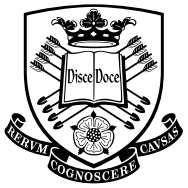

The University Of Sheffield.

Understanding Application and Tribological Mechanisms of Lubricants and Friction Modifiers in the Wheel-Rail Interface

By:

Matthew Harmon

A thesis submitted in partial fulfilment of the requirements for the degree of Doctor of Philosophy

The University of Sheffield
Faculty of Engineering
Department of Mechanical Engineering

August 2018

Summary

A literature review that focussed on friction management products identified a number of areas that were lacking in research. These were that research generally focussed on one scale of test without considering how the results may be affected by changing the scale of the test/experiment. The other main conclusion was that whilst there was a large body of research that focussed on friction management product performance, relatively little considered how the product was applied to the wheel-rail interface and what happened once it was in it. Additionally, there was a lack of small-scale laboratory methods that were validated against full-scale and field data. This led to the following aims of the thesis:

- Assessment of fundamental product properties and how they relate to product performance
- Bench mark tests to assess performance based on available test platforms across a range of scales
- Develop new test methods to assess product properties and product application in the field
- Understand the transferability of laboratory results to the actual, real world contact and between different laboratory test scales

After analysing field operations, tackiness was chosen to focus on as an indicator of grease pick-up performance. A new test method was developed based on an existing tribometer. The method was able to differentiate between different greases, as well as changes in amount of tackifier additive present in the grease. Friction Modifiers (FM's) were also tested using the same procedure and ranked according to how tacky they were. Pick-up tests using a Scaled – Wheel Rig (SWR) showed that the ranking for tackiness was the same as the ranking for pick-up. The tackier the FM or grease the greater the pick-up. Additionally, the ranking was the same when the test was repeated using a Full-Scale Test Facility (FSTF). This means that the ranking of pick-up was independent of slip, load and lateral displacement of the wheel. Carry-down tests of grease using the SWR were performed and showed that an applicator bar that gave more pick-up did not necessarily result in more carry-down. This is because where on the wheel the grease gets picked-up is equally important. If the grease is collected by the wheel near to the flange tip, it does not enter the contact and is wasted. These types of tests have not been done before and the fact that the same results are seen across the test scales shows that the small-scale tests can be used to predict performance in the field. This can lead to these tests being incorporated into standards or used in quality assurance procedures.

The other main outcome of this work is that longitudinal vibration has been shown to change depending on grease presence and top-of-rail contamination. Grease affected the vibration in the 700-1200 Hz range, whereas contamination (by leaves or water) on top of the rail affected the vibration across the frequency range. Additionally, it was shown that the vibration dramatically increased depending on the amount of wheel sliding due to leaf contamination. This could lead to longitudinal vibration being used as a condition monitoring device in known problem areas as an early warning system, or near lubrication sites to monitor lubrication effectiveness. Additionally, it could be used to indicate carry-down distance of friction management products.

Nomenclature

COF	Coefficient Of Friction
EPSRC	Engineering and Physical Sciences Research Council
FM	Friction Modifier
FSTF	Full-Scale Test Facility
GDU	Grease Distribution Unit
km/h	Kilometres per hour
MC4	A typical grease applicator used in the field
MC4-GG	MC4 applicator supplemented with GreaseGuide™
mph	Miles per hour
NDT	Non-Destructive Testing
PSD	Power Spectrum Density
PTV	Pendulum Test Value
QRTC	Quinton Rail Technology Centre
RCF	Rolling Contact Fatigue
RSSB	Rail Safety and Standards Board
SUROS	Sheffield University ROlling and Sliding
SVR	Severn Valley Railway
SWR	Scaled-Wheel Rig
TOR	Top Of Rail
TORFM	Top Of Rail Friction Modifier
TOR-ML	A typical TORFM applicator bar used in the field
Tγ	Wear number
UMT	Universal Mechanical Tester

μ	Coefficient of Friction
d	Wear depth (mm)
F	Force (N)
H	Hardness of the softest contact surfaces
k	Wear coefficient
l	Sliding distance (m)
P	Normal load (N)
p_o/k	Load factor, normal contact pressure divided by shear yield strength
Ra	Surface roughness parameter, arithmetical mean deviation of the assessed profile
V	Total volume of wear debris formed (mm^3)
γ	Creep
ϑ	Angle

Contents

Acknowledgements

I would like to thank my supervisors, Professor Roger Lewis and Anup Chalisey for their support and guidance during my PhD. I would also like to thank all the RA's, technical staff and my fellow PhD candidates in the department who have helped me figure out issues, taught me how to use the test rigs and systems in the department. Lastly, I would like to thank the CDT manager, Kim Hyde for organising the training and development opportunities for the CDT and her continued support through my PhD.

This project is funded by Rail Safety and Standards Board (RSSB) and the Engineering and Physical Sciences Research Council (EPSRC). RSSB also provided technical support through regular updates and meetings with Giulia Lorenzi and Anup Chalisey. I also presented regularly to the Adhesion Research Group which RSSB organise.

1 Introduction

1.1 Background

The wheel-rail interface is an extremely complex system. It is required to carry the load of the train, as well as transfer the traction and braking forces within the small area of contact between the wheel and rail, often approximated to 1 cm^2. The contact is further complicated by being an open system, which means there are many sources of contamination that can affect it. The open nature means that environmental conditions can cause the contact conditions to change in a relatively small time or distance and even between each rail or bogie. Differences in trains such as different axle weights, suspension properties and wheel profiles also change the contact conditions. Maintaining the conditions within the contact at the optimum level can help reduce wear, RCF, noise, vibration and energy requirements; this leads to benefits across the industry as maintenance cost and time is reduced, passenger safety and satisfaction is increased, and running costs are reduced.

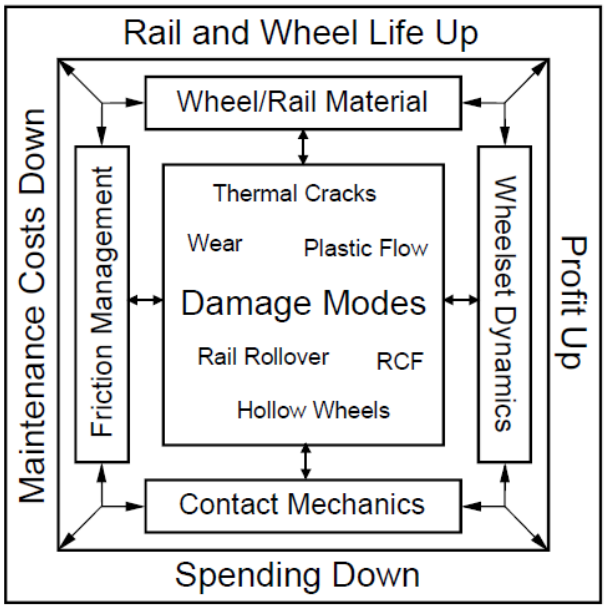

Figure 1- Wheel-rail interface systems diagram [1]

Figure 1 [1] highlights how the diverse aspects involved in the railway influence each other and the importance of considering the entire system when making a change to one aspect. For example, when introducing a new wheel material to reduce wear and increase time between reprofiling, the effect of this new material on Rolling Contact Fatigue (RCF) has to be taken into account as well.

In order to ensure safe, smooth, train operation, the friction level between the wheel and rail can be changed by introducing different products to the wheel-rail interface. This can include traction enhancers (used to improve traction in low adhesion conditions), lubricants (often applied in curves to reduce the forces in the contact) or friction modifiers (used to provide an optimised level of friction). Understanding how these products work and interact with the wheel-rail interface (including any contamination that may or may not be present) is vital to optimising their use for different traffic types and different operating conditions.

1.2 Aims and Objectives

From the literature review undertaken in chapter 2 the following aims were decided upon:

- Assessment of fundamental product properties and how they relate to product performance
- Bench mark tests to assess performance based on available test platforms across a range of scales
- Develop new test methods to assess product properties and product application in the field
- Understand the transferability of laboratory results to the actual, real world contact and between different laboratory test scales

To meet these aims a number of work packages were created as seen in Figure 2. The green boxes highlight the data gathering phase, yellow boxes highlight laboratory tests and orange boxes highlight field tests.

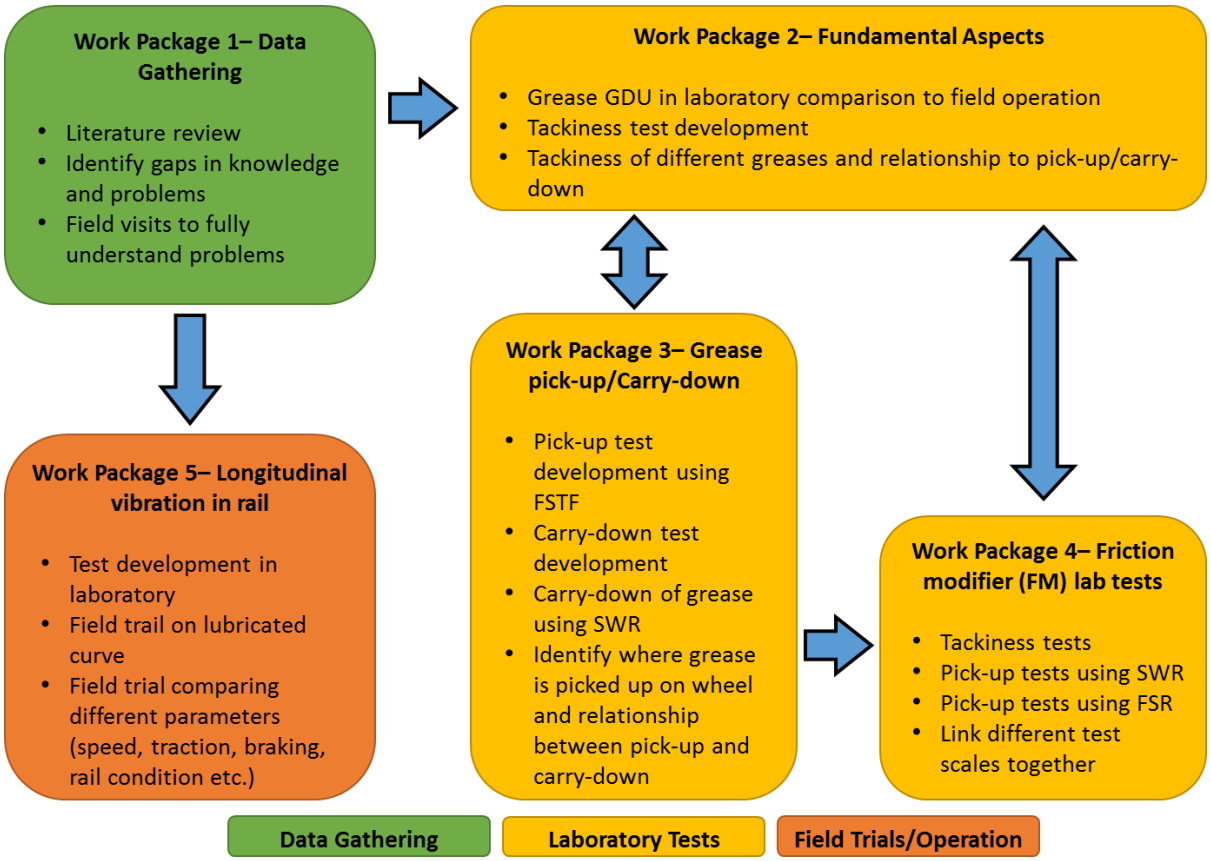

Figure 2- Work packages and how they link together

These work packages were influenced by gaps identified in the literature review and ensured the aims of the work were met. They focused on the physical application of grease and friction modifiers. This was because there is a large body of work already done on the benefits of these products, but there was little work on how to apply them, where they go once they are applied, and how far down the track their benefits are seen. The work packages also included tests at different scales. This is because the smaller the test scale, the quicker and more controllable the tests. However, this comes at the expense of representing the actual conditions seen during

real world operation. The reasons for using the different tests chosen in this work are discussed in much more detail in Chapter 3.

1.3 Outline of Thesis

Initially a review of the current research is presented in Chapter 2. The review focusses on applied products to the wheel-rail interface, in particular Top Of Rail Friction Modifiers (TORFM's) and curve lubricants. The review also helps form the aims and objectives described above. Chapter 3 describes the test rigs used in the subsequent work. This chapter also discusses the various benefits/drawbacks of the different test scales used. Throughout the thesis, different test scales have been linked together. This is important as there will always be differences between laboratory tests and field conditions and little work has been done in this area. Chapters 4-8 contain experimental results. Within each chapter, the results for that section are presented along with a short discussion on the results. Chapter 9 discusses the outcomes of the research, the impact and how the different chapters link together in much greater detail.

Chapter 4 contains various small bodies of work carried out to understand the operation of Grease Distribution Units (GDU's) in the field. Chapter 5 describes a new test method for evaluating the tackiness of grease. The method was developed to link the tackiness of a product to the pick-up by a wheel and there was not a suitable test found in the literature to evaluate tackiness. Chapter 6 describes a new method for assessing the carry-down of grease in the laboratory. This was to be able to measure the effectiveness of changes in pump/GDU characteristics with respect to grease carry-down. This has not been done in the laboratory before and enables different parameters to be tested in a controlled environment. This chapter also analyses scaling effects between two scales of test rig in the laboratory. Chapter 7 details work carried out to use the vibration in the rail as a method for monitoring the amount of grease present in a curve. This method of monitoring the amount of grease can be developed to use as a condition monitoring system or use as a grease carry-down measurement in the field. This is a new method to detect the presence of products on the rail. It also looks at how vibration changes when rail is contaminated with leaves or water and how this could be extended to function as a condition monitoring system for use in problem areas. Chapter 8 describes various work undertaken using friction modifiers. This chapter utilised the same methods that were created for use with grease and linked three different scales of test rig together. This ensured that the new small-scale test methods developed in Chapter 5 and 6 were validated against full-scale data. Chapter 9 discusses the outcome of this research; how it can be used in the field and future directions the work could be taken.

1.3.1 Research Highlights

There are four key areas of work that this research has developed:

- Grease pick-up and carry-down from a GDU can be measured in the laboratory using new test methods developed on two different scales (a Scaled-Wheel Rig and a Full-Scale Test Facility
- A test method to quantify the relative tackiness has been developed in the laboratory. This uses a simple bench-top tribometer to rank products according to their tackiness.
- The contamination of the wheel-rail contact can be inferred by measuring the vibration of the rail as a train passes.

- The relationship between tackiness and product pick-up has been proven using the results from three different test scales.

Further details on these highlights and how they can be applied can be found in Chapter 9.

1.4 Publications

1.4.1 Arising From This Work

1. M. Harmon, R. Lewis, "Review of top of rail friction modifier tribology," *Tribology: Materials, Surfaces and Interfaces*, vol. 10, no 3, pp. 150-162, 2016

2. P. Temple, M. Harmon, R. Lewis, M. Burstow, B. Temple, and D. Jones, "Optimisation of grease application to railway tracks," *Proc. Inst. Mech. Eng. Part F J. Rail Rapid Transit*, vol. 232, no. 5, pp. 1514–1527, 2018

3. M. Harmon, B. Powell, I. Barlebo-Larsen, R. Lewis, "Development of Grease Tackiness Test", *Tribology Transactions,* 2018, pp. 1-10

1.4.2 Arising From Internal Collaboration

4. L. Buckley-Johnstone, M. Harmon, R. Lewis, C. Hardwick, and R. Stock, "Assessment of Friction modifiers performance using Two Different Laboratory Test-Rigs," in *The Third International Conference on Railway Technology: Research, Development and Maintenance*, 2016, pp. 1–16

5. S.R. Lewis, D.I. Fletcher, L. Buckley-Johnstone, B. White, M. Harmon, C. Grigson, H. Brunskill, L. Zhou, T.R. Kempka, R. Lewis, "A Re-Commissioned Flexible Full-Scale Wheel/Rail Test Facility" *Proceedings of 11th International Conference on Contact Mechanics and Wear of Rail/Wheel Systems,* 2018, pp. 1-10

1.4.3 Arising From External Collaboration

6. M. Harmon, J.F Santa, J.A Jaramillo, Alejandro Toro, A. Beagles, R. Lewis, L. Buckley-Johnstone, "Evaluation of the Coefficient Valuation of the Coefficient of Friction of Rails in the Field and Laboratory Using Several Devices", in *Proceedings of 11th International Conference on Contact Mechanics and Wear of Rail/Wheel Systems,* 2018, pp. 1-10

2 Wheel-Rail Contact and Third-Body Materials

This chapter will focus on reviewing research that is currently published with regard to applied products to the wheel-rail interface, in particular Top of Rail Friction Modifiers (TORFM's) and lubricants. Initially a short overview of the wheel-rail contact will be presented in order to put the research into context. Then all third-body substances will be discussed as the rail will rarely (if ever) be clean in the field, and so the interaction between any applied product and what is on the rail already is an important aspect to consider. During the review of existing research, any gaps in knowledge and ideas for further work will be identified and explored.

2.1 Contact Conditions

Higher pairs such as ball bearings or gear teeth are other engineering examples where similar loads are supported by small areas. However, these are generally closed systems with defined contact conditions and little plastic flow occurring due to relatively low slip values and are often fully lubricated systems. This makes the analysis more straight forward and as a result, the relationships and theories developed from these systems are of little use when applied to the wheel-rail contact.

As a train travels down the track, the location of the contact patch on the rail is likely to change due to the dynamic nature of the system. Three broad areas of contact between the rail and wheel can be defined as shown in Figure 3 [2]:

- *Wheel tread-rail head contact (Region A).* This occurs most often, occurring on straight track and high radius curves; it has the lowest contact stresses and lateral forces.
- *Wheel flange-gauge corner contact (Region B).* The contact patch is usually smaller than the previous region and leads to more severe wear due to the higher stresses apparent in the contact.
- *Contact between field sides of wheel and rail (Region C).* This region is least likely to occur, however, high contact stresses causing excessive wear ensue if contact does take place in this region.

As the contact position moves about on the wheel and rail head, the shape of the wheel and rail profiles will change over time due to wear and material flow. The change in profile will lead to a change in the contact stresses and wear rates. This means the contact patch is constantly evolving, leading to a dynamic system, making accurate prediction of the system even harder.

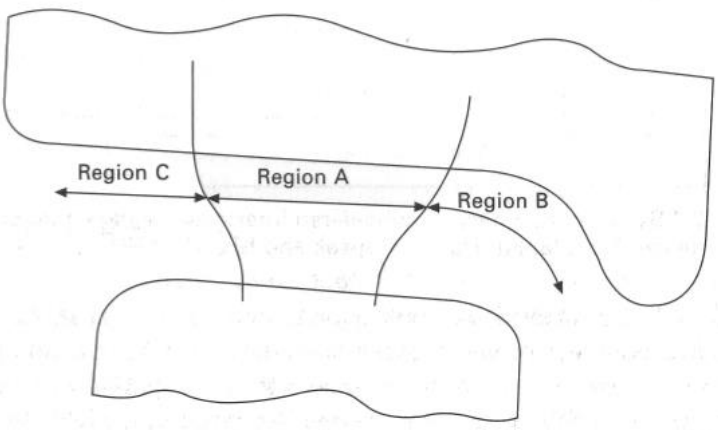

Figure 3- Regions of contact between the wheel and rail [2]

In 1881 Heinrich Hertz determined a relatively simple analytical model for determining the size and loads of the contact patch when two curved bodies are in contact with each other [3]. This model is still used as a starting point for most analysis of the wheel-rail contact today and the following assumptions are applied [4]:

- The surfaces are continuous and non-conforming (i.e. the size of the contact is small compared to the size of the curved bodies)
- Each solid can be considered as an elastic half-space
- The strains are small
- The surfaces are friction less (i.e. smooth)

These assumptions can be invalid when applied to the wheel-rail contact. For example, the open nature of the system means that the contact will be rough and contaminated. Also, when looking at gauge corner contact, the radius of curvature is small enough that the size of the contact cannot be considered insignificant compared to it [5]. However, Hertzian contact analysis is still often used as a starting point for both simple and more complex models. A study recently developed a model for the effect of third-body layers on the traction coefficient which showed good correlation to twin disc experimental results and was based on Hertzian analysis [6].

Numerical solvers have been developed using Hertzian analysis as a base for calculating the contact areas and stresses. Studies have been done comparing these numerical solvers to Hertzian contact and finite element modelling (which includes plastic deformation and actual wheel and rail profiles). The studies have concluded a good correlation for the rail head contact, but significant differences for the rail gauge corner contact, as expected due to the limits of the assumptions [7].

More recently an ultrasonic method has been used to measure the actual contact [8], [9]. Again the studies concluded a good correlation between the methods on a global level. However, at a local level there were differences. It is expected these are caused by a difficulty in ensuring the surfaces are similar between the model and the method.

2.2 Friction, Creep and Damage Mechanisms

Friction is the force that resists two bodies in relative motion and therefore occurs everywhere in the world around us. The coefficient of friction is the ratio between the friction force and the normal force holding the surfaces together. The term traction is given to the force that generates motion between a wheel and a surface, and the coefficient of traction is the ratio between traction force and normal force.

According to shakedown theory (described in section 2.2.3) as friction increases in the wheel-rail interface, plastic deformation increases, leading to a greater rate of strain accumulation and greater RCF/wear. This is shown clearly in the shakedown plot (Figure 14), which will be discussed further in a later section. Life of components can be extended by introducing lubricants (often liquid, but solid lubricants do exist) which provide a low shear strength layer to reduce friction between two surfaces in motion. There are three distinct regimes that occur in liquid lubrication [10]:

- Boundary Lubrication- constant conditions between surfaces despite the lubricant being present. This means the laws of dry friction apply
- Mixed Lubrication- partially separated surfaces with some asperity contact
- Hydrodynamic Lubrication- surfaces are fully separated by the lubricant layer

In the hydrodynamic region the shear stress of the lubricant determines the level of friction. Whereas in boundary and mixed lubrication, there is solid contact between asperities which determines the level of friction. Figure 4 shows a standard Stribeck curve which shows how the three different regimes have clear differences in the coefficient of friction.

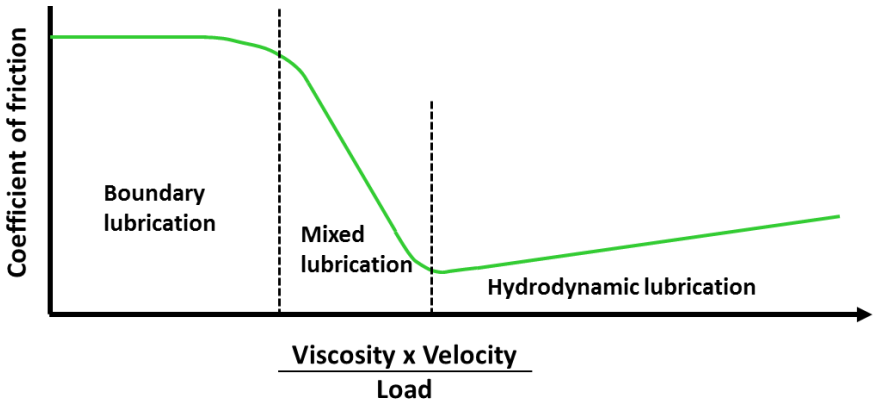

Figure 4- Stribeck curve showing the different lubrication regimes [11]

When the rail is contaminated by oil or is fully lubricated with grease it typically operates in the hydrodynamic region with the level of friction determined by the shear stress of the lubricant [12]. When the rail is wet, it is in the boundary lubrication regime with an associated high coefficient of friction caused by asperity contact [12]. Understanding which lubrication regime the contact is operating in can aid in: designing representative tests, understanding the results from testing, and how to change the contact properties to optimise friction. For example, the fact that oil contaminated contacts operate in the hydrodynamic region explains the low friction values in Figure 6. This is particularly important in top of rail products, where sufficient levels of adhesion are required for traction and braking, so alternative solutions to traditional lubrication are required.

It is important to define different levels of friction in order to better understand the effect of different contaminants. The following definitions have been taken from recent work [13]:

- Medium low: $0.1 < \mu < 0.15$
- Low: $0.05 < \mu < 0.1$
- Exceptionally low: $0.02 < \mu < 0.05$

2.2.1 Creep

Creep (γ) is a measure of how much slip there is in the contact usually expressed as a percentage of the wheel velocity. Slip occurs due to tangential forces in the trailing area of the contact. Creep curves which plot traction coefficient against creep can be used to evaluate different contact conditions. Full slip usually occurs in a dry contact at creep values of 1-2 %, but there are many factors which can affect the creep curves such as humidity, contamination etc.

Figure 5 shows that as the tractive force increases the slip region in the contact increases, and the stick region reduces, until a maximum value where there is no stick region at all and the contact is in full slip.

Figure 6 displays data from experimental work carried out in 2008 which used a twin disc machine to simulate different contact conditions [14]. This work shows the effect of different contaminants on the creep curves and illustrates the dramatic effect that these contaminants can have on the traction coefficient and hence the traction level.

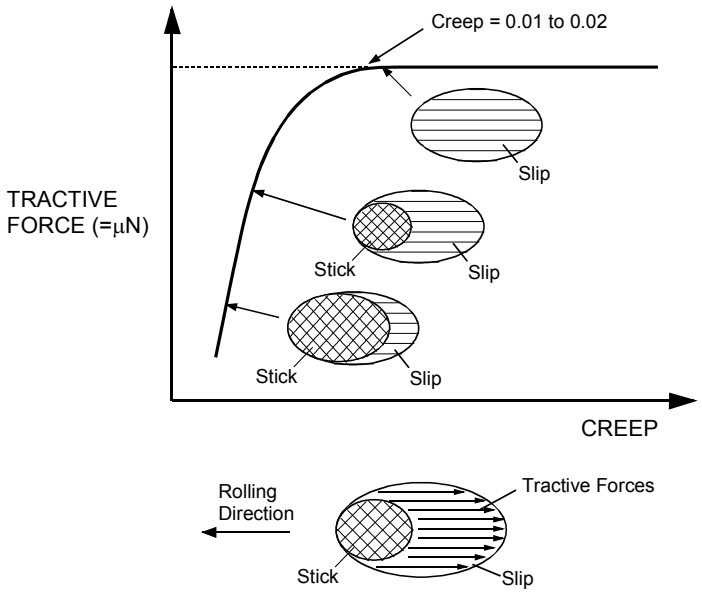

Figure 5- Relationship between traction and creep [5]

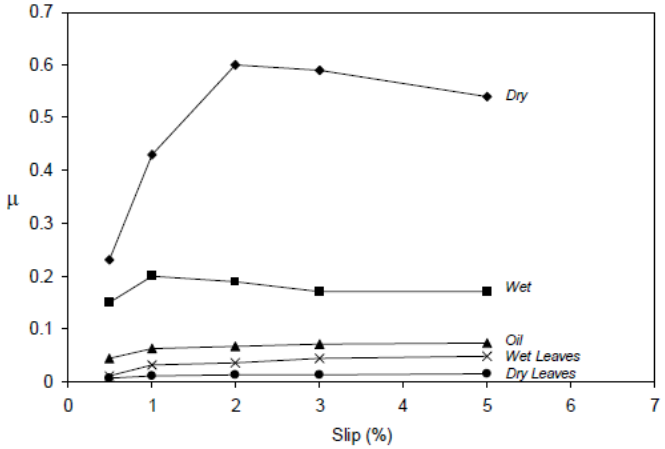

Figure 6- Creep curves for simulated contact conditions [14]

2.2.2 Wear

The wear of a material depends on the tribo-system as a whole. The system not only includes the material properties and stresses the contact is under, but also other factors such as environmental conditions and contamination of the contact. Wear can occur by a number of different mechanisms:

- *Adhesive wear*- actual contact between the two surfaces occurs at asperity junctions which weld together. When the surfaces are moved relative to each other these junctions break apart often leaving the tip of one surface adhering to the other.
- *Abrasive wear*- this type of wear is caused by the asperities of a harder surface moving relative to a softer surface creating long parallel grooves in the sliding direction (Figure 7). This is called two body abrasive wear; three body abrasive wear can be caused by a harder contaminant particle trapped between two moving surfaces.
- *Oxidative wear*- oxides form on the surface of the material which are then broken away (Figure 8). This mechanism is heavily dependent on the ability of the material to oxidise and the availability of oxygen. The process is also reliant on the contact conditions (temperature and humidity).
- *Thermal wear*- this type of wear is linked to the increase in temperature caused by friction generated in the contact. The extreme case is where the material is heated to such an extent that it behaves as a viscous fluid and can be displaced. However, even mild thermal input can lead to residual thermal stresses eventually leading to thermal fatigue and loss of material. Also, the severity of the other mechanisms can be enhanced by a reduction in hardness associated with an increase in temperature.

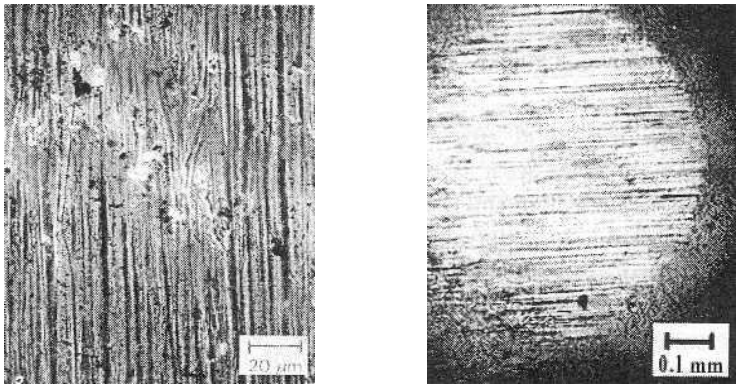

Figure 7- Severe Abrasive Wear [15]

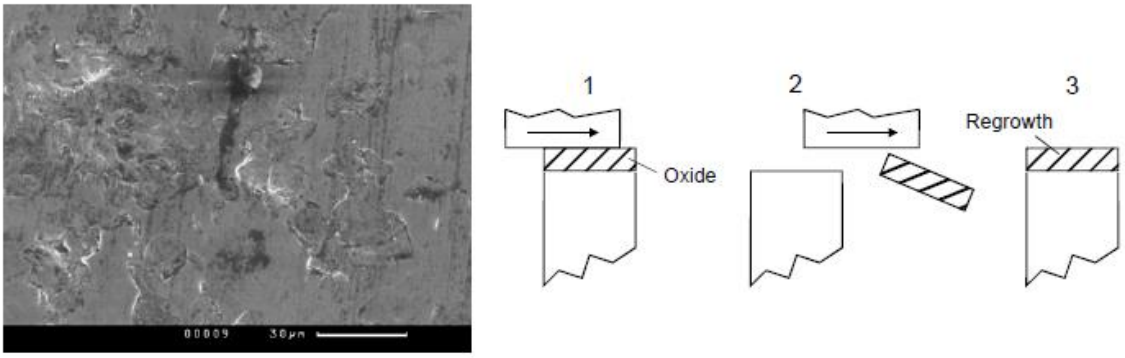

Figure 8- Oxidative Wear [5]

The rate that wear occurs at is often split into three different regimes [16]: mild, severe and catastrophic. The regimes are not split on a specific wear rate, but are based on observation of a sudden jump in wear rate as the severity of loading is increased. Figure 9 demonstrates how the different regimes can easily be seen by twin disc testing as significant changes in the wear rate. The changes in the regime in this case are caused by an increase in slip level which increases the severity of the contact conditions. Increasing the temperature, contact pressure or sliding velocity will have the same effect.

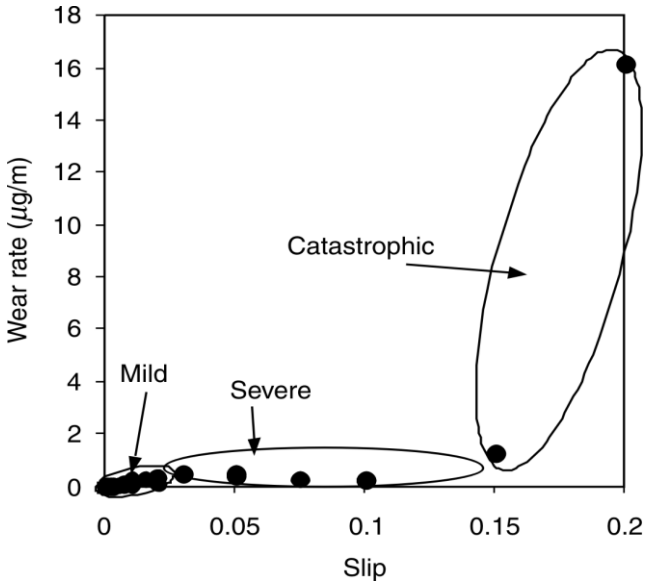

Figure 9- Graph showing the changes in different wear regimes [17]

Additionally when components are first run together the wear rate can be high. However, as the components wear, they improve in conformity and the wear rate drops (referred to as running in) until other processes take over near the end of the component's life and the wear rate increases again. Other non-linear behaviours also can occur. Figure 10 shows two examples of this and how the wear rate changes over a typical component life [18].

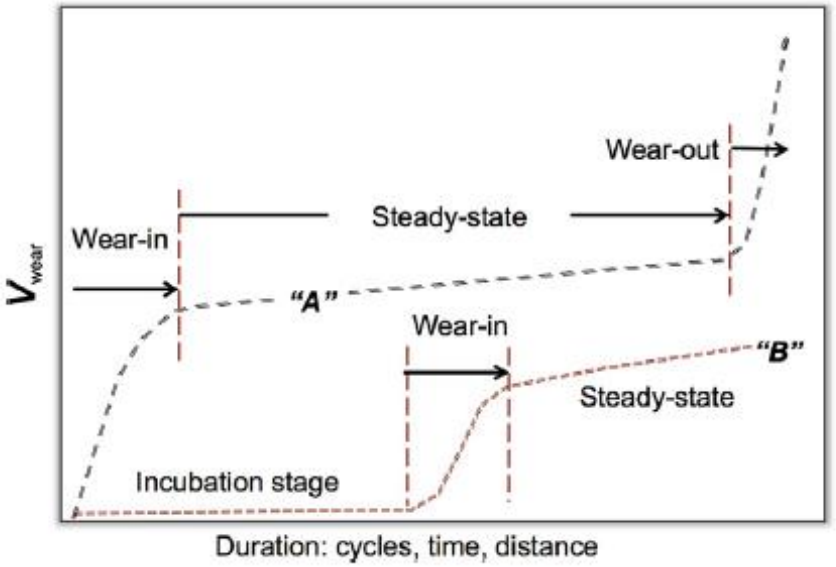

Figure 10- Two different non-linear wear behaviours [18]

Often when attempting to model the wear situation the Archard model [19] (Equation 1) is used as a starting point. This equation is used because it is simple to understand and use, but is often found to over predict the wear volume of a situation. The wear coefficient changes for each material combination and it is also important to be aware of which wear regime the system is currently in as this will also effect the wear coefficient.

$$V = \frac{kPl}{H} \tag{1}$$

Another approach which is widely used is the $T\gamma$ (wear number) approach [20]. This method has wear and fatigue combined in a single parameter referred to as damage. It also relies on correlations between certain $T\gamma$ numbers and the wear/fatigue performance found on the track, which can often be an issue if new rail steels are introduced for example. The wear number is representative of the energy consumed in the contact patch but it does not differentiate between different forms of energy (wear, heat, noise etc.). Wear coefficients are determined from experimental data from rolling/sliding tests which have been well researched for dry contacts, but there are some tests now which are using wet contaminated contacts [21], [22]. However, there is still limited experimental data for friction modifiers.

Wear maps for a material can be created which help in the analysis of wear data. They provide easy analysis of wear as the various mechanisms or regimes can be simply identified. They are usually defined in terms of slip or contact pressure. Data used to create the maps can be limited which restricts how useful the maps can be; nevertheless maps can be used to focus further testing and eventually lead to theory supported by experimental evidence [23]. For example, rail steel regimes have been well defined in terms of wear rate, metallographic features and wear debris, but the mechanisms which lead to the changes in regimes is not currently understood fully; although temperature is expected to play a role as increased temperature can prompt a reduction in material properties. Another cause could be the change in conditions from partial slip to full slip in the contact [17]. Figure 11 shows a wear map with typical contact conditions overlaid onto it. It shows that rail gauge/wheel flange contact results in more severe wear which matches field observations.

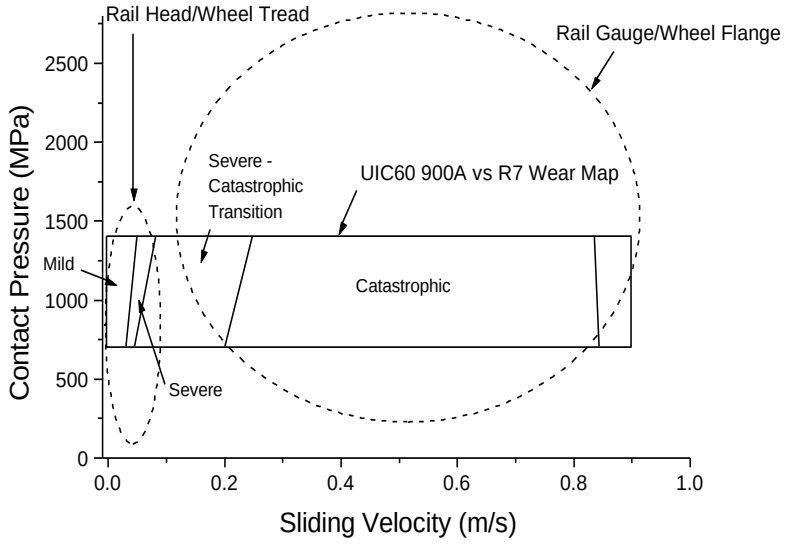

Figure 11- Wear map displaying wheel-rail contact regimes [23]

2.2.3 Rolling Contact Fatigue

Rolling contact fatigue (RCF) is the accumulation of fatigue damage caused by many passes of wheels, resulting in cracking on wheels and rails. Each wheel that passes a particular point on the track exerts a load cycle as the wheel approaches, passes over and continues down the track from the particular point. RCF leads to maintenance requirements (rail grinding, regular Non-Destructive Testing) which is costly, but prevents safety issues, as missed cracks can grow quickly and lead to rail breaks.

Squat defects are a type of RCF found mainly on straight track indicated by a dark spot on the rail surface and a widening of the contact band. Head check defects are more common on the outer rail of corners and do not often cause cracks which propagate to failure. However, they do cause chips of rail gauge corner to break away and the many small surface cracks obscure NDT results. This means the condition of the sub surface is unknown and leads to pre-emptive rail replacement when the original rail may not contain any dangerous cracks. Figure 12 and Figure 13 shows typical RCF defects.

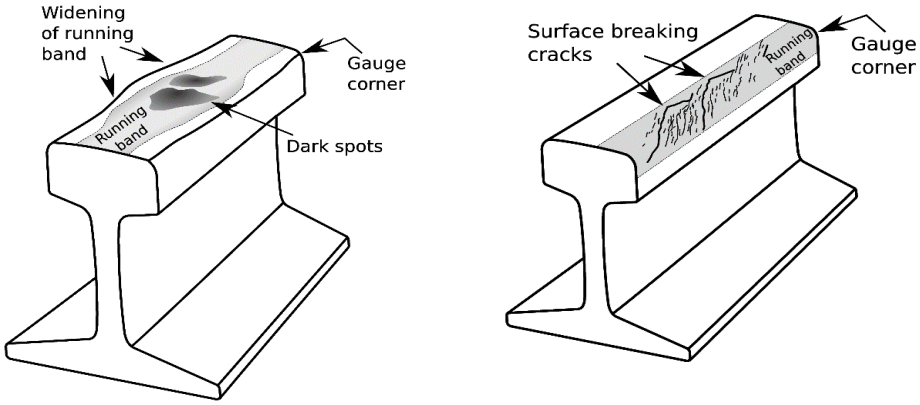

Figure 12- RCF damage types [24]

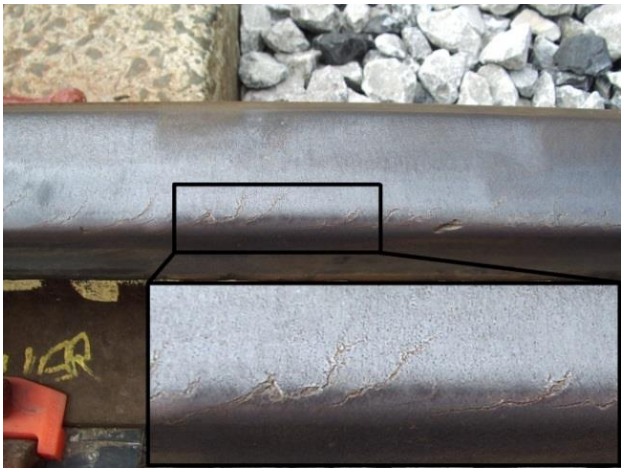

Figure 13- Visual appearance of head check defect type [24]

In pure rolling the maximum shear stress occurs below the surface of the material. As a tractive force is applied, shear stress increases and the location of the maximum stress moves towards the surface. At the surface there is less material surrounding the maximum stress to dissipate it and so more plastic deformation occurs here. The damage to the material is worst if the material enters the ratcheting region; this occurs when the wheel-rail load and contact pressure is higher than the elastic limit and causes permanent plastic deformation leaving residual stress in the rail every time a wheel passes over a particular area. Large strains can accumulate due to ratcheting until the ductility limit of the material is reached when either a crack is initiated if it is subsurface, or wear debris is formed if it is accumulated at the surface [25]. Due to the rolling/sliding nature of the contact a cyclic build-up of plastic deformation occurs which is the origin of RCF and wear. The shakedown map (Figure 14) shows reducing the friction can lead to an increase in load factor without the material entering the dangerous ratchetting region [5].

However, this may not work in all circumstances as reducing the friction by applying a lubricant could change the crack growth mechanism (Figure 15). This may lead to an increase in severity of cracks and again emphasises Figure 1, which shows that the whole system must be considered when making a change to one aspect. Shakedown occurs when the contact pressure exceeds the elastic limit of the material, but is lower than the pressure required to cause ratcheting. This is because the first few load cycles cause residual stresses which can protect the material from further yield leading to higher load that can be safely be run on the rail without further damage.

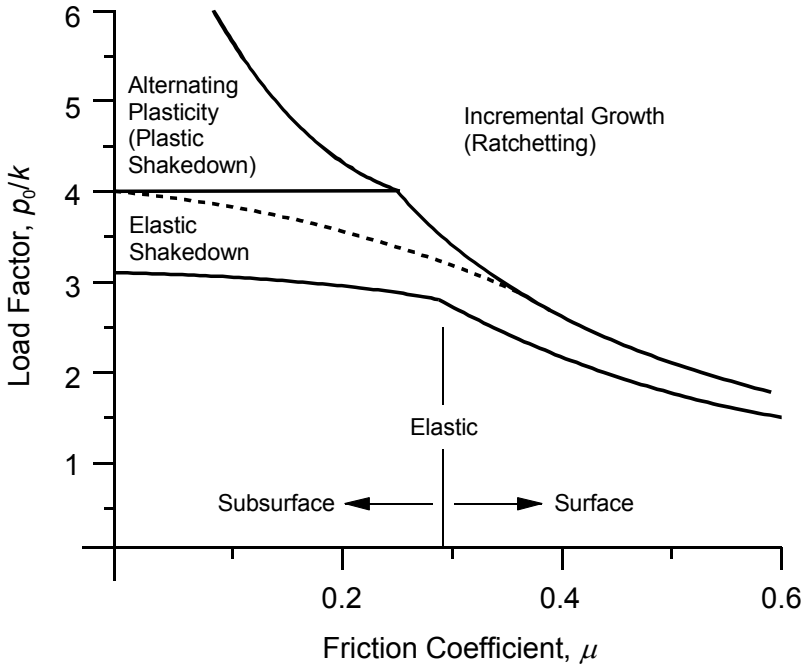

Figure 14- Shakedown Plot [5]

Wear and RCF are both caused by the gradual accumulation of plastic deformation. If material removal due to wear occurs at a faster rate than crack growth then the material will ultimately be left without any cracks in it. This depends on the material/wheel combination as some rail steels wear more rapidly than others. Also different types of traffic will cause different amounts of wear/RCF. Some trains may cause cracks and little wear on a section of track; and when a different type of train runs along the same section of track, it may cause a higher wear rate removing the cracks caused by the previous train. Currently, all relationships between RCF and wear are experimentally based with the typical wear depth per wheel pass is 1 nm. Figure 15 illustrates how wear truncates a crack.

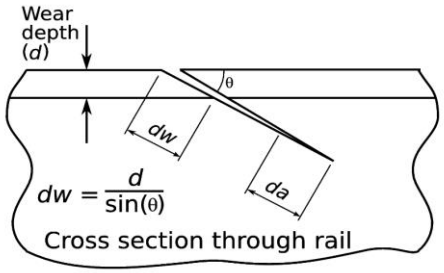

Figure 15- RCF/wear interaction [24]

2.2.4 Mechanisms of Crack Growth

Surfaces are known to be more severely damaged in the presence of a lubricant than when they are dry; although rails do no always have oil/grease applied they can get wet in the rain, and the water can act as lubricant. The exact mechanism behind this process is currently unknown but there are several proposed mechanisms to explain this phenomenon with the reality likely to be a mixture of all of them, Figure 16 shows diagrams of how the different mechanisms act:

- *Shear mode crack growth*- the compressive wheel load as a wheel passes over the crack applies shear to the crack, with the presence of the lubricant allowing the faces to slide more easily, accelerating crack growth. This mechanism is supported by experiments with different lubricants although nobody has found a way of directly measuring this effect.
- *Hydraulic crack growth*- lubricants which are virtually incompressible can act as a hydraulic fluid which transmits the surface contact pressure into the crack, which provides a tensile crack opening stress to occur. This only works if the crack is completely sealed to provide a pressure peak which is unrealistic in a 3D contact.
- *Fluid entrapment crack growth*- similar to previous mechanism with the same associated issue of the sealing of the crack is unlikely to be realistic. This mechanisms explains why only a driving wheel causes crack growth as a braking wheel drives out the fluid from the crack rather than sealing it.
- *Squeeze film lubrication*- this mechanism assumes that the rapid compression of the crack caused by a passing wheel causes a pressure peak inside the fluid which is large enough to cause crack growth regardless of any fluid leaking out.

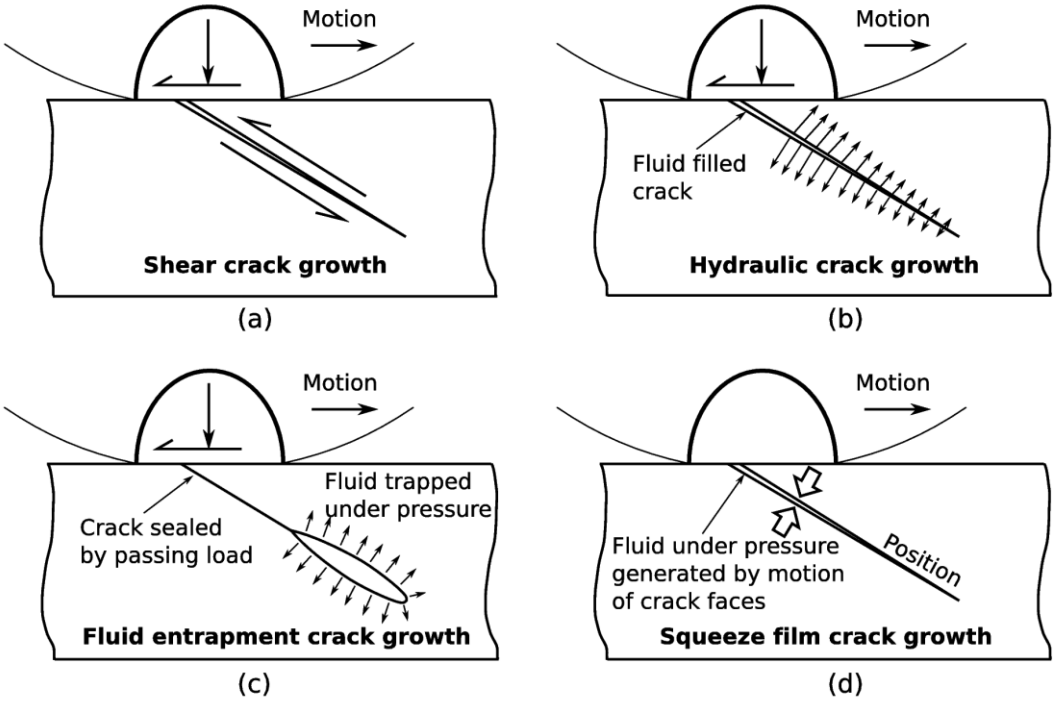

Figure 16- Mechanisms of crack growth [24]

It is possible to get empirical crack growth rate laws from using the above mechanism as a starting point and applying fracture mechanics, but it takes many runs of a model to examine

the stress cycle appropriately. Figure 17 shows that at different lengths, crack growth is driven by different processes. In the initial stage, small cracks created by the mechanisms above are driven by ratchetting; however as the crack length increases the contact stresses become more important and drive the crack growth rather than ratchetting. When the crack length reaches approximately 40mm bending stresses dominate the crack growth and cracks can grow very quickly. This illustrates that it is important to catch cracks before they reach the third phase, and start being driven by bending stresses. The very fast crack growth can lead to catastrophic failures. The bending stresses arise from the fact that the rail is supported on sleepers rather than being continuously supported.

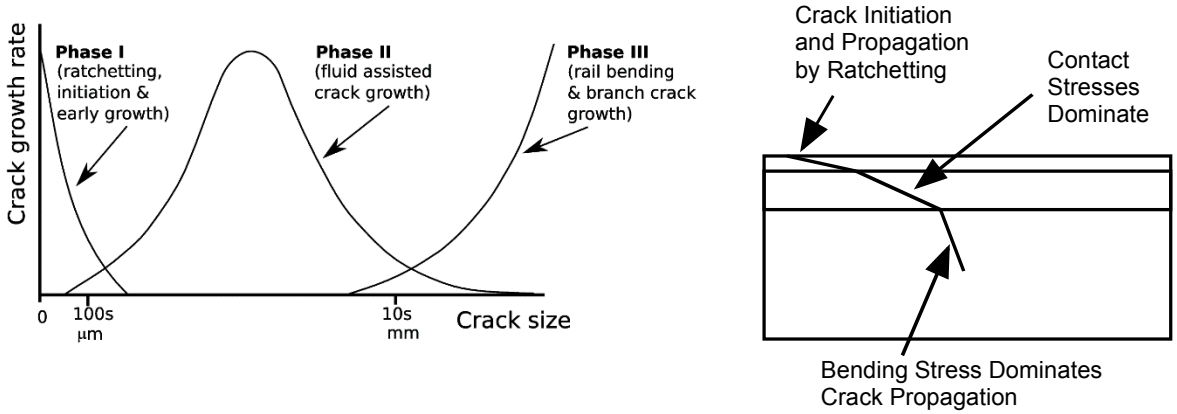

Figure 17- Crack growth stages [24]

2.2.5 Corrugation

Corrugation is defined as a short wavelength variation in profile on the rail head causing noise, vibration and poor ride quality [21,22]. The mechanisms which cause corrugations are linked to plastic flow of material and wear and therefore corrugations are more severe at higher friction levels.

There are different types of corrugation [26]:

- *P2 type*- found where there is a stiff track construction (concrete rail supports) and is caused by the resonance of the vehicle's unsprung mass on the track stiffness
- *Pinned-Pinned type*- also known as roaring rails due to the associated noise increase. This is found on mainline railways as is caused by vertical rail vibration between sleepers. Even small amplitude defect on the rail causes there to be a loss of contact in the troughs, which means the impact forces on the peaks will be several times the static wheel load. This causes a deterioration of the rail support structure.
- *Torsional resonance*- also known as rutting. This is a longitudinal variation in slip and wear at the wheel-rail contact due to resonance of driven wheelsets. This occurs primarily on the low rail in curves or where traction/braking is severe due to one wheel of an axle beginning to slip, driving the opposite wheel into a roll-slip oscillation

2.3 Friction Force Modelling

There are many different models that have been developed to model the wheel-rail contact. A recent report commissioned by RSSB [28] has reviewed current models that are applicable to model water effects. It determined that the Polach model [29] is most suitable for analysing the effects of water on friction in the wheel-rail contact. This is because it is already implemented in multi-body simulation software, fully published, computationally fast, and hence easy to implement. This model can take into account contamination in the contact by describing changes to the initial slope of the traction curve and properties of the interfacial layers.

FASTSIM [30] is an algorithm that calculates the total force in rolling contact from a given spin and creepage. This model is very simple but has a poor relevance to the UK rail network. However, it is the basis for many of the more complex models, including the Polach model and other modified FASTSIM variants [31]. The Spiryagin model [32] is very similar to the Polach model as it is based on FASTSIM and extends it by making the friction coefficient dependant on slip velocity. It is also slightly more computationally expensive when compared to the Polach model.

CONTACT [33] was originally a simple half space based model, but has been recently extended to include a third-body layer, the elastic properties of which can be adapted, and include a falling friction law. However, its computational effort is high, and is not as widely available or as suitable for multi body simulations as other models. Including a third-body layer is a recent development and therefore there is currently no research which validates how well the model predicts the effect of the third-body layer.

The Extended Creep Force (ECF) model [34], [35] is based on a model put forward by Tomberger [36] which itself is based on FASTSIM. Tomberger extended FASTSIM, adding a temperature model, an interfacial fluid model, and microcontact model. This made the Tomberger model more applicable to wheel-rail contact and UK conditions. However, it is not widely validated (possibly due to the fact the algorithms were not fully published). ECF extended the Tomberger model to allow the effect of solid interfacial layers to be taken into account. The ECF model is not fully published, but has been validated against railway operations. It has High Pressure Torsion (HPT) tests built into the inputs to characterise the behaviour of the third-body layer [37], and has been shown to increase the prediction quality when compared to other creep force models [34].

The Popovici model [38] is a mixed lubrication model which models the interfacial layer as a viscoelastic lubricant, sharing the load between the lubricant and asperities. It reduces to simple Coulomb friction model for a dry contact. It is therefore another model that can be used to describe contaminants very well. It is slightly more computationally expensive and not fully published like the Polach model is.

NUCARS is a multi-body rail vehicle dynamics simulation computer programme, which contains a feature to accurately simulate top of rail friction modifiers (provided the creepage and force characteristics are known). For dry, clean conditions, simulations rely on Kalker's original theories, which are well validated and widely used. NUCARS can model friction modifiers by specifying the coefficient of friction and "percentage of kalker coefficient" as inputs to the simulation. A kalker coefficient defines the initial slope of the creep curve and as creep forces are lower for contaminated contact conditions, a percentage value of the coefficient can be used to model the contaminated contact. Figure 18 shows an example of the difference the selection of percentage makes. This programme has been shown to provide a good fit for friction modifiers to experimental data, but is less accurate for lubricants [39]. The

criticisms of this programme are that one "percentage Kalker coefficient" is applied to all areas of the simulation which is quite a large simplification, and it relies on inputs from portable tribometers which are known to not be accurate, especially when friction modifiers are present [40].

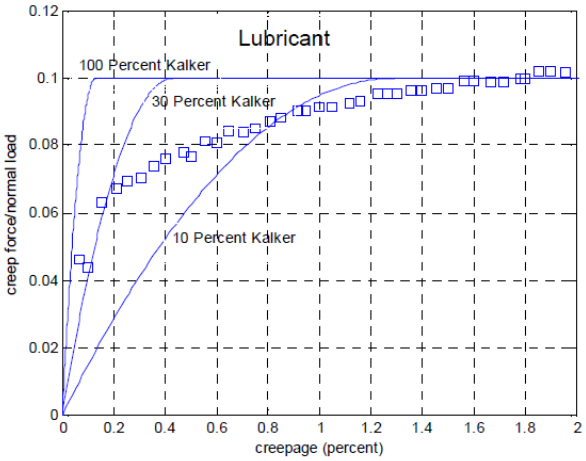

Figure 18- An example showing selection of different Kalker coefficients compared to experimental data for inputting into NUCARS [39]

A new degraded adhesion model has recently been designed [41]. This model allows for removal of unknown contaminants and subsequent adhesion recovery. Additionally, less inputs are required due to the simplicity of the model. This has been shown to provide similar computationally times as other models which do not consider degraded adhesion, as well as a close fit to experimental data.

2.4 Third-Body Materials

In most engineering applications contact areas are in closed systems where the sources of contamination are carefully controlled. This is opposite to what occurs in the wheel-rail interface, where the open system means there are many different sources of contaminant and environmental conditions can vary in relatively short temporal or spatial intervals. In this thesis, contaminants mean any material that is unintentionally present on the rail or wheel. The contaminants mix with the oxide layer and wear particles found on top of rails to create a third-body layer and so depending on what contaminants are present, different third-body layers can be found. The effects the contaminants have are mainly characterised by changes to the level of friction and electrical isolation of the wheel-rail contact. Track circuits detect a train when its wheelsets 'short' the track circuit by providing an electrical path between the two running rails; if the third-body layer isolates the wheelset then train detection can fail, resulting in a potential dangerous situation [42].

This thesis has split the most popular materials that can be found in the wheel-rail interface into two distinct categories: contaminants and applied substances to manage the friction level. If the friction level becomes too low, the safety of the train network can be compromised by trains passing signals at danger or overshooting station stopping points, and can also lead to wheel slippage. If the friction level increases too much then the efficiency of the network as a whole decreases due to factors such as an increase in fuel consumption. When attempting to alter the friction in a particular area there are a number of considerations such as how to apply it to the contact patch, where geographically to introduce it and how much of it to apply.

Additionally, because friction is a system parameter, what works well for one system/area may not be applicable to a different area with different traffic or characteristics.

2.4.1 Contaminants

The main substances generally considered are leaves, oxides, solid particles and water from rain or dew.

Leaves can fall directly onto the track or be sucked onto the track by the aerodynamics of passing trains [43]. Once on the rail, the crushing and compression of the leaves results in a black lubricant strongly adhered on the rail. This results in issues with braking, accelerating and track circuit isolation [44]. This black layer is the product of a chemical reaction between the bulk rail material and the leaves [45]. Often the effects of the leaf layer is counteracted by applying sand which helps remove the layer, improving electrical contact as well as providing more traction [46]. Wheel slip can also lead to an improvement in adhesion when a leaf layer is present as the wheel slip helps to remove the layer without some of the negatives of applying sand [46].

Solid particles will initially be crushed into smaller fragments by the contact pressure as a wheel passes over it, then some of the particles will be ejected from the contact, whilst others will form a particulate agglomerate with steel wear debris and even become embedded into the rail or wheel [1], [47]. The solid contaminants can be a variety of things: sand, crushed ballast, soil debris. Particles such as grit salt, which is used to prevent ice formation on the roads during the winter months, can find its way into the contact [48]. This grit increases the formation of the oxide layer, increasing the severity of its effects. In dry conditions the salt acts as a solid lubricant to reduce traction, and in wet conditions can increase corrosive pitting.

A thin film of moisture is often present on the rail either through rain or dew. A wet rail has been shown to lower the wheel-rail adhesion level, an example is displayed in Figure 6 [14]. This low adhesion has a negative effect to train operation. Data from 2014 has shown that there is an increase in the number of station overruns during the hours when dew is expected to be present on the rail (early morning and late evening) [49]. Another detrimental effect of this layer is an increase in RCF. This is because the water is forced into a crack, lubricating the faces and the compression of the crack causes the water to be forced into the tip creating a widening (mode 1) of the crack [47]. There have been studies to investigate if using a hydrophobic top of rail product would reduce the effect of this contamination [50]. However, it concluded that there was not a convincing case for applying hydrophobic products although there may be some benefit in further investigating their role in suppressing the formation of an oxide layer.

Oxides can form a layer on top of the rail as discussed earlier. This process is heavily dependent on the ability of the material to oxidise, the availability of oxygen, and the contact conditions (temperature and humidity). The oxide layer has the effect of reducing the traction coefficient in the contact; the reduction is small in dry conditions but the effect is much greater in wet conditions (a reduction of up to 4.5 times from the reference value [48]). Additionally the oxide layer is removed after many cycles in the dry condition due to abrasive wear, but in wet conditions the layer is removed at a much lower rate [48]. There is great variety in an oxide layer that is formed on the rail due to a variety of environmental conditions that the rail can face. Therefore, it is very difficult to characterise exactly how an oxide layer will behave in a laboratory setting. A recent paper [6] has analysed the third-body layer after performing twin disc testing and found it to consist of iron and iron oxides. Figure 19 shows the optical results

of the testing with a 50 μm thick layer of oxide on the surface of the disc. The third-body layer in this case is thicker than would be found on the wheel or rail in service use which has been seen to be 15 μm thick [51].

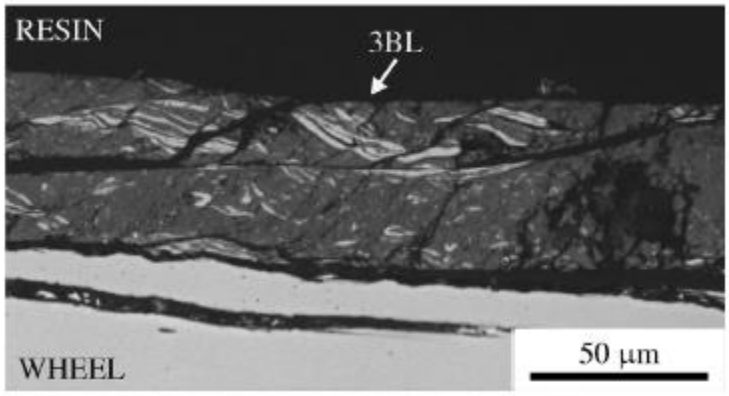

Figure 19- Optical investigation of oxide layer [6]

2.4.2 Applied Substances

Applied substances include anything that is applied to control friction and/or wear in the wheel-rail contact. This substances can broadly be split into grease/lubricants, Friction Modifiers (FM's) and traction enhancers. Traction enhancers are out of scope of this thesis but are included here to highlight the differences between the different products. Within these categories there is often confusion in the industry and in academia about what to call certain products, in particular Top Of Rail (TOR) products. A recent paper [11] has attempted to define terms to bring clarity to this issue. From the paper, TOR products are classified according to their drying behaviour with non-drying products called *TOR lubricants* and drying products called *TOR friction modifiers.* Figure 20 shows the different coefficient of friction that these products operate in. Traction enhancers are not shown on the figure as they do not operate in one band. Traction enhancers are applied in areas of low coefficient of friction and increase it to dry levels.

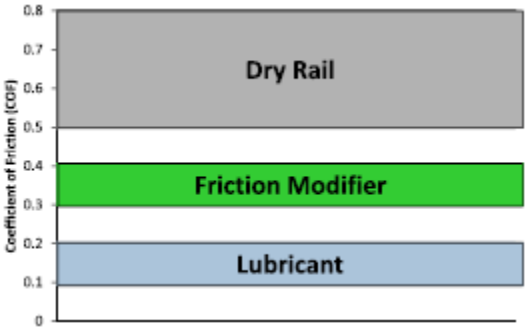

Figure 20- typical coefficient of friction ranges [11]

Greases and lubricants on the rail reduce the coefficient of friction usually to a level below 0.1 The exact level of friction is extremely sensitive to the film thickness between the wheel and rail but even small amounts can cause traction loss [52]. Often grease acts in the boundary lubrication regime which means that some asperity contact still occurs. Lubricants can be found on top of the rail due to deliberate application to achieve a perceived benefit, migration from gauge face lubricants onto the rail head and even oils dripping from passing trains. Eurostar estimates that lubrication saves £1,000,000 per year in maintenance and wheel replacement

demonstrating the positive impact of lubrication. Additionally, the American Association of Railroads estimates that wear caused by ineffective lubrication costs in excess of $US 2 billion per year [53].

TOR lubricants provide friction through a mixed lubrication regime and can be oil based, grease, or hybrid (a mixture of oil and water) [54]. These products stay 'wet' over a long period and have constant transfer between wheel and rail. The products still allow contact between the surface of the wheel and rail and so a slight change in quantity applied dramatically changes the friction level. Oil also has the same effect on RCF as water, provided that there is enough time for the oil to seep into the crack, causing it to grow. Additionally it has been shown that in the presence of water and oil mixtures, the oil is dominant and traction coefficients are the same as having only oil present [55].

A friction modifier differs from a lubricant as it aims to deliver a targeted friction coefficient without negatively affecting the train operations when braking and accelerating or causing surface damage. In Top Of Rail Friction Modifiers (TORFM's) this is often 0.3-0.4; the upper limit of a friction modifier is so that rolling resistance is not significantly increased, improving energy efficiency of the railways. Current products are water based with a solid suspension; as the water evaporates, the solid particles are left behind in the third-body layer on top of the rail delivering the required friction level. The products are wet near to the applicator and material transfer takes place between the wheel and rail, once the product is dry, there is little material transfer [11]. Solid friction modifiers do exist as well which are made of an easily sheared material to aid material transfer. There can be issues with increased wear due to indentation and scratching if the solid particles are too large which means extensive analysis is required in order to optimise toughness, hardness and size of the friction modifier's solid particles [56], [57]. There are two products that are called friction modifiers that are used on the UK rail network. They are Keltrack, which is a water-based product and Railguard, which is an oil based product and so is a TOR lubricant.

Traction enhancers are used solely to improve traction in low slip conditions. Sand is the oldest traction enhancer and is still used all around the world. There are products, often in a gel form, which are also used as traction enhancers. Sand can cause a reduction in traction in dry conditions as it produces a low shear strength layer in the contact patch [58]. In wet conditions or where leaves are present, it can return the traction levels to dry or higher as the sand particles can cut through the lubrication layer. Though this comes at a cost, as the harder sand particles cause a significant increase in the wear rate (through abrasive wear mechanisms) and also has the same isolation issue as a leaf layer [59]–[61]. Other studies have shown that sand can increase traction in water/oil contaminated contacts after an initial reduction [62], [63]. Therefore, traction enhancers/sand are only deployed to recover traction if wheel slippage is detected. Modern traction enhancers use steel shot or alumina rather than sand to reduce issues with wear and track circuit isolation [58]–[65]. A twin disc, laboratory based study has shown that alumina particles are suitable for adhesion recovery as although they lead to abrasive wear, the wear is less than the spalling damage caused by sand [65]. However, the study also showed that sand out performed alumina particles in terms of adhesion recovery for leaf layers.

2.4.3 Effect on Friction

It has been shown that even a small amount of oil/grease (deposited by leaking from passing trains or migration from gauge face) can cause traction loss [52], [62]. This is because it creates

elastohydrodynamic lubrication whereby the viscosity of the oil dramatically increases due to the pressure exerted on it in the contact by the wheel load. If the film thickness is thicker than the surface roughness then a very low friction coefficient results due to no asperity contact.

Friction modifiers eliminate the negative gradient on creep curves. This is important as the negative creep characteristics are unstable and lead to oscillations which cause noise and squealing.

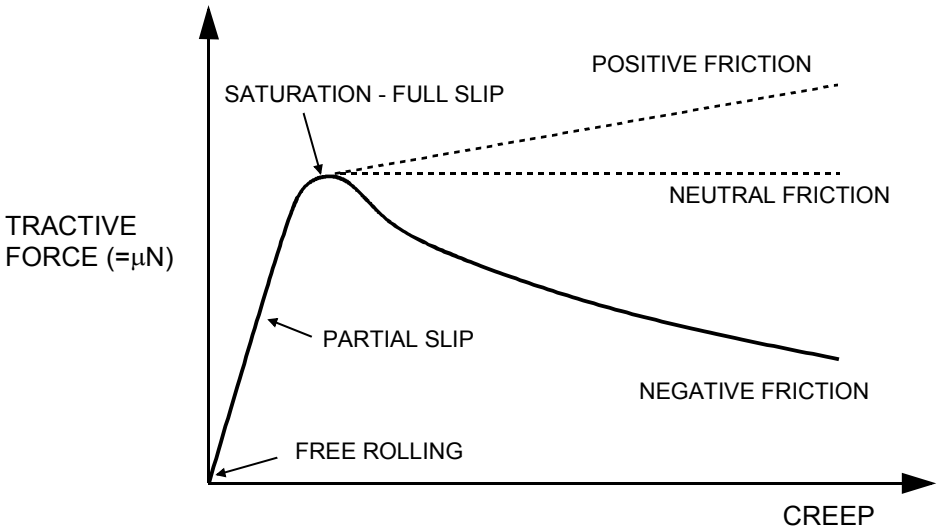

Figure 21- Behaviour of Friction Modifiers [1]

Figure 21 illustrates the effect that different products can have once full slip has been reached:

- Friction modifiers provide neutral friction creep characteristics [66]. In some countries a product which gives neutral creep characteristics are called high positive friction modifiers.
- Traction enhancers are used to increase adhesion in the contact especially when braking and display positive friction creep characteristics. These products are sometimes referred to as very high friction modifiers. These types of products are out of scope of this thesis.

2.4.4 Application, Amount Required and Carry-Down

Friction modifiers can be applied via trackside applicators or from train mounted systems [67] which are popular as no access to the tracks is required and the amount of friction modifier used can be more easily controlled. The solid stick versions are applied via a spring loaded device on the train and form a film on the wheel which is then transferred to the rail.

Trackside applicators as shown in Figure 22 are common with greases where ‘bulbs’ of grease are pushed up above the track to be picked up by a passing train. The problems associated with these are that the environmental conditions (temperature/humidity) could affect the bulbs, i.e., if it is too hot the grease just spreads around and the bulbs do not stand up to be picked up by the passing train. Also, as the tank of grease is by the track, there could be separation within the tank causing issues. Additionally different trains will have different contact on the rail so may miss the bulbs completely.

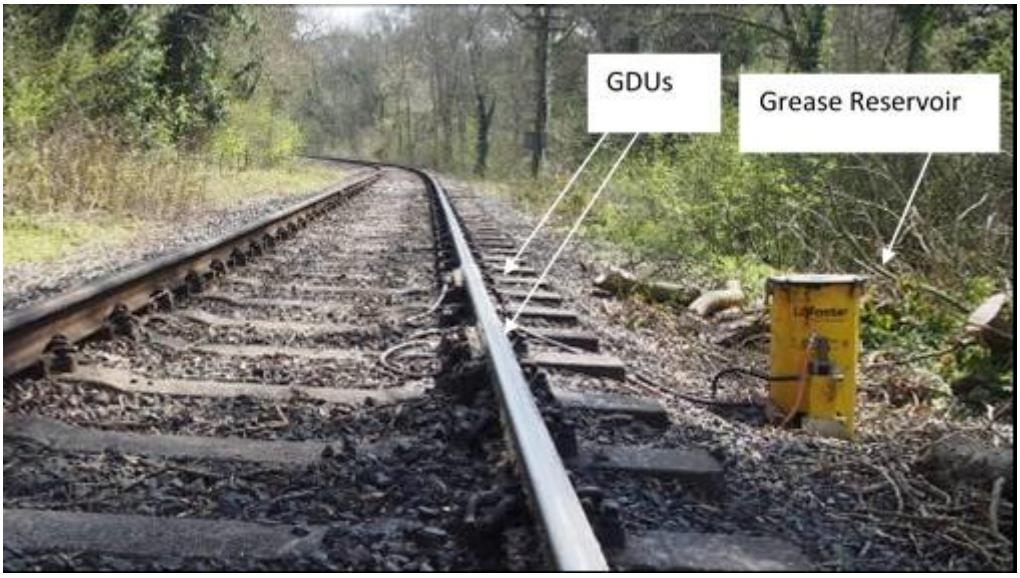

Figure 22- a typical wayside GDU [68]

Recent work using vehicle dynamics simulations [69] to predict the extent of wheel-rail relative displacement when running on a section of track, has shown that the wheels of some vehicles may not move close enough to the gauge face of the rail to pick-up grease from lubricators installed on straight sections of track. This is due to due to differences in vehicle suspensions and wheel profiles, and has been corroborated by measurements from vehicles in the field. This leads to a subsequent risk that the rail/flange contact on the following curves may not be adequately lubricated. Figure 23 compares the simulated movement of a wheel relative to the rail for two different vehicles, with different wheel profiles, running over two different pieces of straight track with different lateral alignment quality. The red and blue dotted lines indicate the amount of relative movement between the wheel and rail required for the wheel flange to pick-up grease from the lubricator GDU for the two different train types. The results show that, because of the higher wheel-rail conicity and stiffer yaw suspension, the wheels of the passenger vehicle (red line) exhibits very little movement relative to the centre of the track and are therefore unlikely to get close enough to the lubricator to pick-up grease from the GDU. On the other hand, the freight vehicle (blue line) shows much larger lateral movements and might, therefore, be expected to be better at picking up grease from lubricators located on straight sections of track. Figure 24 shows the difference between the two wheel profiles.

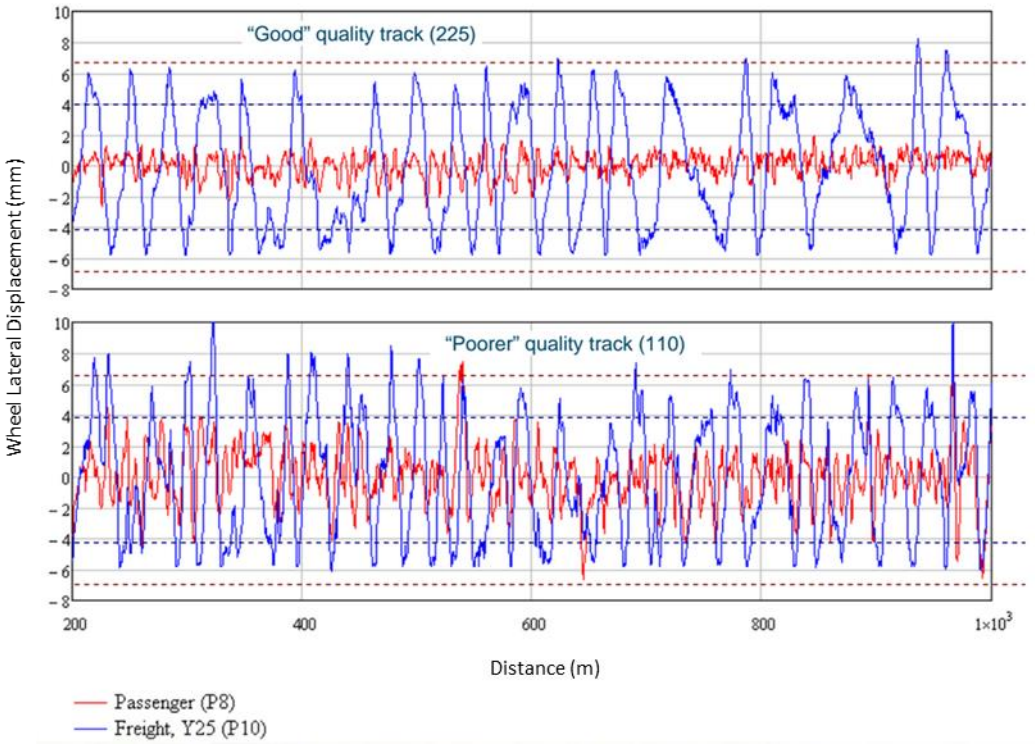

Figure 23- Predictions of wheel-rail lateral displacement for example freight and passenger vehicles on differing quality track, showing that the wheels of passenger vehicle with P8 wheel profiles exhibit much less lateral motion than a freight vehicle with P10 wheel profiles [69]

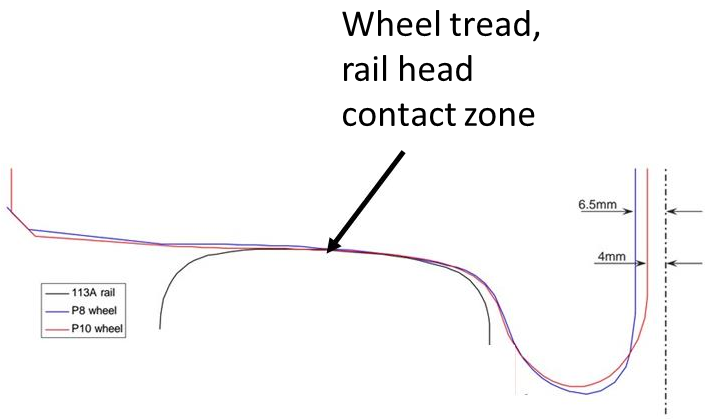

Figure 24- P8 and P10 wheel profiles [69]

Currently the practice of how best to deliver the friction modifier/lubricant to the contact is often based on experience and judgement rather than a theoretical basis supported with experimental evidence. This is starting to change as more experimental research is published and the industry seeks to optimise its processes.

A recent field test using a TOR lubricant [70] showed that the friction coefficient was highly dependent on the amount of lubricant applied and if too much is applied then the friction coefficient is too low for safe operation of the train. Additionally, if the amount of TOR lubricant applied is too little then the friction coefficient is again too low. This supports the

statement that TOR lubricants work in the mixed mode lubrication regime and that a very close control of application rates is necessary to obtain a desired friction level [54].

A Full-Scale Test Facility study which used Keltrack (a water based suspension) applied via a spray atomiser found that the FM applied every 250 wheel passes had the same effect as applying it every 50 passes, and applying it every 500 passes only had a partial effect compared to the dry conditions [71]. This conclusion supports the earlier field test conclusion that there is an optimum amount of FM and also showed that increasing application of FM beyond this limit has no benefit. This conclusion is further supported by a Japanese paper which looked at subway lines in Tokyo and twin roller tests [72]. This paper found that during twin roller tests there was no difference in creep characteristics after a 0.4 s spray and a 1.0 s spray whereas there was a difference when compared to a 0.2 s spray. The same paper made some observations based on a field trial. It concluded that both trains spraying friction modifier onto the low rail was the most effective configuration when changing between one or two trains spraying the modifier, and between spraying either rail or both.

A Scaled-Wheel Rig (SWR) to analyse pick-up and carry-down has been built at The University of Sheffield [68] as described in section 393.4. This research modelled how a grease bulb grows and looked at the difference between worn and new profile wheels. Testing also showed relationships between wheel displacement and mass of grease pick-up, and mass of grease pick-up with increasing pump output. Differences between different grease applicators is also analysed. This test rig has yet to be validated on full-scale rigs or in the field. However, if grease output and pick-up data is compared to simulated vehicle motion then positioning of applicators and its settings can be improved to ensure adequate lubrication.

Carry-down can be defined as the distance from application point over which the product is found to have a noticeable effect on the friction characteristics of the contact. Field testing has shown that a TOR material can produce a 35 % reduction in lateral force (with associated decrease in wear and RCF) at 2 miles down the track from the application point [73]. Additionally, carry-down is affected by the amount of FM applied. However, Eadie et al. [74] showed that there is an optimum amount beyond which increasing the amount of FM has no effect on the carry-down distance. In North American heavy haul railway's, TOR friction control is already well implemented [74]. This paper describes implementation strategies as well as noting that in one traffic direction there is little evidence of product carry. This leads to the conclusion that the product mainly remains on the wheelset rather than being continually transferred between wheel and rail.

Field studies in Australian heavy haul lines with grease have shown that longer applicator bars, by around 50 %, perform better and can achieve a 60 % increase in carry-down [75]. Additionally, less 'splash' of grease and hence less wastage was reported if the distance from outlet port to top of rail is reduced. Another recent study has looked at different types of lubricant and assessed their carry-down (called spread extent in the paper) as well as lateral force reduction and effect on braking [76]. Carry-down was assessed by measuring the friction level directly before applying lubricant, and then measuring the friction level at points down the track until the friction level returned to its pre-application level. It showed that the solid lubricant had significantly poorer carry compared to the oil, grease, and water-soluble lubricants. Interestingly, the amount of product used had no significant effect on carry-down. This paper also showed that the solid lubricant had the smallest effect on braking when the contact was dry, but when the contact is wet, the water soluble lubricant has the smallest effect

on braking. Similar research for TORFM has not been carried out and is currently an area where there is scope for new research.

Water based friction management products have been shown to be vaporised quicker in high contact temperature scenarios (high axle loads, hot weather, tight curves etc.) [77]. This research was carried out on a pin-on-disc machine, but the effect of this quicker vaporisation on performance, carry-down etc. has not been explored using conditions that are more realistic.

2.4.5 Applied Substances Tackiness

Tackiness is described as the ability of a product to form strings or threads [78]. It is often confused with adhesion which refers to the ability of the product to stick to a surface. Tackiness is important in the wheel-rail contact as a tackier product will form longer strings, enhancing product pick-up from the GDU to the wheel. Tackiness performance of a product can be improved by incorporating additives to it. Tackiness additives are often high molecular weight polymers, susceptible to breakdown by high shear rates [79].

The simplest method of determining tackiness is a finger test. A blob of a product is squeezed between finger and thumb and then this finger and thumb are pulled apart. A similar test using a spatula is shown in Figure 25. This is currently used at the end of a grease manufacturing line during quality assurance to determine if the grease is an acceptable tackiness. The results from this test are based on observation, "feel" and are qualitative. For quality assurance purposes, a more standardised and quantative measurement would be extremely beneficial and also allow comparison of different grease formulations.

Figure 25- Current tackiness test

A more sophisticated method of measuring the tackiness is an open siphon technique described in detail in "Lubricant Additives" [79]. This method measures the length of a formed string of grease, the longer the string, the tackier the grease. Another test method is an approach/retraction method [78]. This method has been validated with cone penetration tests by comparing the cohesiveness results and has shown good correlation between the two methods. It uses a measured force during retraction to calculate the energy required to break the product strings as a measure of tackiness. The final test method found uses a Capillary

Break-up Extensional Rheometer to measure the string formed during retraction of two discs [80]. The diameter of the strand is measured via a laser as a function of time.

Work carried out by Strasburger et al. [81] showed different forms of separation according to the force trace produced during the test as seen in Figure 26. The results were obtained using an approach-retraction method. There were clear differences in the traces depending on the type of separation. Initially, the separation is characterised by the flow of the liquid where the force rises to maximum and then decays to zero as seen in Figure 26a. After a threshold value, cavitation causes a rapid decrease in force after the maximum value before a sharp turn and decaying to zero as seen in Figure 26b. Figure 26c shows a transitional period trace where there is both cavitation separation and separation by flow. The reason given by Strasburger et al. [81] for cavitation causing the rapid decrease in force is that at peak force, the tension in the liquid is released by bubbles which grow and join together to form a cavity. The expansion of this cavity causing the break of the fluid layer and the rate of decay of the force is related to how quickly this cavity expands. Cavitation causes the rapid break of any grease strings formed and so lowers the measured tackiness.

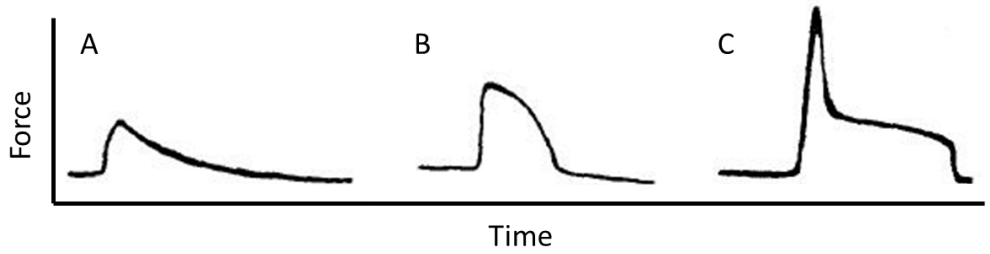

Figure 26- Typical force traces for approach-retraction experiment results. A) trace typical of separation by flow between two surfaces B) trace typical of transition region between flow separation and cavitation separation C) trace typical of separation by cavitation [81]

The polymer chains in greases must have the capacity to expand for a substance to be tacky and the important parameters governing tackiness are the molecular weight and the flexibility of the chains of molecules [79].

There is currently no one method that is universally accepted as a measure of tackiness. The only published research found describes the test methods rather than research into tackiness itself and focusses on oils. Therefore, there is a need for development of the current available test methods for other products to ensure they are reproducible and produce consistent results.

2.4.6 Testing Standards

Currently there is no testing standard for Top of Rail Friction Modifiers (TORFM) although the European Committee for Standardisation (CEN) are currently developing a standard to encompass all friction management products. BS EN 15427 [82] is a standard relating to application of flange lubricants, but there is no equivalent for application of friction modifiers. BS EN 16028 [83] is a standard for lubricants and within it, Annex L, there is a section for solid stick testing using twin-disc machine. This could be used for solid stick friction modifiers, although there is no mention of friction modifiers in the standard. There are also gaps in the standard. For example, there is no specification for pre-conditioning the discs or for cooling the discs during running. This means repeatability of results is hard to gain between different users using the same products and this standard.

There is a Network Rail standard which defines the minimum requirements for rail curve lubricants [84]. The standard details the properties of the lubricant as well as specifying two laboratory tests to analyse the lubricants pumpability and wear/retentivity properties. Although these tests and the minimum requirements are for curve lubricants, a similar process and testing philosophy could be applied to friction modifiers.

2.4.7 Effect on RCF and Wear

Greases can reduce wear rates in sharp curves by up to twenty times, this demonstrated the importance of effective flange lubrication [85].

Oil also has the same effect on RCF as water provided that there is enough time for the oil to seep into the crack. Additionally it has been shown that in the presence of water and oil mixtures the oil is dominant and traction coefficients are the same as having only oil present [55].

Friction modifiers primarily aim to reduce RCF and wear, therefore reducing maintenance requirements and improving safety. Friction modifiers achieve this reduction by improving steering in curves and hence, reduce lateral forces. A study using a full-scale wheel-rail rig showed that after a small initial increase in wear, rails applied with a FM had no further wear compared to dry tests which wear continued throughout the test [71]. The same study found no cracks after running the tests in the rails applied with FM, compared to the dry rails which had cracks visible to the naked eye after half the running distance of the tests. The same conclusions have been found by field testing using a heavy haulage line in China [86] and in America [87]. FM's have this effect as they reduce the coefficient of friction in the contact patch when compared to dry contact. This has means that the forces, and consequently the contact stresses also reduce which results in less plastic deformation.

Twin disc testing has shown that with gauge lubricants, increasing surface roughness decreases retentivity and decreasing retentivity leads to increases in wear [88]. It is thought these relationships are driven by crack pressurisation of the liquid lubricant and so TORFM should not have the same relationships once they have "dried", although there is currently no literature found which looks at this relationship with TORFM.

As RCF and wear has been shown to reduce when using a premium grade rail [89], [90] and using a FM reduces RCF and wear even further; optimising both of these parameters can produce very low wear rates and very little RCF.

2.4.8 Effect of the Third-Body Layer on Products

Understanding of the effects of the third-body layer on the performance of applied products is important as the rail will very rarely be clean in the field. A study on the effect of an artificially created oxide layer using a pin-on-disc and disc-on-disc apparatus concluded that a FM is still effective under a wide range of oxide contamination on the rail head [91]. The same study also looked at the effect of grease on the performance of FM. It determined that grease affected the FM by disturbing the film adhesion to the surface and reducing the friction level. However, it did show that there was still an increase in friction coefficient with a FM present and so displaying that the FM can cope with light grease contamination. This study was the only work found which looked at FM's interaction with other substances.

Another study using pin-on-disc looked at the temperature, humidity and oxide contamination on the performance of friction modifiers [92]. It showed that the humidity had an obvious effect on the retentivity and the friction levels of the FM. It also showed that the levels of oxide present made a difference as well.

Field observation has shown that the grease protects the rail by keeping the friction coefficient below 0.3 when it has evolved from a liquid product to a thin, transparent solid layer [85]. The composition of this layer is unknown, but is likely to be a mixture of whatever is present on the rail when the grease was applied.

2.4.9 Other Effects

Almost all the field studies reviewed [93]–[98] showed that a TORFM reduced the noise of a train on straight track and also in subsequent curves due to a reduction in roll-slip oscillations by reducing lateral/flanging forces. The studies also concluded that FMs are an effective method of reducing all forms of rail corrugation and in particular rutting. There have also been reports of reductions in low frequency vibrations observed when a FM is applied. This suggests that the benefits of applying friction modifiers extends beyond simply the wear and RCF and also applies to the whole industry rather than specific vehicle types. This is supported by an evaluation of field trials in Europe and Japan [99] which looked at a variety of studies on the effect of FM on short pitch corrugation growth. It concluded that the studies had included a large variety of contact conditions that showed a universal reduction in corrugation when FM was applied when compared to no FM present. This infers that the effect of FM is not limited to just one type of vehicle or configuration but its benefits are universal across the industry.

Fuel consumption of a train would be reduced due to reduced rolling and curve resistance when using a TORFM [73], [87]. One study has estimated that 81 litres of diesel could be saved with an application of 1 litre of a TOR lubricant [98], this figure was attained via scaling from a laboratory test and so it is unknown how accurate this figure is. A passenger would also feel a benefit due to a reduction in the noise and vibration of the vehicle they are travelling on. These benefits are also apparent with gauge face lubrication [85].

A field study of a passenger transit system showed no negative effects of friction modifiers on traction or braking [100]; however, it has been noted that one German railway experienced braking issues at some application sites with a TOR product [70], it is unknown if this was an TOR lubricant or TOR friction modifier.

Friction Modifiers have also been shown to have no negative effect on track isolation [101]; this study used a twin disc tester and static test and neither showed a difference in measured impedance during the application of a FM. This is important as introducing new materials into the industry can cause questions about safe running of the trains and so the lack of effect of the FM on impedance is a positive factor.

Applied products have been shown to reduce the number of coarse particles into the air by up to 95 % depending on which product is used [77] due to a shift from dry contact to boundary lubrication, as well as some particles becoming trapped in the product. Grease and TOR lubricant were shown to also decrease ultrafine particles, but water based FM increased the levels of ultrafine particles. These tests were carried out on a pin-on-disc machine which is not wholly representative of wheel-rail contact, further tests should be carried out to confirm these conclusions.

2.4.10 Modelling of Effects

One of the easiest ways of modelling the effects would be to use the Tγ approach (as detailed in section 2.2.2). As mentioned previously this approach relies on wear coefficients from experimental data which at the moment is limited for applied products. One paper which has produced friction modifier wear data [102] has published data for both small-scale twin disc testing and full-scale rig tests.

Modelling the effects of friction modifiers on contact conditions is important when carrying out rail vehicle dynamic simulations. An evaluation of the NUCARS computer programme for simulating the effect of FM has been carried out [39]. NUCARS allows the user to specify a percentage of Kalker coefficient which best applies to their FM/lubricant characteristics. However, as creepage/force characteristics are difficult to obtain in the field due to current portable tribometers not producing reliable data, and the results of the simulation being very dependent on the Kalker, coefficient the results of the simulations cannot currently be trusted.

Within the other models discussed earlier in section 2.3, the ECF and CONTACT models have the capability to model the effects of friction modifiers. CONTACT's ability to include a third-body layer is a recent development and therefore there is currently no research which validates how well the model predicts the effect of the third-body layer on the wheel-rail contact. The ECF has High Pressure Torsion (HPT) tests built into the inputs to characterise the behaviour of the third-body layer [37] and has been shown to increase the prediction quality when compared to other creep force models [34].

2.5 Field Measurement Techniques

It is difficult to get a measurement of the relative wheel-rail position in the field or what contaminants are present on the track. One way would be to use an instrumented train, however the cost and logistics are usually prohibitive to use in a field trial. One way to find where the wheel-rail contact is to spray the rail with paint before the train passes. Where the paint is worn away after a train passing is where the contact has occurred. A measure of the actual wheel-rail contact has been made in the lab using ultrasound [103], however this has not been used in the field to date.

To detect the presence of grease there are a couple of methods that have been used. Glitter has been mixed into a grease reservoir which over time gets carried down the track [104]. Wiping your finger on the track can also be used to detect if grease is present [75]. Neither method provides a friction measurement or a quantitative measure of the amount of grease present. A recent study [105] has used the longitudinal vibration in the rail to measure the presence of grease. In this study, a lubricator was switched off and the vibration measured over time. It found that the 400-1000 Hz frequency range increased in amplitude as time increase and the grease was consumed. Measuring the ration between lateral and vertical loads (L/V) has also been used in field studies [76], [106]. The reduction in L/V can be up to 60 % with the presence of curve lubrication.

To measure friction there are two different devices that are commonly used. A pendulum rig (Figure 28) is described further in Section 3.1. The exact coefficient of friction levels the pendulum gives will not be replicated in the wheel-rail contact. This is because the pendulum measure the friction between a rubber specimen and the rail instead of a steel-steel contact. It can be used as a comparative measure, i.e. dry vs greased etc. A hand pushed tribometer can

also give a friction measurement. This uses a small wheel pushed against the rail to give a COF measurement. Again the absolute values will differ due to differences between the wheel used in the tribometer and the loads/speeds of a train. However, it has been used in many field tests [40], [75], [107] and as with the pendulum, it can detect a change in COF.

2.6 Grading of Research

In order to gauge the current status of research in this area, a grading system has been created scoring each reference according to a set of criteria. This methodology has been used before in industry reports [28]. It is important to note that the criteria focusses on the research's validation and scaling from laboratory to the field, rather than a fundamental assessment of the research. Review papers and textbooks have not been included in this evaluation. This review is focussed on friction management in the rail industry rather than all rail research. The seven criteria are:

- *Peer reviewed publication.* This determines if the research has been accepted by the author's peers.
- *Conclusions evidence in paper.* This determines if the conclusions in the paper is supported by results within the research.
- *Theory supported by testing.* This determines if the theory presented is supported by testing or modelling.
- *Testing supported by modelling.* This determines if the testing carried out has been supported by models and vice versa.
- *Scale test.* This determines if the testing has been carried out on small-scale test rigs to simulate the contact and gain control over specific variables.
- *Full size test.* This determines if the testing has been carried out using a full-scale test rig to simulate the contact.
- *Real world measurements.* This determines if there has been testing carried out/measurements taken during live operation of the railways.

The research is marked against the criteria above and categorised into A, B or C. Category A research fulfils at least 70 % of the criteria, category B research fulfils at least 45 % of the criteria and Category C research fulfils less than 45 % of the criteria. Each reference is also assigned a primary and secondary group according to the main focus of the research:

- *Wheel-rail contact* covers dry contact research. The *modelling* section covers research which deals with modelling of the wheel-rail contact and the *tribological effect* section covers research that has looked at the tribology of the contact using physical testing
- *Traction enhancers* covers all research which has focussed on traction enhancers such as sand or traction gels. This category is further split into *modelling, practical considerations* (covers such things as track isolation, pick-up of product, carry-down of product) and *product performance* (covers such things as retentivity, RCF and wear damage, friction performance etc.)
- *Friction modifiers* covers all research which has focussed on friction modifiers. This category is also further split into *modelling, practical consideration* and *product performance*
- *Grease/lubricant* covers all research which has focussed on greases or lubricants. This category is also further split into *modelling, practical consideration* and *product performance*

- *Contaminants* covers all research which focusses other things that effect the wheel-rail contact and aren't covered in the above categories. These things include oxide layers, leaves, oil etc. This category is further split into *tribological effect* and *modelling*

Clearly this procedure will differentiate the well validated (using a number of different test scales) research, from research which has only been carried out on one test scale and could be an area for future work. A paper which is in a peer reviewed journal, presents conclusions supported by evidence in the paper, puts forward theory that is supported by modelling, includes a scaled test, a full-scale test and real world measurements would give industry confidence that the conclusions of the paper are accurate. Whereas a paper which only uses a scaled test to support a theory is less robust. It should be reiterated that research is categorised according to the criteria detailed above and is not a criticism of the research in general.

The full table detailing the grading of each individual reference is included in Appendix A. The chart displaying the results of the grading is shown in Figure 27. It is important to note that this paper has focussed mainly on contaminants and applied products, so there is a large body of research on dry wheel-rail contact that is not included here. It is immediately obvious that most of the research is in category B with only four of the papers assessed being given category C. This is mainly due to only one scale of testing or one method used in each assessed piece of research. The research that is categorised A is mainly because it has used other scales or modelling to support the initial findings of the research. The small number of category A research illustrates that there is a lot of work to do to relate lab work to the field and vice versa. There are also a comparatively large number of papers that focus on modelling of the wheel-rail contact, but the modelling of contaminants or applied products is an area where there is a large gap in the research found. This is thought to be due to the complexity of including a third-body into the modelled contact and the associated computing cost involved.

For TORFM, the research to date has mainly focussed on the performance of the products. Although more recently research has started to be published which focusses on the practical considerations involved. This is still an area where more work could be done to ensure the full benefits of these products are realised. Additionally, due to the number of different product philosophies (as discussed in section 2.4.2 above) there seems to be very little understanding of the fundamental properties behind how each of the different products work and produce the benefits described in the literature. Looking at Figure 27, it appears as though there are more papers that concentrate on friction modifiers compared to other products. This is also due to the variety in products called friction modifiers. This means there is more scope for research as the variation in products that work in different ways, requires more work to fully understand how the products function, and the benefits they bring. This can be compared to traction enhancers/lubricants which have a set of standards that any new form of these types of products must meet in order to be used on the rail network.

Figure 27- Summary of grading of research

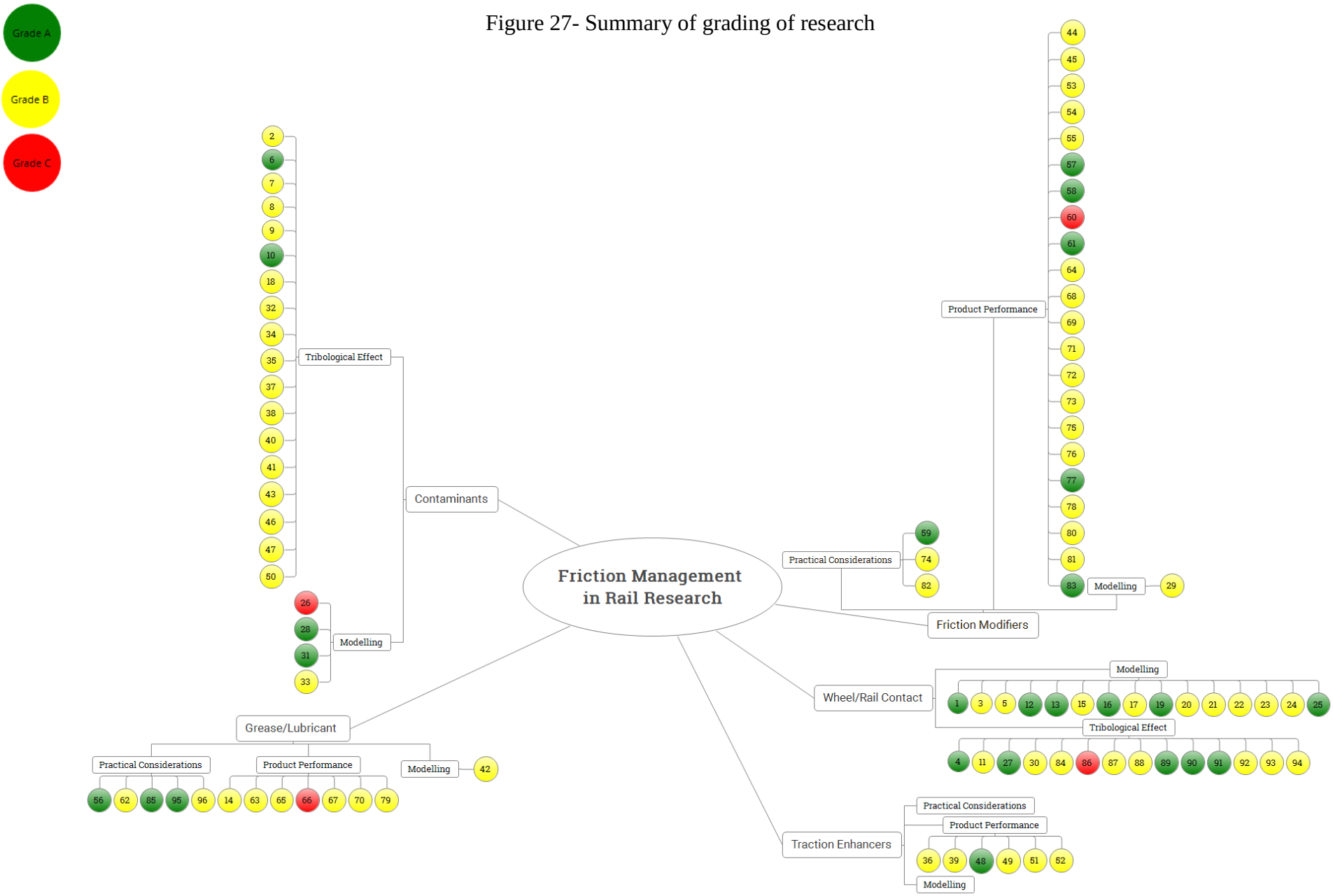

2.7 Summary

A recent report by a Vehicle Track Systems Interface Committee (VT/SIC) [108] highlighted that an optimised coefficient of friction was a positive area of development and could start by better understanding the conditions within the contact patch. The areas that affect this behaviour are many and include third-body layers, temperature and relationships between regions of stick and slip in the contact. The findings in the report are supported by the analysis of the quality of research in the previous sections which has highlighted that much of the research is of 'average' quality, and that there is less research into the practical considerations of the products.

One criticism of the much of the academic literature on the subject of friction modifiers is that there are not many research studies which focus on how much product is required or where to apply it to achieve the benefits that much of the research has found. The main benefits of reducing RCF and wear as well as the secondary benefits of reducing noise and vibration are well documented; however, there are significant gaps in knowledge when trying to understand the behaviour of the friction modifier for use in the field. For example, understanding how far down the track the effects of applying the product lasts for is an important consideration when attempting to choose where and how often to apply a product. Another important consideration is the effect of contamination of the friction modifier. This review has only found one paper which looked at the interaction of FM with grease, but research looking at other forms of contamination such as sand or the interaction with different oxide layers is currently lacking. The most recent papers do start to tackle these issues, which shows that the academic research is starting to focus on the gaps in knowledge. Friction modifiers is a term applied to many different products that are fundamentally different and work in different ways. This has led to confusion and some papers claim to report results for friction modifiers when in fact the product that is tested is actually a top of rail lubricant. Recent publications [54] have attempted to clarify this issue and it is hoped that in the future the industry will have a clearer understanding of the different products and how they function.

How the different scales of testing compare to field conditions is another area which there is scope for more research. If the relationship between the different scales is fully understood then it would help answer the questions in the previous paragraph as the representative, smaller, faster, cheaper tests can be carried out to ascertain certain factors and focus the more expensive, slower testing scales. This research into scaling would also help with the development of testing standards (there are currently no standards for how TORFM should behave, although CEN is currently working on developing them).

From the evidence presented in this review there are a number of areas to focus further research on:

- Assessment of fundamental product properties and how they relate to product performance
- Bench mark tests to assess performance based on available test platforms across a range of scales
- Develop new test methods to assess product properties and product application in the field
- Understand the transferability of laboratory results to the actual, real world contact and between different laboratory test scales

By linking these areas of research together, a suite of new laboratory test methods that are validated against full-scale and real world data have been developed. This means that there are simple, quick tests available that give reliable indicators on real world performance. This leads to an improvement in overall efficiency of the railway industry as research into different operating scenarios/friction management products and equipment, can be performed quickly and easily in the laboratory. This can lead to bespoke and optimised products, application amounts and condition monitoring systems for each operating scenario.

3 Test Capability and Scales

There are many different scales of testing in order to analyse the wheel-rail contact ranging from simple table top tribometers to field testing. Choosing the appropriate test methodology is a trade-off between many factors including cost, complexity and control. It is usually the case that the simple test rigs are able to give results from specimens reasonably cheaply and quickly compared to more complex methods at the expense of accurately portraying the system being analysed. Increasing the complexity of the test methodology to representative test conditions not only leads to the increase in costs and time, but control over the individual parameters being investigated is lost, introducing a source of error into the investigation. Using real rail material cut out to form specimens to put into smaller test rigs is one way of being able to compare full-scale field tests to small-scale laboratory experiments [23]. The main differences between the different scales often comes from the difference in environmental control.

An example of how different test scales can interact is a study that attempted to correlate ball-on-disc with full-scale rail performance tests using the Transportation Technology Centre Inc. (TTCI) test track loop [109]. One of the issues faced was that the wear data was reported using different units (depth of wear track for ball-on-disc and total area loss for full-scale test), once this was overcome by getting the wear data from ball-on-disc experiments in total area loss the two sets of data could be compared. It showed that there was a good correlation between the two scales with the ball-on-disc providing a pre-screening of rail performance to select the best materials to take forward to full-scale test.

Studies have started to look at the differences between the different scales used when evaluating rail contact conditions. It has been shown in a small study that there is a reasonable correlation between small-scale and full-scale results [23], [102]. Different scales of test rigs were compared using modified wear number approach (see section 2.2.2 for more details on wear number) [102]. The wear number was divided by the contact area to allow the different scales to be compared and results plotted on the same graph.

Full-scale tests and twin disc tests have been shown to provide the same performance ranking of different greases [85]. This shows that even if the exact values are different, the small-scale tests do provide useful qualitative data. Other studies have also found that whilst the same trends are observed the exact values can differ greatly between full-scale tests and actual field trials [90]; this could mainly be due to the lack of control over what is on the rail in field trails. It has been noted in one study [71] that the FM used was seen to build up on the test rail, something which has not been noted from field observations. This illustrates the difference between carrying out a test on the same short section of rail at similar contact and environmental conditions compared to what actually occurs in the field.

Adhesion levels in twin disc testing are within the range that are known to occur in the field as seen in Table 1 [14]. This shows that this approach is suitable to compare adhesion levels for a variety of conditions. Conversely, twin-disc tests involving contaminants, for example sand, are often more severe cases then would be met in real application. This is due to the contaminant being more easily entrained into the contact as there is no surrounding air current, and the point of application is much closer to the contact [102]. This means that these sort of tests are only really useful as qualitive tests between different contaminants/products rather than investigation into real application values.

Author	Test Apparatus	Load (kN)	Rolling Speed (km/h)	Test Condition	Peak μ	Slip at Peak μ (%)	Stable μ (5% Slip)
Zhang et al. [110]	Full-Scale Test Facility	44	10-70	Dry	0.5-0.57	2	0.5-0.57
		67	10-70	Dry	0.44-0.55	1-2	0.44-0.52
		44	120-240	Wet	0.07-0.13	0.5-1	0.065-0.12
		67	80-240	Wet	0.05-0.11	0.5-1	0.05-0.105
		67	140-300	Oil	0.045-0.055	1	0.044-0.052
Jin et al. [111]	Full-Scale Test Facility	135	140-300	Oil	0.04-0.05	1	0.037-0.048
Harrison et al. [40]	Push tribometer	Unknown	Unknown	Dry	0.52	1	0.5
				Dry	0.7	2-5	0.7
Nagase [112]	Instrumented bogie on test vehicle	Variable	Variable	"Dry"	0.2-0.4	Unknown	Unknown
				Wet	0.05-0.2		
				Oil	0.05-0.07		
				Leaves	0.025-0.10		
E. A. Gallardo-Hernandez and R. Lewis [14]	Twin-disc	7.7	3.54	Dry	0.6	2	0.54
				Wet	0.2	1	0.17
				Oil	0.07	1	0.06

Table 1- Table showing comparison of traction coefficients derived by a variety of test methods [14]

Table 2 shows some of the different test scales available at The University of Sheffield to highlight the advantages and disadvantages of different scales.

Test Rig	Advantages/Disadvantages
Bruker Universal Mechanical Tester (UMT) (ball-on-disc or pin-on-disc)	Small, simple machine Environment can be controlled Not realistic contact geometry Ball is not same material as would be used
High Pressure Torsion	Realistic normal stresses in contact Applies torque to rotate specimens relative to each other. Not realistic contact geometry
Plint TE54 mini traction machine (ball-on-disc or twin-disc)	More realistic contact as both the ball and the discs are being driven Ball is not same material as would be found on the railway
SUROS- twin-disc test machine	More realistic contact as both test pieces are being driven Can use realistic materials for both discs
Scaled- Wheel Rig (SWR)	Real rail and GDU Scaled wheel Simple to use Pure rolling contact only No speed control
Full- Scale Test Facility (FSTF)	Realistic contact geometry and loads as using real wheels and rails Same section of wheel and rail run on each pass so effects such as carry-downand retentivity difficult to measure Longer test runs then previous test rigs due to need to lift, rotate and move the wheel-rail back to starting positions

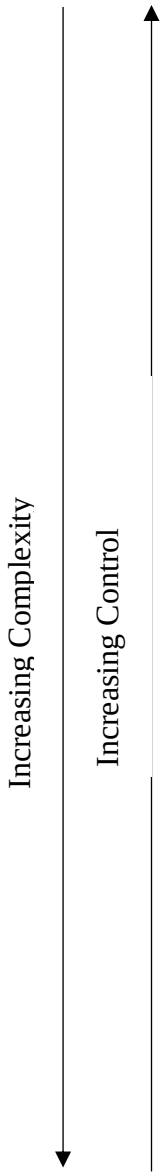

Table 2- Different test scales available at The University of Sheffield

3.1 Pendulum

The pendulum rig (as shown in Figure 28) was original designed to measure the friction between car tyres and roads and also between a shoe and the floor. It works on an energy loss principle. A swinging arm with a rubber plate attached to the end contacts the surface and pushes a needle up a scale. The higher up the needle is pushed the lower the Pendulum Test Value (PTV) and smaller the coefficient of friction. This is because it has lost less energy during contact with the test surface than a test where the arm doesn't reach as high on the scale. The coefficient of friction in this test is found using Equation 2 [113]. This empirical relationship is due to the rubber test specimen being spring loaded.

$$\mu = \left(\frac{110}{PTV} - \frac{1}{3}\right)^{-1} \quad (2)$$

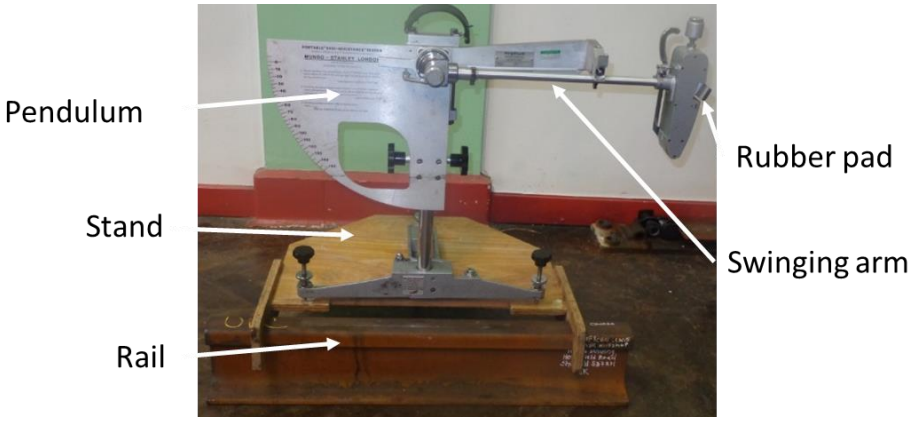

Figure 28-Pendulum test setup in the lab

The pendulum is simple, easy to use and portable. This makes it ideal for measuring different conditions. The friction measurement is from a pure sliding, rubber on steel contact. This means that the exact friction coefficient would not be replicated in a wheel-rail contact. However, the relationships derived would still be valid so allow comparison between conditions/locations.

3.2 Bruker Universal Mechanical Tester (UMT)

A Bruker UMT TriboLab is a modular tribometer that can be configured to perform many different tribological tests. The tribometer mainly consists of an upper drive, lower drive and load cell. The upper drive can move in all three axes and at different rates. Different sized balls or pins can be attached to the upper drive depending on desired application. The lower drive can be either a linear or rotary depending on the type of motion desired. The load is applied vertically and can be varied (1 mN to 1 kN) depending on load cell used. The humidity/temperature can also be controlled using an environment chamber module.

It can be configured in ball-on-disc or pin-on-disc configuration. Neither configuration is ideal for simulating the wheel-rail contact. This is because pin-on-disc is a pure sliding contact and the pin will wear throughout the test, changing the contact pressure making it difficult to control the contact conditions. Ball-on-disc is also not ideal as the ball is usually made from a different steel and so the material behaviour is different. The modular and small-scale nature of the UMT means that it is ideal for testing lots of different conditions quickly to influence larger scale, more representative tests. The UMT is controlled by creating a test script, defining the parameters which the computer then implements when the script is run.

3.3 Sheffield University Rolling and Sliding (SUROS)

The University of Sheffield Rolling and Sliding (SUROS) machine is a twin disc tester capable of carrying out a variety of tests [114], for example the rig can develop an entire creep curve automatically [115]. Figure 29 shows the test rig which is based on a Colchester lathe fitted with an AC motor to provide rotation to each of the discs individually. Load is applied via a hydraulic actuator and friction measured on the lathe side shaft via a torque transducer. Figure 30 shows the dimensions of the discs typically used and how they are machined out of real wheel and rail steel.

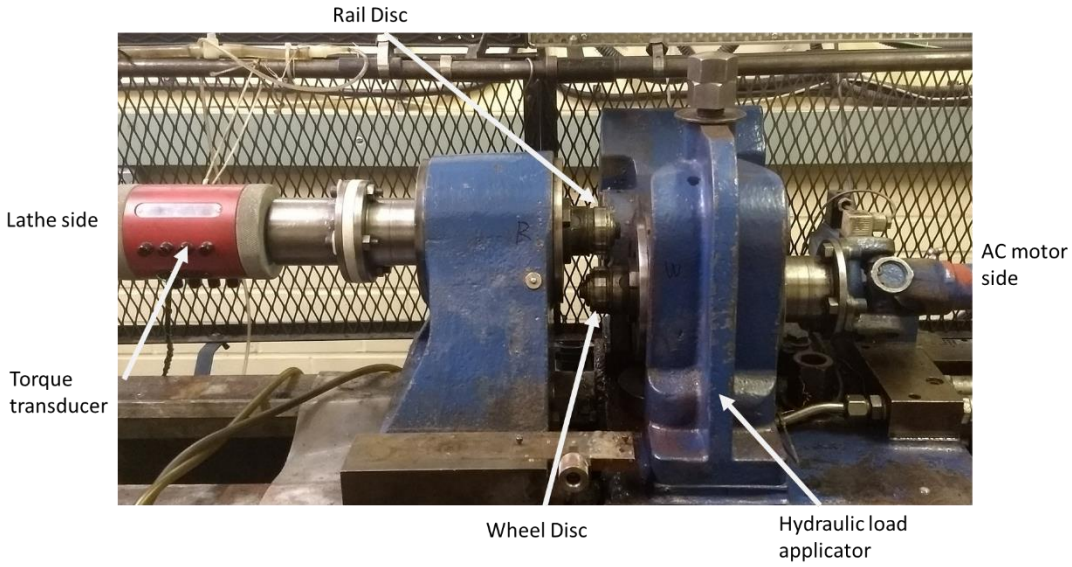

Figure 29- Photograph of SUROS test area

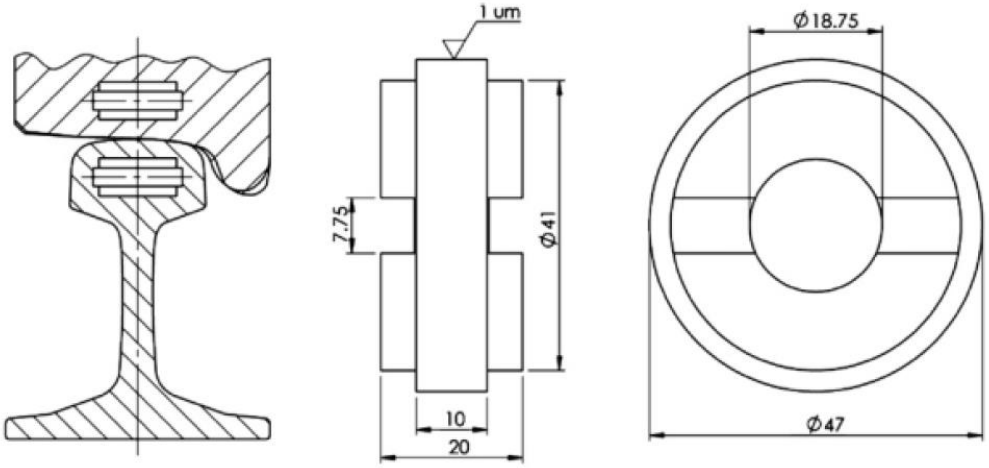

Figure 30- Dimensions of SUROS disc

SUROS can generate contact pressures equivalent to actual wheel-rail contact conditions (although the contact shape is different). The speed of each disc can be varied to produce the desired slip ratio (the ratio between the speed of the rail disc and the speed of the wheel disc). The nominal surface speed is approximately 1 m/s which is slow for a train but this is considerably faster than the larger scale test rigs. Different contaminants/products can be applied to the surface of the discs if desired.

3.4 Scaled- Wheel Rig (SWR) with Lubrication Equipment

A bespoke rig designed for pick-up assessment (from [104]) was used in the work (see Figure 31), with some adaptation to improve operation and adjustment. A reduced diameter wheel is mounted on a trolley, which is mounted on a T-section bar to provide parallel controlled motion, with the tread of the wheel thus rolling along a section of real rail inclined at 1:20. The trolley is in two parts, the lower with roller bearings interfacing with the bar and the upper part able to be adjusted to set the wheel position laterally with respect to the rail. The neutral position of the wheel is found from analysing standard track gauge and wheelset back-to-back

measurements for the GB network; the distance from wheel flange back to rail gauge face is 37.5 mm (Figure 32). The size of the wheel was determined (approximately 1/5 scale, 180 mm diameter) so that it was large enough that the circumference was longer than the grease applicator bar and the length of rail was sufficient to allow the wheel to pass the applicator bar. The wheel profile used was that of a new P8 profile [116], commonly used for passenger rolling stock in Great Britain. For this test rig, the wheel-rail surface contact is in pure rolling and there is no speed control, slip or angle of attack applied.

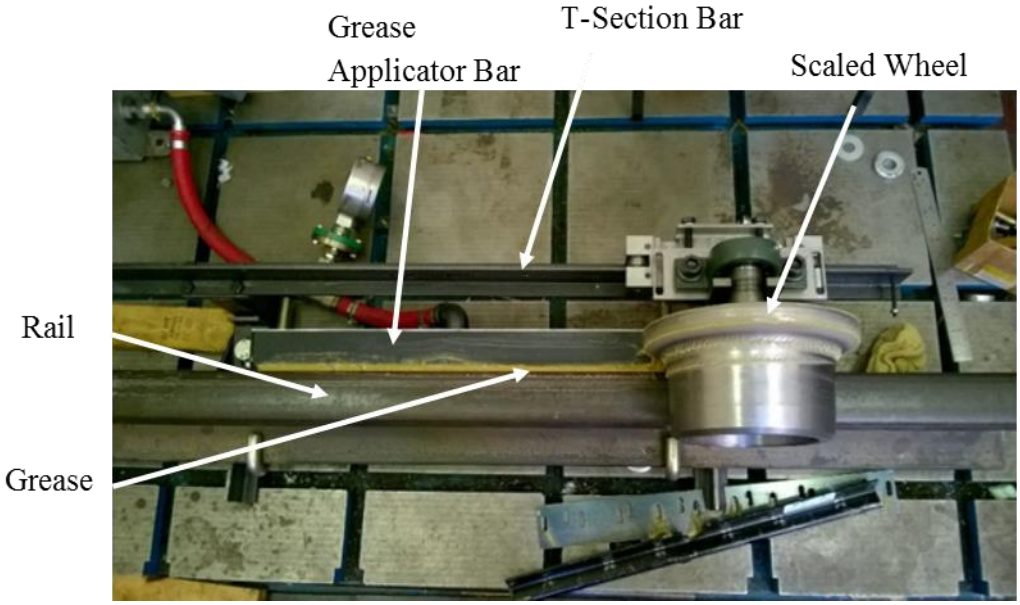

Figure 31- Plan view of SWR

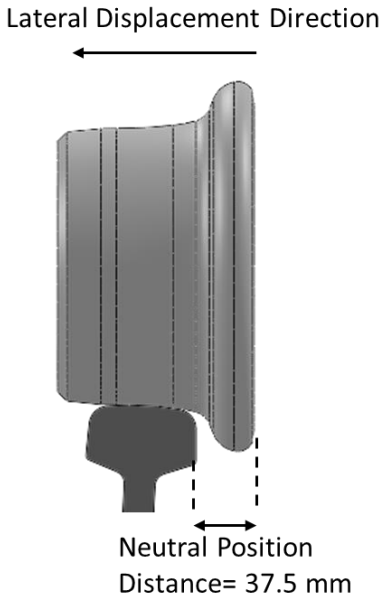

Figure 32- Neutral position diagram

A L.B. Foster supplied Protector IV lubricator cabinet with pump, motor and controller was used to control grease supply during the experiments. Any GDU can be fitted to the rail. Two examples supplied by L.B. Foster are: the standard MC4 (Figure 33) is a bar type GDU with 18 outlet ports, through which grease is pumped forming separate bulbs which are available to

be picked up by passing wheels. The second variant is of the same base design, but is supplemented by the patented GreaseGuide™ (GG) (Figure 34). This additional element comprises a foam pad which forms a ledge alongside the bar. Both GDU's can be mounted at different heights.

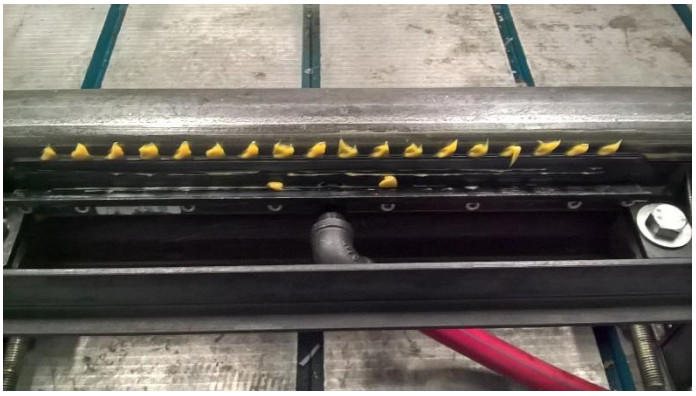

Figure 33- MC4 GDU

Figure 34- MC4-GG GDU

This set-up is easy to use and allows the interaction between the wheel and different GDU's to be studied. The main disadvantages are that there is no load or speed control on the rig.

3.5 Full-Scale Test Facility (FSTF)

The Full-Scale Test Facility (FSTF) is a full size fixed-axle-location P8 profiled wheel that is loaded against a section of rail which slides on a slide bed as seen in Figure 35. Normal load, slip and rail velocity are controlled by three separate actuators (labelled 1, 2 and 3 in Figure 36 respectively). Normal load is applied vertically above the wheel, rail velocity is controlled by moving the slide bed and slip is applied via a chain attached to the rim of the wheel that moves at a set velocity relative to the slide bed.

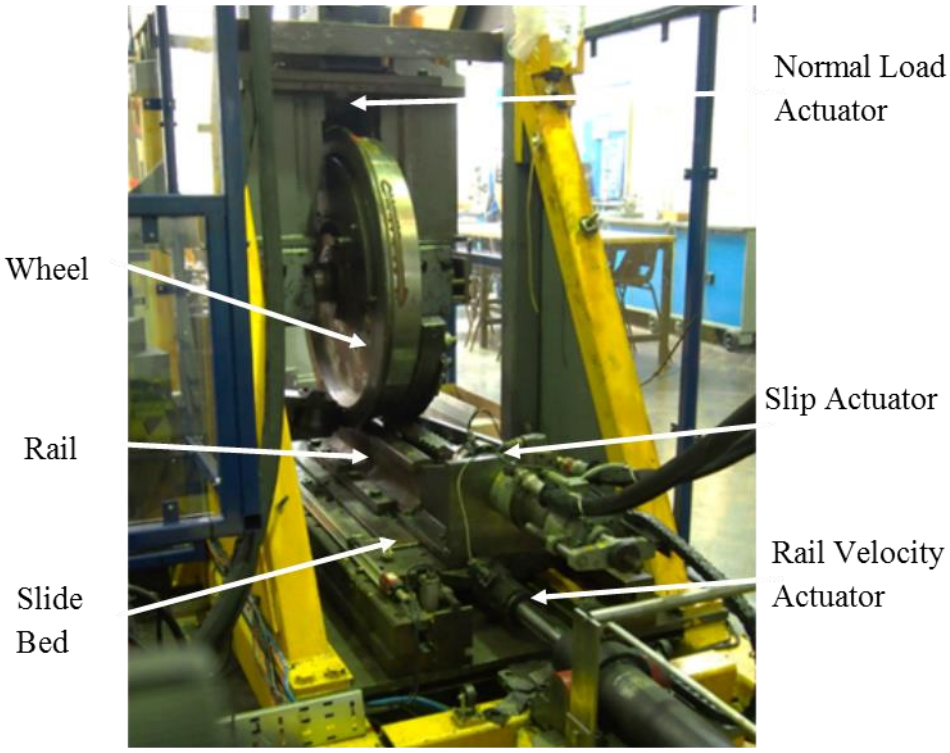

Figure 35- Full-Scale Test Facility (FSTF)

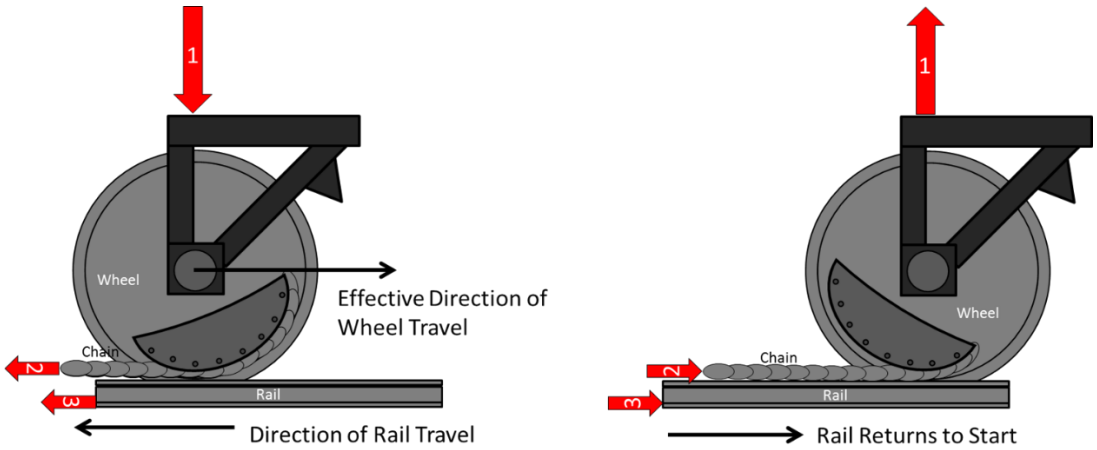

Figure 36- FSTF schematic

This rig allows actual contact pressures similar to a real wheel-rail contact to be achieved as well as controlling the slip values and providing the actual geometry. This means that it is ideal for controlled testing that cannot be carried out in the field. The main disadvantage to the FSTF is that the slide bed only moves at a maximum of 100 mm/s, which is significantly slower than in field operation.

3.6 Field Testing

Field testing means any testing which uses a real train and rail track. This can be at a dedicated test loop/closed section of track or taking measurements as trains that are in service pass by. Field testing can be extremely costly (both in terms of time and money) compared to laboratory testing and the complexity of the system means that it can be difficult to isolate the conditions being tested. However, it is vital that the conditions in the field are understood to ensure

laboratory tests are replicating the right conditions or the limitations of the laboratory testing are understood. Some of the key variables that laboratory testing must take account of are contact pressure, slip, speed, rail/wheel materials and surface condition (roughness, oxides etc.). Not all of The limitations that affect all laboratory testing when trying to replicate field conditions are:

- The same "wheel" contacts the same section of "rail" whereas in the field a wheel travels down a long section of "fresh" track. This has an effect on the surface condition as well as the temperature of the contact. High temperature can build up due to the cyclic reloading of the test specimens and lack of heat transfer away from the contact (particularly twin-disc testing). Additionally the use of one 'wheel' means that there is no steering forces acting in the rigs as there would be in the field as the wheelset self-steers during curving.
- The contact point and load is always the same, whereas in the field different profiled wheels in a variety of worn conditions with different axle loads run on the same track.
- The longitudinal forces provided by a train's traction system during acceleration and braking will change the contact stresses, influencing the wear.
- The environment within the laboratory is relatively constant when compared to normal track conditions which can vary greatly in time and location.
- Contamination of the wheel and rail, for example by leaves, ballast dust etc., does not take place in the laboratory but can be artificially introduced to the contact to analyse their effect.

Field testing can also be used once laboratory tests have been completed to validate and prove that any benefit shown in laboratory tests is replicated in real life, minimising the amount of testing required. Figure 37 shows a flow chart of an ideal test procedure. Ideally, there would be an initial field measurement phase to understand fully the conditions of the system to be tested. Then laboratory tests at different scales can be carried out (starting at small-scale test rigs and working upwards). Modelling can also be used to help validate laboratory tests as well as define future tests. Finally, field testing can be carried out to prove the laboratory results. This procedure means that industry can be confident that a benefit shown in the laboratory can be achieved in real life. This is because the different test scales and modelling will all have different limitations so by using different scales, all of the limitations mentioned in the previous paragraph can be mitigated.

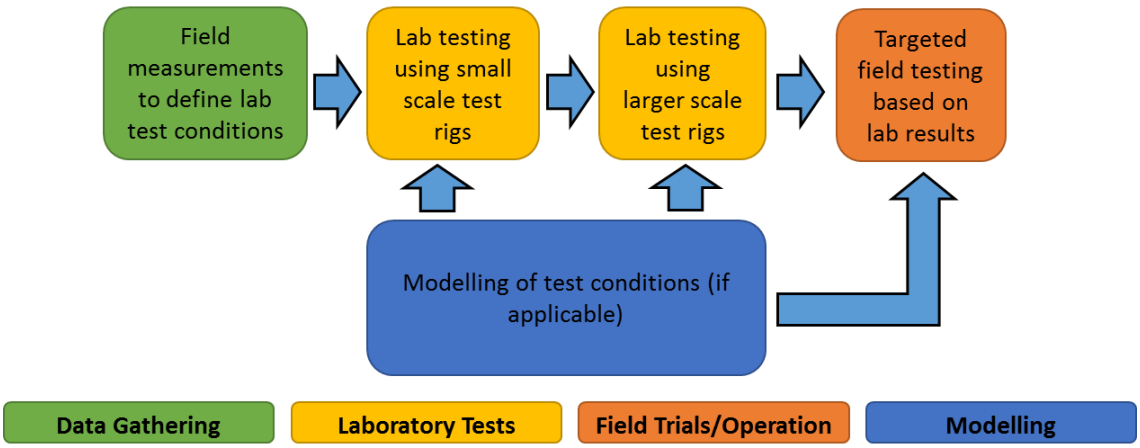

Figure 37- Flow chart of ideal test procedure

4 Grease Distribution Unit Operation

There is a large variety of greases available, all with various properties depending on the desired application. Greases are made up of a base oil, a thickener (to solidify the oil), and additives (to provide targeted properties). They are used to lubricate curves, as an oil on its own would not stay in position between different train passes. Under high shear loads the viscosity of the grease decreases to a similar viscosity as the base oil, providing the required lubrication. The grease used in all the laboratory tests is designed for use in trackside lubricators and approved for use on the UK network by Network Rail.

Understanding how the lubrication equipment works in the field is vital to designing representative laboratory tests. The relative position of the wheel and rail as a train travels through a lubricator site is an important parameter in determining how grease is picked-up by the wheel, and carried-down into subsequent curves.

Grease bulbs produced in the laboratory using a Grease Distribution Unit (GDU) were compared to bulb measurements undertaken by Network Rail and L.B. Foster in the field. Variations along the grease bar in the laboratory are also analysed. This was to ensure that the grease bulbs produced in the laboratory are of similar size and shape to bulbs commonly found in field operation. In the field, the grease will be subjected to different temperatures as the seasons change. To understand what effect this has on the grease a pumpability test was carried out at different temperatures.

4.1 Test Methodology

4.1.1 Laboratory Equipment

To get an accurate measurement of the distance between the wheel flange and gauge face, a bulb of putty is attached to the rail. The Full-Scale Test Facility (section 3.5) was used to carry out a trial run to find: the best shape to make the bulb, to ensure it does not interfere with the wheel-rail contact, and to make sure the bulb remains attached to the rail.

4.1.2 Field Measurements

A location at the Severn Valley Railway (SVR) was chosen as the lubricators were working well (no blocked ports) and the speed of the trains is relatively constant. The site is halfway between Bewdley and Arley near to Trimpley reservoir as shown in Figure 38. The site consists of one track with two-way traffic. The GDU (Figure 39) consists of two MC4 grease applicator bars supplied with grease from a grease tank next to the track. The lubricators are installed in straight track before a curve, thus relying on the wheel flange moving laterally enough to pick-up grease from the lubricator site and carry it into the curve.

To see how the wheel picks-up grease from the GDU, a camera was installed that records video as the train travels over it (Figure 39). A light was installed next to the camera to help produce a better image. Adhesive putty was attached to the rail before and after a lubricator so that the actual distance between the rail gauge face and wheel flange can be measured.

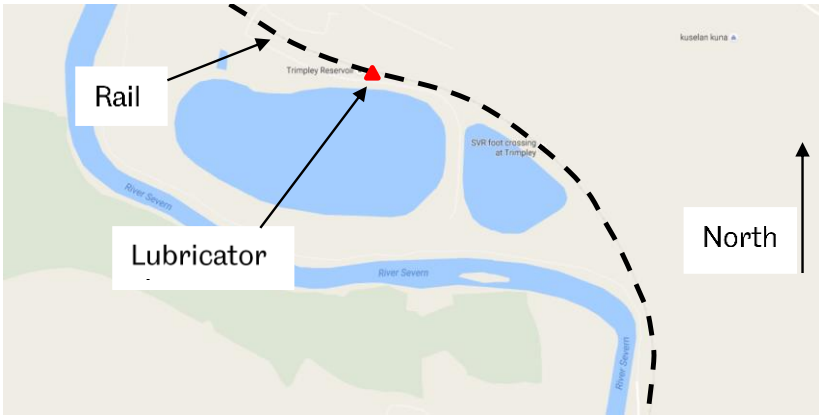

Figure 38- Location of measurement site

Figure 39- Test set-up

4.1.3 Grease Bulb Measurement

The test equipment described in 3.4 was used in the laboratory to produce grease bulbs. Previous work done at The University of Sheffield [117] used a procedure to gain a steady state amount of grease on the GDU. This procedure involved pumping the grease for 0.3 s and rolling the wheel along the rail at a lateral displacement of 8.5 mm. This was repeated three times. The amount of grease left on the GDU after three passes was compared to after more than three passes and no difference was found. The grease bulbs at port numbers 1, 5, 9, 14, and 18 were measured using the following sequence:

- Prepare GDU with grease bulbs
- Insert graph paper (cut to rail profile) into bulb (as shown in Figure 40)
- Draw around the grease bulb
- Remove graph paper and scan into computer
- Use ImageJ analysis software to measure the grease bulb depth at 1.5 mm height intervals

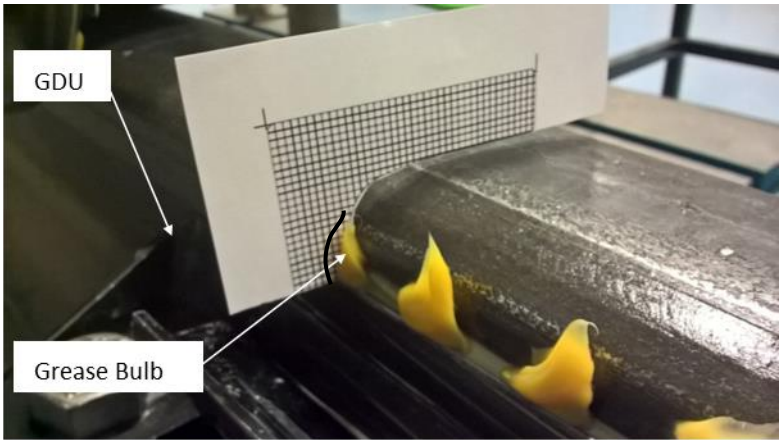

Figure 40- Measuring the size of the grease bulb in the laboratory

4.1.4 Grease Pumpability

To investigate what effect variations of temperature will have on the grease bulbs the standard MC4-GDU was put into an environment chamber. The pump cabinet was too large to fit into the chamber so a standard hand pump was used. The test set-up is shown in Figure 41. The grease bulb size was measured for all 18 ports of the GDU at four different temperatures: -20, 0, 20, 40 ℃. The maximum pressure required to pump the grease was also recorded except at -20 ℃ as the pressure gauge had a working temperature of 0-70 ℃. The grease and environment chamber was left for 30 minutes once it had reached the required temperature to allow the grease to reach the same temperature. This test follows the same procedure as described in the Network Rail standard [84] which defines the minimum requirements for rail curve lubricants. The standard has the performance targets detailed in Table 3.

Performance Targets	
Maximum Peak Pressure (bar)	2.5
Minimum Average Height (mm)	8
Minimum Average Depth (mm)	4
Maximum Standard Deviation in Height (mm)	2
No drooping after 30 mins	

Table 3- Performance targets from curve lubricant standard [84]

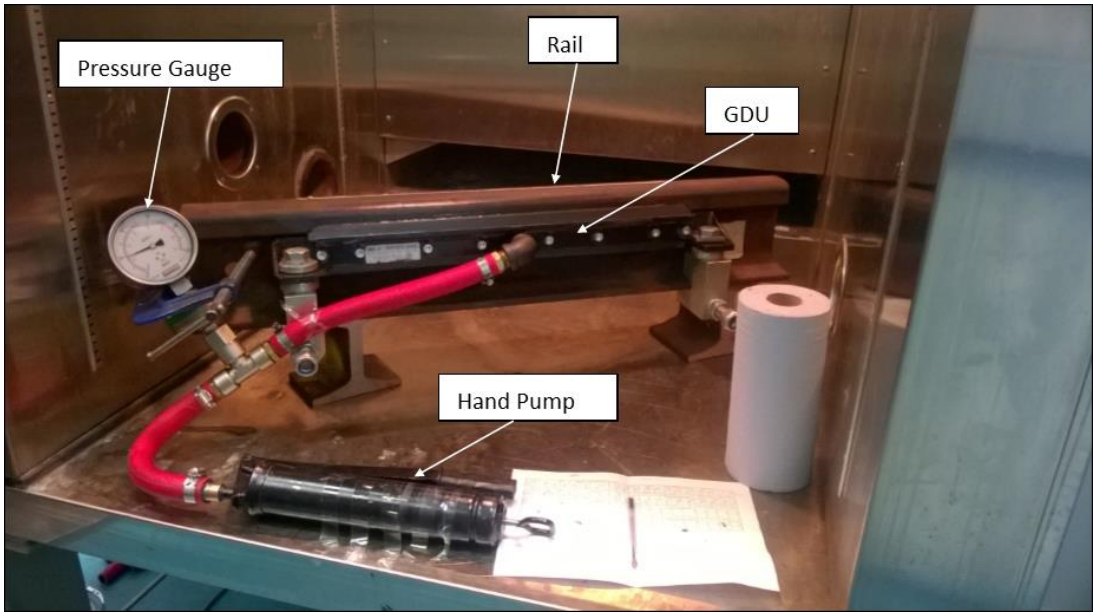

Figure 41- Set-up of the pumpability test

4.2 Results

4.2.1 Laboratory Gauge Face/Wheel Flange Distance

Figure 42 shows the shape of the putty bulb pre and post-test. The bulb was smeared with grease to prevent the wheel from knocking the bulb off the rail. This shape of bulb was superior to other shapes tested as it always stayed attached to the rail and showed enough deformation to get a measurement. In Figure 42B, the wheel flange has clearly deformed the putty, squeezing it into a thinner profile. This can be measured to give an accurate distance between the gauge face of the rail and the wheel flange.

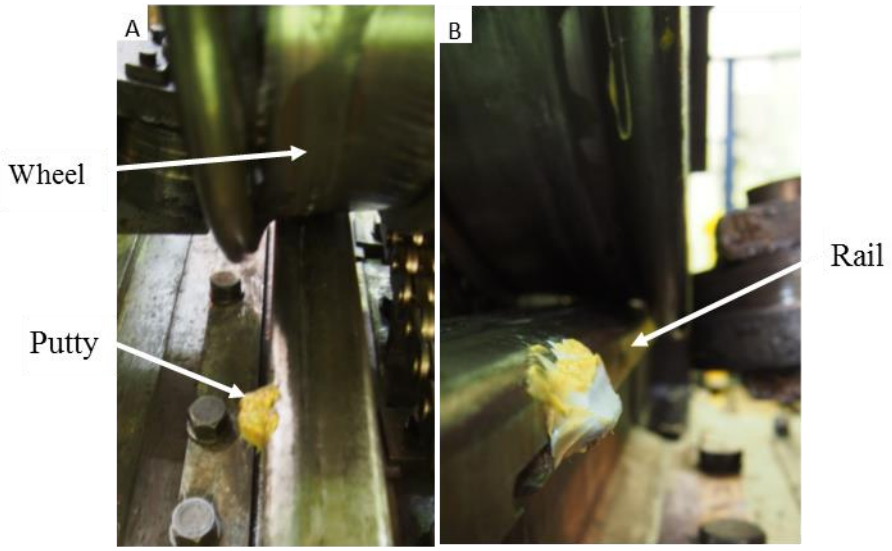

Figure 42- Shape of putty bulb on rail A) before test B) after test

4.2.2 Field Gauge Face/Wheel Flange Distance

Figure 43 shows the position of the three measurement locations within the lubricator site: one just before the first applicator bar, one in between the two applicator bars, and one after the second applicator bar.

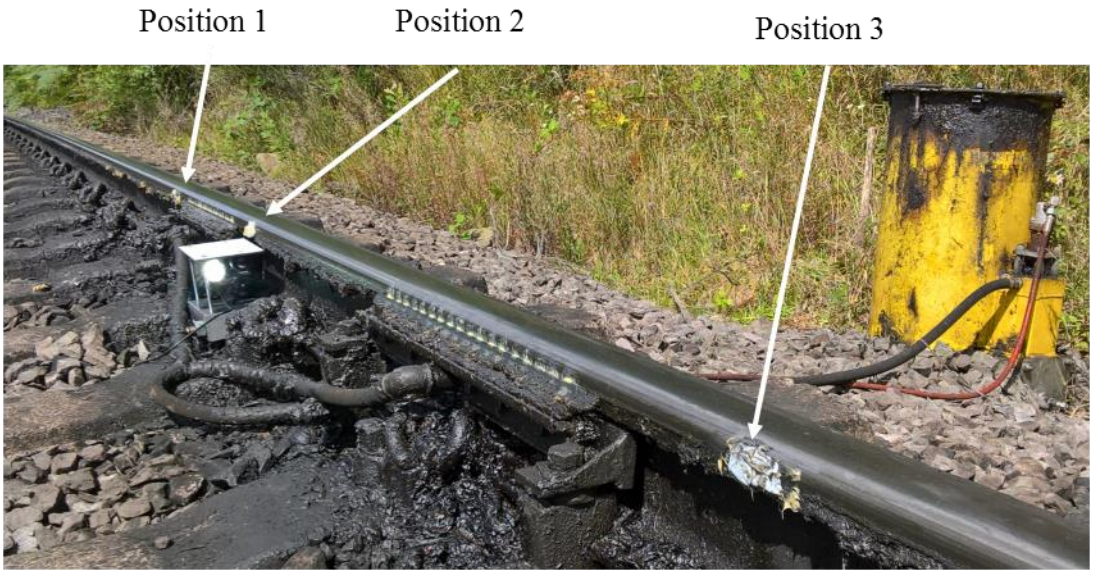

Figure 43- Position of the measurements within the lubricator site

Figure 44 shows the results from three trains passing through the lubricator site. It shows that there is variation from train to train and between the three different sites. If the gap between the gauge face and wheel flange is too big (i.e. the measured width is too large) then there is a chance that grease will not be picked up. However, the width of the grease bulbs is much larger than any of the measured widths (as seen in 4.2.5). This means that the wheel flange will always pick-up some grease.

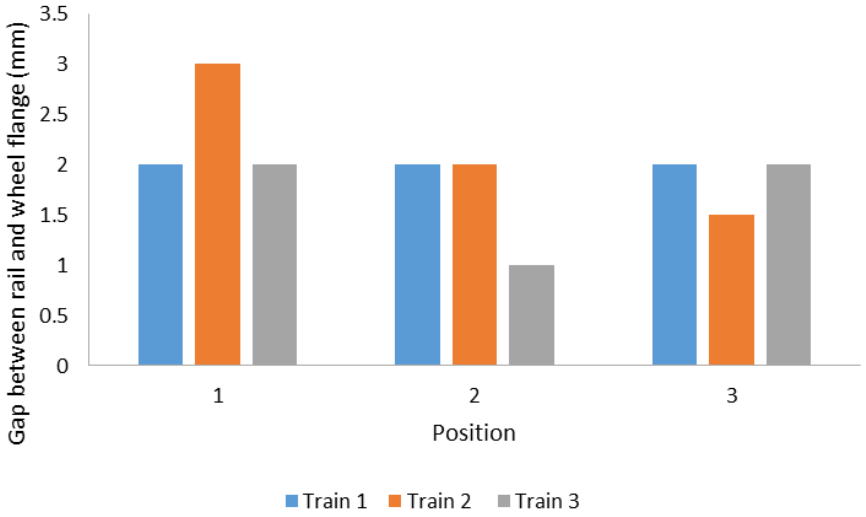

Figure 44- Measurements from three trains passing through lubricator site

4.2.3 Camera

Figure 45 shows images captured by the video camera during a train passing through the lubricator bar. Three different trains were recorded passing through the site. In Figure 45A, the untouched grease bulbs are clearly seen. Figure 45B was taken just after the first wheel has passed through the site but before the second wheel. The grease bulbs are no longer present, as the wheel has made contact with the grease, picking some of it up. Grease strings that form when the wheel passes through the grease are clearly seen. Some of this grease is wasted as it will not end up in the wheel-rail contact in the subsequent curves.

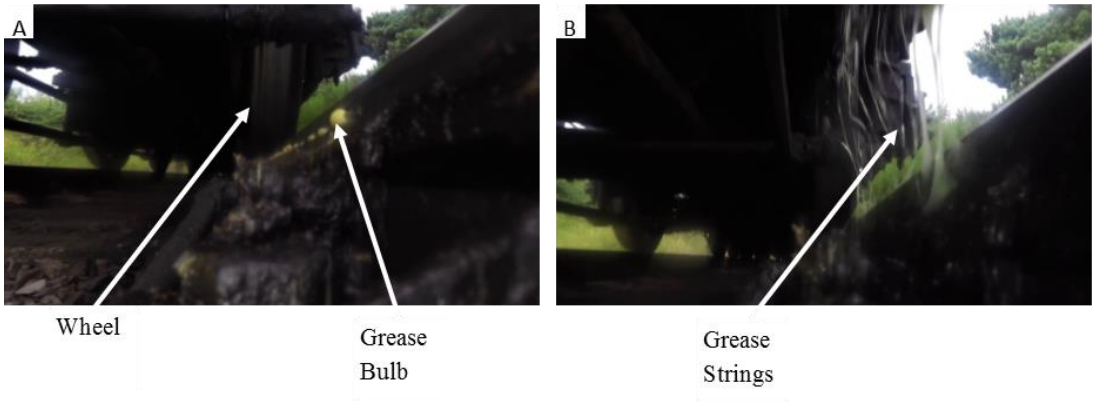

Figure 45- Still images captured from video camera A) before contact between first wheel of train and grease bulb B) After first wheel has passed through lubricator site but before second wheel

From watching the videos, it is clear that the first wheel of a train picks up the majority of the grease. After this, the grease bulbs are too small for the wheel flange to contact them. The grease bulbs grow whilst the train is passing through the site as more grease is pumped from the grease tank. When the grease bulbs reach a sufficient width, the wheel picks-up the grease starting the process again. After the train has passed, the grease bulbs continue to grow due to a small amount of pressure remaining in hose connecting the tank to the applicator bar. This means that the grease bulbs are at their largest for the first wheel of a train. This is shown in Figure 46.

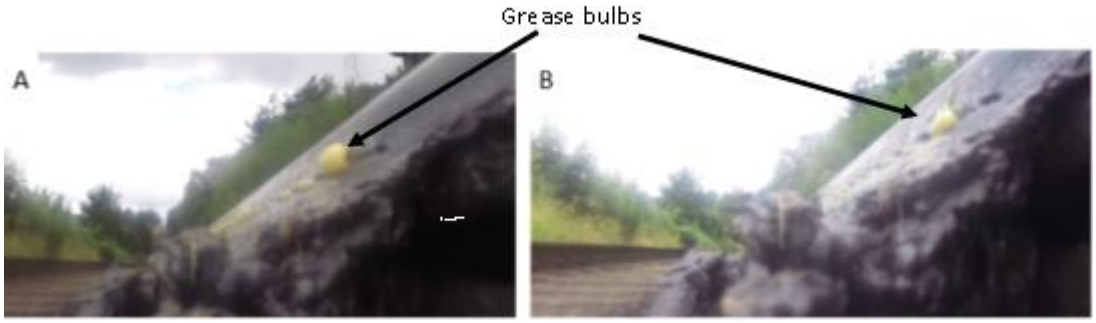

Figure 46- View along lubricator A) before train has passed B) after train has passed

4.2.4 Grease Bulb Laboratory Variability

Figure 47 shows how the location of the port affects the grease bulb shape and how the bulb shape changes between different repeats. It highlights that there is variation from port to port as well as between different repeat tests.

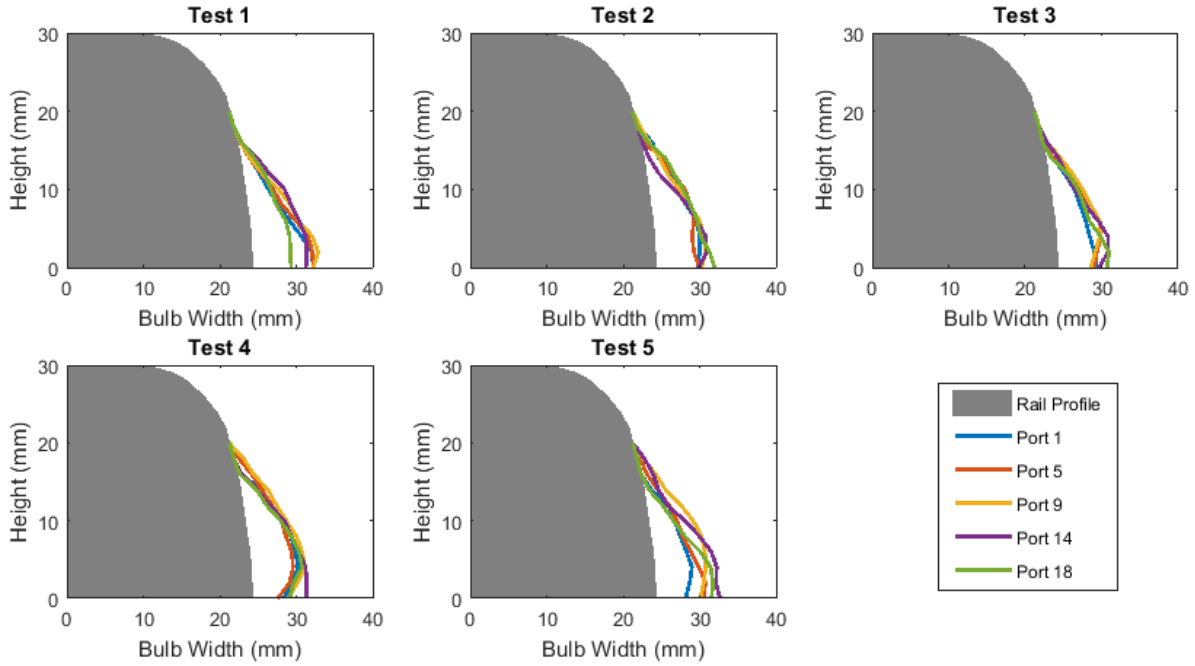

Figure 47- Variation in bulb shape from five ports across five tests

Figure 48 shows the variation in bulb shape when comparing the average of the measured ports. There is reasonable correlation between the repeats, especially above 5mm in height.

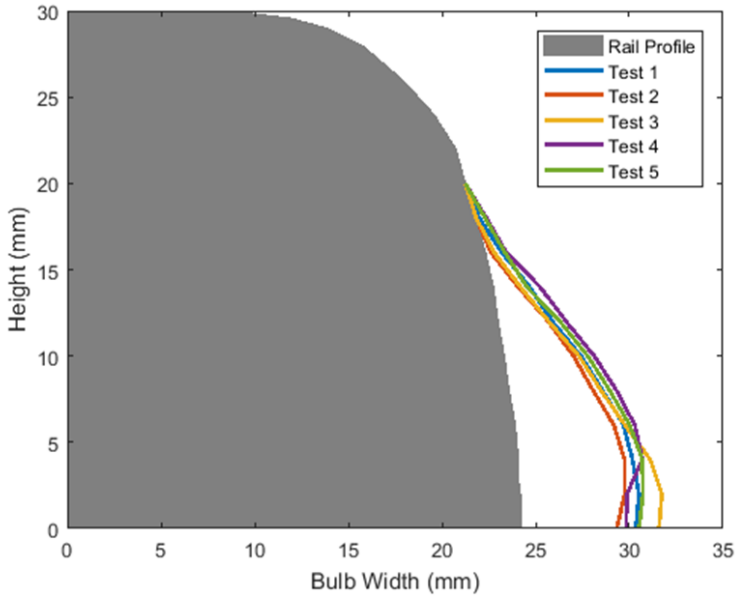

Figure 48- Variation in average bulb shape from the five repeats

4.2.5 Grease Bulb Laboratory vs Field

Field measurements were made using the same method as described in section 4.1.3 by L.B. Foster and Network Rail [69]. Three different locations were measured near to Hereford. Each location comprises of two GDU's on each rail. The GDU's were the same type as used in the laboratory tests. Figure 49 shows an example of one of the field location measurements.

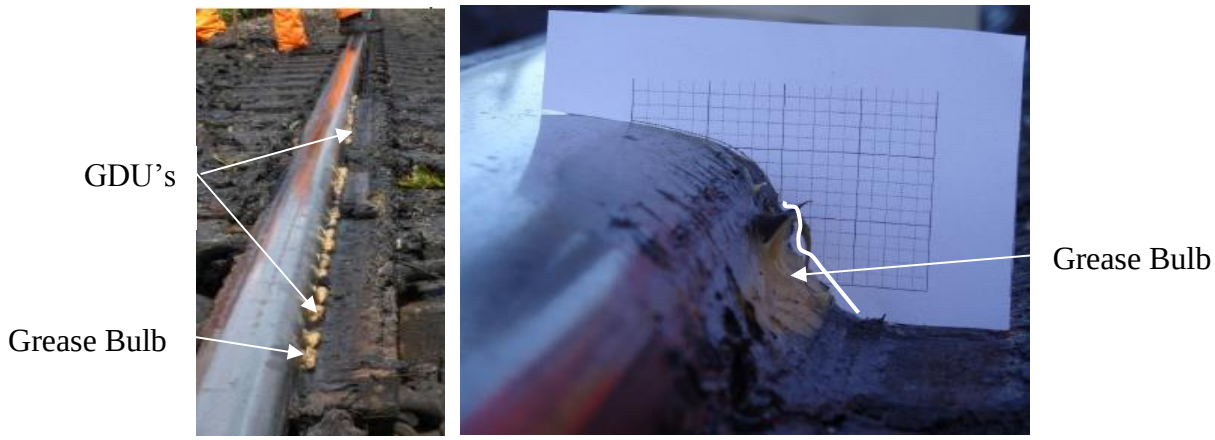

Figure 49- Example measurement of grease bulb in the field [69]

Figure 50 compares the average bulb shape from the laboratory (averaged across all ports and repeats) to the average bulb shape measured in the field at three different locations. It highlights that there is no one bulb shape to try and replicate due to the considerable difference in the bulb shapes between different locations.

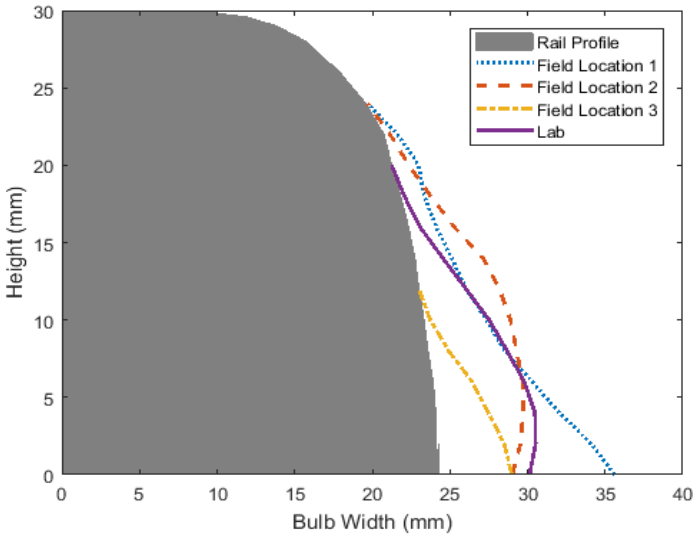

Figure 50- comparing averaged laboratory bulb shape to measurements taken at three different field locations

Figure 51 shows the variation in four different ports at field location 1. At this field location there are four GDU's, each of the four ports measured is at the end of one of these GDU's.

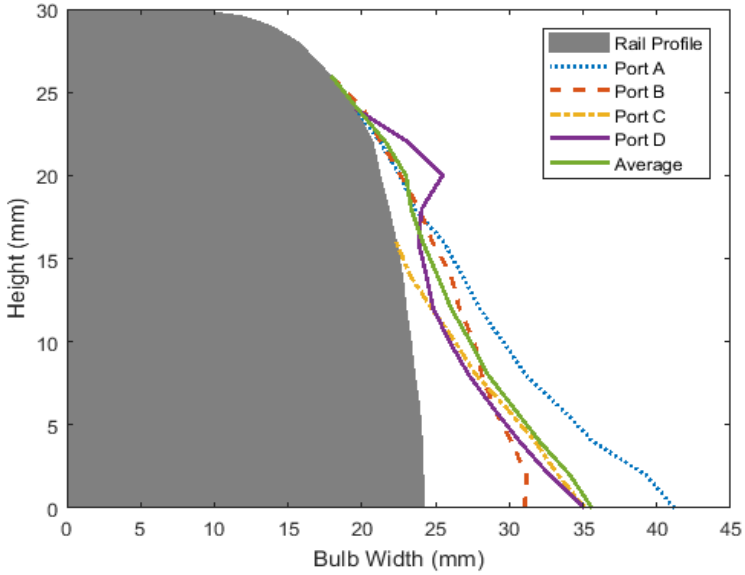

Figure 51- Port variation across field location 1

4.2.6 Grease Pumpability Test

Figure 52- Figure 54 show how temperature affects the bulb height and depth along a MC4 GDU for three different greases (Grease A, Grease B and Grease C). The figures show a two point moving average to show the trend more clearly. In general the bulbs are larger in the middle of the GDU compared to the bulbs at the end of the GDU. There is not a clear temperature trend with any of the greases. This suggests that the greases perform in a similar way at various temperatures.

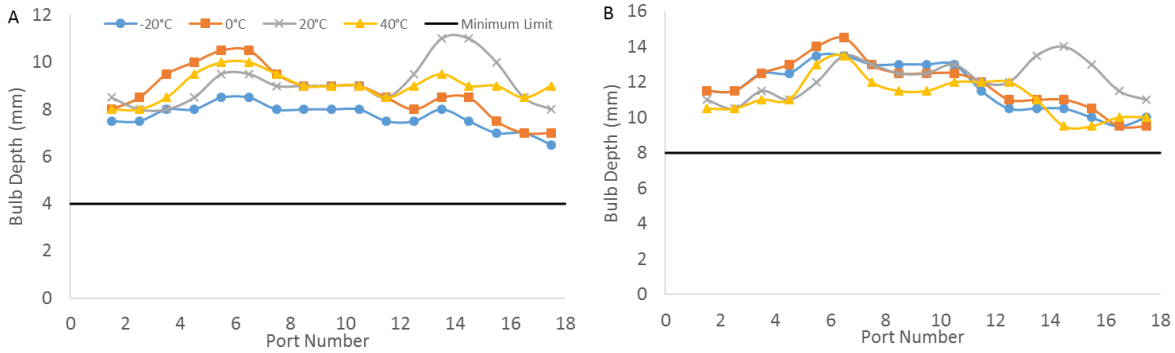

Figure 52- Temperature effects on bulb size along a MC4 GDU for Grease A

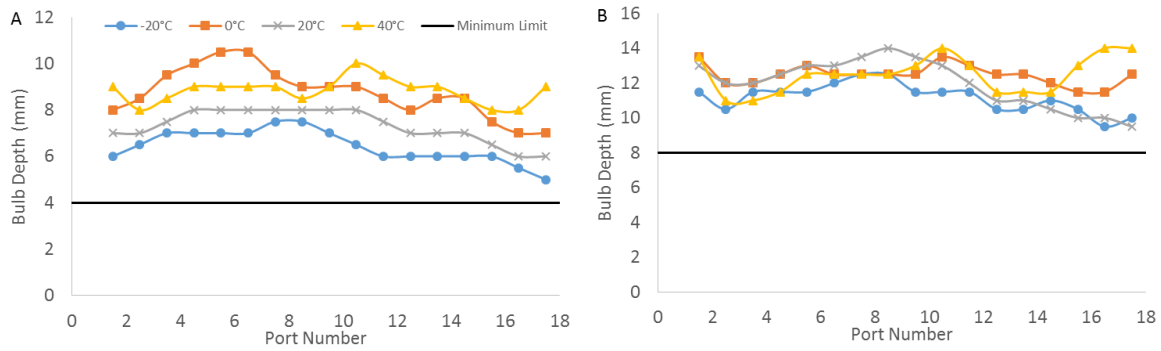

Figure 53- Temperature effects on bulb size along a MC4 GDU for Grease B

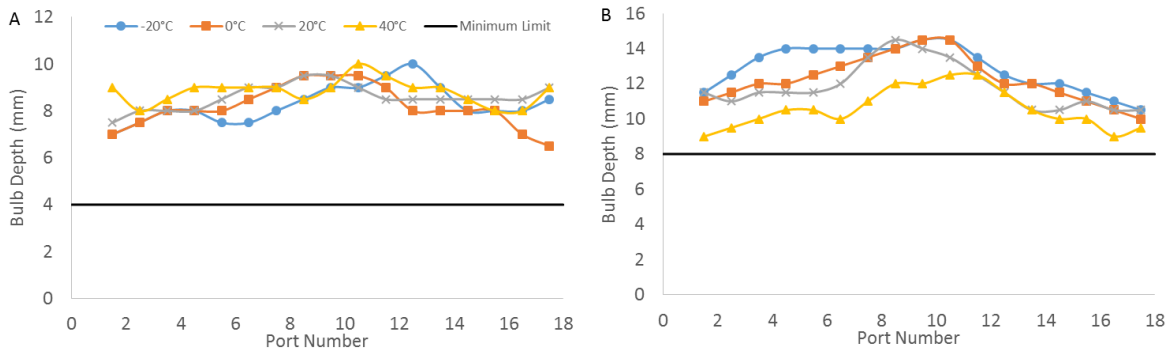

Figure 54- Temperature effects on bulb size along a MC4 GDU for Grease C

Figure 55 shows the peak pumping pressure at the different temperatures for the three greases. again there is no clear trend between temperature and pumping pressure. All three greases meet the criteria specified in Table 3.

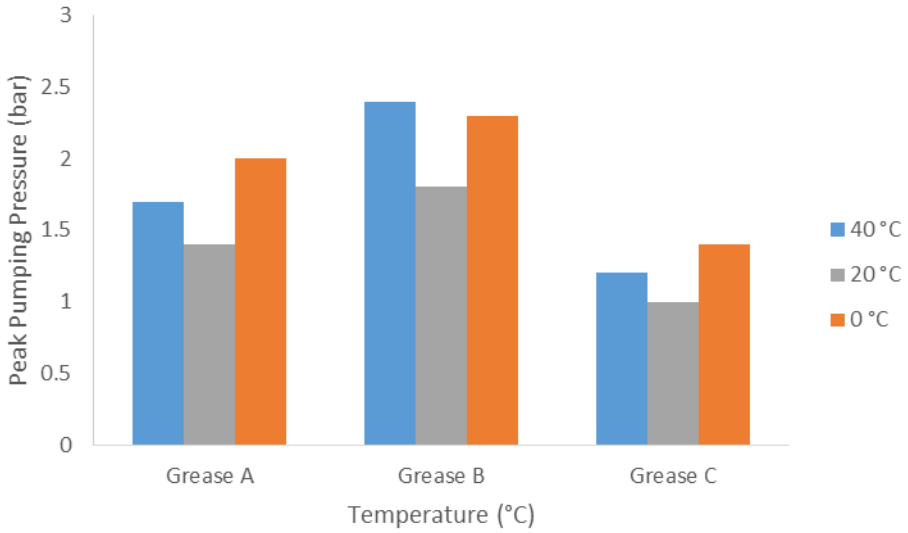

Figure 55- Peak pumping pressure at different temperatures for three different greases

4.3 Discussion

Figure 47 shows the difficulty in trying to produce a bulb shape that is consistently the same in the laboratory with five different bulb shapes produced from five different repeats. Figure 48 shows that this does not make much difference when averaged out across the different ports.

The difference in average bulb shape is small between different repeats for bulb height greater than five millimetres. This is important as if the wheel flange contacts the bulb at the lower heights (below five mm bulb height); the grease deposits higher up the wheel flange, away from the contact area and so is unlikely to be in a useful position to feed the contact patch. This has been shown in previous research [117]. It has indicated that grease is required near the flange root of the rail. In order to reach this area the grease bulb should "grow" up the gauge corner of the rail increasing its height. However, the bulb should not be too close to the top of the rail, otherwise there is a risk that the grease will spread onto the top of the rail contact which can cause traction problems for the train. The bulb shapes shown in Figure 47 and Figure 48 have enough height to deposit grease across the wheel flange without contaminating the top of rail.

Figure 50 shows that there is no one shape bulb that is present in the field as at the three different locations there is a significant difference in shape and volume of the average bulb. This is further emphasised in Figure 51 which shows a difference between ports at the same location. This could be due to the wheel position being at different lateral displacements at these different locations. A small gap between the gauge face and wheel flange will have a smaller bulb as more of the grease transfers to the wheel as it passes. Figure 50 also displays that the average laboratory bulb fits in well with the field data. The differences in bulb shape in the field (seen in Figure 50 and Figure 51) are also much larger than seen in the laboratory, highlighting that the current method does a reasonable job of producing the same bulb shape between repeats.

4.4 Conclusions

Videos have been made of a lubricator site in operation. They have allowed analysis of how the wheels of a train interact with a grease applicator and the grease bulbs. Measurements have also been made of the distance between the wheel flange and the rail gauge face. The measurements do have small variability, but as long as the grease bulb width is always larger than the distance between the wheel flange and gauge face, the wheel will pick up grease. This allows laboratory tests to be refined to mimic the conditions seen in field operation.

This work has shown how in the field there is not one bulb shape as there are large variations between different locations as well as between different ports at the same location. This makes it difficult to produce a bulb in the laboratory that reproduces field conditions precisely. The current laboratory method does produce a consistent bulb shape that can relate to conditions seen in the field when averaged out across the GDU.

5 Grease Tackiness

Greases are widely used in many different applications to improve the performance of systems and protect components from failure. Understanding the properties of a grease and impacts of additives is vital to selecting the appropriate grease/additive to use.

Grease is applied to the gauge corner of rail in curves. This reduces the friction and forces in the wheel-rail contact to reduce wear and RCF, prolonging the life of the wheel and rail. The grease transfers to the wheel flange from lubricators, often placed next to the rail in straight track. The wheel then carries it down the track lubricating the rail in the subsequent curves. There are also train based applicators that apply grease directly to the wheel. How much grease gets picked-up and carried-down the track is important to ensure adequate lubrication of curves. Therefore the tackiness of the grease plays an important part in this transfer process, ensuring enough grease is transferred from the lubricator to the wheel and then from the wheel to the rail. The work presented in section 4.2.3 clearly show s of grease forming during a wheel rolling through a GDU site. Tackiness has been defined and discussed further in section 2.4.5.

Currently there are no standard tests for grease tackiness and very few studies of tackiness in the literature. A standard laboratory test is required for tackiness for quality control purposes, for greases to be optimised for their specific application, and to be able to predict future performance in an application.

5.1 Aim

The aim of this work was to devise a test method to quantify tackiness of grease. Initially, test parameters had to be determined that would produce consistent, reproducible results. To prove the test method works, the effect of roughness on tackiness and different greases were tested. Also, the effect of preparation the grease pre-test was analysed. Finally, the effect of adding small amounts of tackifer additive on the tackiness was assessed.

5.2 Test Methodology

A Bruker UMT as described in section 3.2 was used in this work as its modular construction meant it could be tailored to fit the requirements. A linear lower drive with a vice was used to hold the lower specimen in position. A 50 N load cell was used to provide a suitable level of resolution. Figure 56 shows a typical test set-up. The upper specimen diameter is 29 mm; both specimens have a slight convex surface and machined from stainless steel 316. A video camera was used to record the test. A syringe was used to apply grease to the lower specimen using a mass balance accurate to ± 0.0005 g to measure the amount of grease. The grease used was a standard multi-purpose grease.

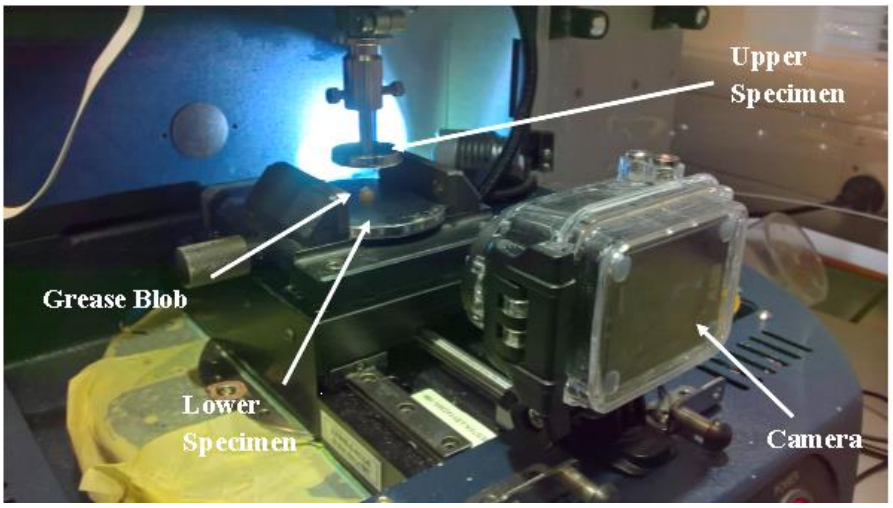

Figure 56- Typical test set-up

The method is an approach-retraction type experiment. This method was chosen due to its simplicity to implement.

All test followed a standard procedure:

- Specimens pre-smeared with a small amount (< 0.05 g) of grease. The amount of grease used to pre-smear the specimens has no effect on the results.
- Blob of grease applied to lower specimen via syringe using mass balance
- Test script run:
  - Lowers upper specimen until set force is reached for 10 seconds
  - Retract upper specimen at set speed until grease strings broken
  - Excess grease removed from upper specimen
  - Lower specimen re-weighed to measure the grease pick-up onto the upper specimen

Figure 57 shows a schematic of the different stages of the test:

- Stage 1: the upper specimen is lowered until a set force is reached
- Stage 2: the upper specimen is held in position at the set force for a set time
- Stage 3: the upper specimen is raised, pulling the grease upwards forming a grease "string"
- Stage 4: the upper specimen continues to raise, the grease "string" is broken and some of the grease is transferred to the upper specimen

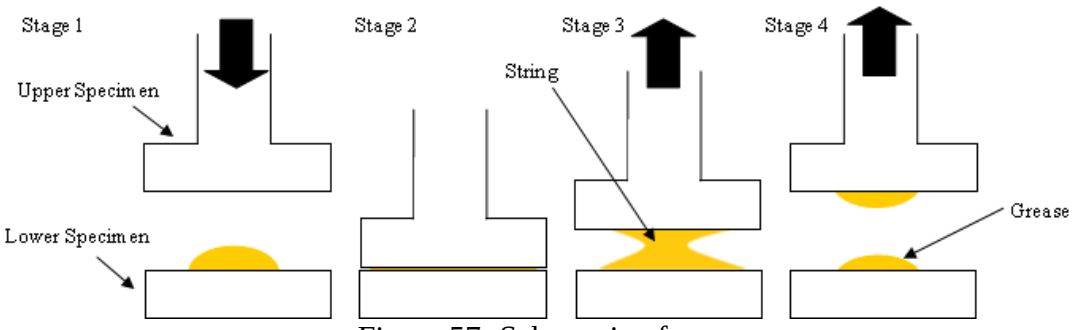

Figure 57- Schematic of test

Figure 58 shows an example of a typical force-distance graph produced from the tests. This graph is just for the retraction period (stage 3 and 4 in Figure 57) and not the loading period (stage 1 and 3 in Figure 57) of the test. The force tends to zero as the grease strings break. This shape of graph is typical for slow rates of separation caused by the grease flowing between the two test specimens [81]. From work carried out by Achanta et al. [78] the three distinct regions represent different properties of the grease:

- Region A- the work done against the grease resistance
- Region B- the work required to start separation
- Region C- the work required to break the grease strings. This region allows tackiness to be calculated.

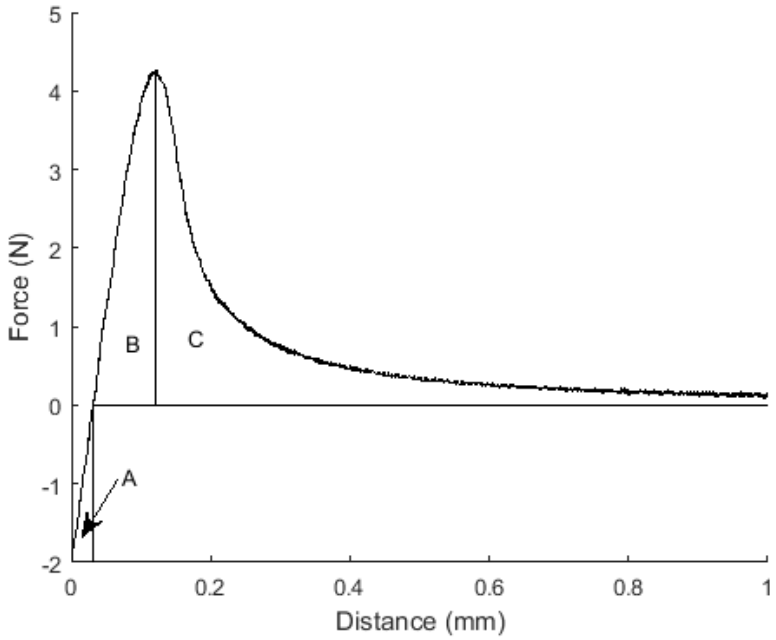

Figure 58- Example force response graph for stage 3 and 4

The area of Region C is calculated using a Matlab script. The Matlab script integrates the area under the curve from the maximum force value to where the force drops below zero. This is illustrated in equation 3.

$$Work\ Done = \int_{x=y_{max}}^{y=0} F dx \tag{3}$$

Figure 59 shows an example of a test half way through the top specimen retracting. The grease string can clearly be seen and is almost broken.

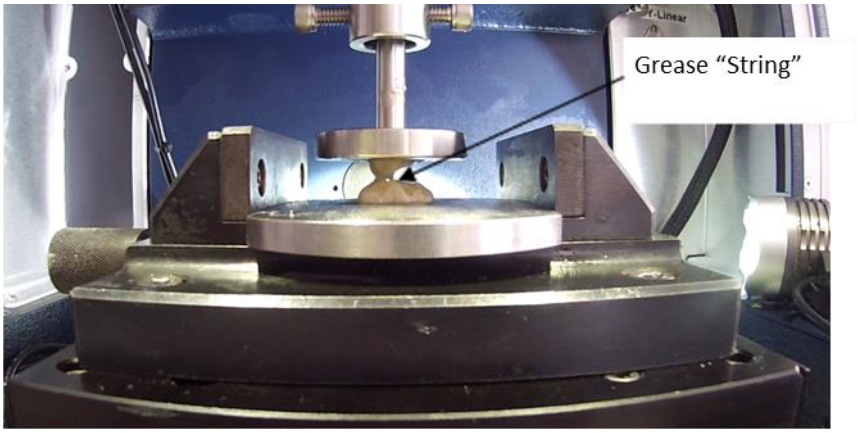

Figure 59- example test run

Before carrying out testing, a number of parameters had to be determined:

- Initial compressive force
- Initial grease amount
- Retraction speed
- Repeatability of results

Each parameter was varied in turn in a preliminary study to analyse its effect and to decide what setting to use in the main investigation. All of the parameters used in all of the tests can be seen in Table 4.

Report Section Number	Initial Compressive Force (N)	Retraction Speed (mm/s)	Initial Grease Amount (g)	Distance of Retraction (mm)	Number of Working Steps	Specimen Type
5.3.1 Repeatability of Results	2	0.25	0.1	8	0	Smooth
5.3.2 Initial Compressive Force	1/2/5/10	0.25	0.1	8	0	Smooth
5.3.3 Initial Grease Amount	4	0.25	0.05/0.1/0.2/0.3/ 0.4/0.5/0.75/1.0	8	0	Smooth
5.3.4 Retraction Speed	4	0.25	0.1	8	0	Smooth
5.4 Effect of Specimen Roughness	4	0.25	0.5	10	0	Smooth and Rough
5.5 "Working" of grease	2	0.1	0.1	8	0/5/10/15/20/ 30/40/50/100	Smooth
5.6 Tackifier Additive	4	0.25	0.5	10	0	Smooth

Table 4- Summary of all test conditions

5.3 Preliminary Study Results

5.3.1 Repeatability of Results

Figure 60 shows the effect of repeating tests with the same parameters. The initial grease amount was 0.1g, the retraction speed was 0.25mm/s and initial force was 2N.

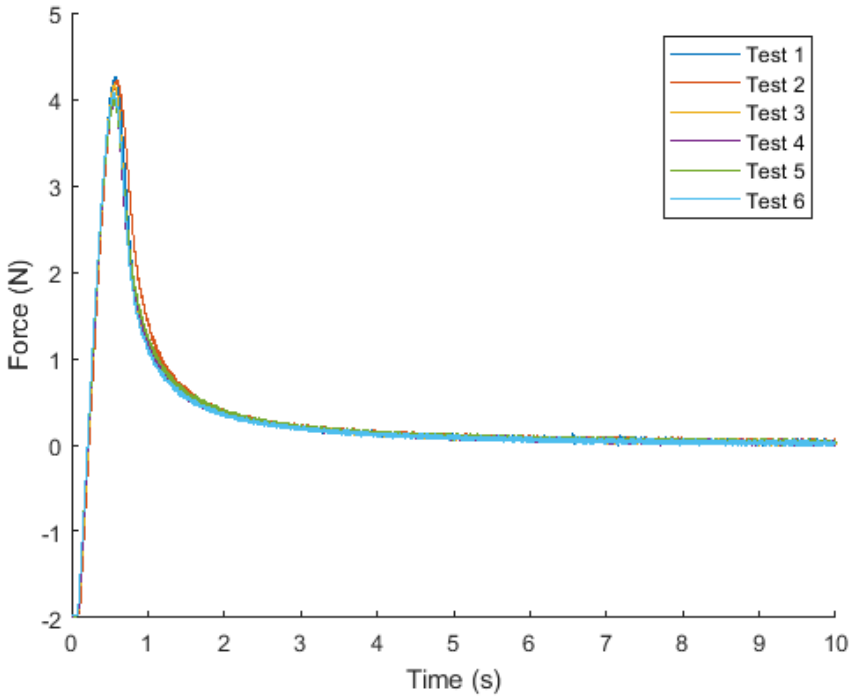

Figure 60- Graph showing repeats of the same parameters

Figure 61 shows the average value for the spread of data for each test. This quantifies the average deviation between each individual repeat and the average of all six. This value is the mean absolute area and is calculated as shown in equation 4. A spread value of 0.015 means that on average, the force measured in that particular test run, deviates by ± 0.015 from the average of all six repeats. The maximum accuracy parameter is less than 0.02. This indicates that the procedure produces repeatable, consistent results as the deviation from the average is small.

$$Spread = \sum_{i=1}^{n} \frac{|F_i - F_{average,\ i}|}{n} \quad (4)$$

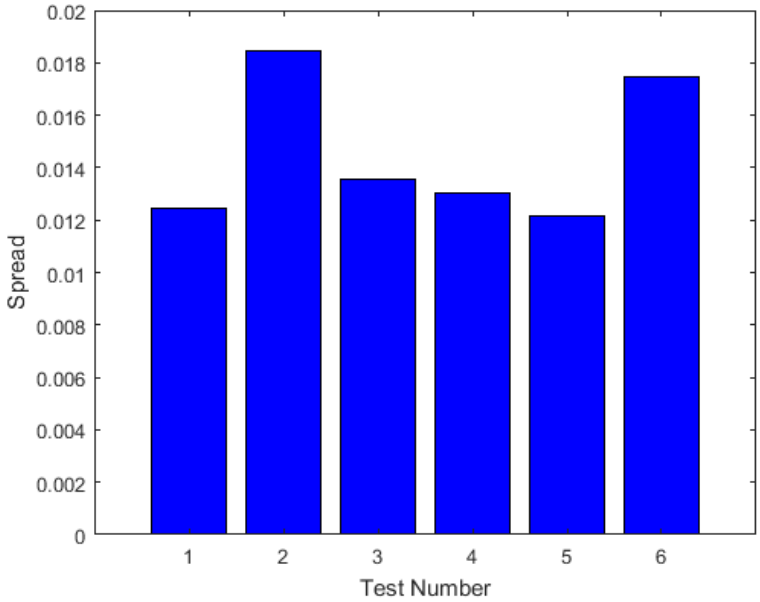

Figure 61- Spread of data

5.3.2 Initial Compressive Force

Figure 62 shows how the initial compressive force affects the force curve. It clearly indicates that the maximum pull off force increases as the initial compressive force increases. The shape of the graph also changes as the initial force is increased. This is due to cavitation effects as described in section 2.4.5 causing the rapid decrease in force. From the graph it was decided to use an initial compressive force of less than 5 N to avoid the cavitation effects. The speed of retraction was 0.25 mm/s and the initial grease amount was 0.1 g.

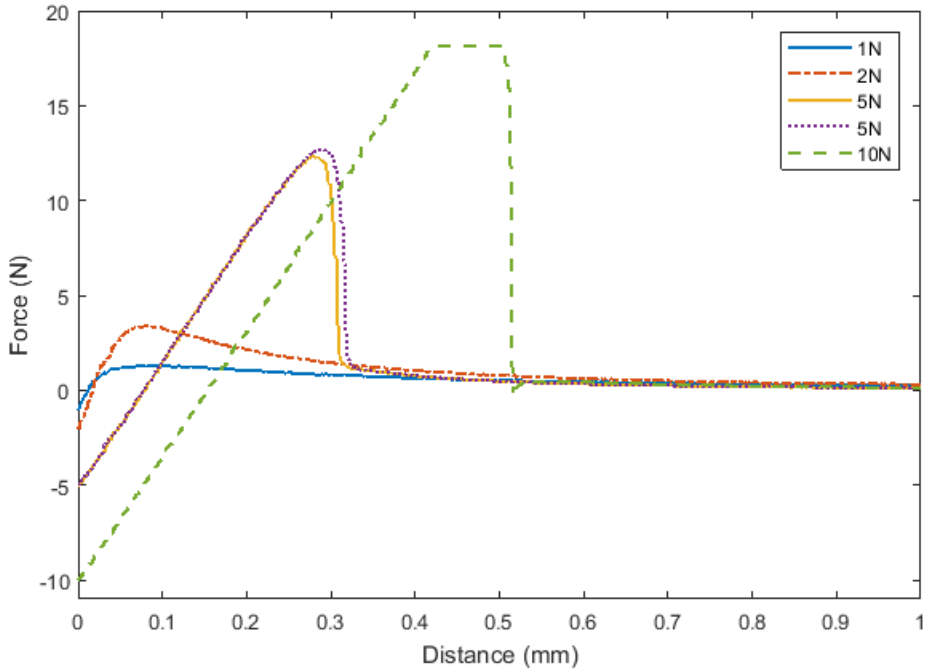

Figure 62- Effect of changing the initial compressive force

5.3.3 Initial Grease Amount

Figure 63 shows how the initial grease amount influences the force curve. It clearly shows that as the amount of grease increases, the maximum pull off force decreases. This is due to the same compressive force being supported by more grease. The shape of the curve also changes as cavitation effects occur less with more grease present. From the graph it was decided to use an initial grease amount of 0.5 g. The larger grease amounts would have been more preferable, but some grease was squeezed beyond the diameter of the test specimen above 0.5 g of grease. The initial compressive force was 4 N and the speed of retraction 0.25 mm/s.

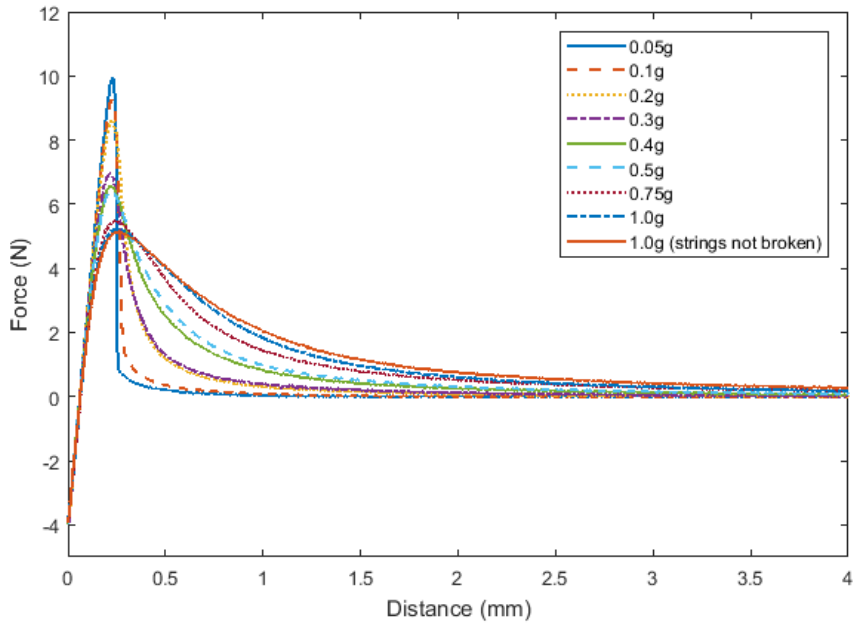

Figure 63- Effect of changing the initial grease amount

5.3.4 Retraction Speed

Figure 64 shows how the retraction speed affects the force curve. As the speed increases the peak pull-off force increases apart from at 0.5 mm/s where the shape of graph changes. Again the change in shape is due to cavitation effects decreasing at the higher speeds. The initial compressive force was 4 N and initial grease amount was 0.1 g. It was decided to use a retraction speed of 0.25 mm/s as 0.5 mm/s makes the separation occur over a very short time period. The cavitation effect will be reduced in future tests as the initial amount of grease will be increased.

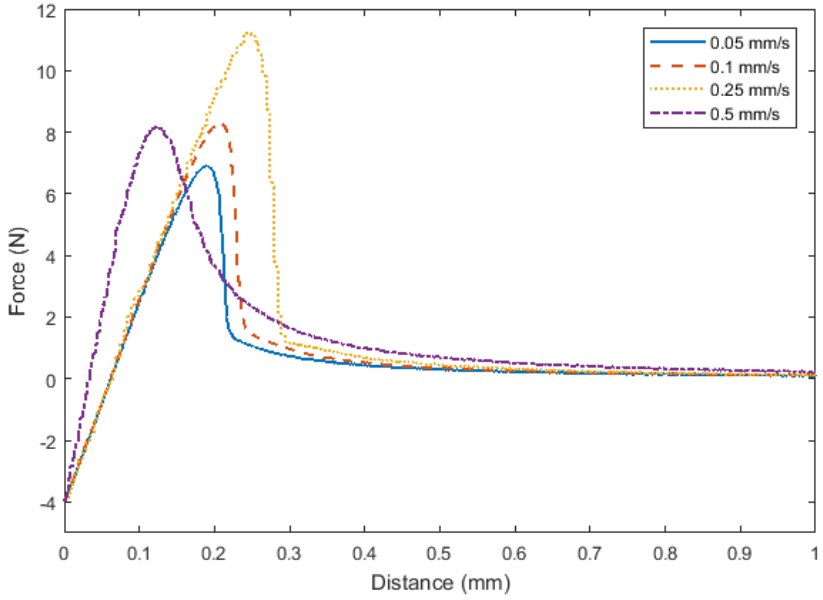

Figure 64- Effect of changing the retraction speed

5.3.5 Discussion

Figure 65 shows the work done to break the grease strings for each of the preliminary tests. The ideal case is to maximise the work done to break the grease strings as this leads to a reduction in error overall. Overall, Figure 65 supports the conclusions above. There is a clear direct correlation between initial grease amount and work done to break the grease strings (Figure 65C). The graph levels out because the as the amount of grease increases, some gets squeezed beyond the circumference of the specimen and so is lost from the test. There is also a linear correlation between retraction speed and work done (Figure 65B). For the different compressive force graph, there is a clear increase with the work done dropping once cavitation effects start occurring (Figure 65A) as seen in Figure 62. Figure 65D shows that the method produces repeatable results.

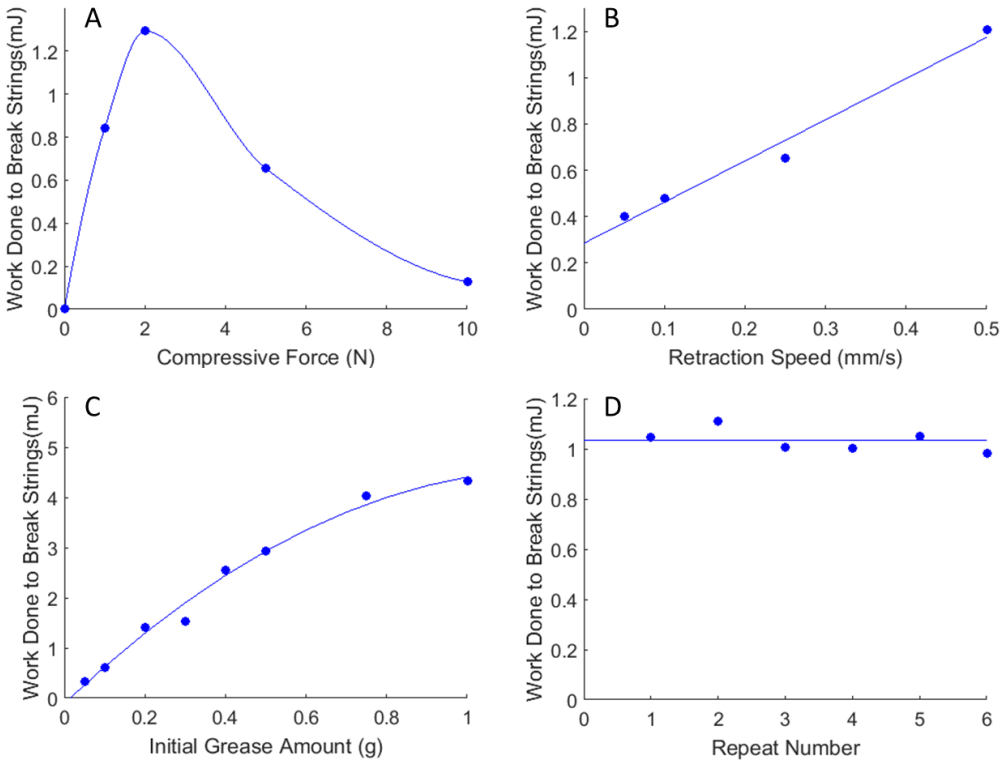

Figure 65- Work done to break grease strings for A) compressive force B) retraction speeds C) initial grease amounts D) repeats of same parameters

5.3.6 Observations

The initial tests showed that the method produces repeatable results. The force curve is influenced by cavitation effects, the parameters detailed in Table 5 to take forward to further tests were chosen to avoid cavitation:

Compressive force (N)	4
Retraction speed (mm/s)	0.25
Initial grease amount (g)	0.5

Table 5- Chosen parameters from preliminary study

The retraction speed of 0.25 mm/s caused cavitation effects to be seen in 5.3.4. However, the increased grease amount to 0.5 g will mean the separation is caused by the flow of the grease rather than by cavitation. These parameters are not representative of wheel-rail contact as usually there is more grease present, there is a greater compressive force, the speed is much faster and the wheel rolls over the grease rather than a straight vertical retraction. However, the parameters chosen will allow repeatable, reproducible results so that comparisons between tests can be made and this method can be used to inform future tests in more realistic conditions. This is because it the relative performance of products that is important to measure rather than absolute values due to similar test conditions as found on the railway network.

5.4 Effect of Specimen Roughness and Different Greases

To investigate what effect the specimen roughness had on tackiness, two specimen pairs were made, one with an *Ra* of 3µm and a smoother pair with a *Ra* of 0.6 µm. Twelve different greases were tested on both pairs of specimens using the standard test method described in section 5.2 and the conditions shown in Table 5. Some of the greases are different formulations of the same grease. This means that they share the same base oil but have altered additive amounts or different additives altogether to alter the properties of the grease.

5.4.1 Results

Figure 66 shows the results from the testing with different greases using the different roughness specimens. It clearly shows that the rough specimens require more work to break the grease strings, with a couple of exceptions. The graph also shows that the test method is able to differentiate between different greases/different formulations of the same grease.

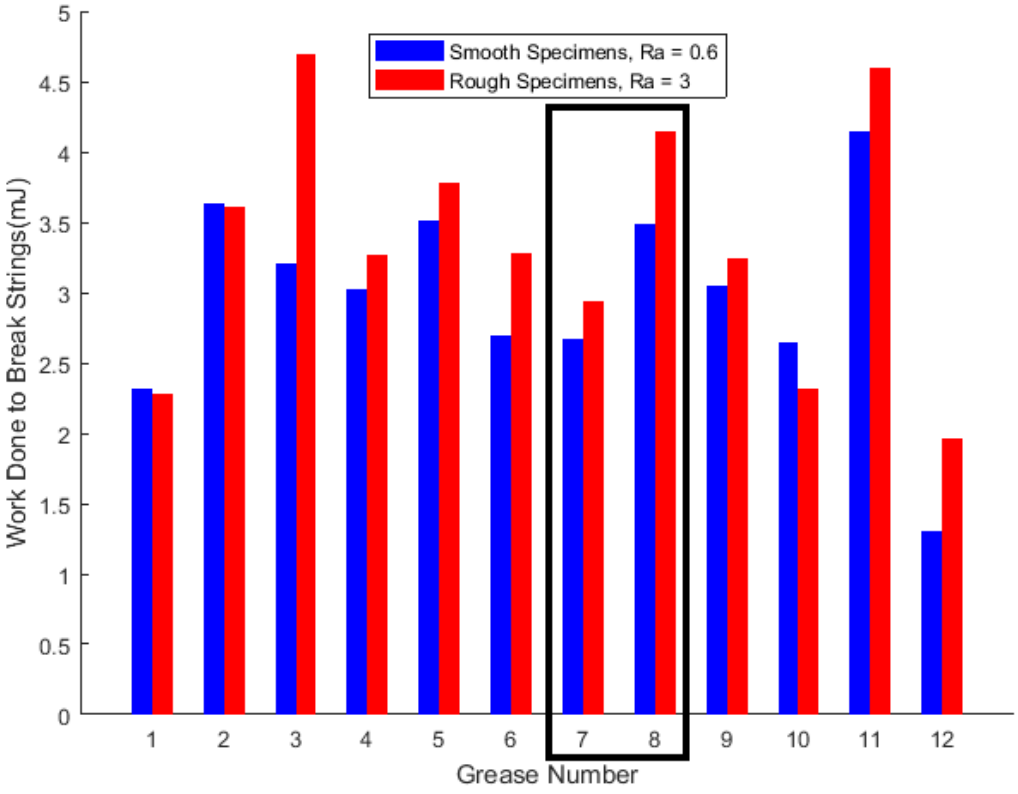

Figure 66- Effect of roughness on the work done to break grease strings. Grease 7 and Grease 8 are used in Figure 68

Figure 67 shows the percentage of grease picked-up on the upper specimen. There are no clear conclusions that can be drawn from this graph. This is because the smooth specimens pick-up more grease on some occasions and the rougher specimens pick-up more grease on other occasions.

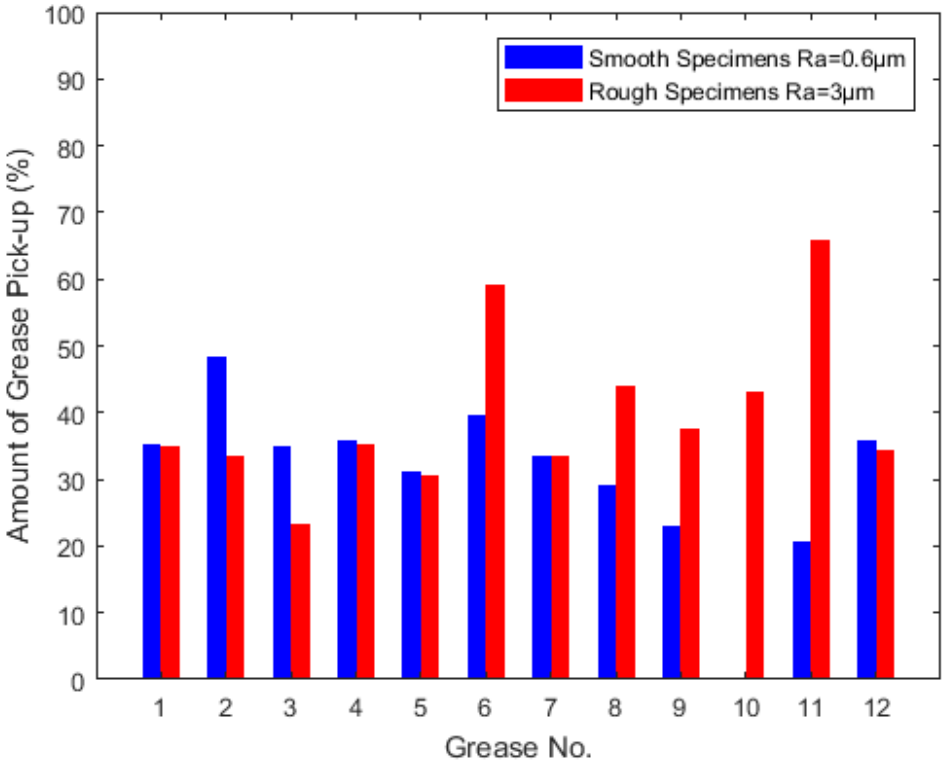

Figure 67- Amount of grease pick-up on upper specimen

Figure 68 compares the pick-up of two greases on a wheel from previous work done at The University of Sheffield. The tests used a scaled-wheel on a short section of rail with two different grease applicator bars tested. Figure 66 and Figure 68 support the hypothesis that the tackier the grease, the greater the pick-up. This is because the tackiness will cause longer strings to form which will cause more of the grease to transfer to the upper specimen. It is difficult to know why this hypothesis is not supported in Figure 67. It is expected that this is because the contact conditions and motion is completely different between moving two conical plates vertically and rolling a wheel along a rail.

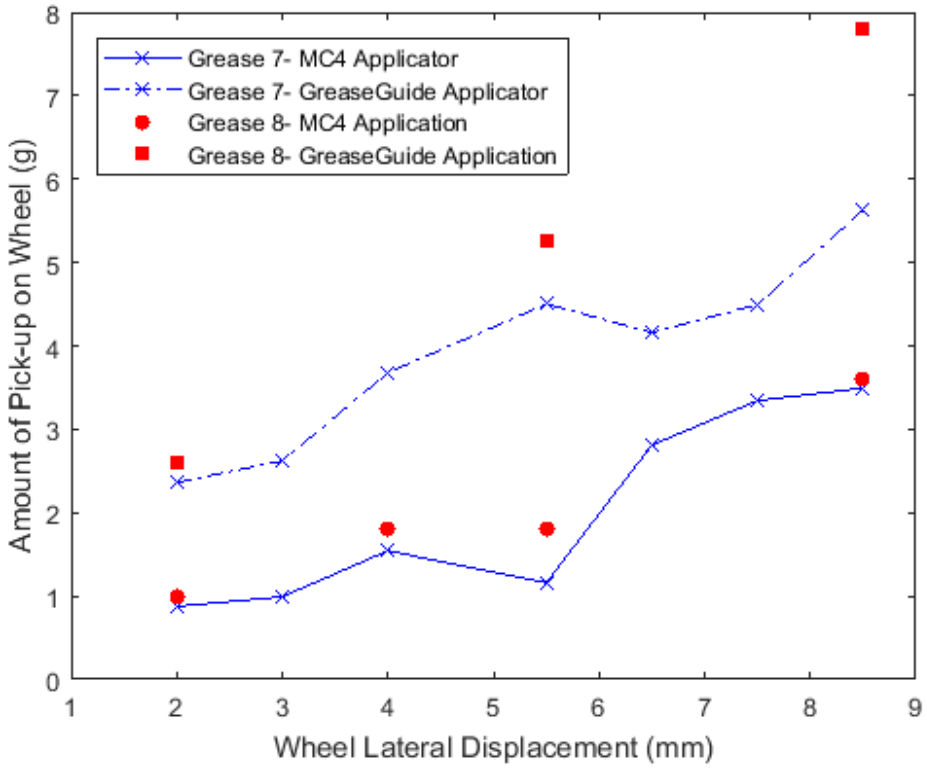

Figure 68- Comparing pick-up of grease on a wheel from a scaled-wheel rig at the University of Sheffield for two different greases (Grease 7 and Grease 8 in Figure 68) and two different grease applicator bars.

5.4.2 Observations

This section of work has shown that rougher specimens cause more work to be done to break the grease strings and hence mean the grease is seen as more tacky. The tests have also been able to differentiate between many different greases and even between different formulations of the same grease. This has been further extended to a more realistic wheel-rail test rig where the grease with a higher tackiness has resulted in a higher pick-up of grease onto the wheel.

5.5 Preparation of Grease

There has been anecdotal evidence that preparation of a grease prior to carrying out a tackiness test with it changes the tackiness of the grease. Preparation of the grease in this study means applying small amounts of compressive force to the grease before starting the separation test. Whilst this does not happen in the railways, it is a useful adaptation to the procedure that could be used to extend this same method to other industries. This would allow grease manufacturers to have one test apparatus at the end of a production line that could be used for multiple applications/greases rather than only for railway greases.

5.5.1 Test Methodology

To investigate if this does occur and to attempt to quantify the effect, a modification to the standard test script detailed in section 5.2 was made (changes to script are highlighted in bold text below). A preparation stage was included prior to carrying out the "test" stage

- Specimens pre-smeared with a small (<0.05 g) amount of grease
- Blob of grease applied to lower specimen via syringe using mass balance
- Test script run
    - **Preparation stage**
        - **Lower upper specimen until force of 2 N is reached for 2 seconds**
        - **Retract upper specimen at set speed for a small distance as shown in Table 6**
        - **Repeat previous two steps a set number of times**
    - Test Stage
        - Lower upper specimen until force of 2 N is reached for **2** seconds
        - Retract upper specimen at set speed until grease strings broken
- Excess grease removed from upper specimen
- Lower specimen re-weighed to measure the grease pick-up onto the upper specimen

There were two types of preparation investigated with the parameters detailed in Table 6:

- Type A- peak force is reached during preparation stage, but strings are not completely broken
- Type B- peak force not reached during preparation stage

Type	Distance Retracted (mm)	Speed of Retraction (mm/s)
A	0.1	0.1
B	0.05	0.05

Table 6- Parameters used during the preparation stage of script

Figure 69 shows how the two types of preparation are different as it can clearly be seen that in type A, the peak force has been reached before the grease is compressed again. There is a slight overshoot of force as the grease is compressed, it is not expected that this makes a difference to the results. The graph shows five preparation steps.

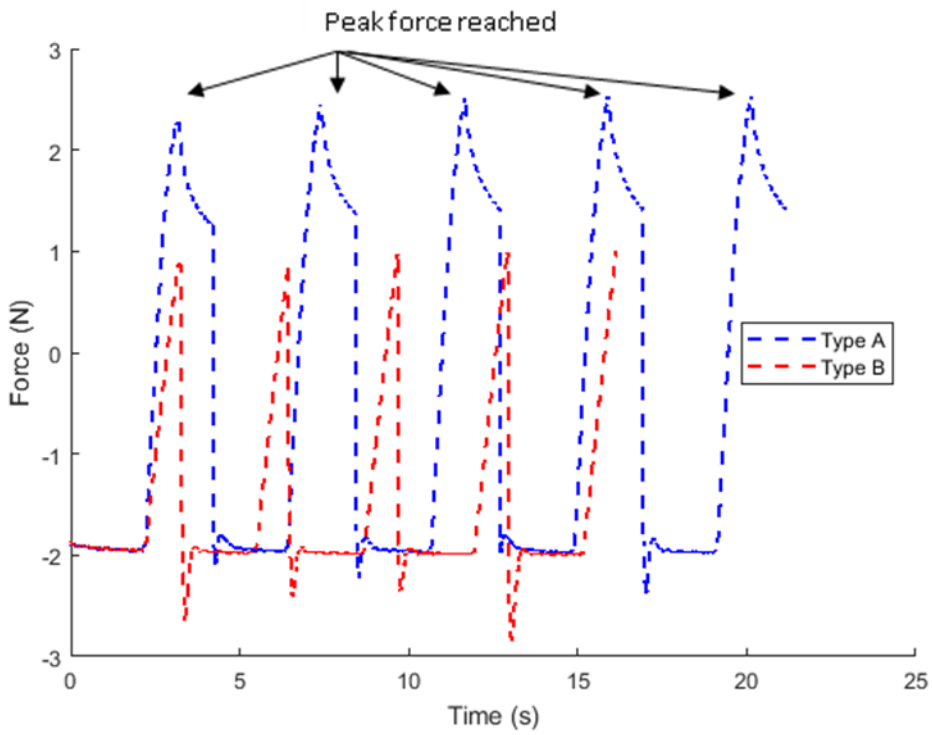

Figure 69- Force time graph of five preparation stages

5.5.2 Results

Figure 70 shows the different response of the grease as the upper specimen retracts with prior preparation of the grease. It can clearly be seen that preparing the grease, where the peak pull-off force is reached on each preparation step (Type A in Figure 69) causes a reduction in the tackiness and a reduction in the maximum pull-off force of the grease. Whereas, preparing the grease where the peak pull-off force is not reached on each preparation step (Type B in Figure 69) causes an increase in the tackiness of the grease and an increase in the maximum pull-off force.

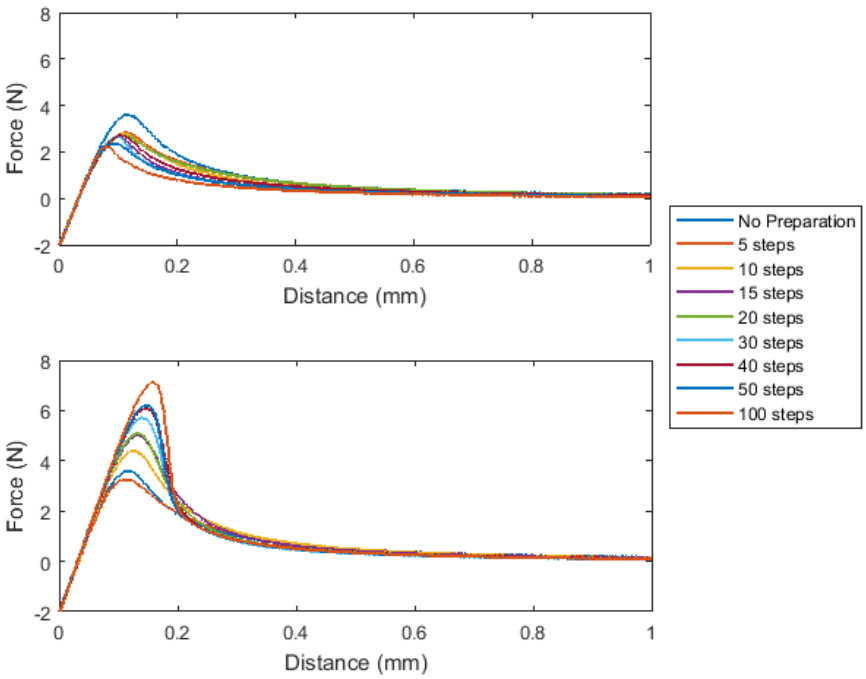

Figure 70- Effect of previous preparation of grease for A) Type A preparation and B) Type B preparation

To show the effect of prior preparation of the grease, Figure 71 shows the peak pull-off force reached against the number of steps the grease was worked for before the test was carried out. This figure supports the observations in Figure 70. Furthermore, for type A preparation it appears that the reduction in tackiness is linear as the number of preparation steps increases. Whereas, for type B preparation the relationship is quadratic.

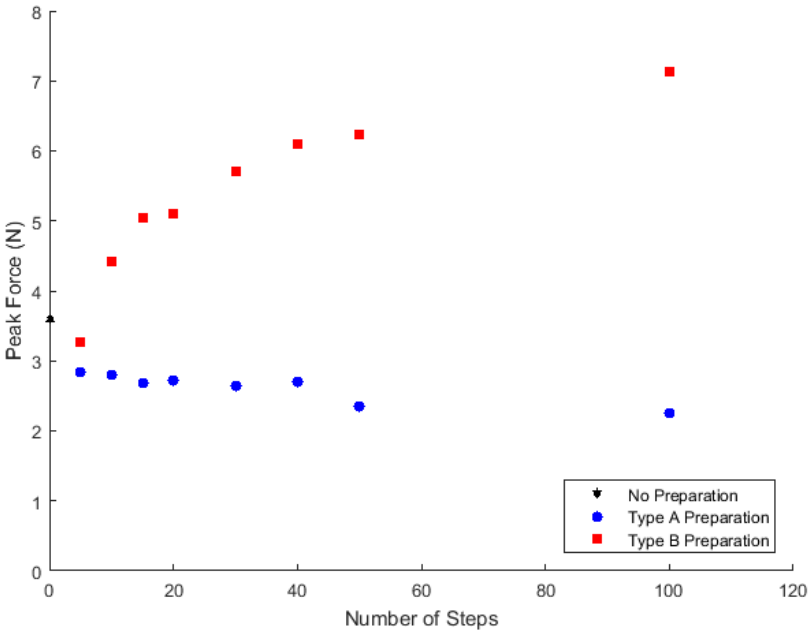

Figure 71- Peak force reached during test for differing number of worked steps prior to test being carried out

Figure 72 shows the work done to break the grease strings. Type B preparation required more energy than type A preparation to break the grease strings. This is due to an increase in tackiness with this type of preparation. For the total work done there is actually a decrease in the work required to break the grease strings compared to no preparation. For the first 0.3 mm of retraction there is an increase in work for type B preparation and a decrease in work for type A preparation.

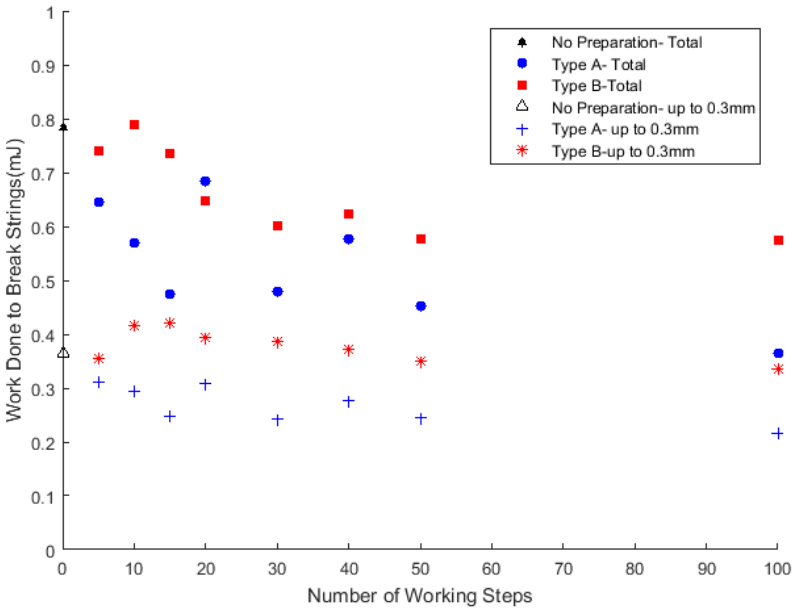

Figure 72- Work required to break grease strings for both types of preparation

5.5.3 Discussion

Figure 70 and Figure 71 support each other. Both figures show a decrease in peak force for type A preparation and an increase in peak force for type B preparation. This is explained by understanding how the chains of molecules in the grease respond to the two different preparation types. For type A preparation, the maximum pull-off force is reached which shears some of the long chains of molecules into smaller chains. This would happen at each preparation step so the more steps there are, the smaller the chains of molecules, which need less force to cause separation when the upper specimen retracts fully. These shorter chains are also less elastic than longer chains causing the reduction in tackiness. This explains the linear relationship seen in Figure 71 and Figure 72 for type A preparation. For type B preparation, the maximum pull-off force is not reached and the preparation steps have the effect of aligning the chains of molecules in the grease. This has the effect that when the upper specimen is retracted fully, more chains of the molecules share the load and can be extended elastically. Hence, more force is required to pull the specimens apart and an increase in tackiness. Figure 70B also shows that for an increasing number of steps, cavitation effects start occurring as the shape of the graph changes. Two things preparation together cause the quadratic relationship seen in Figure 71 for type B preparation. First, the cavitation effect places an upper limit on the tackiness of the grease [81] and the more preparation steps that occur, the greater the cavitation effect. This is indicated in Figure 70B where the greater the number of preparation steps, the steeper the gradient of the line after the peak force has been reached. Secondly, the

preparation of the grease is aligning the molecules, but they can only be aligned by a finite amount. Initially, the chains are aligned randomly. Once preparation of the grease starts the chains get more aligned as the number of preparation steps increases. Therefore, once the majority of the molecules are aligned, further preparation of the grease has little effect.
Figure 72 shows the work required to break the grease strings. For type A preparation there is a decrease in work required for both the total and first 0.3 mm of retraction results. This is expected due to reasons described in the previous paragraph. For type B preparation there is a difference between the total and first 0.3 mm of retraction results. The reasons for this are discussed further in section 5.7. The first 0.3 mm of retraction is the correct results as the preparation causes an increase in tackiness. However, after 15 preparation steps the tackiness starts reducing with increasing number of preparation steps. This is caused by cavitation occurring breaking the grease strings quicker. This shows that whilst increasing the number of preparation steps beyond a certain amount increases the adhesion of the grease (shown by increase in peak force), it reduces the tackiness.

5.5.4 Observations

This section of work has shown that preparation the grease prior to testing changes the response of the grease. If the maximum pull-off force is not reached during preparation then the peak force seen increases with the number of steps the grease is worked for. If the maximum pull-off force is reached during preparation the opposite occurs. This is due to changes in the arrangement and length of the chains of molecules in the grease. The work done to break the grease strings for the initial period of retraction shows that if maximum pull-off force is not reached during preparation, the tackiness increases until cavitation effects occur and tackiness starts to decrease again. If maximum pull-off force is reached during preparation of the grease, then tackiness is reduced.

The test method has been shown to differentiate between different levels and types of preparation. This extends the usefulness of this test as it allows the standard procedure (with a small modification to the method) to be applied to different applications. This would allow grease manufacturers to have one test apparatus at the end of a production line for quality assurance purposes, instead of potentially many types of test apparatus that are only used for one specific application.

5.6 Tackifier additive

To test how sensitive the test method is, small amounts of a tackifier additive were added to the grease in increments of 0.1 % by weight starting at 0 %.

5.6.1 Test Methodology

The standard test method described in section 5.2 was used in these tests. The initial grease amount was 0.5 g, the retraction speed was 0.25 mm/s and initial force was 4 N. Initially the test samples were mixed by hand prior to the test starting out. The results were found to contain a lot of scatter between different repeats (each percentage was repeated five times). Therefore an improved method of preparing the grease samples was devised:

- Base grease added to mixing pot (~70 g)
- 0.1 % by weight tackier additive added to mixing pot
- Mixed by hand for 3 minutes
- Sample removed via syringe (4-6 g)
- Previous steps repeated to get all 5 samples
- Syringes placed in dry ultrasonic bath for 10 minutes and heated to 40 °C
- Samples prepared 48 hours before testing to allow cooling of the samples back to room temperature

5.6.2 Results

Figure 73 shows the effect of adding small amounts of tackifier additive. This data is from the initial hand mixing of the grease samples. It shows that there is an increase in tackiness when the additive is added compared to no additive. However, between the different amounts of additive, there is little difference. This is thought to be due to poor mixing of the specimens and the small quantities used meaning that it is uncertain that the correct ratio of grease and tackiness made it onto the test specimen. This is illustrated by the large error bars.

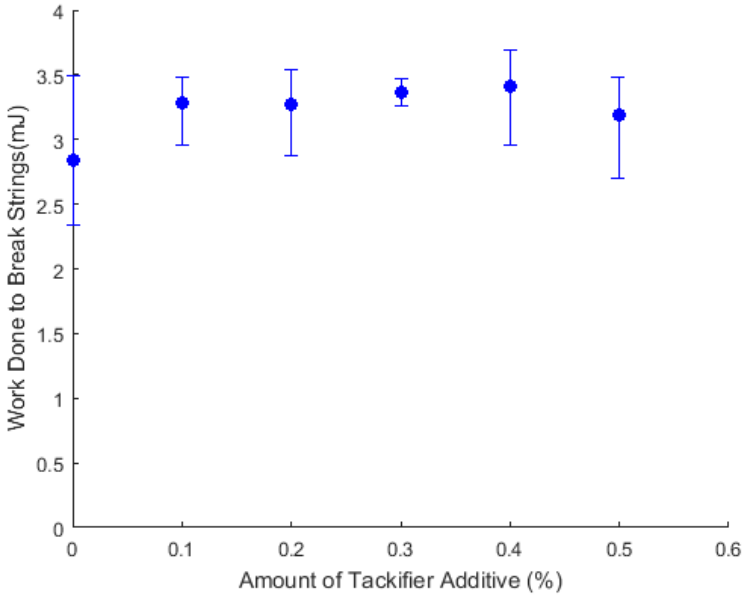

Figure 73- Work done to break grease strings with different amounts of tackifier additive- initial data

Figure 74 shows the effect of adding the tackifier additive on the tackiness of the grease. This data used the improved mixing method. The values here are lower than in Figure 73, this is likely due to the test occurring on different days and different times of day so the laboratory environmental conditions caused this change. The overall trend is for a decrease in tackiness for an increasing amount of tackifier additive. This is not correct, as the additive should increase the tackiness. It is interesting that as the period that the work done is calculated over gets smaller, the relationship changes. This is discussed further in section 5.7.

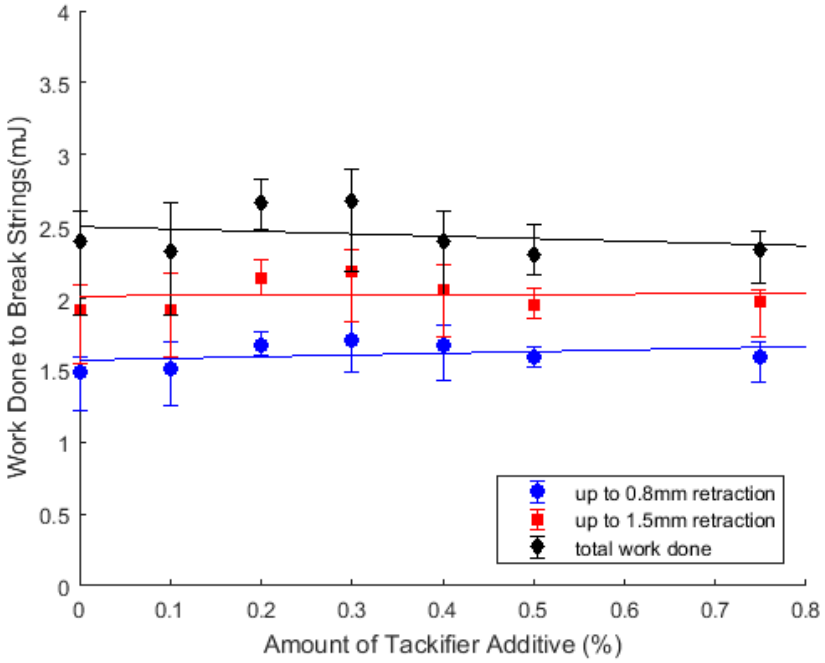

Figure 74- Work done to break grease strings with different amounts of tackifier additive- improved grease mixing method used

Figure 75 shows the change in standard deviation in the work done calculation using the two different mixing methods. It shows that the second, more sophisticated mixing method has a

significantly lower standard deviation. This is because it ensures the mixture is mixed properly, increasing the chances of getting the correct ratio of tackiness to grease onto the test specimen.

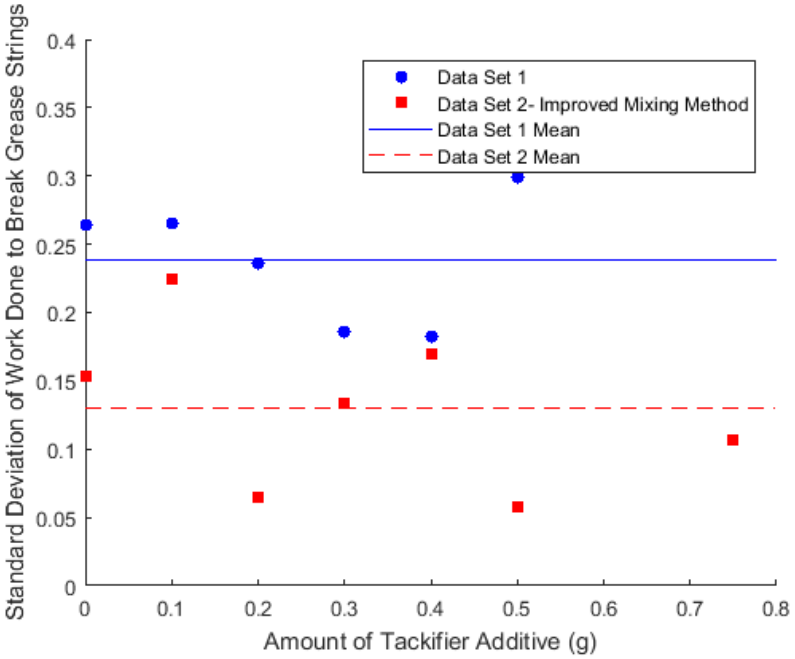

Figure 75- Standard deviation for the two mixing methods

Figure 76 shows a section of the force- distance graph for the mean values of each of the different tackifer amounts. This graph helps to explain the results in Figure 74. The results for 0.4 %, 0.5 % and 0.75 % have a higher peak force than the smaller percentage results. What happens after the peak force has a significant effect on the overall work done. The force for the smaller percentages does not decrease as quickly as the higher percentages, this leads to the smaller percentages having a higher overall work done to break the grease strings. This is for the improved mixing method.

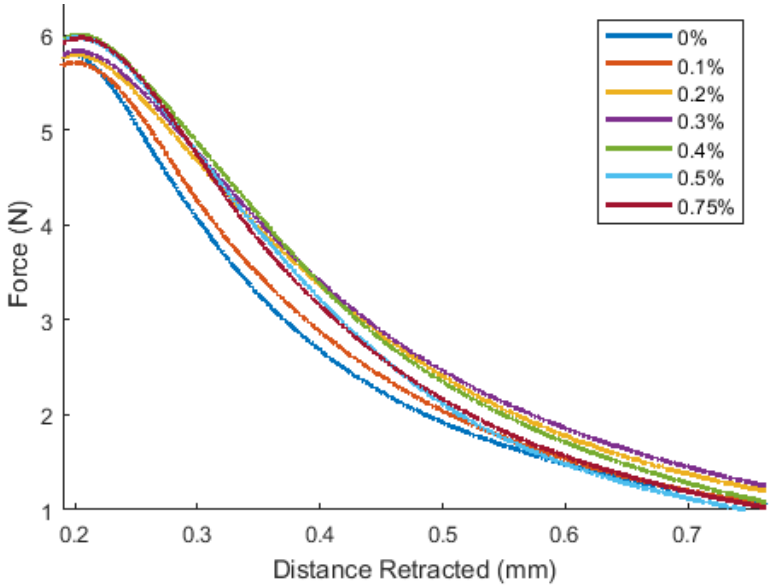

Figure 76- A section of the force-distance graph for different tackifier amounts- improved mixing method.

Figure 77 shows the mean peak force for both mixing methods. It again shows that the second, sophisticated method is significantly better at mixing the grease as the error bars are smaller and the trend of increased peak force for increasing tackifier additive is supported by theory.

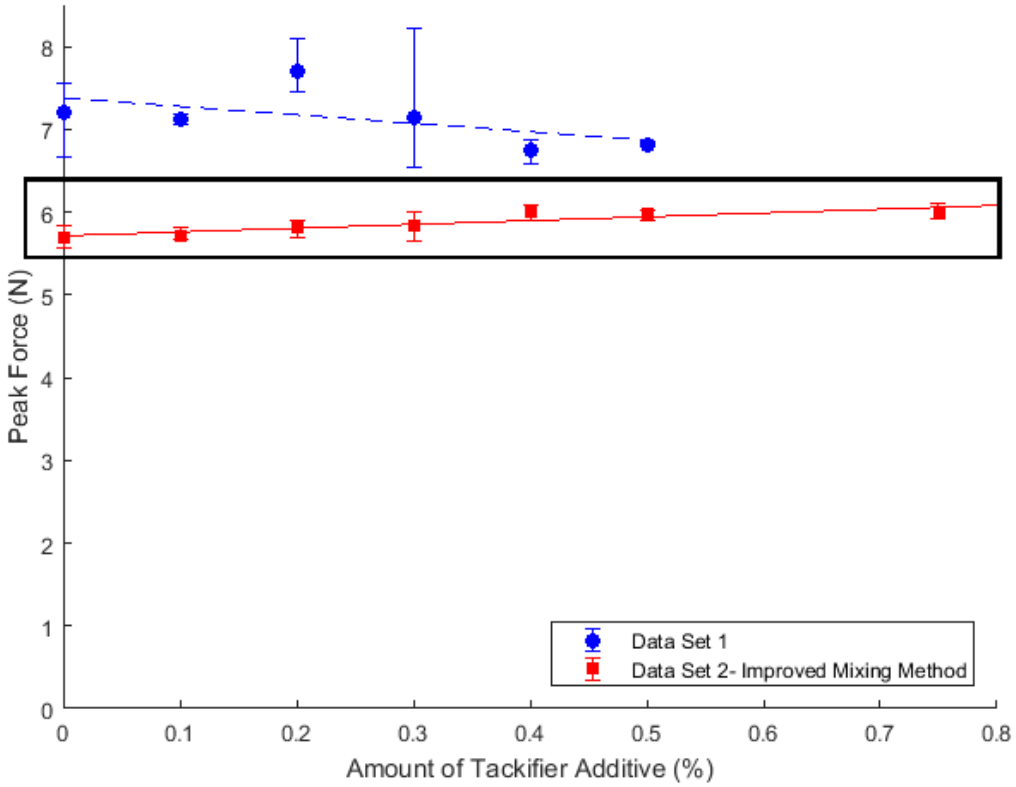

Figure 77- Peak force vs amount of tackifier additive for both mixing methods. Data set 2 is enlarged in Figure 78

Figure 78 is an enlarged section of Figure 77 to show the results from data set 2 more clearly. It is important to note the y-axis scale.

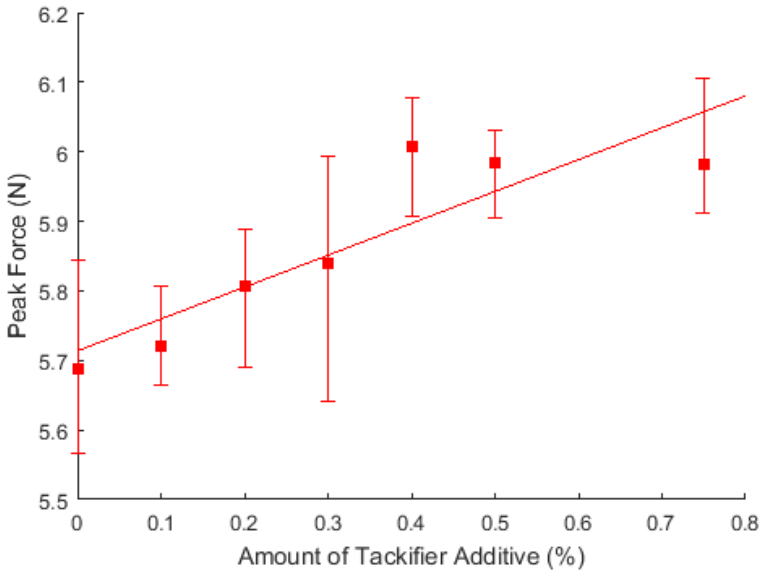

Figure 78- Zoomed in peak force vs tackifier additive graph from Figure 77

Figure 79 shows the amount of grease transferred to the upper specimen during testing. There is a slight decrease in grease picked up by the upper specimen, but this could just within the error of the experiment and the tackiness of the grease does not affect the pick-up of grease in this case due to the very small changes in tackiness.

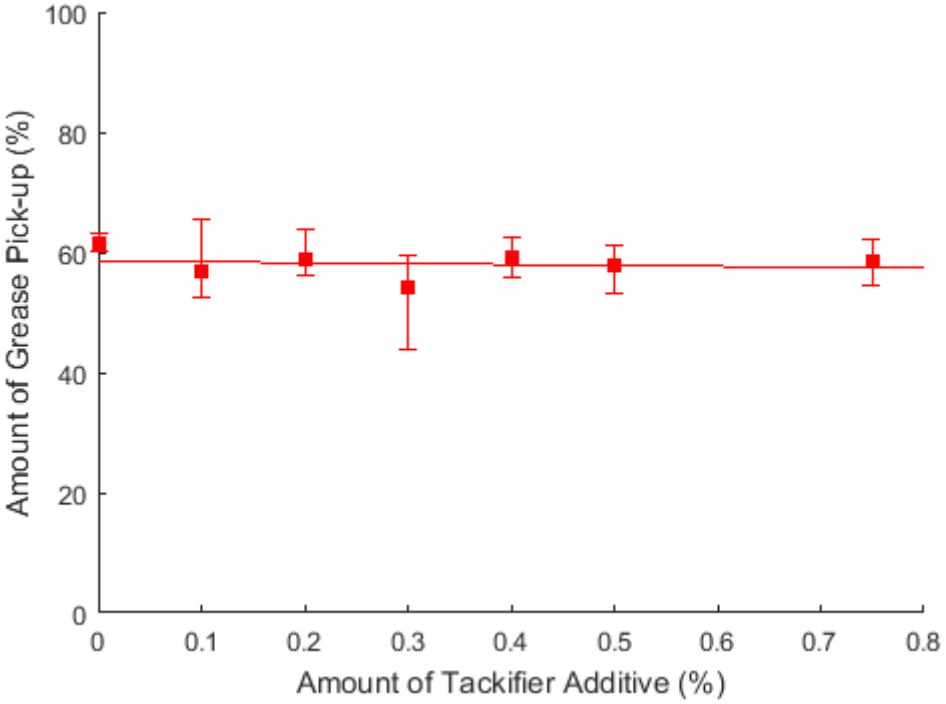

Figure 79- Amount of pick-up of grease on upper specimen

5.6.3 Observations

This section of work has shown that the test method does detect small changes in the grease, but careful preparation of samples is important to ensure any experimental error is not greater than the measured changes in tackiness.

5.7 Discussion

The results shown in sections 5.5- 5.6 show that the work done to break the grease strings is not a reliable way of showing how the tackiness changes when the differences are very small. This is due to the way the work done is calculated rather than the parameter itself. The maximum peak force shows the relationships more clearly. However, the maximum peak force is an indicator of adhesion rather than tackiness as it shows how much force is required to separate the two plates.

The work done is calculated using a matlab script to integrate the area under the force-distance graph. The script calculates the area from the maximum peak force to where the curve reaches zero. However, as the force decreases towards zero the error in recorded force increases. A further source of error is the fact that once the specimens have been separated, a portion of the grease has been transferred to the upper specimen. As this grease has a mass and the force is measured in the vertical plane, the grease will exert a small force on the upper specimen due to gravity. Although this force from the grease is very small, (less than 0.1 N) this will have an effect, particularly near the end of the retraction period when the recorded force is very small due to the grease strings being very thin. The effect of these errors can be seen in Figure 72 where there is one anomalous result at 20 preparation steps for the total work required to break the grease strings. The reason for this can be seen in Figure 80 where although the peak force for type A preparation is lower, it has a higher force for a longer time (the retraction occurs over 8 mm) once both curves approach zero.

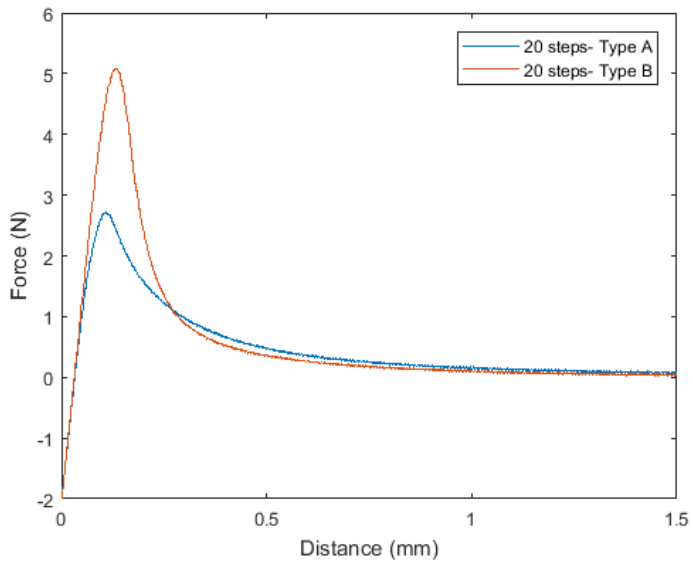

Figure 80- Force vs distance retracted with 20 steps of preparation for both types

A large proportion of the work done is expended in the initial period following the peak force. This explains the results in Figure 72- Figure 74 where if the period the work done is calculated over is reduced to cover just the period immediately after the maximum peak force the results are correct. This is because the errors discussed in the previous paragraph have a significantly smaller effect when the force is larger. The length of this period is influenced by the test conditions and can only be determined by analysing the force-time graph. The length of this period should be chosen so that as much of the data is captured as possible.

The method developed here is a new method to measure the relative ranking of the tackiness of products. The method is:

- Pre-mix grease with additional additives using ultrasonic bath
- Specimens pre-smeared with a small amount (< 0.05 g) of grease
- Blob of grease applied to lower specimen via syringe using mass balance
- Test script run:
  - Lowers upper specimen until set force is reached for 10 seconds
  - Retract upper specimen at set speed until grease strings broken
  - Excess grease removed from upper specimen
  - Lower specimen re-weighed to measure the grease pick-up onto the upper specimen
- Integrate the area under the curve from peak force to when the force reduces to below 0.1 using a Matlab script

5.8 Conclusions

A test method using a standard tribometer has been developed using an approach-retraction method. Initially, different test inputs were investigated to understand how the parameters affected the results. Parameters were chosen to limit the cavitation effects seen in results. The test method has been shown to be able to differentiate between different greases and so can be used as a benchmarking method. The effect of adding small amounts of a tackifier additive has shown that whilst it is difficult to get the right quantities of additive onto the test specimen, the effect of the additive can be seen in the maximum pull-off force results and tackiness of the grease. Preparation the grease prior to testing has an effect of the response of the grease and can be incorporated into the test method if required. The tackiness of the grease should be calculated by integrating the area under the force-distance graph from the maximum peak force to a period when the force is considered to be too low to be reliable. The length of this period is affected by many parameters so can only be determined by analysing the force-distance graph first. This is done to reduce errors in detecting small forces.

6 Grease Pick-Up and Carry-Down Performance

A recent masters project carried out at The University of Sheffield [118] studied the interaction between the wheel and grease bulbs from a grease distribution unit (GDU). The project used a rig with a scaled-wheel combined with a standard applicator system from the field (described in section 3.4). To analyse the effect the scaled-wheel had on the results of this project, the same GDU system was installed onto a Full-Scale Test Facility (FSTF) at The University of Sheffield (FSTF described in section 3.5). Tests were carried out at the same test parameters as the previous project [118] with the results compared.

A series of tests to assess how grease is transferred back to the rail once a wheel has picked it up is also carried out. The tests use the SWR described in section 3.4. The test parameters have been chosen to match previous grease pick-up work [117], [118] to explore if there is a relationship between pick-up and carry-down. Carry-down is defined in this context as the distance travelled down the track where the grease has an effect.

6.1 Validating Effect of a Scaled Wheel using a FSTF

6.1.1 Test Apparatus- Full-Scale Test Facility

Figure 81 is a photograph showing the attachment of the standard MC4-GDU to the FSTF. Other aspects of the FSTF can also be seen in the photograph. The lateral position of the wheel is set by lifting the wheel off the rail and manually moving it to the desired position. The wheel is only fixed on the ‘field’ side of the rail (opposite side to the GDU). During operation the wheel was observed to move laterally, increasing the gauge face to wheel flange back distance. This movement is variable from one wheel pass to another which will lead to increased variation in the results.

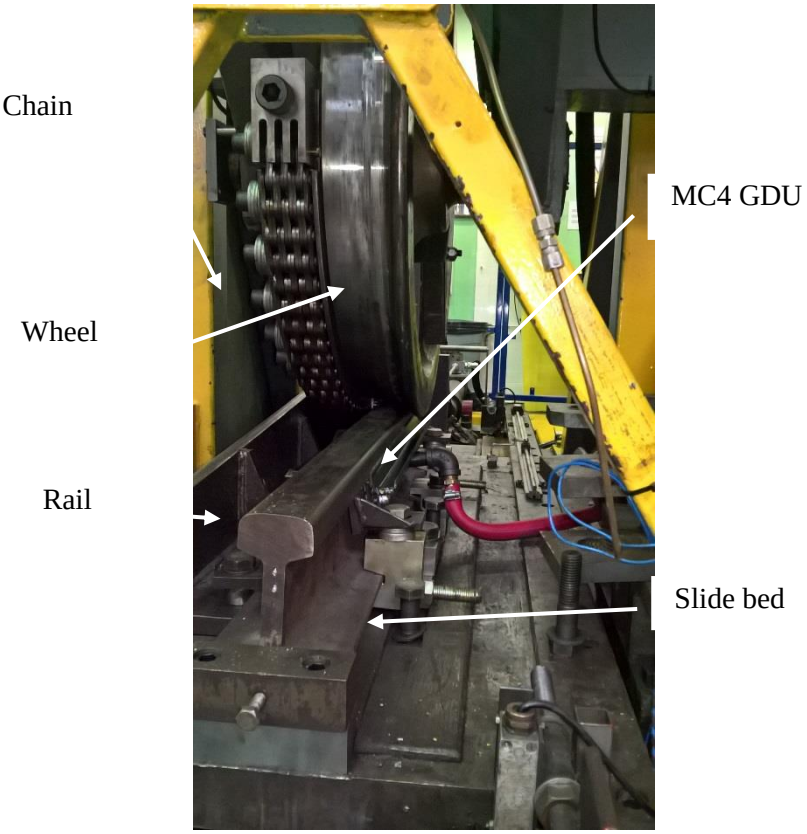

Figure 81- Set-up of MC4-GDU on FSTF

6.1.2 Test Methodology

Tests were carried out using the FSTF at lateral displacements and pumping durations to match the SWR [118] study, with each parameter tested three times. Grease pick-up was measured by mass of the grease adhering to the wheel and photographs were taken to capture the pattern of grease pick-up. The mass of grease was recorded using a set of scales that is accurate to ± 0.005 g with a tare mass of multiple cotton pads taken before using them to remove the grease from the wheel. The following additional parameters were used:

- Maximum contact pressure was 1000 MPa
- Rail velocity was 100 mm/s
- Slip was 0.5 %

To replicate field conditions as much as possible, and because for each test the grease had been removed for weighing, the level of grease on the GDU/rail was prepared prior to each test commencing. This meant establishing a base level of grease on the GDU/rail that is considered to replicate a standard established state in service. While this inevitably introduced a degree of tolerance, it was considered important to enable the test to represent a comparison in service rather than from clean rail. Due to the design of the FSTF, the preparation procedure carried out on the SWR for the standard MC4 had to be modified as it was not practicable. The bar was not wiped in between each measurement, to return the grease level to the prepared level, one pump of 0.3 s was added to the existing layer and one pass at a lateral displacement of 8.5 mm was carried out. This same preparation procedure was used for the MC4-GG as well. Pump output measurements were compared to the previous study [118] results to see if there was any

variation. Five measurements were taken at four different pump durations and the output of grease from the GDU weighed.

6.1.3 Results

Figure 82 shows the results from comparing the pump output from this study to values reported in the previous study [118]. The pump outputs a very similar amount for the short pump durations with a small deviation at the higher pump duration. This work focusses on the shorter durations. Therefore the pump outputted the same amount of grease in both studies.

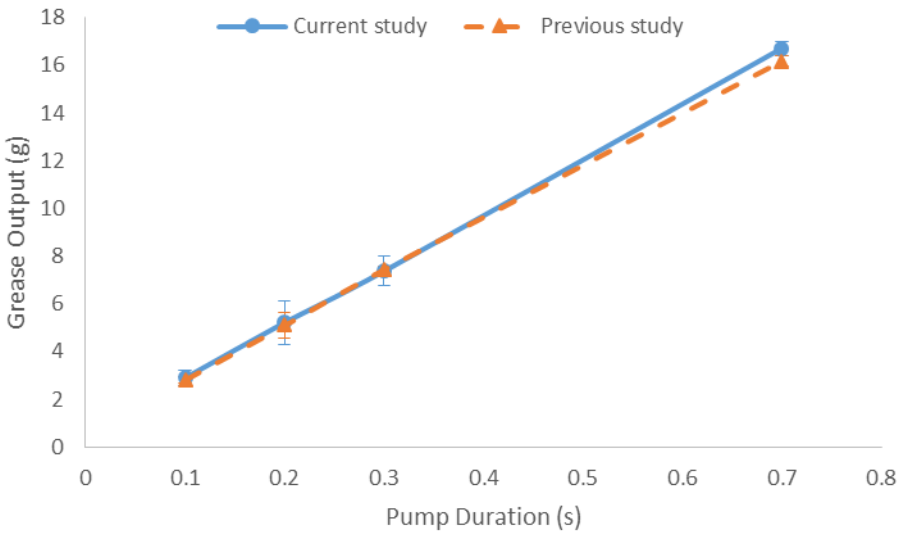

Figure 82- Comparing pump output from this work to previous work [118]

Figure 83 shows how the FSTF results compare to the SWR for the standard MC4 applicator. It can be seen from the graph that for a particular pump duration, there is an increase in pick-up as lateral displacement increases. For the FSTF results there is not a significant difference in pick-up when pumping duration is increased for a particular lateral displacement. This is in contrast to the SWR results which did show an increase in pick-up as pumping duration increases. It is unclear why the FSTF results for the higher pumping durations were considerably different to the SWR results although the different normalisation procedure between the two test rigs will have influenced the results. Data was not collected on the amount of grease forced up or down. The larger flange on the full size wheel could have been responsible for dragging down more grease, and not wiping the grease bar between test runs exacerbated this effect. This would explain why the higher pumping durations did not show an increase in pick-up as more grease was pulled down rather than transferred to the wheel.

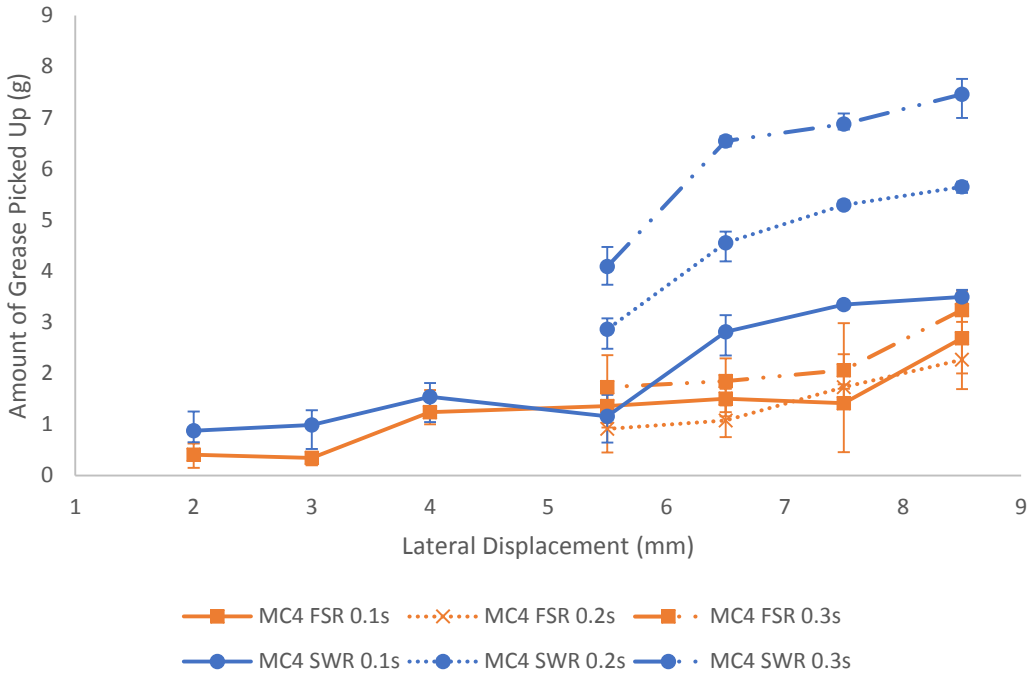

Figure 83- Lateral displacement vs mass of pick-up for both the SWR and FSTF, for different pump durations using the standard MC4 applicator

Figure 84 shows how the FSTF results compare to the SWR results for the MC4-GG applicator. Overall, there is general trend for a small increase in grease pick-up for increasing lateral displacement using both rigs (although there are anomalies within the data which show the opposite). In contrast to the standard MC4 data, there is a clear increase in mass pick-up for increasing pump duration for both test rigs. The error bars showing the maximum and minimum repeat values in Figure 83 and Figure 84 display an increase in scatter within the results for the MC4-GG applicator. This could account for some of the anomalies within the general trends described above, particularly as the range of pick-up values is smaller with the GG installed when compared to the standard MC4 applicator. Increasing the number of repeats would help improve analysis of the data as anomalies would have less effect on the average values. The absolute values of mass pick-up are different between the FSTF and SWR with the FSTF always producing less grease pick-up. The increased size is likely to have an influence as well as the inability to lock the wheel on the FSTF at a particular lateral displacement. Although the absolute values are different, overall the same trends are observed on both test rigs.

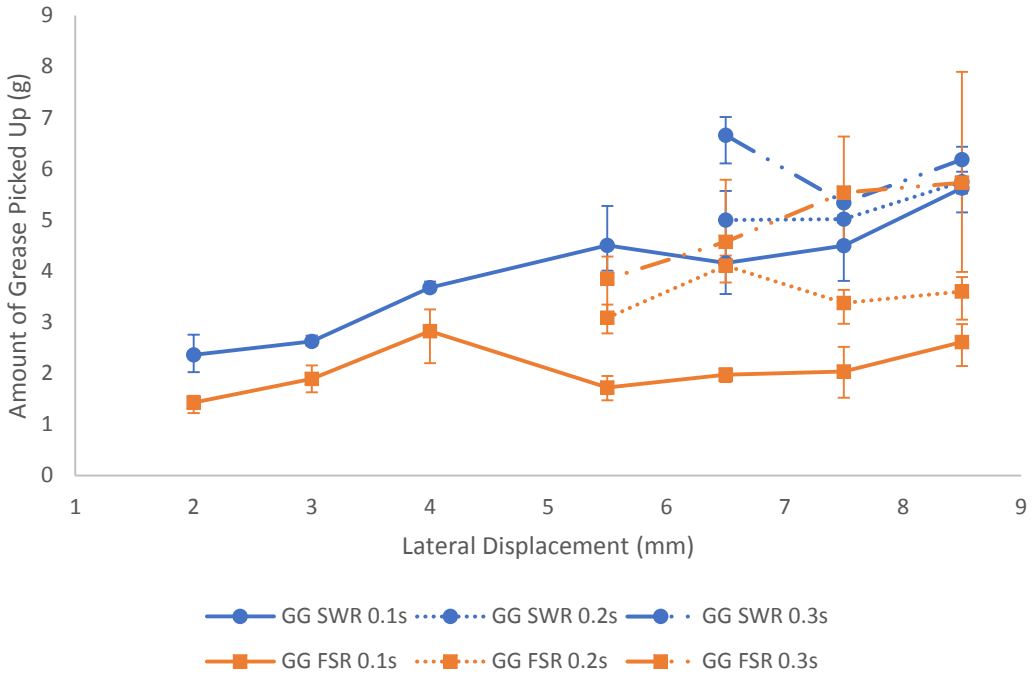

Figure 84- Lateral displacement vs mass of pick-up for both the SWR and FSTF, for different pump durations using the MC4-GG applicator

Figure 85 shows photographs taken after one wheel pass through the two different GDU's. The pumping duration and lateral displacement was the same for both photographs. It can be seen that the GG provides a larger smear of grease across more of the flange toe compared to the standard MC4. These findings are typical of the observations across the different lateral displacements and pumping durations.

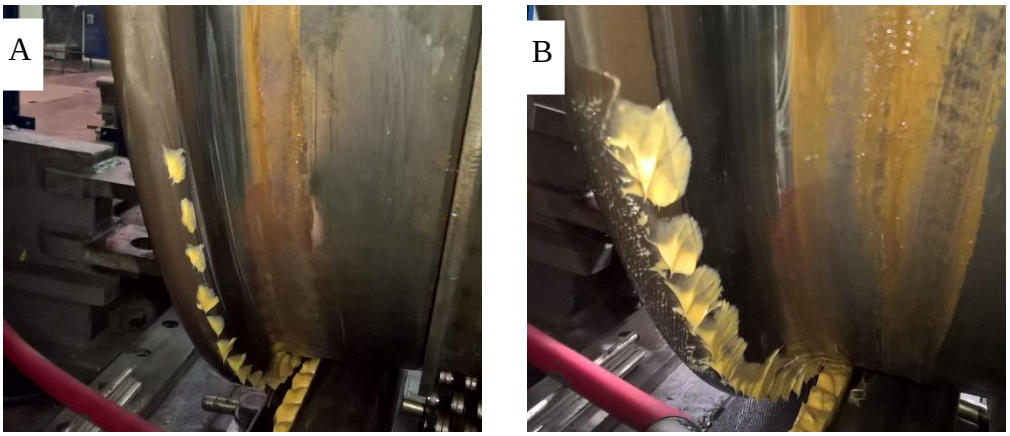

Figure 85- Pick-up of grease onto wheel from one wheel pass at lateral displacement 6.5 mm using A) standard MC4 GDU, B) MC4-GG

6.1.4 Conclusions

The validation tests of the SWR using the FSTF has shown the following:

1. Mass of grease picked up increased with wheel displacement toward the rail for a given grease output.
2. Mass of grease picked up increased with increasing output for a given wheel displacement.

These conclusions are in agreement with the SWR study. This series of tests showed that although the absolute values differ between using the SWR and FSTF, the same relationships do hold for both test rigs. These findings have been shown to be influenced by scale and could further be influenced by wheel speed.

6.2 Carry-Down Scaled-Wheel Tests

6.2.1 Test Methodology

The Scaled-Wheel Rig (SWR) and lubrication equipment described in section 3.4 was used in this series of tests. In order to standardise the grease layer for the MC4 GDU, the wheel was rolled three times at a lateral displacement of 8.5 mm through grease that was pumped for 0.3 s. For the MC4-GG the wheel was rolled six times at a lateral displacement of 8.5 mm through grease that was pumped for 0.5 s.

Due to the large number of variables available it was determined to use test parameters which matched field conditions as closely as possible. The following test parameters were used:

- GDU: MC4 and MC4-GG. Both bars are set at the height specified by the manufacturer
- Pump duration: 0.1s and 0.3s
- Pick-up lateral displacement: 2 mm, 5.5 mm, 8.5 mm
- Carry-down distances: 18 mm and 28 mm
- Grease: RSClare Trackside

Once the grease level was prepared on the grease bar, one pump of the required duration is added and the wheel is rolled through at the set pick-up lateral displacement. The grease bar is removed from the rail and the rail cleaned of grease. The wheel is moved laterally by a set distance (either 18 mm or 28 mm). This causes the wheel flange to contact the rail and allows simulation of the wheel travelling around a curve despite the rail being straight. As two different distances are used, two different curves are simulated: a shallow curve in the case of the 18 mm distance and a sharp curve in the case of the 28 mm distance. The wheel is rolled down the rail and the resultant mass transfer of grease is recorded by wiping the rail with paper towels and weighing them using a set of scales accurate to ± 0.005 g. The wheel returned to the start position and rolled down the rail again. The wheel was rolled down the rail five times for each set of results. It was found that after five passes the mass transfer of grease to the rail was negligible and stayed constant. Each parameter was tested three times.

6.2.2 Results

To show that the change in normalisation procedure for the MC4-GG and the change in grease from previous work [117] does not affect the amount of grease pick-up, the mass of grease pick-up is shown in Figure 86. It shows that for the MC4 bar the trackside grease has a slightly higher pick-up than supreme grease. The MC4-GG also shows a higher pick-up for the trackside grease but the difference is much greater at the high lateral displacement. This is due to the different preparation procedure.

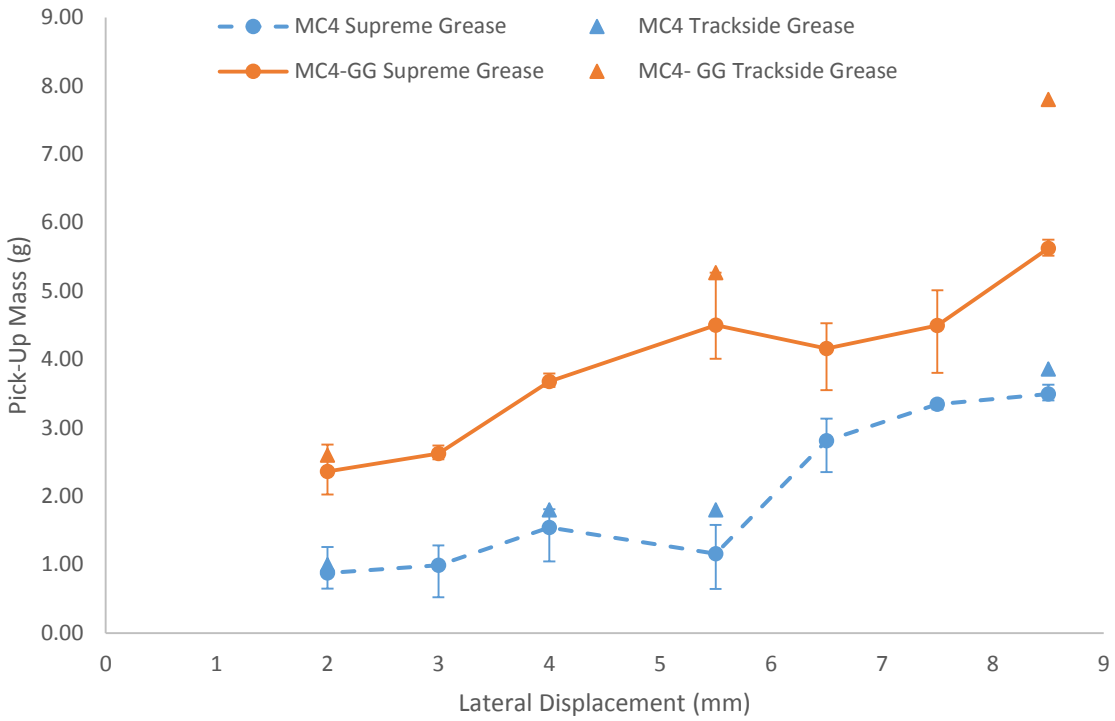

Figure 86- Graph comparing grease pick-up from this tests to previous work [117]

Figure 87 compares the mass transfer of grease to rail to wheel roll number for 2 mm pick-up displacement for the standard MC4 applicator. There is less grease transfer to the rail for an increase in pass number. It can clearly be seen that an increase in pump duration increases the mass transfer of grease to the rail from the wheel. It can also be seen that there is a sharp decrease in mass transfer between the first few passes for the 0.3 s pump duration before the mass transfer remains steady for the later passes. For the 0.1 s pump duration results the drop in mass transfer between each roll is lower than for the 0.3 s pump duration results. This is due to the initial mass transfer being much lower. The increase in carry-down distance results in a small increase in mass transfer to the rail for all roll numbers.

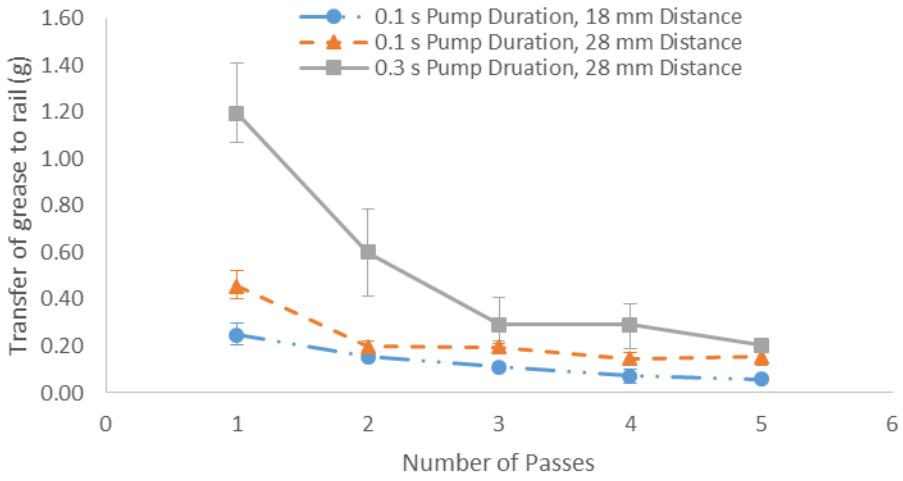

Figure 87- Graph comparing mass grease transfer to the rail and roll number for 2 mm pick-up displacement (MC4 bar)

Figure 88 compares the mass transfer of grease to rail to wheel roll number for 5.5 mm pick-up displacement for the standard MC4 applicator. For an increase in pump duration there is not an increase in mass transfer of grease to the rail, this is in contrast to the result in Figure 87. For roll 1 for the 0.1 s pump duration results, the mass transfer of grease is higher than in Figure 87. The increase in carry-down distance again results in an increase in mass transfer for all roll numbers.

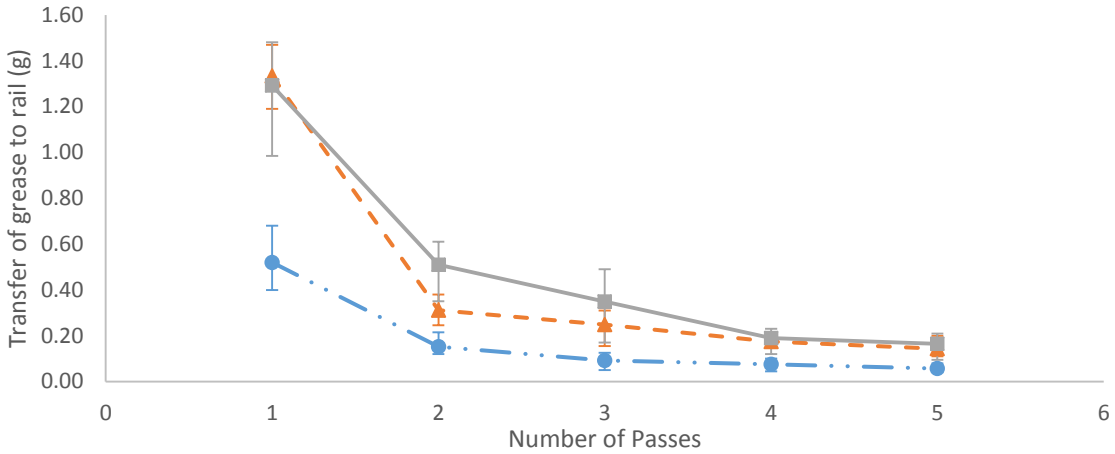

Figure 88- Graph comparing mass grease transfer to the rail and roll number for 5.5 mm pick-up displacement (MC4 bar)

Figure 89 compares the mass transfer of grease to rail to wheel roll number for 8.5 mm pick-up displacement for the standard MC4 applicator. The relationships described previously for Figure 88 are also displayed in Figure 89.

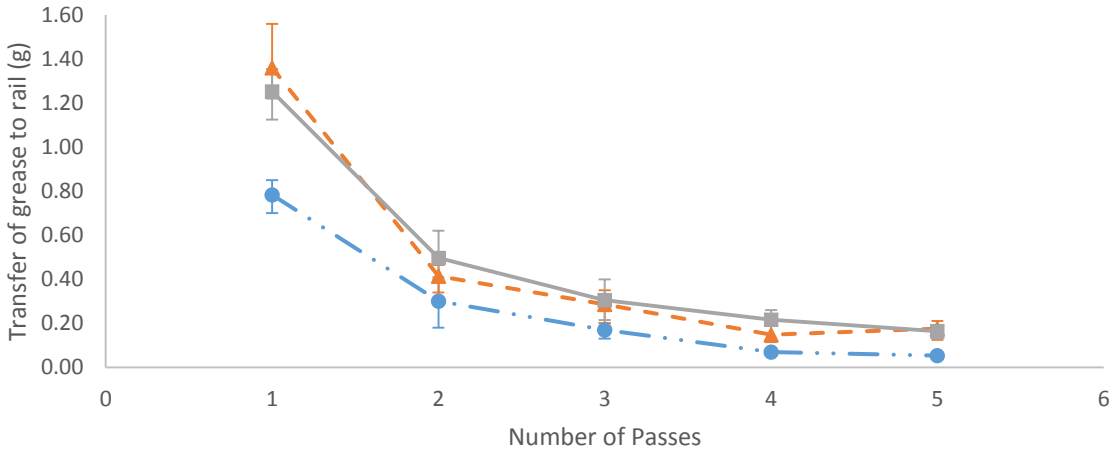

Figure 89- Graph comparing mass grease transfer to the rail and roll number for 8.5 mm pick-up displacement (MC4 bar)

Figure 90- Figure 92 compares the mass transfer of grease to rail to wheel roll number for 2 mm, 5.5 mm and 8.5 mm pick-up displacement respectively for the MC4-GG applicator. In all three graphs the 0.1 s pump duration, 18 mm carry-down distances results in no transfer of grease to the rail from the wheel. For the other results, increasing the roll number leads to a lower mass transfer of grease. In two cases (Figure 90 and Figure 92), the higher pump duration results in a lower mass transfer of grease to the rail. The amount of mass transfer to the rail for

the MC4-GG applicator bar is significantly lower than for the standard MC4 bar (Figure 87-Figure 89).

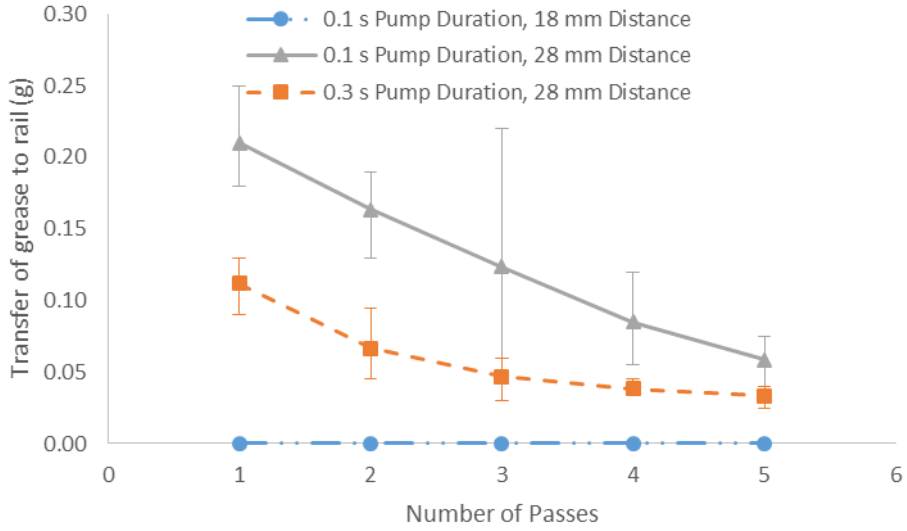

Figure 90- Graph comparing mass grease transfer to the rail and roll number for 2 mm pick-up displacement (MC4-GG bar)

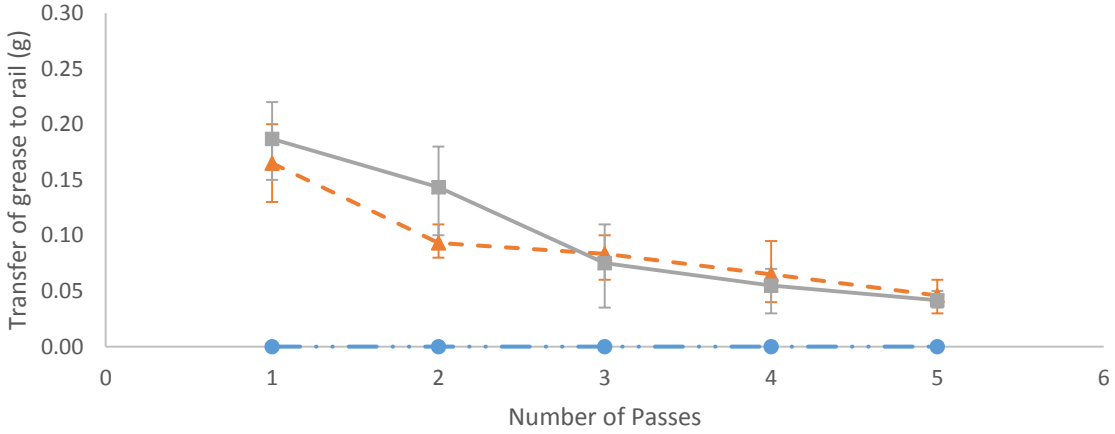

Figure 91- Graph comparing mass grease transfer to the rail and roll number for 5.5 mm pick-up displacement (MC4-GG bar)

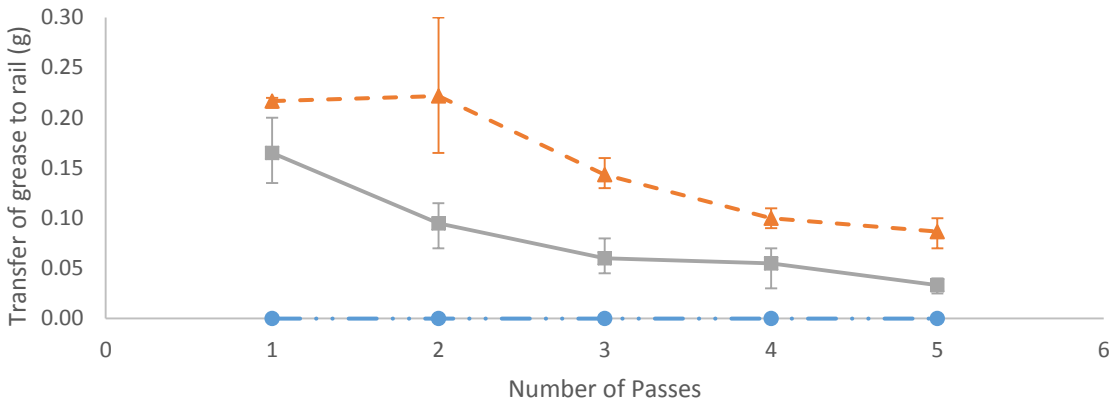

Figure 92- Graph comparing mass grease transfer to the rail and roll number for 8.5 mm pick-up displacement (MC4-GG bar)

6.3 Discussion

The most surprising result from the testing is that the MC4-GG applicator produces less carry-down of grease than compared to the MC4 applicator and in one case resulted in no carry-down of grease. It is surprising because the MC4-GG has been shown to have more grease pick-up than the standard MC4 bar in previous work. Figure 93 shows photographs from one set of parameters for both applicator bars which help to explain the results. It is clearly seen that whilst the MC4-GG bar has more grease on the wheel, very little of it is where contact has occurred, with most of the grease deposited near the flange tip during pick-up. This in contrast to the standard MC4 bar where the grease is deposited nearer the flange root in pick-up and subsequently there is more grease in the contact zone. This shown by the grease being squeezed either side of the contact zone. The reason for this result is due to the mounting height of the applicator bar. The MC4-GG was mounted at a height of 29 mm (as per manufacturers specification) below the rail crown whereas the standard MC4 bar has mounted at a height of 19 mm (as per the manufacturers specification) below the rail crown. The lower mounting height is due to the foam pad needing to be low enough for the wheel flange not to damage it.

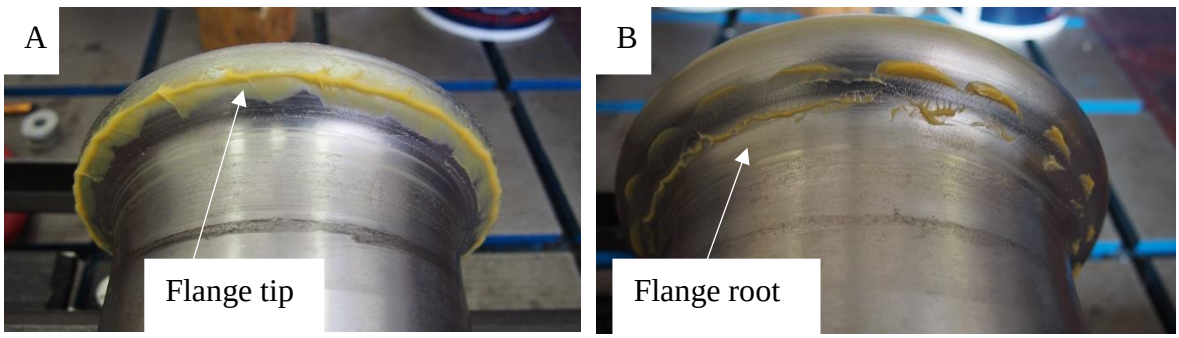

Figure 93- Photographs showing the wheel after one roll for A) MC4-GG applicator B) MC4 applicator. 8.5 mm pick-up lateral displacement, 0.1 s pump duration, 28 mm carry-down displacement

Figure 94- Figure 95 show the wheel-rail position for both carry-down distancess. Both photographs show that a two point contact has occurred between the wheel and rail. This is realistic of field conditions during curving.

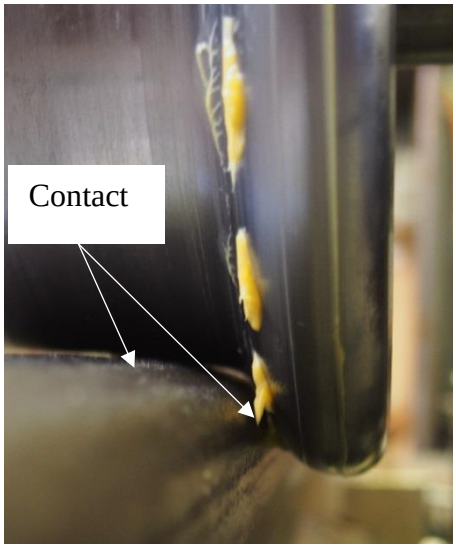

Figure 94- Relative wheel-rail contact for carry-down displacement of 18 mm

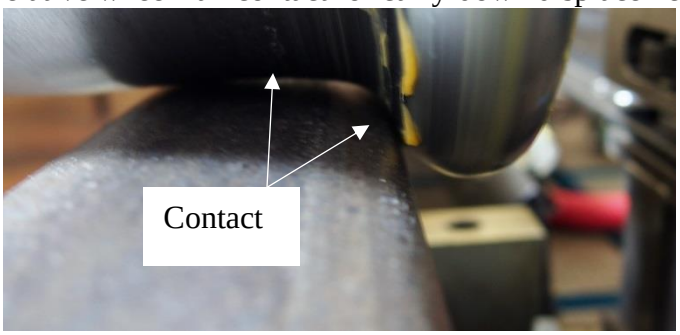

Figure 95- Relative wheel-rail contact for carry-down displacement of 28 mm

Figure 96 shows the wheel after five passes of two different pump durations. It helps to explain the results in Figure 87-Figure 91 which show no increase in grease carry-down for an increase in pump durations. This is because the increase in pump duration results in an increase in bulb size and pick-up of grease to the wheel, but the extra grease is not picked up in an area where contact occurs. It is picked up closer to the flange tip where contact does not occur. This means that although there is more grease on the wheel, there is actually the same amount of grease in the contact area in both cases. However, in the field, hunting of the wheel will occur, which means the contact position will change and this excess grease may be deposited onto the rail.

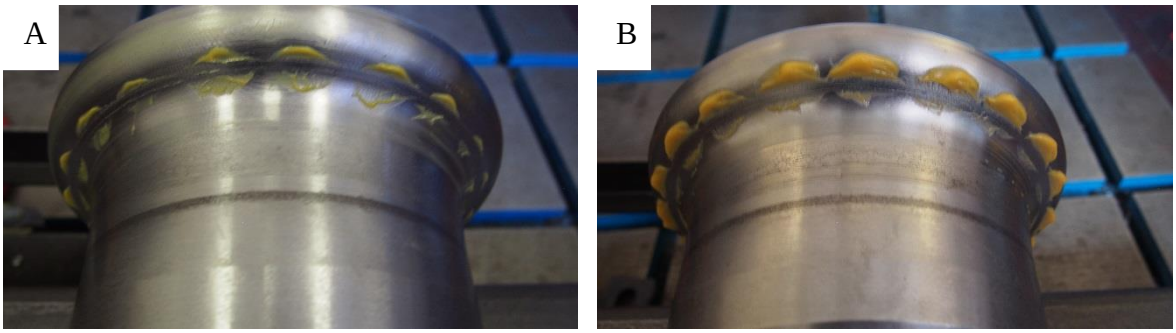

Figure 96- Photographs showing the wheel after 5 passes for A) 0.1 s pump duration B) 0.3 s pump duration. 5.5 mm pick-up lateral displacement, MC4 applicator, 28 mm carry-down displacement

Figure 97 shows photographs of the wheel after one roll at different pick-up lateral displacements. The photographs support the results in Figure 87- Figure 92 where the 2 mm

pick-up displacement has slightly different results than the 5.5 mm and 8.5 mm pick-up displacements. The results are different because there is little grease left on the wheel after one roll from the 2 mm pick-up displacement. This is in contrast to the other pick-up displacements where there is still areas of grease in or close to the contact area to feed the contact with grease, and provide mass transfer to the rail. These photographs also explain why there is a sharp drop in mass transfer to the rail after the first few passes compared to later passes. This is because initially there is a large blob of grease in the contact zone. After the first roll this blob is squeezed either side of the contact zone and subsequently on the next roll there is less grease available to be transferred to the rail.

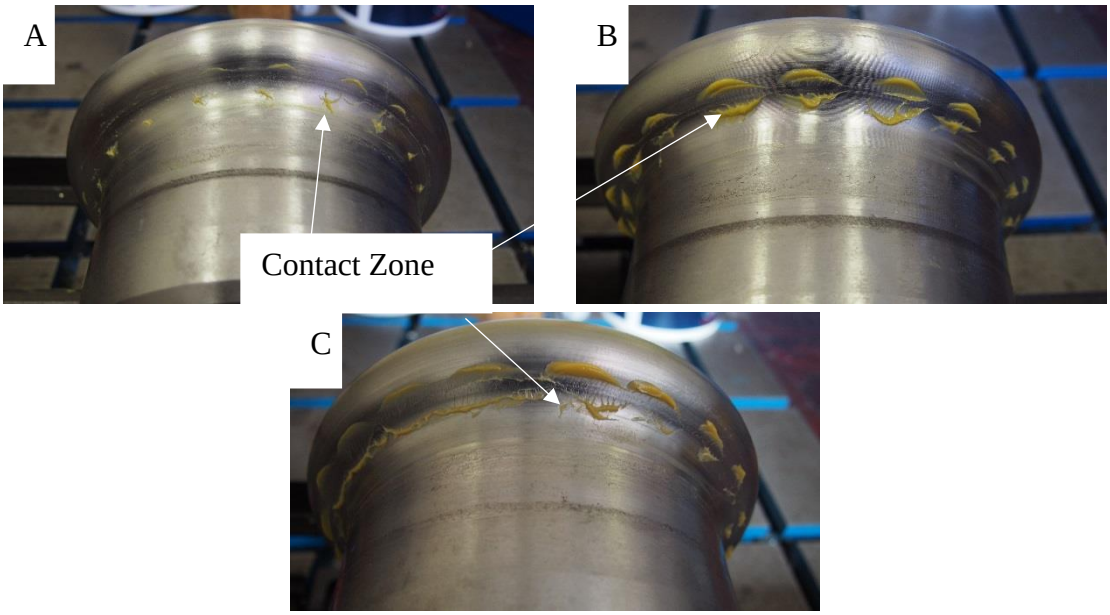

Figure 97- Photographs showing the wheel after 1 roll for A) 2 mm pick-up lateral displacement B) 5.5 mm pick-up lateral displacement C) 8.5 mm pick-up lateral displacement. 0.1 s pump duration, MC4 applicator, 28 mm carry-down distance

Figure 87- Figure 92 all show varying amounts of spread in the results. This is due to the manual nature of the test rig and the variability in achieving a consistent level of grease on the wheel after pick-up. The spread for the MC4-GG (Figure 90- Figure 92) is larger than the standard MC4 (Figure 87- Figure 89). This is due to the reduced mass transfer quantities leading to even a small variation in mass creating a proportionally larger spread. This means that it is difficult to draw conclusions from the data, which has large errors in it, but the general trends are important.

6.4 Conclusions

The most important conclusion from this work is that increasing the pick-up of grease to the wheel does not necessarily lead to increased carry-down. The location of the grease pick-up in relation to the wheel-rail contact is extremely important. This illustrates the complex interaction of wheel-rail contact and to optimise GDU operation, the whole system must be analysed rather than focusing on individual components.

Further work in this area is required in order to relate this work to the field and optimise GDU operation. How much grease is required to produce the required performance benefit is also an important factor. If this is known then the number of passes could be increased until the mass transfer to rail is below this level providing a measure of the distance of carry-down.

7 Grease Condition Monitoring

As a train travels along a track vibrations are created in the rails. This is caused by the roughness of the wheel and rail causing vertical excitations, which radiate away from the wheel-rail contact in all directions [119]. Roughness is the dominant cause of vibration, proved by agreement between models and measurements [120], but other contributors can be irregularities in the wheel or rail, such as wheel flats or rail joints. These dramatically increase the vibration via the same mechanism as roughness. Transverse excitation by the wheel flange contacting the gauge face in curves is another source of vibration. As roughness is the primary cause of vibration, any substance (for example oxides, leaves, friction modifiers etc.) that is present on the wheel or rail that changes the relative roughness will change the vibration in the rail. Additionally, if the substances change the creep characteristics, the vibration will also change. For example, friction modifiers cause positive creep characteristics which will reduce vibration compared to dry, negative creep characteristics. The presence of grease in the wheel-rail contact will have a dampening effect on the longitudinal vibrations in the rail as grease will make the relative roughness smoother and lower coefficient of friction in the wheel-rail contact.

7.1 Aim

The aim of this trial was to evaluate if measuring the longitudinal vibrations of the rail as a train passes a particular point is a reliable way of detecting the presence of grease. Variations between different trains, as well as train travel direction was also analysed. This trial used a test methodology that was initially developed in the laboratory on a scaled-wheel test rig. A second trial took place that looked at how the vibration in the rail changes during braking and during low adhesion conditions.

7.2 Vibration Measurement Equipment

Figure 98 shows a picture of the vibration measurement set-up. The following kit was used:

- Integrated Electronic PiezoElectric (IEPE) Accelerometer. This was chosen as it has an internal electronic preamplifier, which removes the need for an external amplifier. This is attached to rail via mounting block in the correct plane to record longitudinal vibration
- IEPE Signal Conditioner. Constant current battery power supply which provides charge to the accelerometer
- Data Acquisition Card. Receives voltage signal and samples it at the predetermined rate for transfer to PC.
- Laptop with Data Acquisition Software. In this case, a Matlab GUI is used to store the information from the data acquisition card.

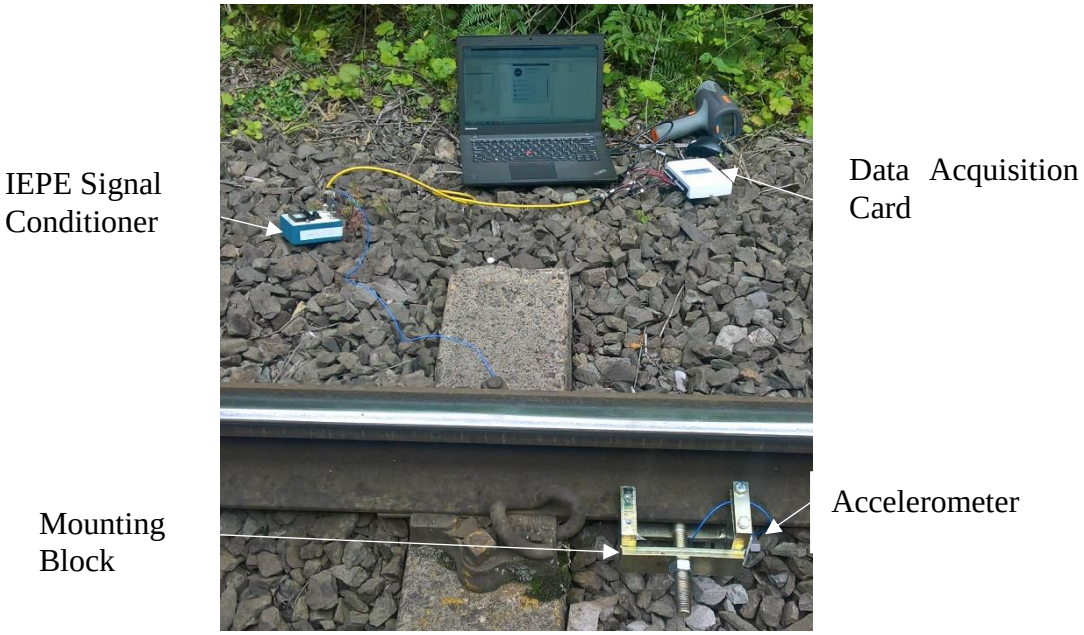

Figure 98- Vibration Measurement set-up of vibration monitoring kit

7.3 Test Methodology

7.3.1 Natural Frequencies

Initially the vibration measurement equipment described in section 7.2 was mounted on the Scaled Wheel Rig (SWR) (as described in section 3.4). The rail was hit with a hammer three times in four different spots (Figure 99 shows a schematic of the hammer hits at points A-D). This was done to gain an understanding of the natural frequency of the test set-up. This is a common technique to find the natural frequencies of small structures [121]. Knowing the natural frequencies of the test apparatus is important in order to characterise the system.

The test was repeated for both a "hard" hit of the rail and a "soft" hit. The hammer was swung by hand and an effort to maintain a consistent force of hit was made. Each measurement was taken three times and the results averaged. Whilst carrying out the field trial at Quinton Rail Technology Centre (QRTC), the rail was hit in six places as shown in Figure 100 (A-F). Again, each measurement was taken three times and the results averaged. This would enable the natural frequencies of the system on a mounted track to be compared to the short section of rail in the laboratory.

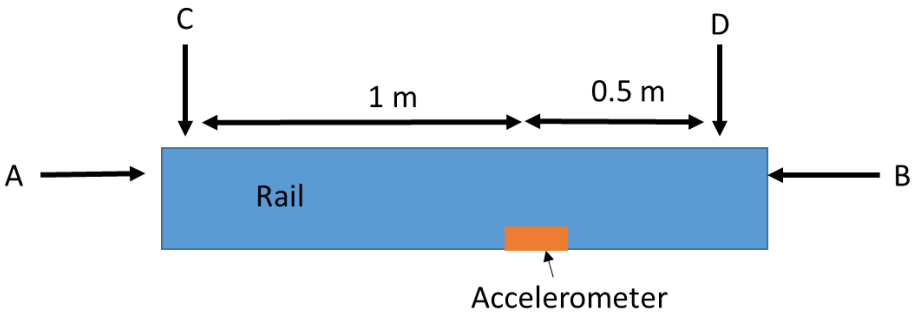

Figure 99- Schematic of hammer hits on SWR

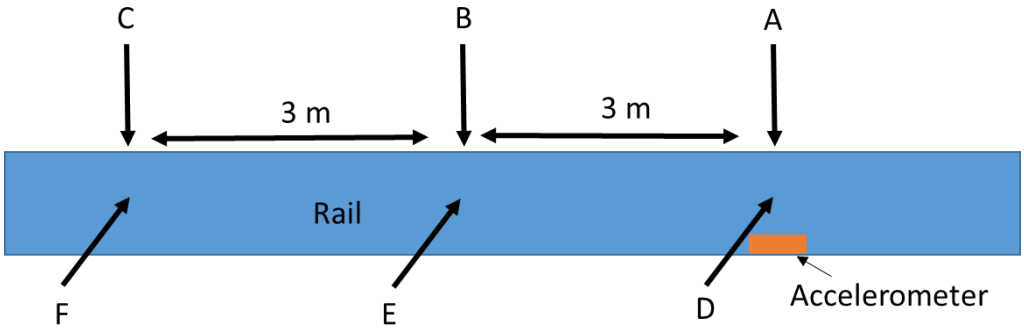

Figure 100- Schematic of hammer hits at QRTC

7.3.2 Laboratory Trial

A short trail run was carried out in the laboratory using the SWR. This compared the vibration in the SWR when the wheel is rolled along a clean rail to when there is grease present on the rail. Approximately 8 g of an approved rail curve grease was applied to the gauge face using a brush along a 1 m section of rail. This is an over application of what would be found in the field, but this test aims to identify the frequency range of interest, and to test the equipment rather than replicate field conditions precisely. The wheel was moved laterally until there was gauge corner/ wheel flange contact and the wheel rolled along a 1:10 inclined rail under gravity. Additionally, tests were performed with the wheel in tread contact with the same amount of grease applied to the top of rail. All measurements were repeated three times and the results averaged. The results are shown in section 7.5.1.

7.3.3 Severn Valley Railway

A field trial was carried out at Severn Valley Railway (SVR). The test equipment described in section 7.2 was mounted at three sites at different distances down the track from the lubricator, as shown in Figure 101. The lubricator (Figure 102) is located halfway between Bewdley and Arley, next to Trimpley Reservoir. This location was chosen as the lubricator was preparation well (no blocked ports) and is a place on the line where speeds are relatively constant. In addition, the lubricator set-up and rail profiles are the same as used on Network Rail track. As there is only one track at this point in the railway line, both directions of train were measured. There were four different trains on track on the measurement day (three steam engine trains and one diesel). One measurement site was on the entry to a curve, one site was halfway round the curve and the final site was at the exit to the curve. As only one set of recording equipment was available, the equipment was moved down to the next site once multiple measurements had been taken, and there was a suitable gap in the train timetable.

Additionally friction measurements were taken at all three sites using the pendulum (described in section 3.1) and hand-push tribometer (Figure 103). The hand-push tribometer is pushed along the rail and the friction is measured via a small measuring wheel that can be set to the top of rail or the gauge corner. The measurements were taken on a different day to the vibration measurements. It was raining lightly during the friction measurements meaning that the rail was wet during the tribometer measurements. Both the coefficient of friction on the top of rail and the gauge corner at all three sites were recorded from the tribometer. For the pendulum results, only the top of rail was measured. Coefficient of friction for three different contact conditions were recorded for the pendulum rig: dry, wet, wet and contaminated. The wet and

contaminated measurements were recorded by measuring the friction on the rail before cleaning it. The dry measurements were recorded by drying the rail, and the wet measurements by spraying the rail with water after dry measurements had been recorded. It is not possible to record the friction for the different contact conditions with the tribometer as a large section of the rail would have to be cleaned/dried which is not feasible. Each measurement was repeated five times.

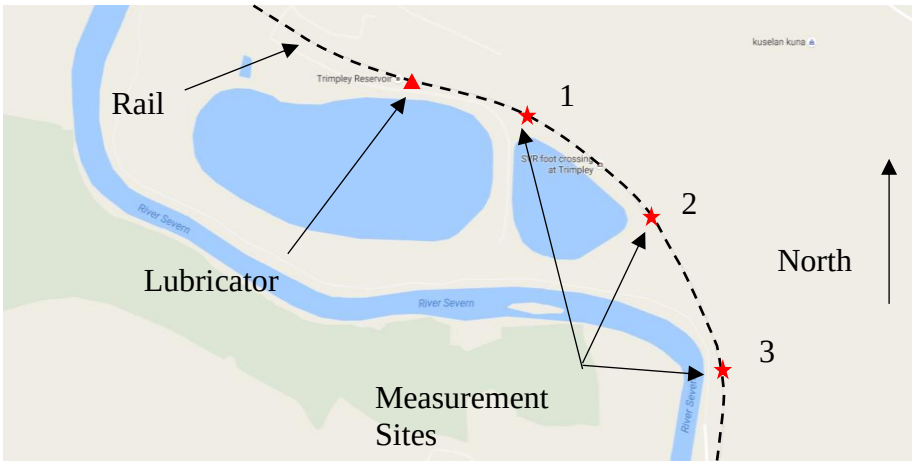

Figure 101- Location of measurement sites

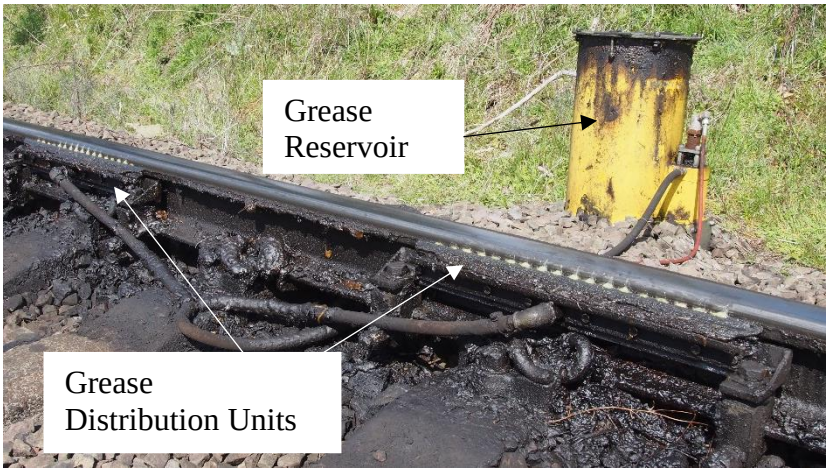

Figure 102- Lubricator Site


Figure 103- Hand push tribometer

7.3.4 Quinton Rail Technology Centre

A second field trial took place at Quinton Rail Technology Centre (QRTC) in Long Marston, Warwickshire. This series of tests focussed on the effect of leaf layer and water contamination in the wheel-rail contact. Two speeds were tested: 10 mph (16 km/h) and 25 mph (40 km/h). The rail conditions tested were:

- Dry
- Damp (caused by dew)
- Leaf contamination
- Wet leaf contamination

Leaf layers were generated by laying leaves on both rails (for 3 m and 6 m). The train was run over the test area five times to condition the layer before a test was completed. Figure 105 shows the railhead after a leaf layer has been formed. To test the effect of water contamination on leaf layer, the wheel-rail contact was constantly sprayed with water throughout the test by an on-board system. When the vehicle had passed over the test equipment the driver either applied the brakes or allowed the vehicle to coast to a stop. Figure 104 shows the layout of the test area and a summary of the different test conditions is shown in Table 7. A number of repeats of each condition were tested. The vehicle was a Class 117 DMU driven by the same driver for each test. The distance it took for the train to stop was also recorded.

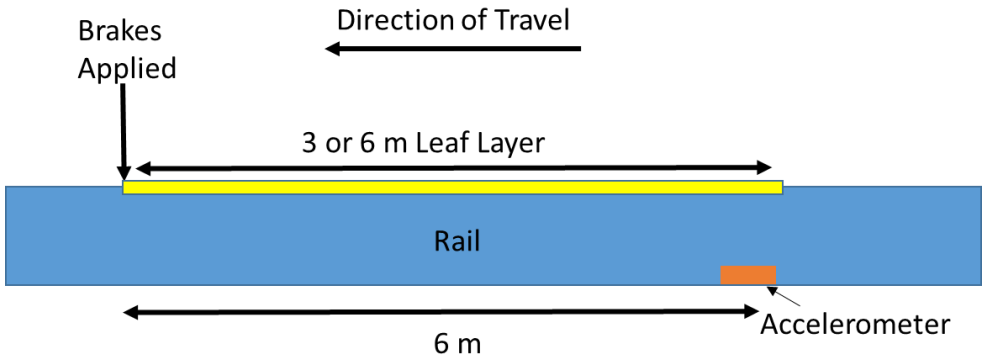

Figure 104- Schematic of QRTC field trail test area

Brake Condition	Initial Speed (mph)	Track Condition
Coast	10	Dry
Brake	10	Dry
Brake	25	Dry
Brake	10	Damp (dew)
Brake	10	3 m Leaf Layer
Brake	10	Wet 3 m Leaf Layer
Brake	25	3 m Leaf Layer
Coast	25	3 m Leaf Layer
Brake	10	6 m Leaf Layer
Brake	25	6 m Leaf Layer

Table 7- Test summary

Figure 105- Photo of railhead showing leaf layer contamination at braking point

7.4 Signal Processing

The raw data from the measurement equipment includes elapsed time, accelerometer output (in volts) and sample rate. To allow the important components of the signal to be differentiated from background noise in the signal a number of steps are carried out to get data into the frequency domain:

- Data Trimming

The first stage of processing is to trim each data set to the period of interest. For example at SVR, the time period was twenty-two seconds. This was the period from when the vibration started to increase to where the vibrations fell back to a "normal" level as shown in Figure 106. The start point for each train was selected manually.

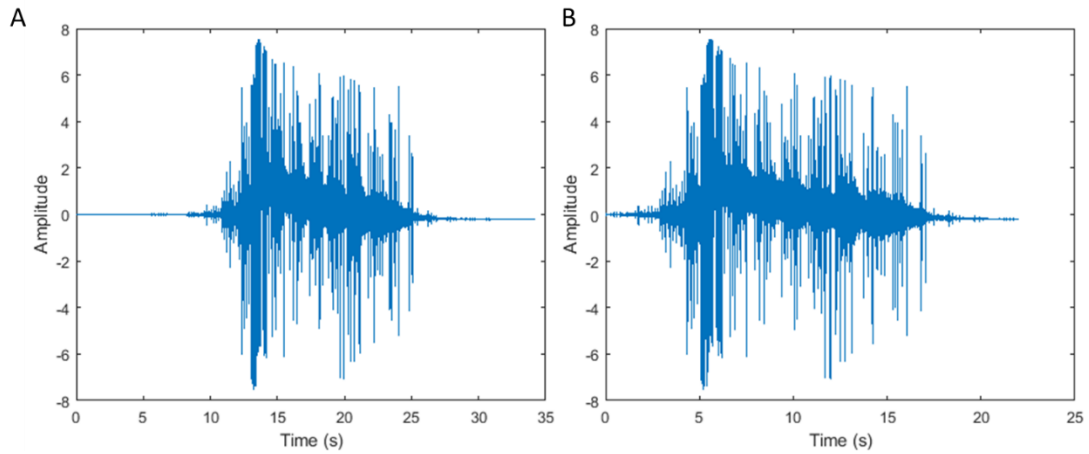

Figure 106- Data trimming example A) Raw data B) After trimming

- Windowing

If both ends of the trimmed signal are not the same, high frequency noise can be introduced when performing the Fourier transform. For this reason a Hanning window is applied to the trimmed data. This applies a cosine function to the data and ensures there is a zero amplitude at each end of the signal as shown in Figure 107.

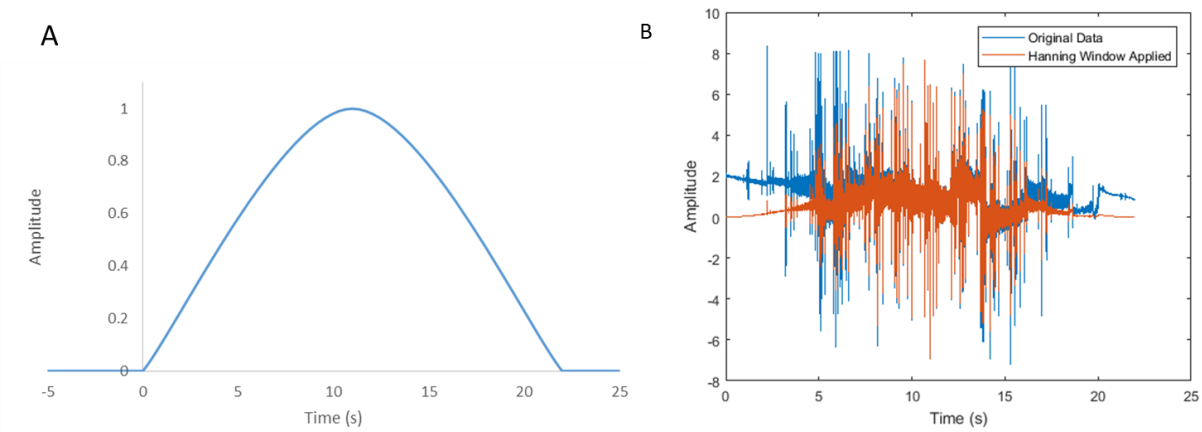

Figure 107- A) Hanning window for 22 second time period B) Example of Hanning window effect

- Filtering

A fourth order, low pass butterworth filter is used to filter out high frequency noise from the signal as shown in Figure 108. A cut-off frequency of 4000 Hz is used. This filter has been used in previous work from laboratory data and has shown to be appropriate for this application.

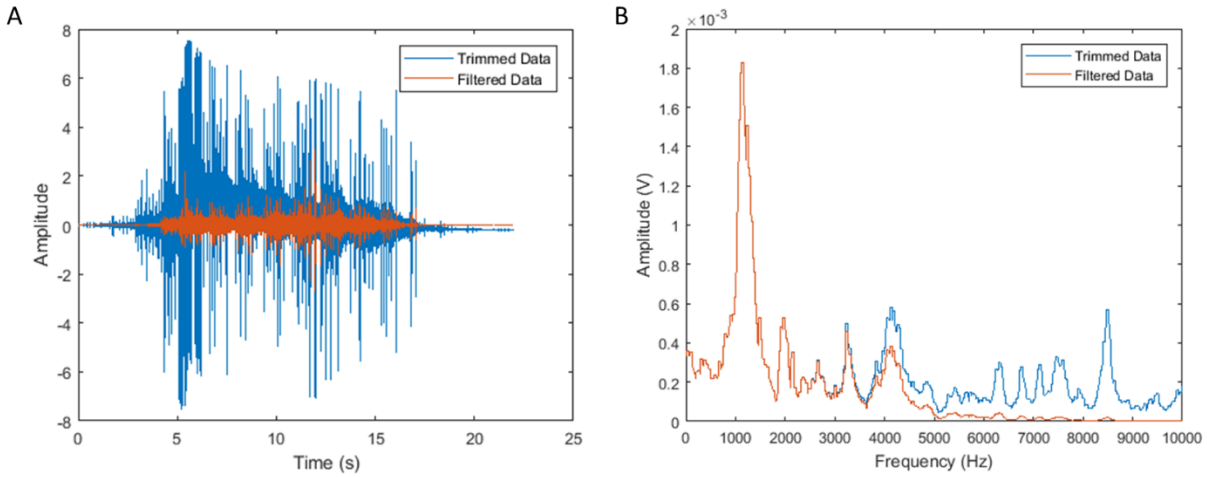

Figure 108- Filtered data example A) Time domain B) Frequency domain

- Fourier Transform

Converting data from the time domain to the frequency domain allows easier comparison between signals as the important components of the signal are easier to identify. A Fourier transform is used to convert the data to the frequency domain, an example is shown in Figure 109A.

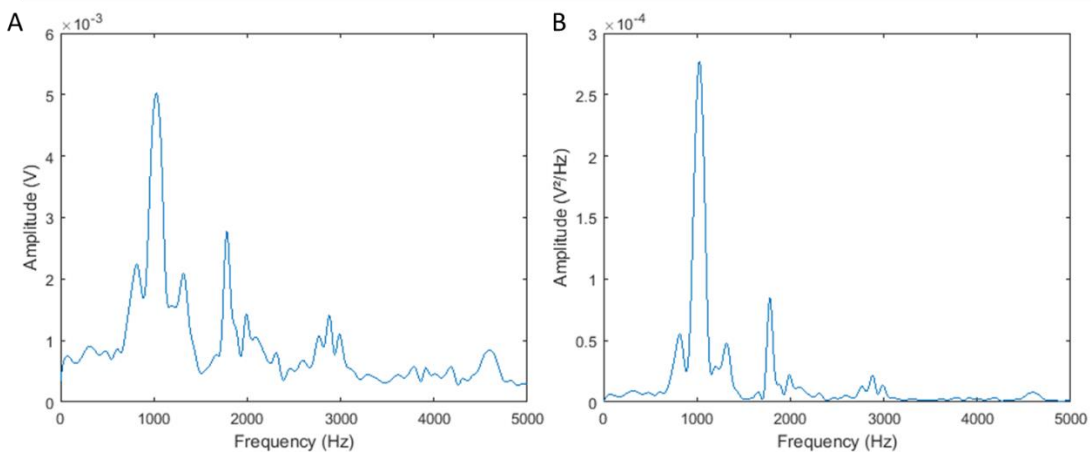

Figure 109- A) Fourier transform example B) PSD example

- Power Spectrum Density

When there is too much noise in the frequency spectrum an extra step is carried out. To get the Power Spectrum Density (PSD), the amplitude is multiplied by its complex conjugate and divided by the frequency. This helps to reduce the noise in the signal, allowing the important frequencies of the signal to be seen more clearly as shown in in Figure 109.

7.5 Results

7.5.1 Natural Frequencies of Measurement Set-Up

Figure 110 shows the frequency response when the rail is hit "hard" with a hammer at four different spots (the four spots are shown in Figure 99) in the laboratory. In each case the graph shown is the average of three hits and the frequency response is attained using the method described in section 7.4. Clearly, when the rail is hit at spot A and B there is a larger response than when the rail is hit at spot C and D. This is because the accelerometer records longitudinal vibration and the rail is hit in the longitudinal direction in cases A and B, but in the vertical direction at location C and D. In all instances, there are two clear peaks in the 1700-1900 Hz region corresponding to the first two natural frequencies of the test equipment.

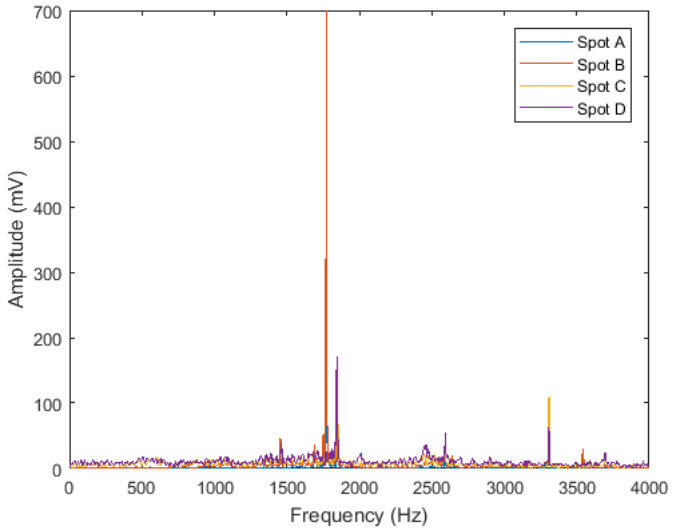

Figure 110- Frequency response recorded when rail hit hard with hammer at four different spots

Figure 111 shows the average PSD for the three locations from the test at QRTC when the rail is hit on the side (the schematic of the hits is shown in Figure 100). It clearly shows large peaks in the 3000-3500 Hz range with the largest amplitude at the same location as the accelerometer and smaller peaks lower in the frequency range. As the location of the hit moves further away from the accelerometer, more of the vibration from the hit is dampened resulting in a smaller amplitude.

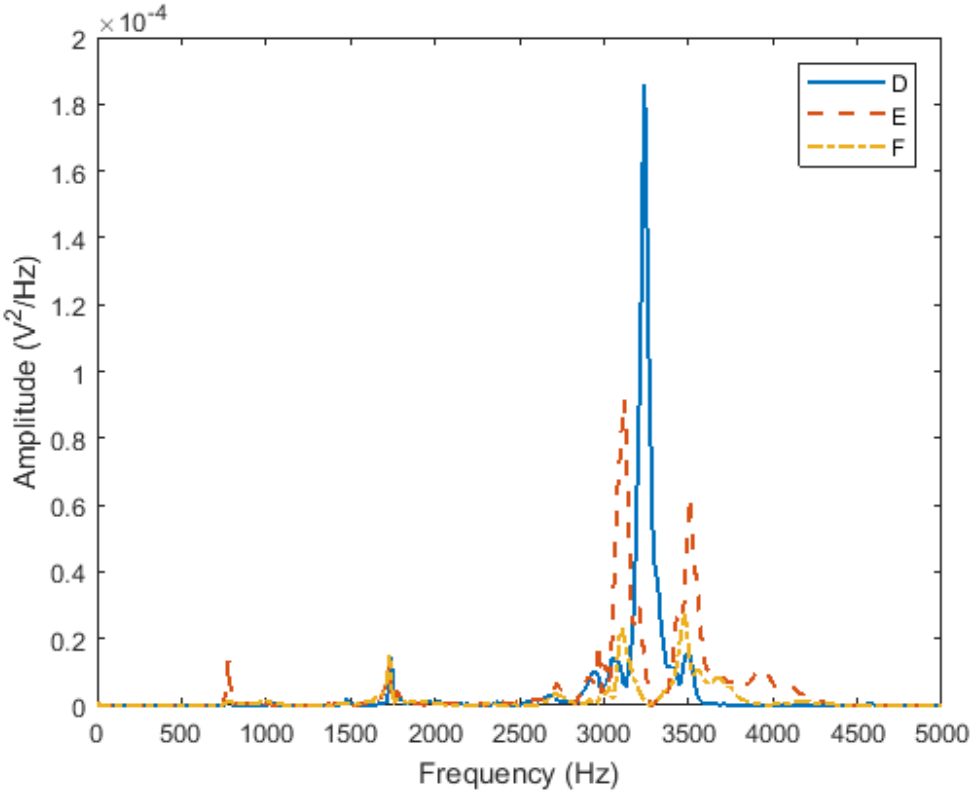

Figure 111- Average PSD for the rail hit on the side

Figure 112 shows the average PSD for the three locations from the test at QRTC when the rail is hit on the top. It shows peaks in the same range as Figure 111 and the same reduction in amplitude as distance from the accelerometer increases. It is important to note the change in y-axis between Figure 111 and Figure 112. The lower amplitude for the hits on top of the rail is due to the accelerometer recording the longitudinal acceleration. A hit to the top of the rail results in less vibration in the longitudinal direction than the hits to the side of the rail.

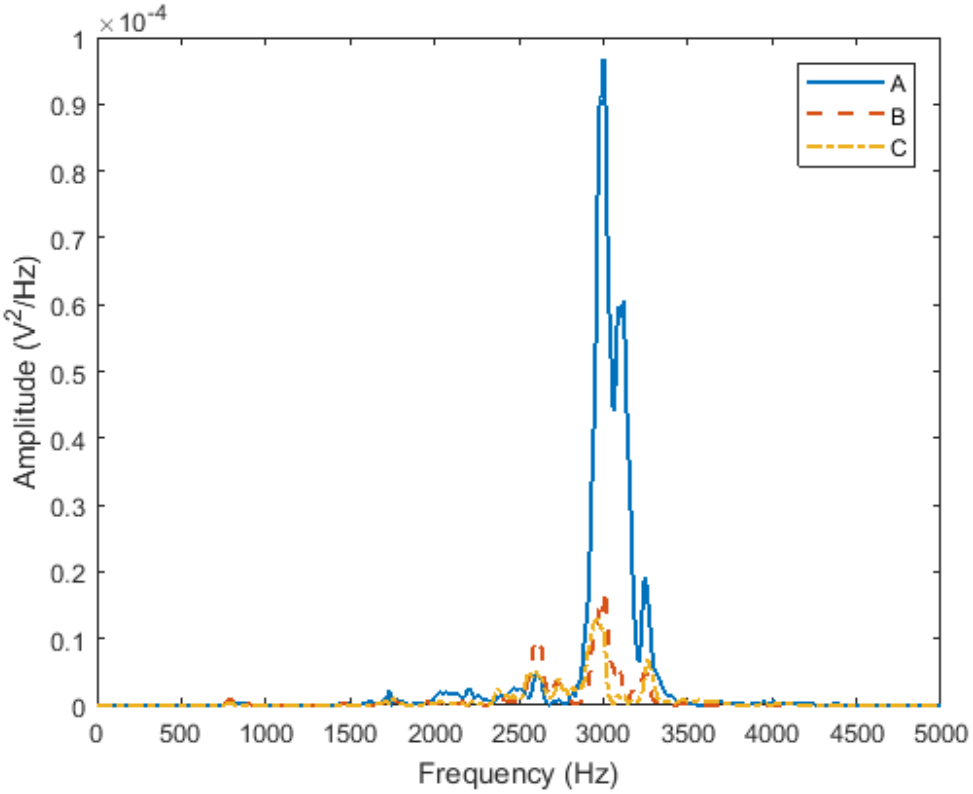

Figure 112- Average PSD for the rail hit on the top

7.5.2 Laboratory Trial

Figure 113 shows the average vibration response in the rail for the different contact conditions tested. For both tread and gauge corner contact the grease reduces the vibration, the reduction is more obvious in the tread contact. For gauge corner contact, the reduction in amplitude is in the 500-1000 Hz range. For tread contact, the reduction in frequency occurs across the whole frequency range.

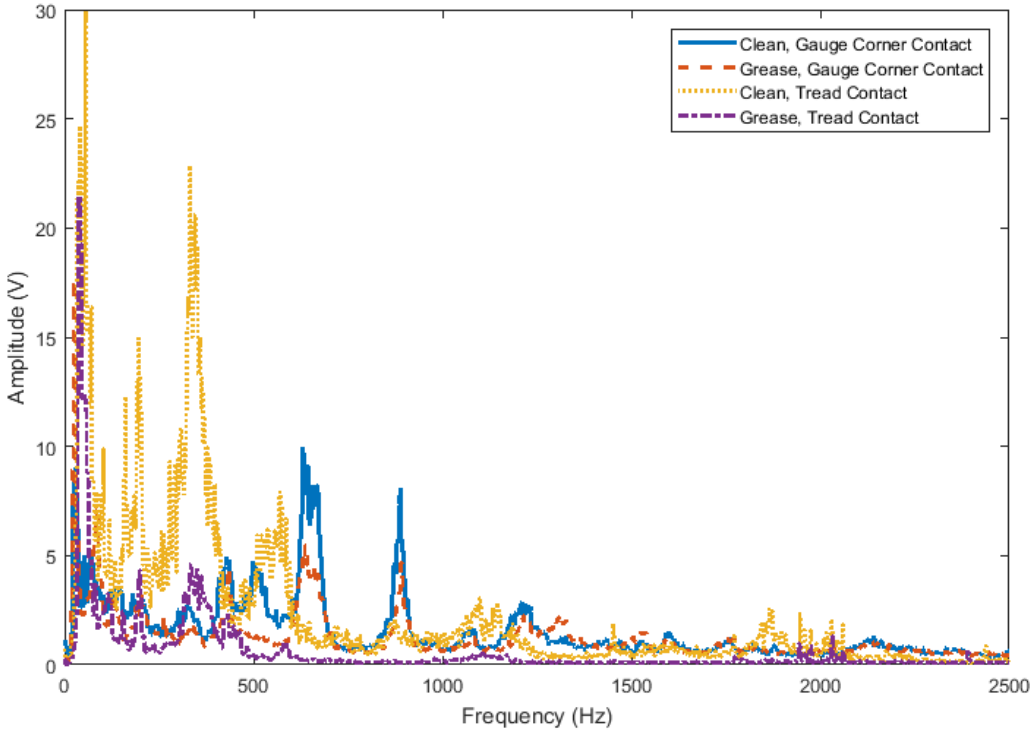

Figure 113- Vibration response from SWR for different contact conditions

7.5.3 Severn Valley Railway Field Trial Results

Figure 114 compares the vibration response in the rail from three different trains travelling southbound through measurement site three. Although there are small differences in amplitude, all three trains produce a similar response with two main peaks (illustrated on graph as primary and secondary peaks) at the same frequencies.

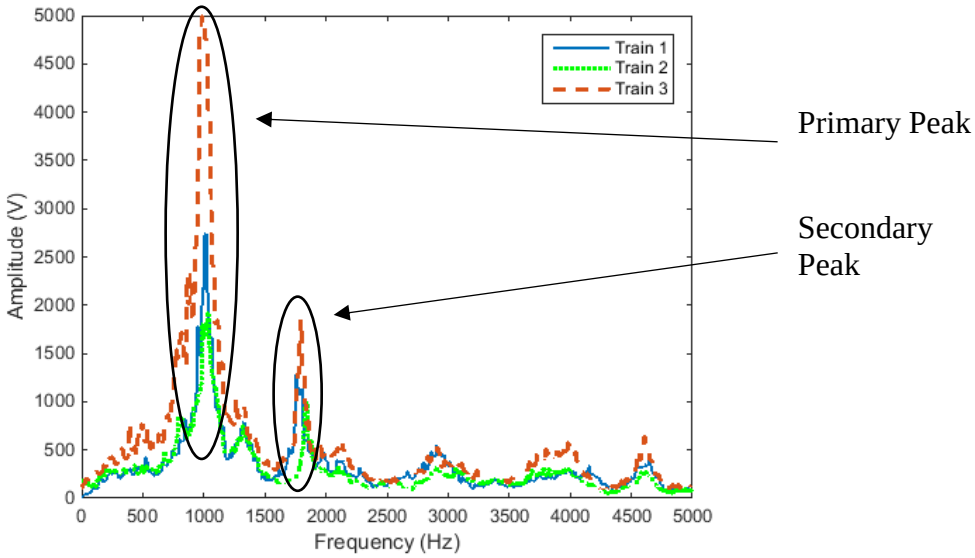

Figure 114- Three different trains passing the same measurement site

Figure 115 compares the vibration response in the rail from the three different sites. In all three cases, the train was travelling southbound. It is clear from the graph that the closer the site is to the lubricator, the lower the vibration. This is seen as a significant reduction in the primary and secondary peaks amplitude and in the case of site one, the secondary peak is almost non-existent.

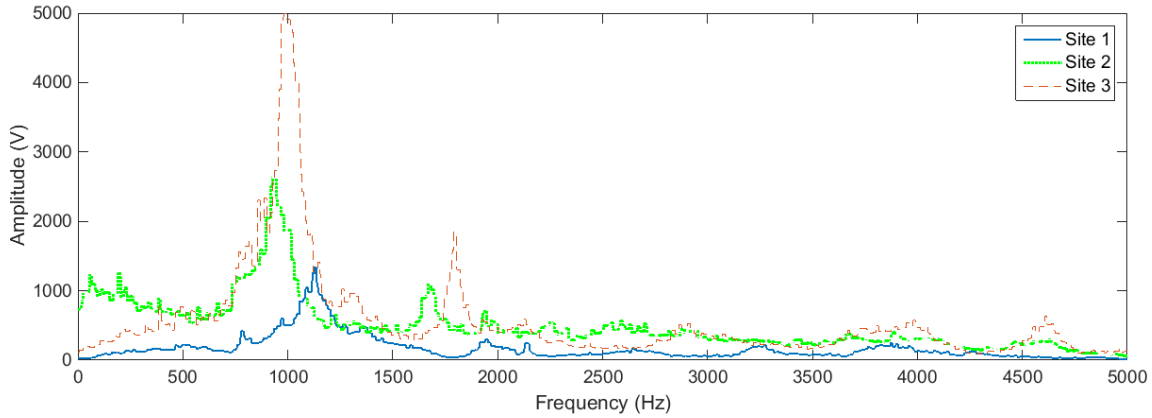

Figure 115- Comparing vibration response from the three different measurement sites

Figure 116 compares the same train passing through measurement site two, travelling northbound and travelling southbound. As in Figure 114 where different trains are compared, there is a small difference in the amplitude of the response, but the peaks are at the same frequencies.

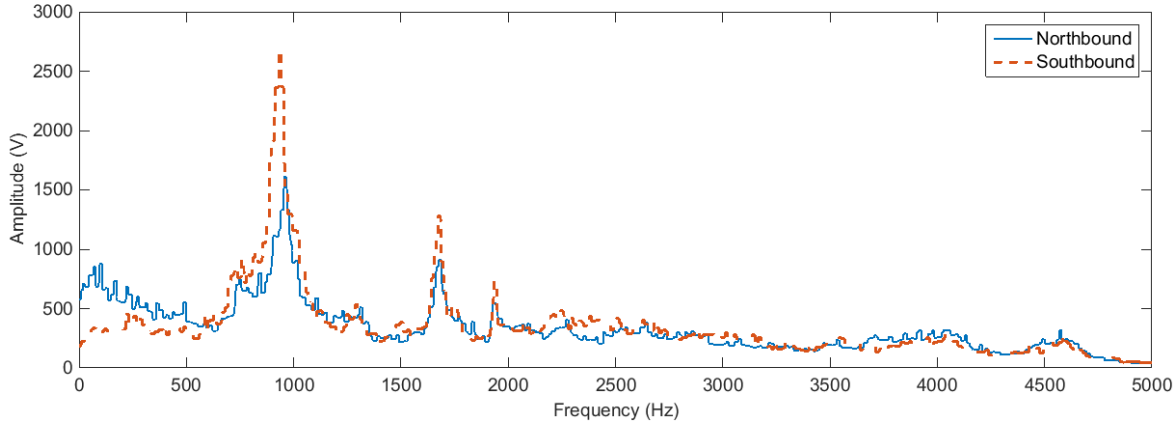

Figure 116- Graph comparing the same train travelling in both directions

Figure 117 shows the results of the friction measurements using the pendulum. The repeat results were consistent (shown by the small error bars). Overall, the trend is as expected, the highest friction coefficient for the dry contact condition. Spraying water onto the rail reduces the friction coefficient, and if water and contamination is present on the rail, the coefficient of friction is even lower. The lowest coefficient of friction was found at site 1. This site is close to the lubricator and the low friction coefficient could be caused by small amounts of grease contaminating the top of the rail. This hypothesis is supported by the fact that the rail without the lubricator on it has a much higher friction coefficient. Site 2 also had a lower friction coefficient than site 3 for the dry and wet condition. This could be because there were more trees overhanging the rail at this point leading to greater leaf contamination at this site.

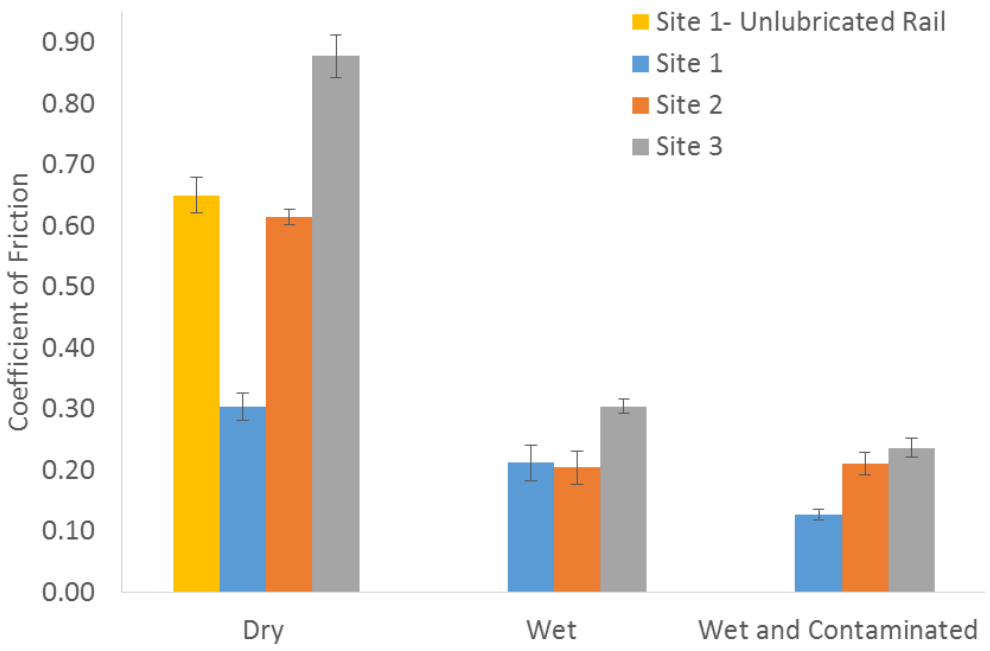

Figure 117- Pendulum friction measurements

Figure 118 shows the results of the tribometer tests. The absolute values cannot be compared to Figure 117 as it is a different contact. The tribometer measures a rolling-sliding contact between a metal wheel and the rail whereas the pendulum measures a sliding contact between rubber and the rail. The rail was wet and contaminated in all the results in the figure. For the top of rail results, the friction coefficient is similar for all three sites. Site 2 is slightly lower, caused by the larger tree canopy mentioned in the previous paragraph. For the gauge corner, the friction coefficient increases from site 1 to 3 (as distance from lubricator increases). This suggests that the amount of grease present on the gauge corner decreases as distance from the lubricator increases.

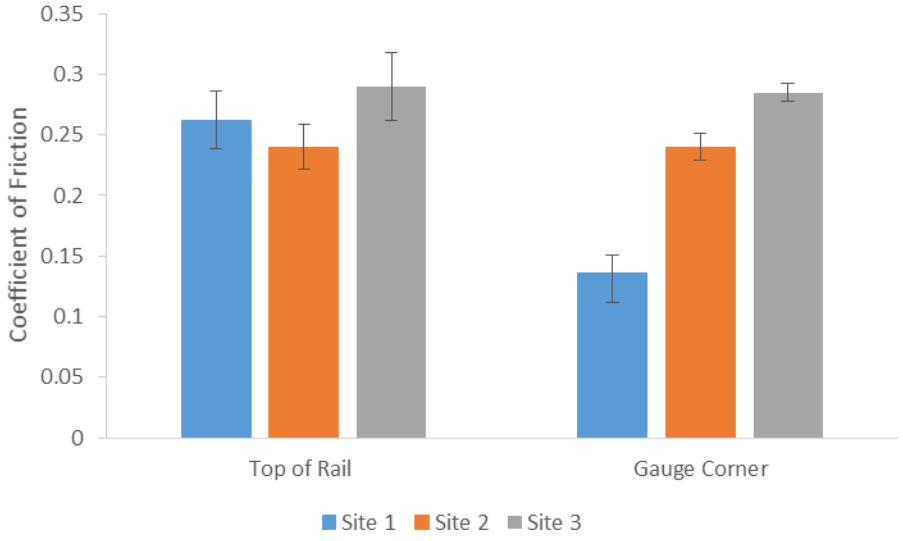

Figure 118- Tribometer friction measurements

7.5.4 Quinton Rail Technology Centre Field Trial Results

Figure 119 shows the vibration in the rail for different conditions, it is important to note the different y-axis scales at the different conditions. The tests shown in Figure 119A were carried out in the morning with moisture from earlier rain and dew present on the railhead. The initial speed of these tests was 10 mph (16 km/h). The railhead was observed to be drying with every pass of the train. This can be seen in Figure 119A as from pass 2- pass 5 there is a small increase in vibration in the rail. Pass 1 has a higher vibration than the other passes despite the rail being in the wettest condition of the five passes. This is caused by oxide having formed on the rail overnight. As this layer has only been formed overnight, it is very thin and so worn away on the first pass of the train. Figure 119C shows five dry coast tests at the initial speed of 10 mph (16 km/h). It shows that there is reasonably good repeatability between the five passes, with the exception of pass 4, which has a higher vibration than the rest. This could simply be down to driver error (braking differently to the previous four tests). Prior to this test the rail was scrubbed using a mechanical scrubber to remove a leaf layer from previous tests. This could explain the slightly lower frequency response below 1000 Hz for pass 1 as the rail was clean. The rail was not scrubbed between each pass so small amounts of dirt/dust etc. would be present on the railhead. Figure 119B shows three dry brake tests at the initial speed of 10 mph (16 km/h). The three tests show broadly the same vibration, but there are differences at certain frequencies and more variation compared to the coast tests in Figure 119C. This is due to the level of braking changing slightly from pass to pass and hence changing the frequency response. Figure 119D shows the vibration in the rail for five dry brake tests at an initial speed of 25 mph (40 km/h). There is no correlation between any of the passes, but the vibration is clearly at a higher amplitude than the 10 mph (16 km/h) tests shown in the rest of the figure. This is due to the faster initial speed increasing the severity of the braking forces. These braking forces are very transient due to variations in wheel slide/braking performance from pass to pass which varies the vibration in the rail.

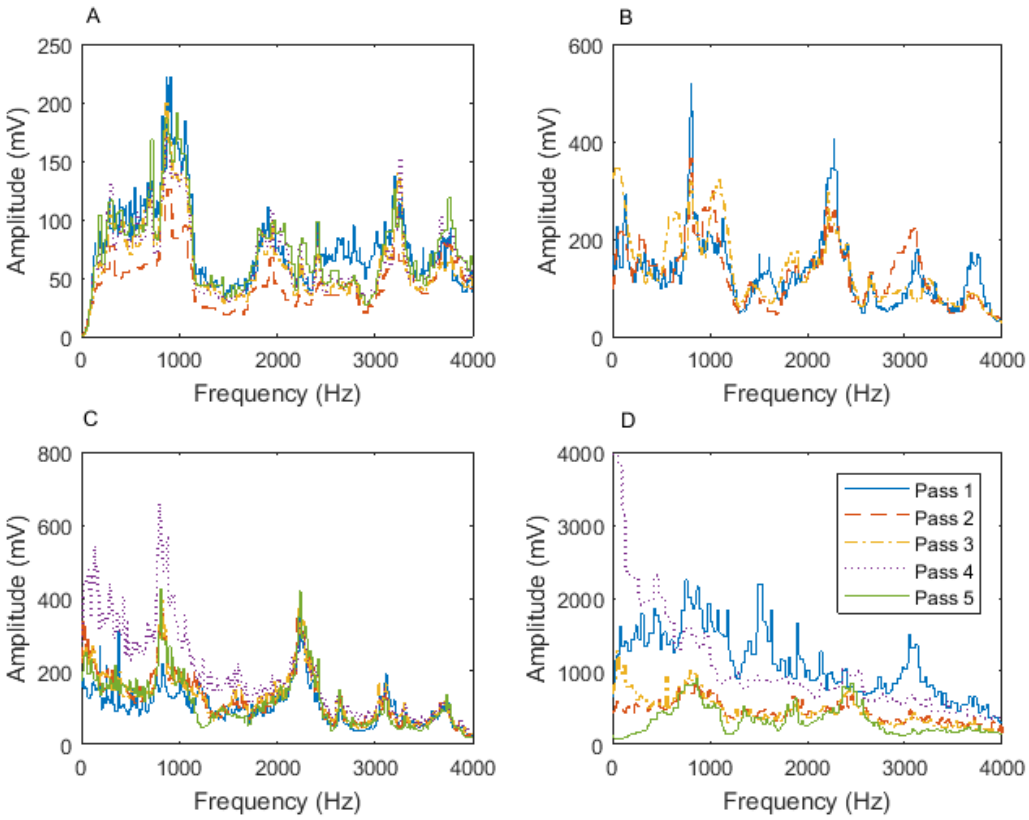

Figure 119- Rail vibration for rail A) Five 10 mph (16 km/h) brake tests at start of day with dew present on the railhead B) Three 10 mph (16 km/h) dry brake tests C) Five 25 mph (40 km/h) dry coast tests D) Five 25 mph (40 km/h) dry brake tests

Figure 120 shows the vibration in the rail when a 3 m leaf layer is applied to both rails just before the braking point. It is important to note the change in y-axis scale between A/B and C/D. The five brake tests shown in Figure 120A were carried out at 10 mph (16 kmh) and there is little variation from test to test. The four brake tests shown in Figure 120B were carried out at 10 mph (16 km/h) with water constantly applied to the contact. Again, there is little variation from test to test. The five tests shown in Figure 120C were carried out at 25 mph (40 km/h) and the vehicle coasted to a stop rather than braking. The five tests shown in Figure 120D were carried out at 25 mph (40 km/h) with brakes applied. There is considerably more vibration at 25 mph (40 km/h) compared to 10 mph (16 km/h) (shown by the higher amplitude). There is also slightly more variability in the response at 25 mph (40 km/h) compared to 10, caused by the same problems described above.

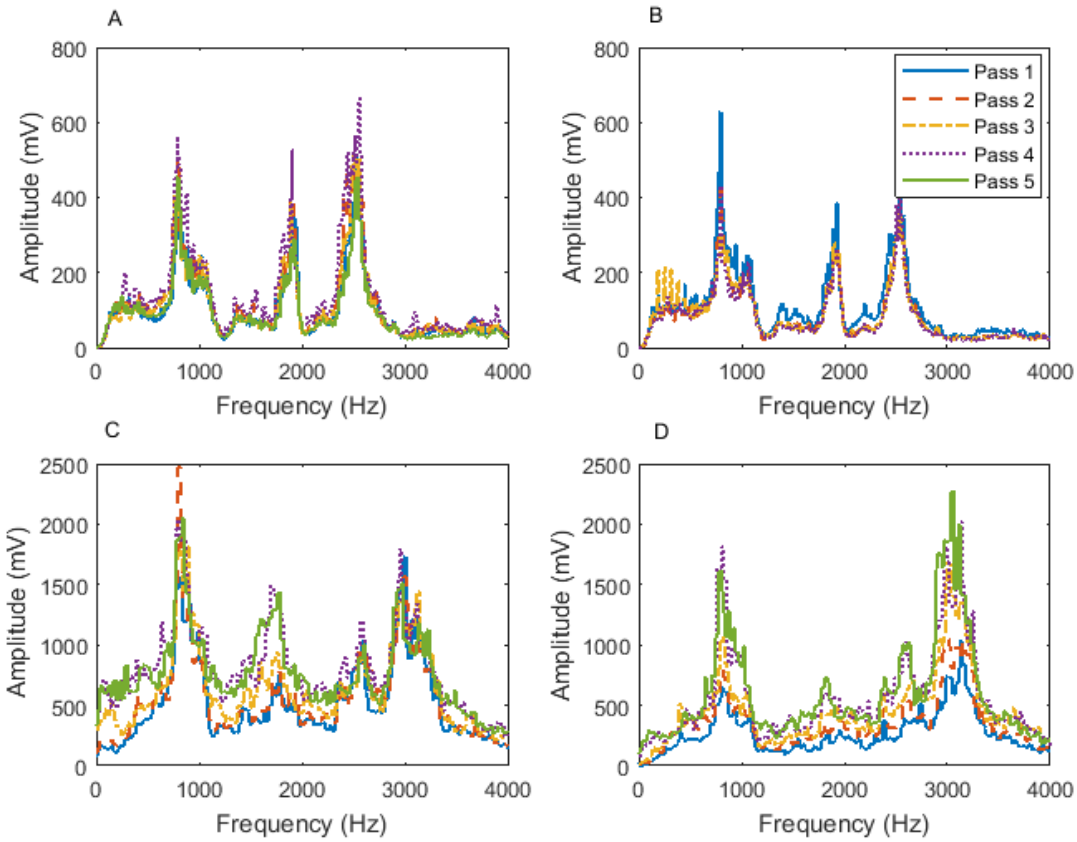

Figure 120- Rail vibration for 3 m leaf contamination: A) Five 10 mph (16 km/h) brake tests B) Four 10 mph (16 km/h) wet brake tests C) Five 25 mph (40 km/h) coast tests D) Five 25 mph (40 km/h) brake tests

Figure 121 shows the vibration in the rail when a 6.6 m leaf layer is applied to both rails just before the braking point. It is important to note the change in y-axis scale between the two subplots. Figure 121A shows the vibration for 10 mph (16 km/h) and Figure 121B shows the vibration for 25 mph (40 km/h). Both plots have a great deal of variability from pass to pass (although it is difficult to draw conclusions from Figure 121A as only two repeats were performed).

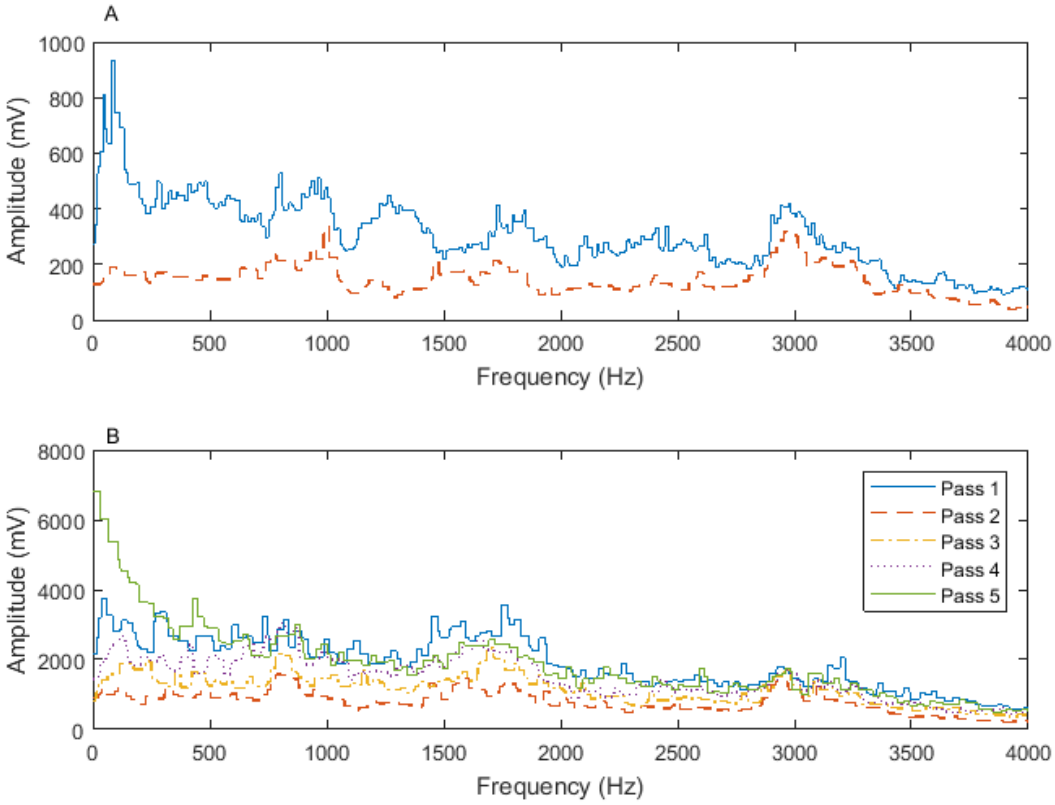

Figure 121- Rail vibration for 6.6 m leaf contamination: A) Two 10 mph (16 km/h) brake tests B) Five 25 mph (40 km/h) wet brake tests

Figure 122 shows the averages for dry (brake and coast tests) and dew brake tests. The dew causes a reduction in amplitude compared to dry. This is due to the low levels of moisture reducing the traction coefficient. The coast tests have an increased vibration compared to the brake tests. This is counter intuitive as one would expect the braking to cause more vibration in the rail. However, during coasting the speed of the train remains higher for a longer period which leads to more vibration than when the train is moving slowly due to the brakes being applied.

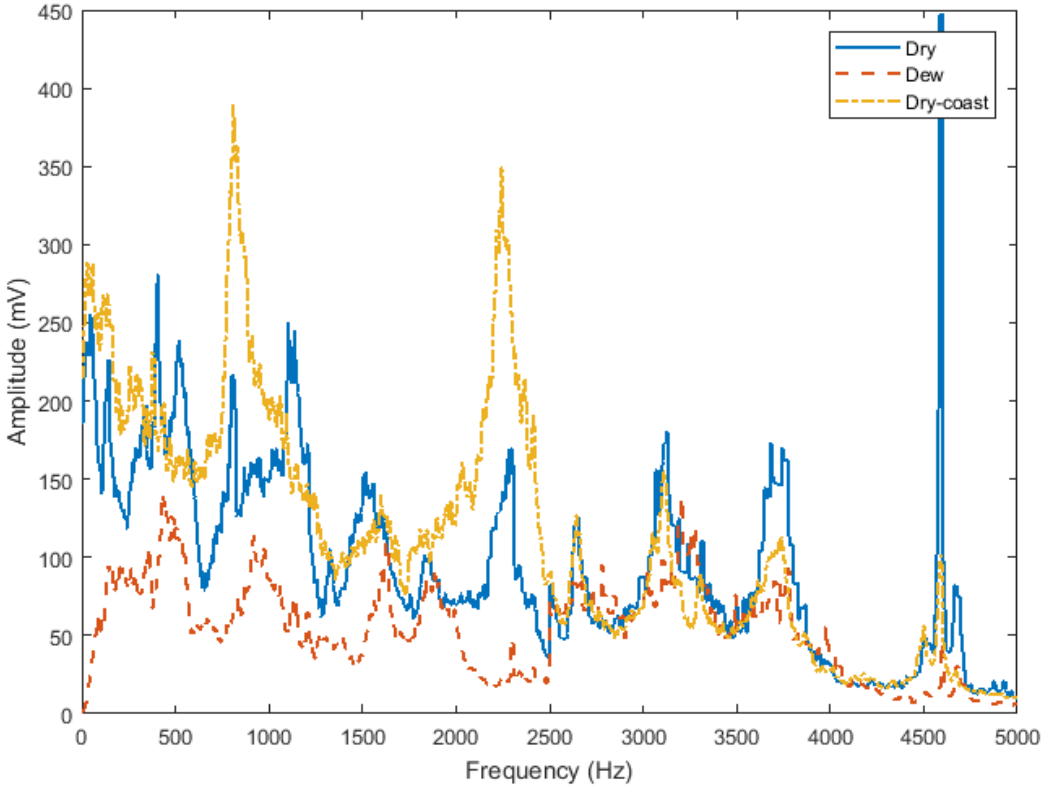

Figure 122- Averages for dry, dew brake tests and dry coast tests

Figure 123 shows the averages when the tests are performed with the 3 m leaf layer. A 'clean' 10 mph (16 km/h) brake average is also included for comparison. As mentioned above, the 25 mph (40 km/h) tests have a higher vibration than the 10 mph (16 km/h) tests. This is because the higher speed causes more severe braking forces which cause more vibration. The leaf layers produce more vibration in the rail than dry, "clean" rail. This is because the low adhesion causes more sliding within the contact which translates into more vibration during braking. The wet leaf 10 mph (16 km/h) tests has a lower vibration than the 10 mph (16 km/h) dry leaf tests. This is because the water is applied as a jet to the contact. This removes some of the leaf contamination and hence a reduction in the vibration. Not all the leaf contamination is removed, if it was the vibration would look similar to the "clean" vibration response. As with the results presented in Figure 122, coasting to a stop causes a higher vibration than braking. Compared to the 'clean' 10 mph (16 km/h) brake tests, the presence of the leaf layer causes three distinct peaks to develop, at 900 Hz, 1800 Hz and 2500-3000 Hz.

Average vibration for the 6 m leaf layer are not presented due to the wide variability in the results distorting any conclusions that could be drawn.

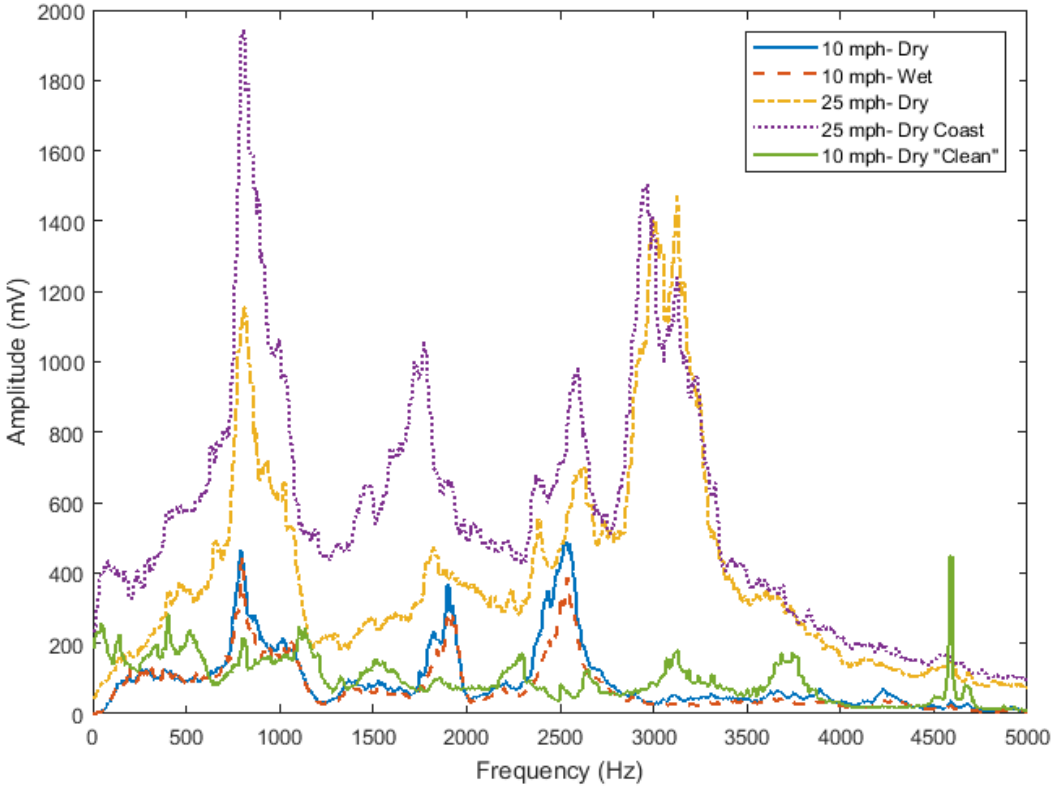

Figure 123- Averages for 3 m leaf layer

Figure 124 shows how the average stopping distance changes for each condition tested. A damp rail produces a slightly longer stopping distance compared to dry as the traction coefficient is reduced, reducing the braking force. The leaf layers in general cause longer stopping distances compared to dry rail and have larger standard deviations due to braking variability caused by leaf contamination causing transience. A wet 3 m leaf layer reduces the stopping distance compared to a dry 3 m leaf layer as the jet of water cleans the contamination from the contact slightly, improving braking performance. The stopping distances show that the leaf layers create low adhesion conditions because they are longer for leaf layers than with dry, clean rail.

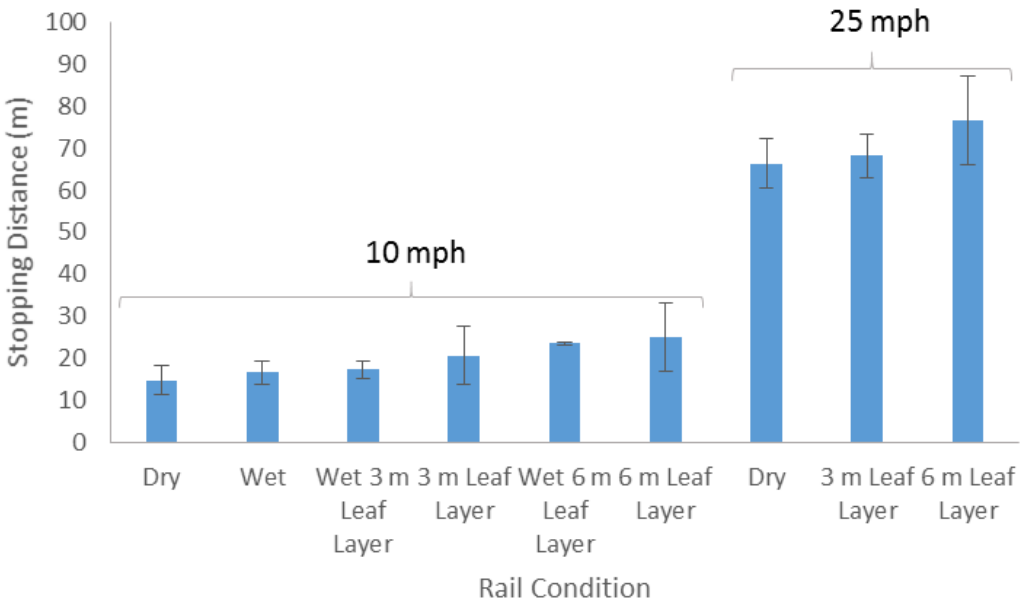

Figure 124- Stopping distances for different conditions

7.6 Discussion

The natural frequencies of the test set-up is much higher in the field (3000-3500 Hz) than in the laboratory (1500-1900 Hz). This is because the rail is supported differently and is much longer in the field.

The results from the laboratory trial (shown in Figure 113) show that the equipment and method is a reliable way of measuring the vibration in the rail for different contact conditions. The area of interest is 500-1000 Hz for gauge corner contact. This area is not near the natural frequency of the test set-up.

The frequency of the primary peak seen in Figure 114 and Figure 116 is approximately 1000 Hz. This is in the middle of the range a previous report [105] found increased, when lubrication was switched off. The secondary peak is outside of the range previously reported. The secondary peak could be caused by differences in the vehicles and track geometries between this test and the previous report [105] or could be due the natural frequencies of the test setup. The natural frequency test was carried out at a different track, on a different day and this could affect the natural frequencies results as the sleeper spacing may be different as well as different support structure.

Figure 114 and Figure 116 show that the vibration response in the rail, at the same measurement site is similar, with only small differences in amplitude for different travel directions or train. Table 8 shows the different speeds of the train passing the measurement site as the data was recorded. A lower train speed would cause a smaller amplitude in the vibration response of the rail. Table 8 supports this as:

- The northbound train in Figure 116 is travelling 7 mph (11 km/h) slower and has a lower amplitude response
- The differences in amplitude seen in Figure 114 correspond to changes in speed shown in the table

Train	Speed, mph (km/h)
Train 1 in Figure 114	24 (38)
Train 2 in Figure 114	21 (33)
Train 3 in Figure 114	35 (56)
Northbound Train in Figure 116	20 (32)
Southbound Train in Figure 116	27 (43)

Table 8- Differences in train speed

The fact that variations in direction or train do not produce a shift in the frequency of the peak means that the changes displayed in Figure 115 must be due to a different reason. The friction measurements for the gauge corner in Figure 118 suggest that the change is due to a different friction coefficient at the three sites. This is because the lowest friction coefficient has a corresponding low vibration amplitude and a high friction coefficient has a corresponding high vibration amplitude. Figure 125 shows photographs of the gauge face from each of the measurement sites. It shows that the changing friction coefficient is caused by different amounts of grease present at each of the three sites. A large amount of grease (shown by a black smear) can clearly be seen in site 1. Site 2 has a small amount of grease whereas site 3 is completely free from a visible amount of grease. This corresponds to the differing levels of vibration seen in Figure 125 and proves that the level of longitudinal vibration can be equated to the amount of grease present on the rail.

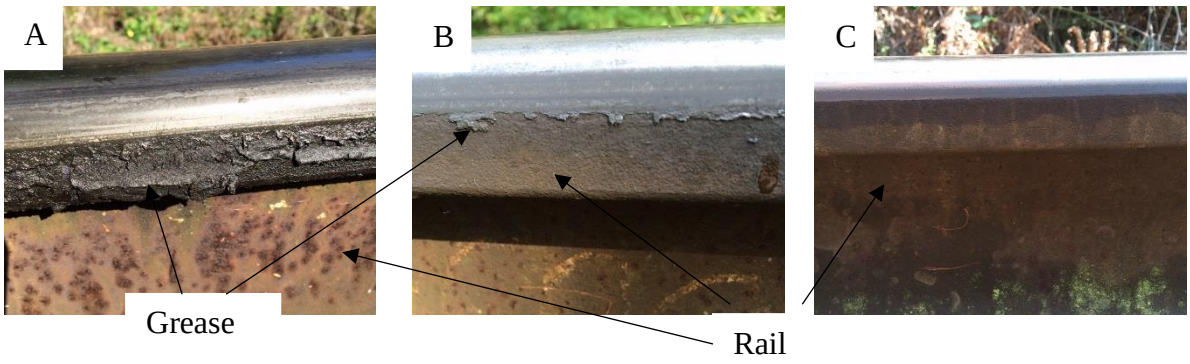

Figure 125- Gauge face view of rail for A) site 1 B) site 2 C) site 3

The results from the QRTC field trial showed how the vibration changed with different track conditions. For the dry tests at the slow speed, there was good repeatability seen in the measurement (Figure 119). When the speed was increased to 25 mph (40 km/h) there was an increase in the variability in the vibration between repeats. In low adhesion conditions, (when the leaf layers were applied), good repeatability between test passes was seen for the 3 m leaf layer (Figure 120). However, the vibration changed significantly between each repeat and was a larger amplitude for the 6 m leaf layer. This is because it creates a more severe low adhesion event as there is more leaf layer present. This could be seen during the tests as the wheels of the vehicle were able to be seen sliding for longer and there was leaf contamination carried down beyond the application zone by the vehicle. Additionally, braking levels were not consistent for each repeat as the driver changed braking levels to reduce damage to the wheels.

The results in Figure 119-Figure 123 show that with a vehicle moving at 10 mph (16 km/h), applying a 3 m leaf layer to the rail prior to a braking point is a reliable way of creating low adhesion. This is shown in the repeatability of the vibration in the rail. By monitoring the

vibration, particularly in the frequency range of the three peaks shown in Figure 123, methods to reduce the low adhesion event can be tested for their effectiveness. However, one of the peaks, 2500- 3000 Hz is close to the natural frequency of the test set-up so could be influenced by resonance effects rather than due to leaf layers.

Table 9 shows the differences in test conditions between the two field trials. The differences mean that it would be difficult to directly compare the two trials as their aims were different. The problems association with the variability seen in repeat measurements at QRTC mean that for development of a monitoring system for grease, sites should be chosen where speed to relatively constant with little acceleration or braking of the train. This helps reduce variation between repeat measurements. The leaf contamination and water leads to changes in the vibration across the measured range (0-4000 Hz), although there are three clear peaks. Whereas the majority of the change in vibration when grease is present occurs in 700-1200 Hz. This is the same result as seen in the laboratory. Grease applied to the top of rail reduced frequencies across the measured range. Whereas grease applied to the gauge corner only reduced vibration in a narrow band. This means it is possible to identify where contamination occurs by analysing which parts of the frequency spectrum change.

Test condition	QRTC	SVR
Track geometry	Straight	Curved
Wheel-rail contact	Tread contact	Gauge corner/flange contact
Speed	Braking/coasting to a stop	Steady speed
Contamination of contact	Leaf layer on railhead	Grease applied to gauge corner
Vehicle used	Class 117 DMU	Steam engine pulling four passenger vehicles

Table 9- Differences between the two field trail methods

Due to the sensitivity of the vibration to small changes in contact conditions it is hypothesised that track and train characteristics will also affect vibration. For example, if the sleeper spacing changes from one site to another or a train has stiffer suspension the vibration may change. Therefore, more data is required from different measurement sites to be able to analyse what the impact of track/train features.

7.7 Conclusions

Travel direction, train speed and different trains do not affect the frequency of the main peaks of the vibration response of the rail. They only effect the amplitude of the response. An increase in train speed leads to an increase in the amplitude of vibration. The further away the measurement site is from the lubricator, the less grease is present on the rail, the higher the coefficient of friction and this leads to an increase in vibration. Therefore, by monitoring the longitudinal vibrations it is possible to detect the presence of the grease. Measuring the vibration during severe braking or low adhesion events caused by contamination to the top of the rail would reduce the effectiveness of a grease detection/monitoring system. This is because of the greater transience involved during braking/low adhesion as well as low adhesion on top of rail causing an increase in vibration during braking. Therefore, a monitoring/detection system would work best where speed of a vehicle is relatively constant with little acceleration

or braking. However, contamination to the top of the rail by leaves affected vibration across the frequency range, whereas grease only affected the 700-1200 Hz region.

8 Friction Modifiers

This chapter uses methods developed in previous chapters for grease tackiness (chapter 5) and pick-up (section 6.1) and applies them to a Top of Rail Friction Modifier (TORFM). Carry-down was not assessed as TORFM dries soon after the applicator and little material transfer takes place. This means that the carry-down method developed for grease is not suitable for use with TORFM because it works differently to grease. The aim of this work was to link three test scales together by using the same products on each of the scales. This would show if using a small tabletop tribometer to measure tackiness could predict the outcome of pick-up tests using the Scaled-Wheel Rig (SWR) (see section 3.4 for test rig details) and the Full-Scale Test Facility (FSTF) (see section 3.5 for test rig details). Additionally, the SWR has not been used for Top Of Rail (TOR) products before, so comparing SWR and FSTF results will validate the use of the SWR for future tests using TOR products.

8.1 Test Methodology

8.1.1 Tackiness

The test method developed in chapter 5 was used to evaluate the tackiness of four variations of the same TORFM. Further details on TORFM's can be found in section 2.4. No adaptation of the test method was needed. This was because even though the method was developed for gauge corner products, it is purely representative of the relative tackiness between the products, rather than representing gauge corner/wheel flange contact that occurs in curves. The method and equipment details can be found in section 5.2. Smooth specimens (Ra= 0.6 μm) and rough specimens (Ra= 3 μm) were also tested to see the effect of roughness on the results. All the combinations of FM and roughness were tested at least three times to demonstrate the repeatability of the method.

The test was repeated on two of the four products a few months after the main study. The two products were from a different batch from the same supplier. Additionally, the laboratory/test environment was not controlled. This means that a small difference in the environmental conditions would be expected between the two data capture periods (although the environmental conditions were not recorded). How these repeat results compare to the previous results gives an indication of how robust the test method is.

8.1.2 Scaled-Wheel Rig Pick-Up

The SWR described in section 3.4 was used to measure the pick-up of three variations of the same TORFM on a reduced diameter wheel. These were the same batch of product as used in section 8.1.1. Only three out of the four TORFM's were tested as there was not enough of FM-D available to carry out this test. A TOR-ML applicator bar was attached to the rail as shown in Figure 126. A hand pump was used to pump the TORFM through the applicator. The scaled-wheel was rolled along the rail, through the 'puddle' of TORFM (see Figure 127 for an example). The weight of TORFM transferred to the wheel during the roll was measured using a mass balance (accurate to ± 0.005 g).

Initially, different parameters were tested using one TORFM before the different TORFM's were compared. This was done to see how different set-ups and pump amounts affected pick-up. Four different pump amounts were tested. The amount of TORFM pumped out varied

between TORFM (due to different viscosities) and between repeats. Therefore, the mass of the TORFM that the applicator outputted was weighed and the results averaged to give an average output for each pump amount and TORFM. Figure 127 shows the shape of a typical TORFM 'puddle' formed by the applicator bar. The bar was set at two height positions. The 'low' position is the height that the manufacturers specify in their manual [122] and the 'high' position was set 2.5 mm higher. The different test conditions for this initial set of tests are shown in Table 10. The amount of pick-up was measured after one wheel pass through the puddle of TORFM. All parameters were tested at least three times and averaged to gain the mean value of TORFM pick-up.

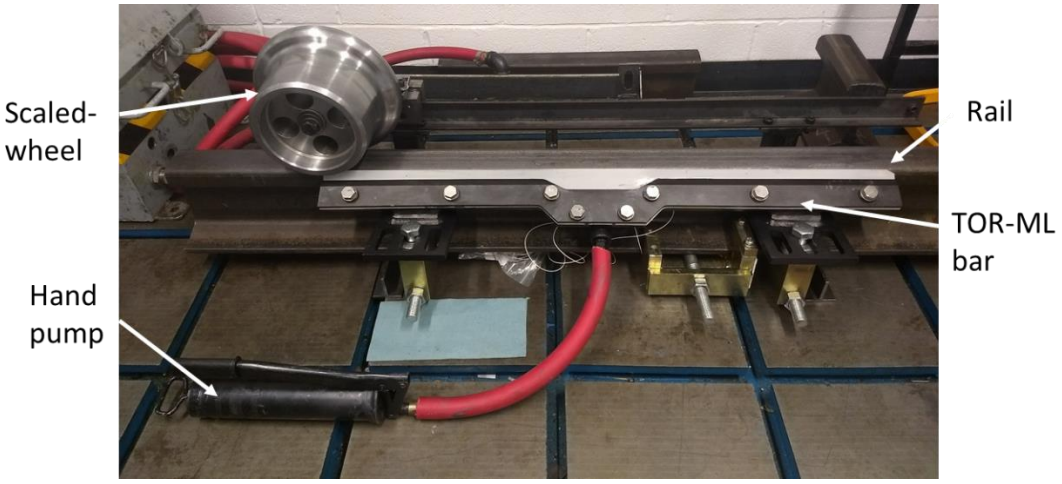

Figure 126- SWR with TOR-ML bar attached

Parameter	Test conditions
Bar height	Low, high
Number of hand pumps	2,4,6,8
Friction modifier	FM-C
Wheel lateral displacement (mm)	0, 4, 8.5

Table 10- Initial SWR test conditions

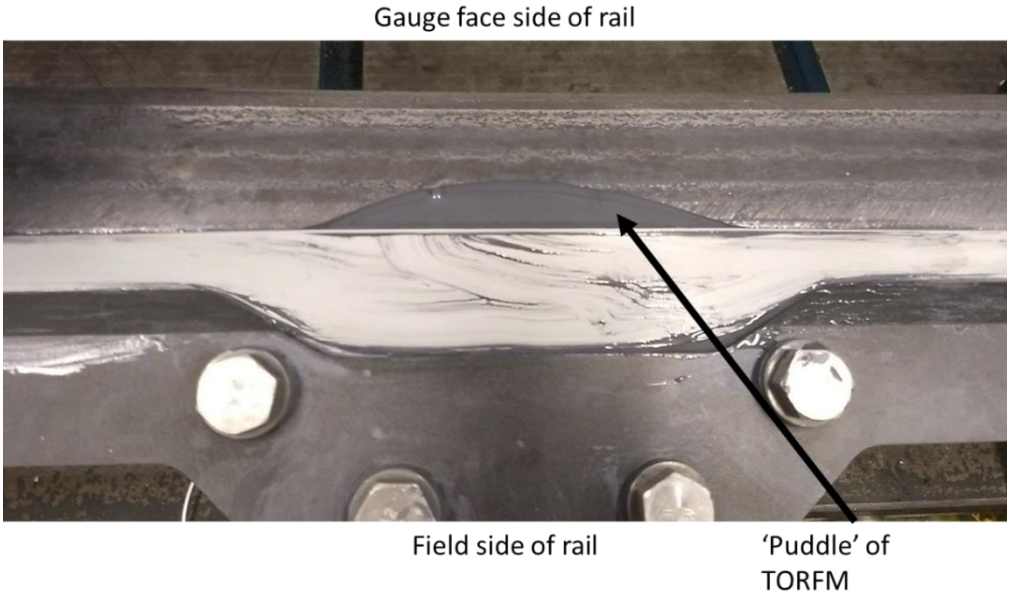

Figure 127- Typical pump output for FM- C, 4 pumps

After this initial phase of testing the pick-up for the three different TORFM's was measured. This was done by rolling the wheel through the puddle of TORFM and weighing the TORFM picked-up by the wheel. The wheel was rolled a further four times, weighing the amount of pick-up each time and not pumping any more TORFM between wheel passes. This gave a total of five wheel passes which simulates five axles of a train passing. Typically twenty axles pass before reapplication of TORFM. Five wheel passes was chosen as after this amount the TORFM measured was zero or close to zero. The test conditions used are summarised in Table 11.

Parameter	Test conditions
Bar height	Low
Number of hand pumps	4,6,8
Wheel lateral displacement (mm)	0,4,8.5
Friction modifier	FM-A, FM-B, FM-C

Table 11- SWR test conditions for different TORFM's

8.1.3 Full- Scale Test Facility Pick-Up

The FSTF described in section 3.5 was used to measure the pick-up of three variations of the same TORFM on a full size wheel. These were the same batch of product as used in sections 8.1.1 and 8.1.2. The TOR-ML applicator did not fit onto this test rig due to where the chain (see Figure 35 and Figure 36) attaches to the wheel. Therefore, a hand pump was used to apply TORFM directly to the top of rail. Figure 128 shows an example of the 'puddle' of TORFM applied directly to the rail before a test starts. It was chosen to apply the puddle to middle of the railhead as if it was applied more to the field side of the rail (to mimic the application shown in Figure 127), the TORFM flowed down the side of the rail before the wheel rolled over the puddle.

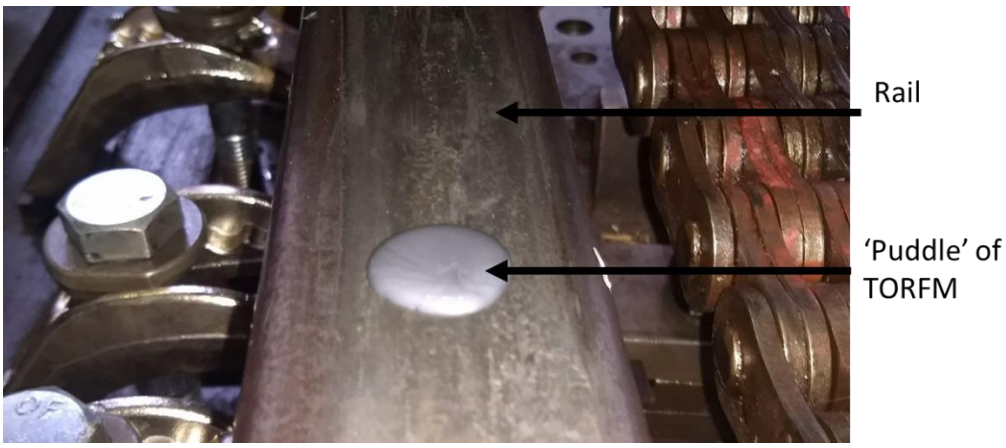

Figure 128- Example of puddle of TORFM applied to rail before test commences

Initially, how the pick-up of TORFM to the wheel changed with different pump amounts, wheel lateral displacement, slip and applied load was studied with one TORFM. This was done by applying a set amount of TORFM, rolling the wheel through the puddle once and weighing the mass of TORFM picked-up on the wheel using paper towels and a mass balance accurate to ± 0.005 g. The parameters tested in this initial work are summarised in Table 12.

Parameter	Test conditions
Pump amount (g)	1.7, 3.4, 6.8
Wheel lateral displacement (mm)	0, 4, 8.5
Slip (%)	2, 5
Load (kN)	75, 85, 100
Friction modifier	FM-C

Table 12- Initial FSTF test conditions

After this initial phase of testing, the pick-up for the three different TORFM's was measured. This was done using the same method as for SWR detailed in 8.1.2 and the parameters used detailed in Table 13. As the amount the hand pump outputted varies between pumps, a syringe was used to apply the TORFM to the rail to ensure a constant volume was applied to the rail each time. As the density of the different TORFM's is similar, as shown in Table 14, the difference in mass of 3 ml of each of the three TORFM's is negligible.

Parameter	Test conditions
Pump amount (ml)	3
Wheel lateral displacement (mm)	0
Slip (%)	2
Load (kN)	75
Friction modifier	FM-A, FM-B, FM-C

Table 13- FSTF test conditions for different TORFM's

FM	Density (g/cm^3)
FM-A	1.08
FM-B	1.06
FM-C	1.07

Table 14- Density of the three different TORFM's

8.2 Results

8.2.1 Tackiness

Figure 129 shows an example of one of the force-distance results. The shape of the graph shows that the separation of the two surfaces is in the transition region as shown in Figure 26. Ideally, the separation would be in the separation by flow region, as this would give the best tackiness result. However, there is not much cavitation, as the slope of the graph after the peak force is not vertical and therefore the test parameters do not need to be changed. All the force-distance graphs for the other tests look similar to this one.

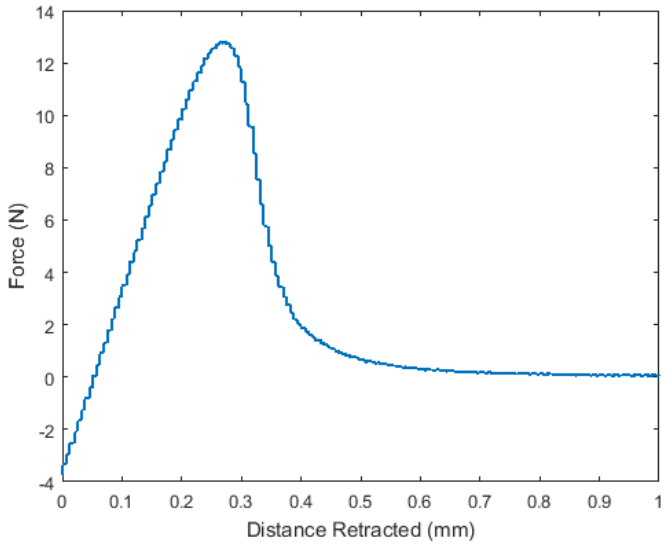

Figure 129- Example result of retraction period of test for a TORFM

Figure 130 shows the average peak force for all the TORFM's and for both specimen roughness's. For all the TORFM's there is a reduction in peak force from the smooth to the rough specimens. The error bars show the standard deviation from the three results so one anomalous result causes a large spread. Another factor is that the TORFM's are a water based suspension and 0.5 g is used for each tests. Therefore, it is possible that the amount of particles on the test specimen varies from test to test causing the spread in the data.

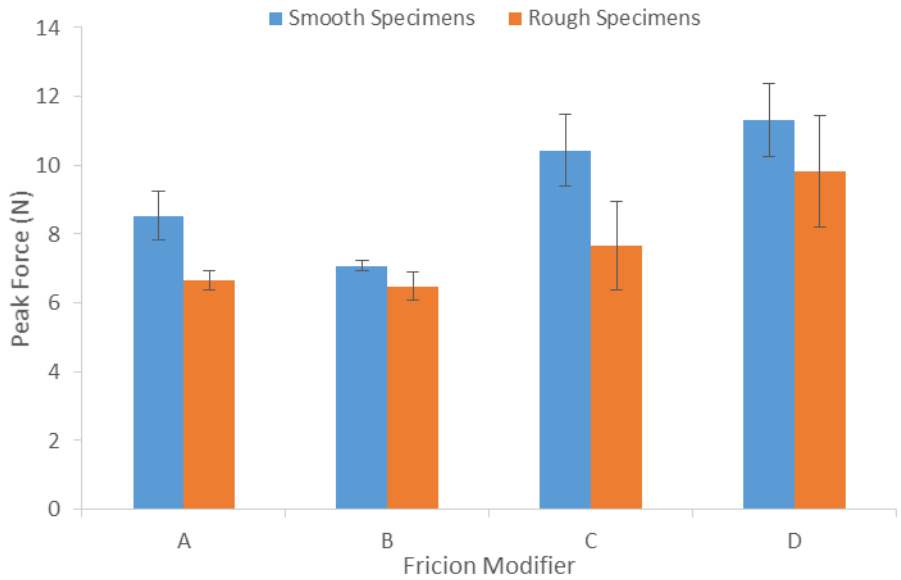

Figure 130- Peak force during separation for TORFM's and specimen types

Figure 131 shows the work done to break the strings during separation. As with the previous figure, there are large error bars. For all the TORFM's except FM-D, the rough specimens cause a reduction in the work done to break the grease strings. This is the opposite to the results seen with grease (Figure 66).

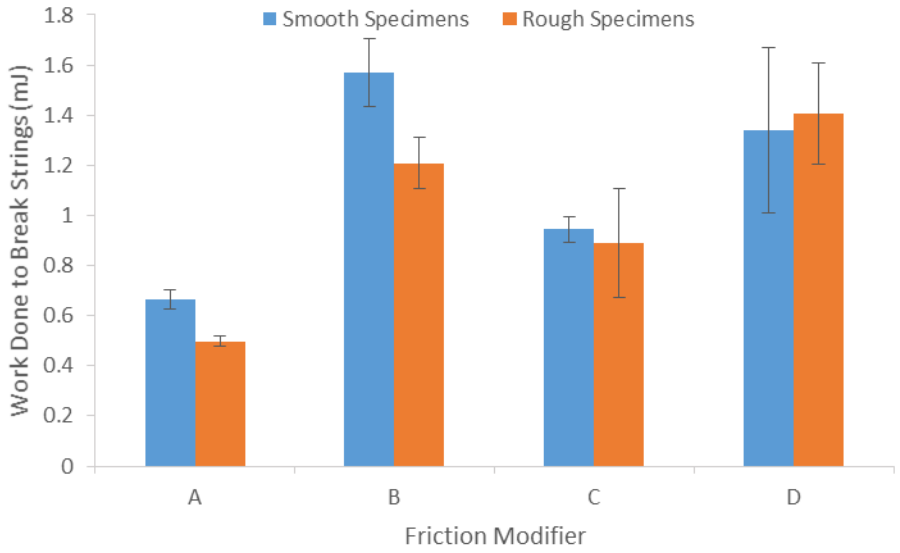

Figure 131- Work required to break strings during separation for both TORFM's and specimen types

Figure 132 shows the peak force for two different batches of two TORFM's. It is immediately apparent that the standard deviation is consistently higher for the second batch. This could be caused by batch two being stored for a longer period. This would allow separation within the product to occur, which is not fully remixed. Both products were mixed the same way (by hand) prior to the tests being performed. For the smooth specimens, FM-D has a higher peak force than FM-C (although batch two produces a slightly lower value). For the rough specimens the FM-D has a lower peak force than FM-C from batch one, but this is reversed in batch two. This is likely to be caused by the separation/inadequate mixing problem mentioned already.

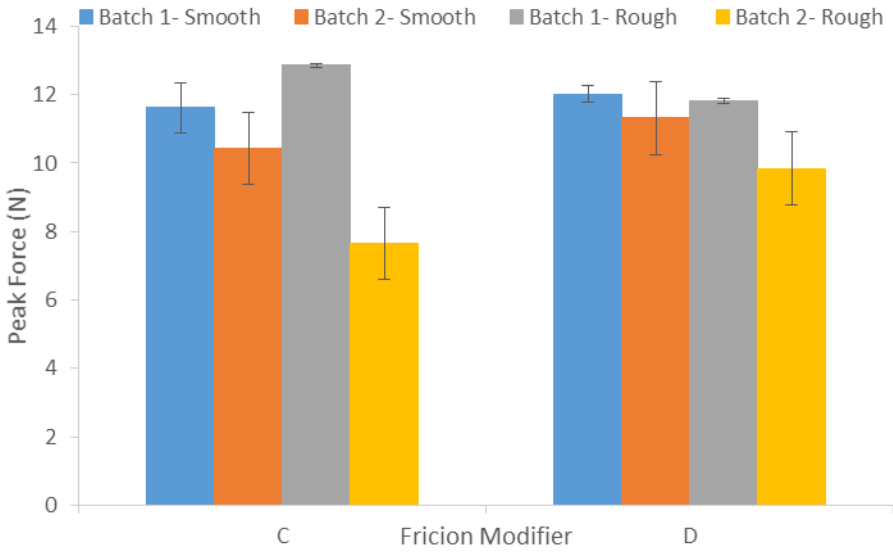

Figure 132- Peak force for two TORFM's from two different batches

Figure 133 shows the work done to break grease strings for two different batches of two TORFM's. As in the previous figure, the standard deviation is much higher in batch two. The same relationship between FM-C and FM-D is seen in both batches for both specimen roughness's (FM-C is less tacky than FM-D). Taking into account the large error bars, there is a reasonable correlation between the two batches. FM-C has a slightly lower result for batch

two than batch one (especially for the rough specimens). Whereas, FM-D has a slightly larger result for batch two than batch one.

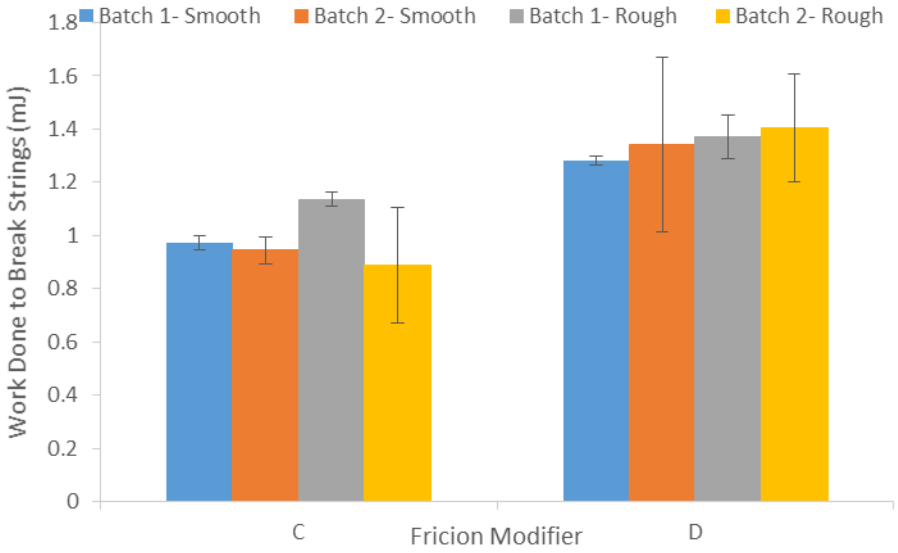

Figure 133- Work done to break strings for two FM's from two different batches

Looking at the individual test results for batch two, the spread in the results was caused by one significantly different result from the other two repeats. An example of this is shown in Figure 134 where the second test result is lower than the other two. Removing this repeat causes the standard deviation to fall to 0.13 from 0.32, which is a similar deviation to batch one (which had a deviation of 0.09). This supports the theory that separation of the product, and not fully remixing the product before testing caused the spread. This is because there is agreement between two out of the three tests, which show that the product is mostly mixed, but occasionally a significant change in tackiness/adhesion caused by a less well mixed part of the product ending up on the test specimen.

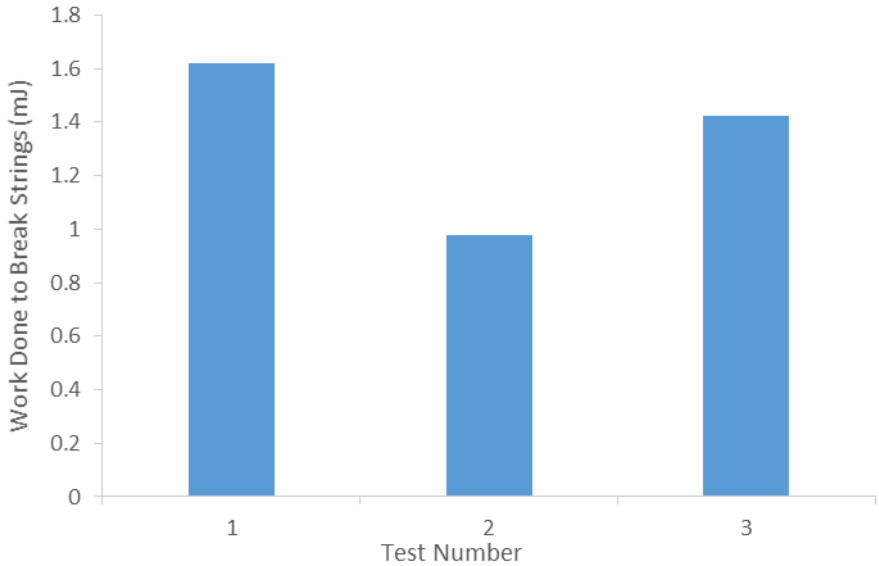

Figure 134- Individual test results for batch two, FM-D, smooth specimens

8.2.2 Scaled-Wheel Rig Pick-Up

Figure 135 shows how the amount of TORFM picked-up by the wheel changes as the height of the applicator bar, the amount pumped out and the wheel lateral displacement changes. Clearly, the more TORFM pumped out, the more is picked-up by the wheel. This is because pumping more out results in a bigger puddle on the railhead and allows more TORFM to flow across the rail and enter the wheel-rail contact band. The high position of the bar results in more TORFM picked-up by the wheel. This is because the high position results in slightly more of the TORFM flowing across the railhead, meaning that the wheel contacts a larger amount of TORFM. In the low position, with the extra small amount of grease pumped out, no pick-up of TORFM was recorded. This was because the puddle produced was not large enough to be in the wheel-rail contact zone. There is not much change in pick-up with lateral displacement of the wheel. This is because the profile of the wheel does not change much in the wheel tread/ railhead contact zone as shown in Figure 24. All the tests show small standard deviation in the results, which shows that the tests are repeatable.

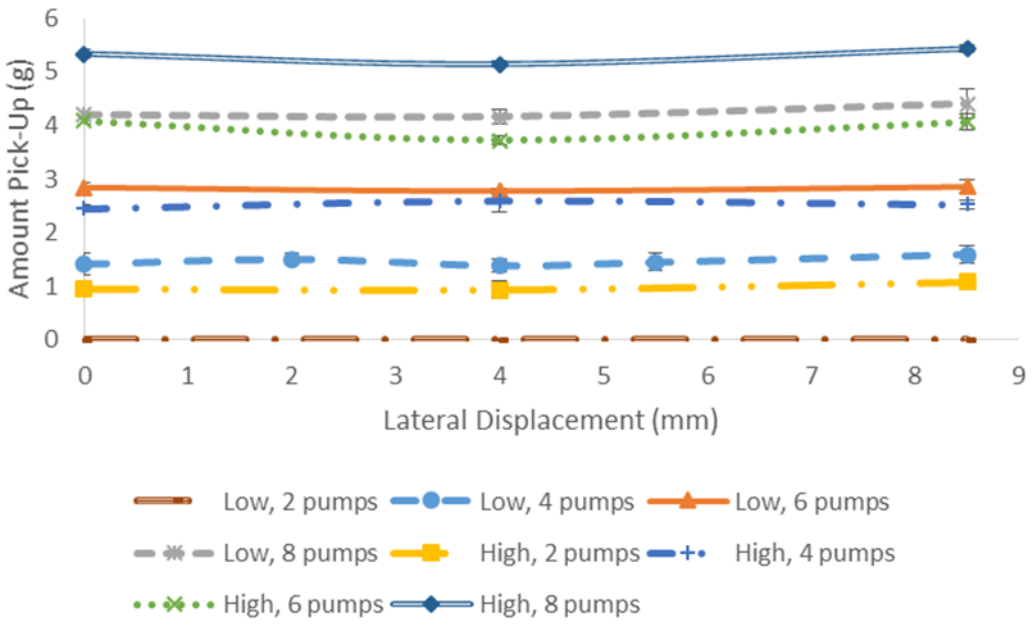

Figure 135- Variation in FM pick-up with changes in wheel lateral displacement

Figure 136 shows the average amounts pumped out, average amount of pick-up and the percentage of picked-up for different pump amounts. The same conclusions as shown in Figure 135 can also be seen in this figure. Additionally, it can be see that for the high applicator bar position, more TORFM is pumped out for the same pump levels. This is due to where the outlet of the applicator sits in relation to the curve of the rail. The high applicator position means that less of the outlet port is 'blocked' by the rail meaning that it is easier for more of the product to flow across the rail. The applicator in the high position also results in a higher percentage being picked up by the wheel. Again, this is because more of the FM flows further across the railhead and into the contact band.

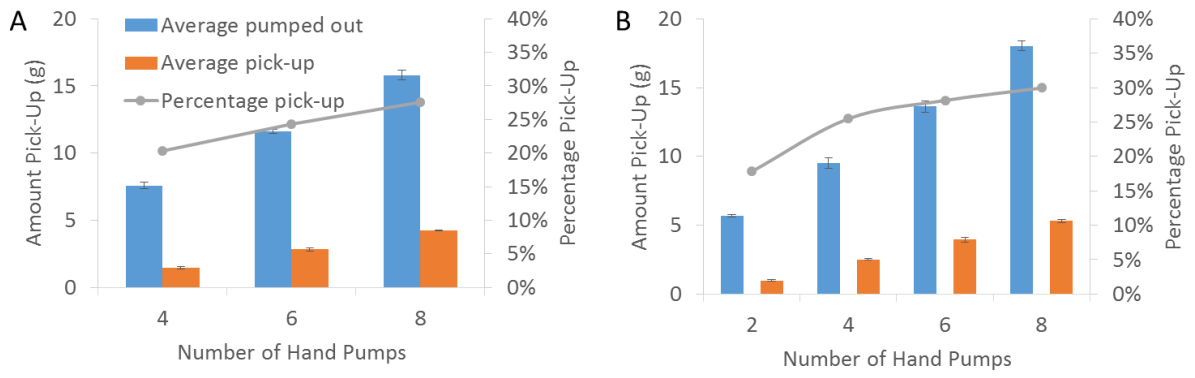

Figure 136- Variation in pick-up with different test parameters for A) low applicator bar, B) high applicator bar

Figure 137 shows the pick-up on the wheel and the post-test puddle on the rail for both applicator bar heights. Clearly, the high applicator bar position has resulted in more TORFM spread across a larger area on the wheel tread and on the rail (shown in Figure 137C compared to Figure 137A, and Figure 137D compared to Figure 137B). Additionally, the high applicator bar has resulted in some of the product flowing on to the applicator and so being lost from the rail as shown in Figure 137D.

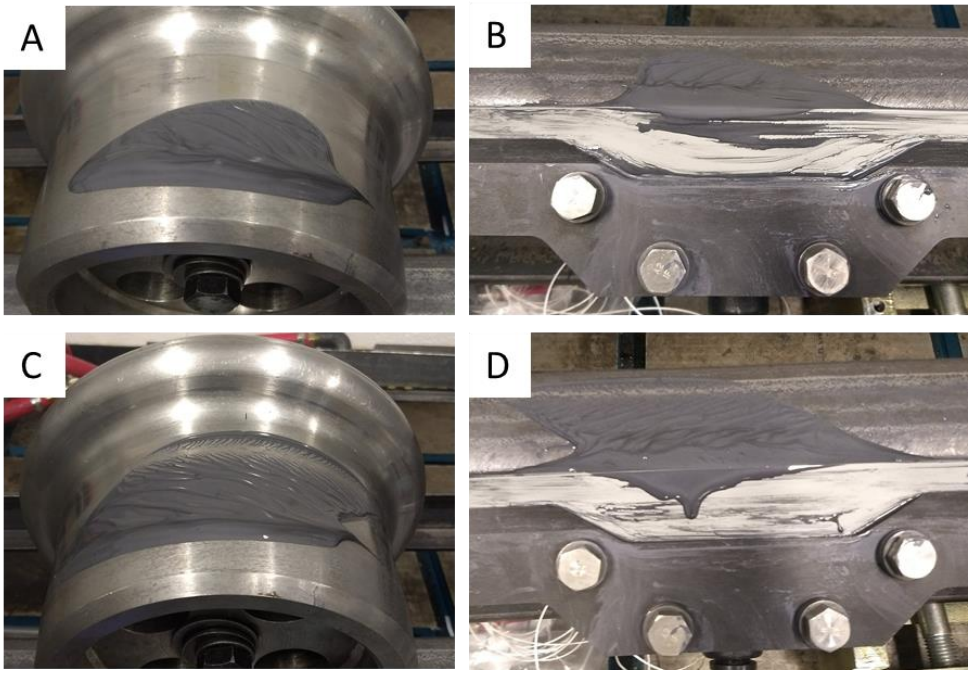

Figure 137- FM-C, 0 mm lateral displacement, medium pump output A) pick-up on wheel, low applicator bar B) puddle on rail post-test, low applicator bar C) pick-up on wheel, high applicator bar, B) puddle on rail post-test, high applicator bar

Figure 138 shows the amount picked-up at different lateral displacements for three different formulations of the TORFM. All these tests were carried out at the low applicator bar height, as this is the height specified by the manufacturer. The same relationships displayed in Figure 135 are shown here for all three TORFM's. Increasing pump amount increases pick-up of FM and lateral displacement has little effect on the pick-up amount.

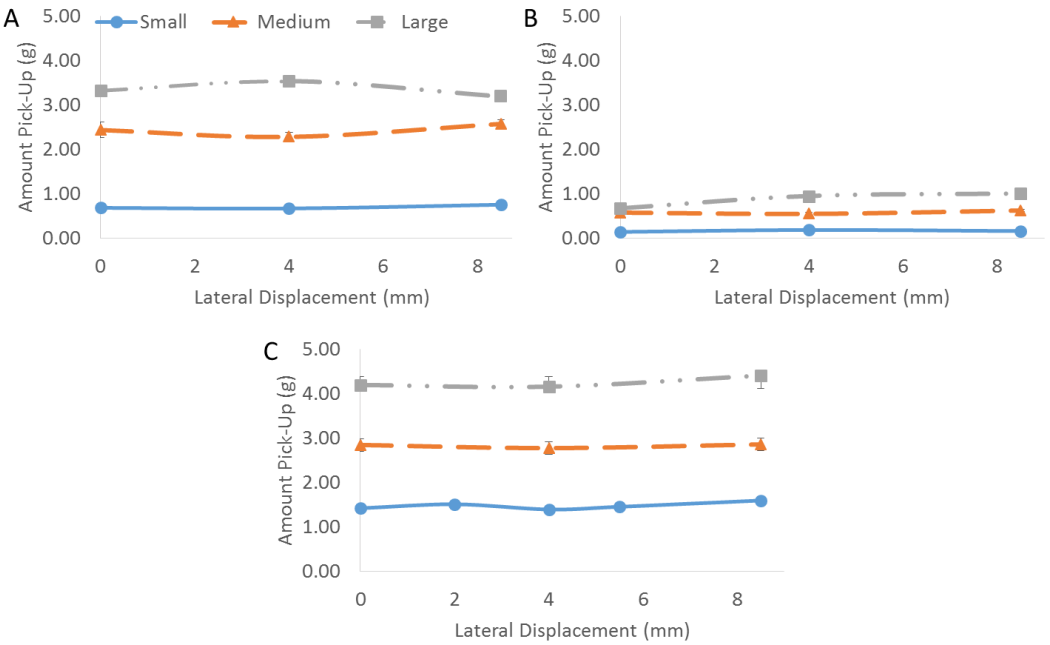

Figure 138- FM pick-up at different lateral displacements after one wheel pass for A) FM-A B) FM-B C) FM-C

Figure 139 shows how the pick-up changes when the wheel is passed multiple times through the same puddle for three different TORFM's. For FM-A and FM-C there is a decrease in pick-up with each pass, until no pick-up of TORFM is recorded. For FM-B the relationship is different. There is an increase in pick-up from pass 1 to pass 2, and then a decrease with each subsequent pass. This is because FM-B is much more viscous and tacky than the other two TORFM's. The first pass of the wheel picks up little TORFM, but drags more of it across the rail. Therefore, when the wheel next passes there is more of it in the contact band for the wheel to pick-up. The more viscous nature of FM-B means that more of it stays in contact band whereas the other two TORFM's flow more easily and spread across the rail more, flowing out of the contact zone. This means that there is more FM-B available on subsequent passes resulting in greater pick-up even on roll 4 and 5. Figure 140- Figure 141 emphasise this by showing how the puddle left on the rail and the pick-up on the wheel changes for FM-B compared to FM-C after each wheel pass.

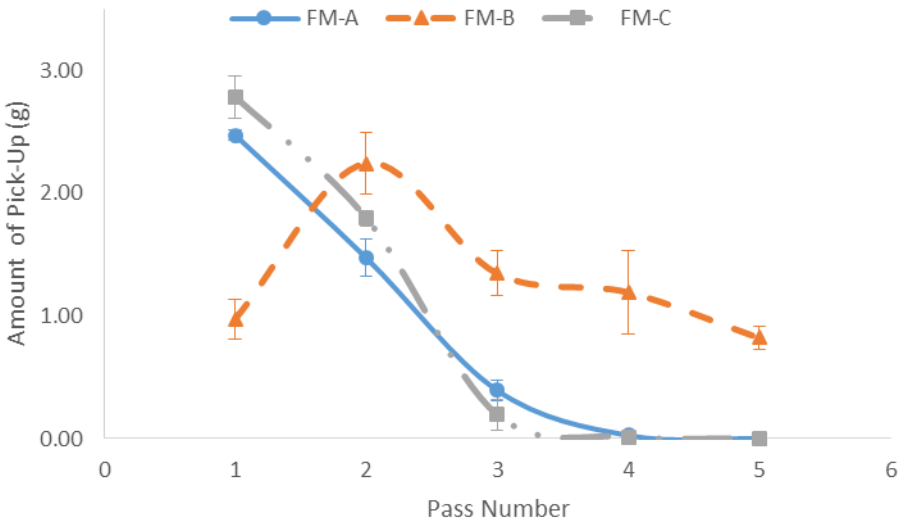

Figure 139- Average pick-up for multiple passes of three TORFM's

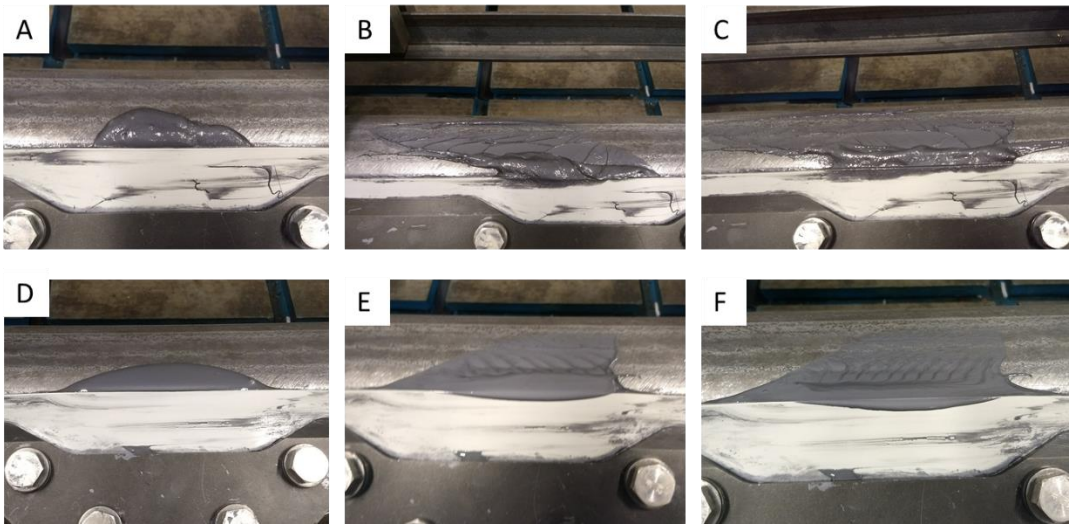

Figure 140- remaining puddle on rail after A) FM-B no wheel pass B) FM-B one wheel pass C) FM-B two wheel pass D) FM-C no wheel pass E) FM-C one wheel pass F) FM-C two wheel pass

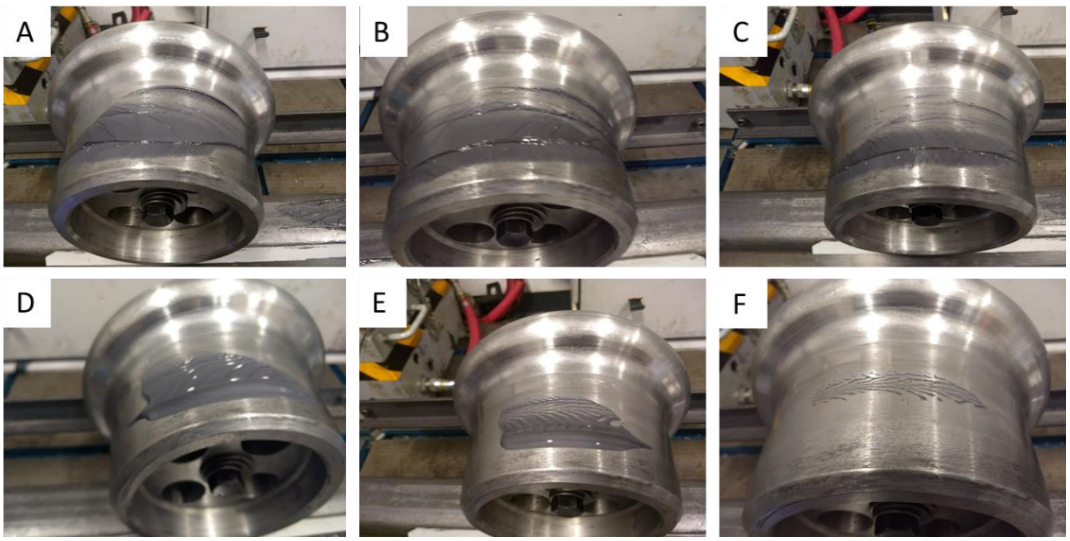

Figure 141- Wheel pick-up A) FM-B one wheel pass B) FM-B two wheel pass C) FM-B five wheel pass D) FM-C one wheel pass E) FM-C two wheel pass F) FM-C three wheel pass

Figure 142 shows how the total pick-up from five passes of the different TORFM's varies, as well as the percentage of TORFM pumped out that gets picked up by the wheel. FM-B has a higher overall pick-up due to reasons mentioned above and if the test is extended for further rolls the difference between it and the other two TORFM's would grow as the pick-up had not reached zero on wheel pass 5 (see Figure 139). FM-A has a lower pick-up percentage than FM-C.

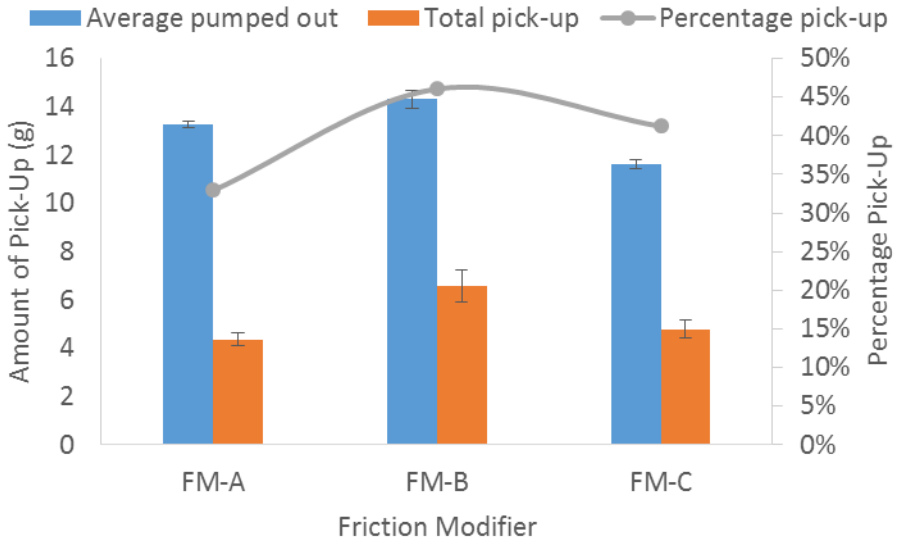

Figure 142- Variation in total pick-up for different TORFM's

Figure 143 shows the pick-up during one roll on two separate testing days that took place one month apart. FM-A and FM-C values are very close whereas there is a difference in the value for FM-B. The order of TORFM in terms of pick-up is the same on both days. This is more important than the absolute values. The differences are caused by environmental differences in the laboratory. The temperature/humidity was not recorded but depending on what other test rigs are running, outside temperature etc., the environment changes. Therefore, it is beneficial that the environment is not shown to change the ranking of which TORFM is better for pick-up

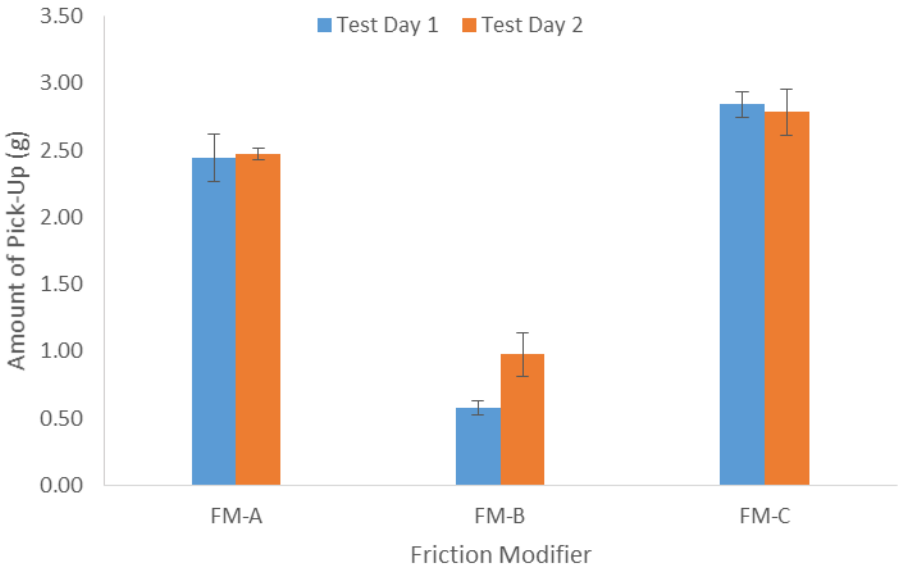

Figure 143- Pick-up from one roll on two different days

8.2.3 Full- Scale Test Facility Pick-Up

Figure 144 shows how pick-up varies under different conditions. Figure 144A shows that as pump output is increased, the amount of pick-up also increases due to there being more product available on the rail. However, if the amount on the rail increases too much it spills over the edge of the rail and is lost. This is why there is a change in gradient in the curve. For future tests, the amount of TORFM pumped out should be below 4 g to ensure that the TORFM stays on the rail where it will be used. The horizontal error bars on Figure 144A are because the pump does not output a uniform amount each time. This is why a syringe was used for further tests as the amount of output can be more carefully controlled. Figure 144B shows that there is a small increase in pick-up with an increase in lateral displacement. Figure 144C shows that increasing slip increases pick-up of FM. However, the increase is very small and there is overlap between the error bars for the two slip levels tested. Figure 144D shows that increasing the contact force between the wheel and rail decreases pick-up. This is because the increased force causes more of the FM to be squeezed out of the contact as the wheel passes across the pool of FM.

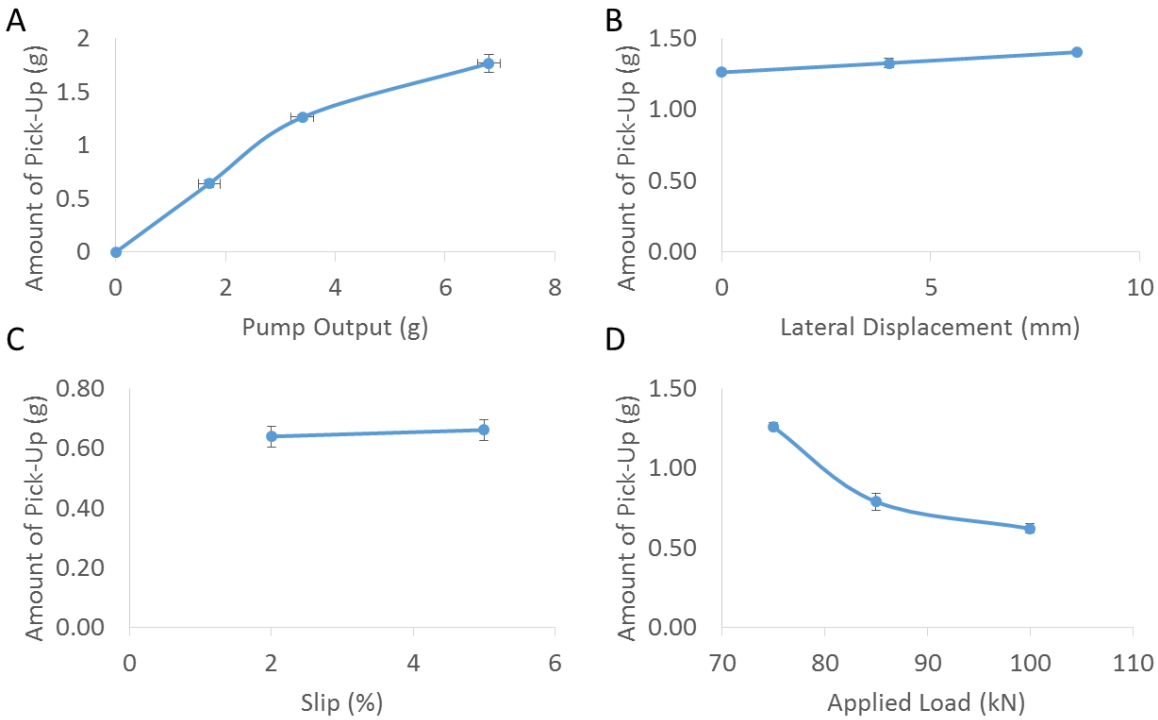

Figure 144- Variation in TORFM pick-up with A) change in pump output B) lateral displacement C) slip D) applied load

Figure 145 shows how the pick-up changes for multiple passes. This simulates a train passing an application site. For FM-A and FM-C there is a sharp drop off after the first wheel pass. Whereas, for FM-B there is an increase in pick-up from pass 1 to pass 2 and then pick-up remains higher than the other two TORFM's. The error bars for FM-B are larger. This is because it is much tackier than the other two and does not flow across the railhead. This means that it stays in place until the wheel contacts the puddle. It is likely that the puddle is not the same shape for each repeat, which has an effect on where the TORFM goes once the wheel has contacted it and thus the shape of the puddle contributes to the larger error bars.

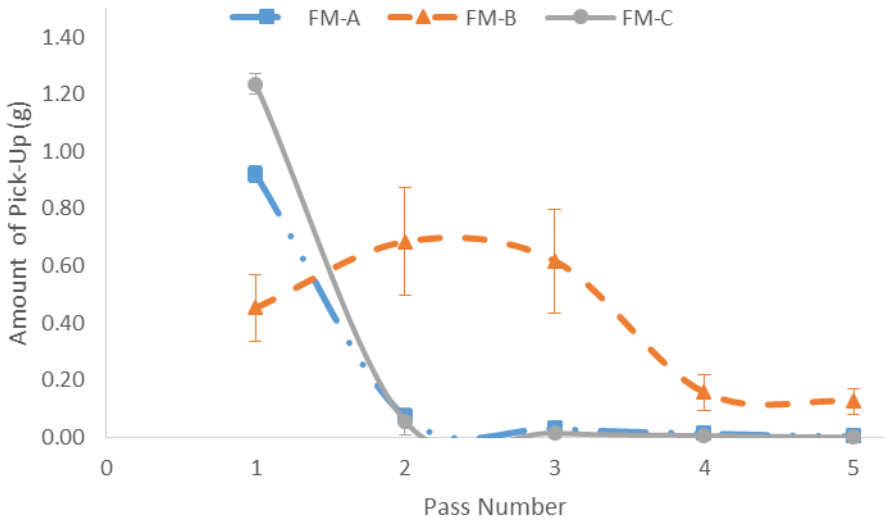

Figure 145- Average pick-up for multiple passes of three FMs

Figure 146 shows the total amount of FM picked-up for the five passes of the wheel. It shows that FM-B has the greatest pick-up by a large margin and FM-A has a slightly lower pick-up amount than FM-C.

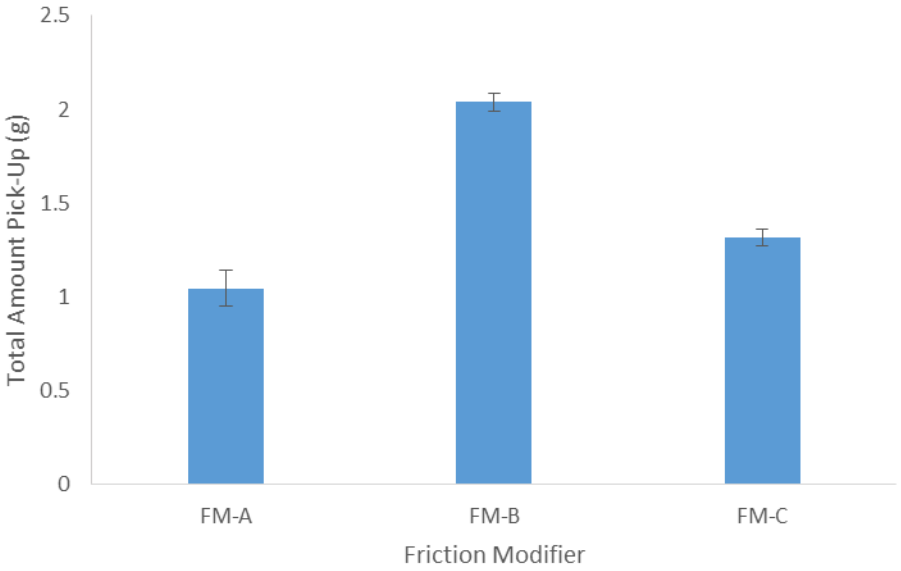

Figure 146- Total pick-up from the five passes for three FMs

8.3 Discussion

Figure 147 shows relative performance of the three TORFM's on each of the test rigs. For Tackiness, the value is derived from dividing the tackiness of the TORFM by the maximum tackiness of the three TORFM's. For example for FM-A:

$$Percentage = \frac{Tackiness\ of\ FMA}{Tackiness\ of\ FMB} \times 100 \quad (5)$$

For the SWR and FSR the percentage is the amount picked-up by the wheel compared to the amount applied to the rail. Figure 147 shows that the ranking of performance is exactly the same for each of the test rigs. FM-B is the tackiest formulation, FM-C is the lowest and FM-B gives the highest pick-up, FM-C gives the lowest. This means that the tackiness test is an indicator of how one TOR product will perform (in terms of pick-up) compared to another. The values of pick-up between SWR and FSTF are different. This is expected due to the different loads, speeds and slip values between the two rigs as well as different application methods. It is more important that the relative ranking is the same rather than focussing on the absolute values. This is because the loads, speeds and slips will be different again in field conditions compared to the SWR and FSTF (as well as many other variations). Therefore, these two test rigs are representative of the relative performance rather than drawing out the exact amounts of pick-up that occurs in the field.

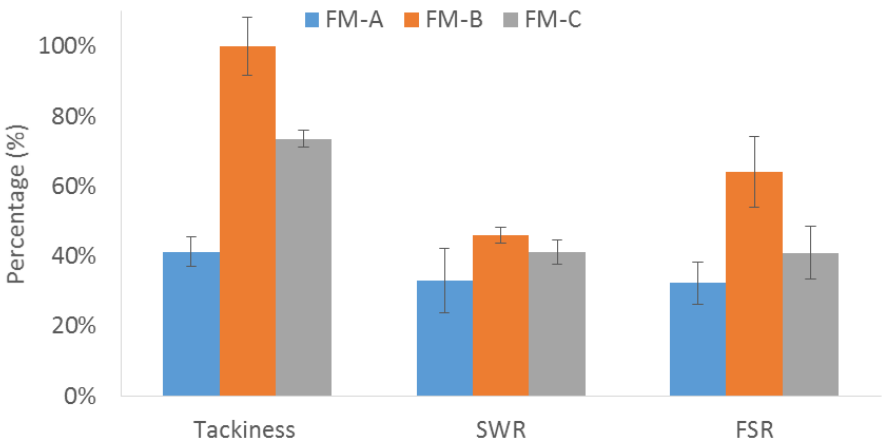

Figure 147- Ranking of the three TORFM's across the different test rigs

In the SWR tests, lateral displacement was shown not to have an effect on the pick-up of TORFM (Figure 135 and Figure 138). However, in the FSTF tests lateral displacement increased slightly (Figure 144B). The increase is small relative to the amount of TORFM picked up and so is considered to not be important. This difference in relationship is caused by the variation in application of TORFM to the rail.

8.4 Conclusions

The tackiness method developed in section 5 for grease tackiness has been shown to be equally applicable to friction modifiers. The results show that the method can differentiate between four very similar formulations of the same product. As in the grease work the roughness of the specimens affects the results. This does not matter as the ranking of the four TORFM's is the same regardless of what specimen roughness is used. However, it would be best if the specimens had the same roughness as the component being simulated (in this case the wheel and rail). This would eliminate a source of error when the results are scaled up to larger test rigs. The results from the two different batches of FM generally show good agreement between each other although there are differences in absolute values. Care should be taken to ensure the products are fully mixed when using products that have been stored for a period of time. If the results show inconsistencies then more repeats should be carried out or remix the product before carrying out the test again. The ranking of tackiness that this test method has given for the three TORFM's is the same as the ranking in the SWR and FSTF tests. Therefore, this tackiness test can be used to predict the outcome of larger scale tests and can be give indicators on how one product's pick-up would compare to another's.

From the SWR and FSTF testing it has been shown that the SWR can be used to rank different TORFM's and could be used to differentiate between different applicator bars using this method. This is because it is easy to attach an applicator bar and the results that this method gives are repeatable with a small standard deviation. As the FSTF has shown the same performance ranking of the three TORFM's as the SWR, it can be concluded that load, slip and speed do not affect the relative performance between different TORFM's.

9 Discussion

The aims of this work (details can be found in section 2.7) were:

- Assessment of fundamental product properties and how they relate to product performance
- Benchmark tests to assess performance based on available test platforms across a range of scales
- Develop new test methods to assess product properties and application in the field
- Understand the transferability of laboratory results to the actual, real world contact and between different laboratory test scales

This led to a number of key outcomes as detailed below. How these outcomes are linked together can be seen in Figure 148.

9.1 Key Outcomes

9.1.1 Fundamental Product Property

Tackiness was identified as a property that is key to the transfer of friction management products. This includes application to the wheel (pick-up) and the distance down the track that the benefits are seen (carry-down). This is because the ability for the product to form strings plays a key role in how much is transferred from the applicator/rail to wheel, and the transfer back from wheel to rail (if applicable). There was not a standard test found in the literature for tackiness, and literature on tackiness in general was found to be lacking. A test based on an approach-retraction style method was developed as an existing benchtop tribometer could be modified to be used in this way. This new test gave results quickly that were repeatable and accurate. The results of the tests were able to rank different products (including different formulations of the same product) according to their tackiness. Initial tests carried out with greases and TORFM's using a scaled-wheel rig ranked different products according to how much of the product is picked up by a wheel. This showed that the tackier the product, more of it is picked-up by the wheel. This confirmed that tackiness can be used as an indicator of pick-up performance and can be used by companies to develop new products or test products meet required standard at end of production line (see items 5-6 in Figure 148). This would lead to a benefit to the railway industry as if a wheel picks up more product, there is a greater chance it will carry it down further, reducing the need for multiple lubricators/prolong life of track and wheels.

9.1.2 Benchmark Tests

The tackiness test described above (section 9.1.1) can also be incorporated into standards that all products that want to be used on the railways have to meet. This would mean that only products that are known to perform well can be used. To enable this, further work to know what a 'good' product tackiness amount in the laboratory would have to be identified.

As well as the tackiness test, the Scaled-Wheel Rig (SWR) has been shown to be versatile in what products, applicator bars and methods can be tested with it. It has also shown agreement with tackiness tests and full-scale laboratory tests and so the test methods for pick-up and carry-

down could also be incorporated into standards for track based applications (see item 7 in Figure 148).

9.1.3 New Test Method to Assess Product Properties and Application in the Field

In order for the outcomes described in section 9.1.1 and 9.1.2 to be realised, more work is required to be done in the field to assess pick-up and carry-down in the field. Currently, the only options to measure carry-down is by visual inspection (difficult to see thin films), friction measurement (measures friction between rail and measurement device so doesn't take into account the effect of the wheel side of the interface) or by lateral force measurements (only for TORFM). Therefore a new method that measures the longitudinal vibration in the rail has been developed and been shown to detect different levels of grease around a curve. Carrying out vibration measurements along with complementary laboratory tests enables the relative performance between laboratory and field to be identified and ensures that the laboratory tests are validated against real world performance (see items 1 and 2 in Figure 148).

9.1.4 Linking Test Scales

The work described in Chapter 8 shows how three test scales are linked together as all three test methods give the same ranking of TORFM formulations. This means that the quicker, easier small-scale tests can be used to narrow down product choices and take a smaller, targeted range of products through to further testing. The interconnecting arrows in Figure 148 empahsise how the different test scales link together.

9.2 Impact and Future Directions

The work presented in this thesis has developed new test methods and has linked different test scales together. Now that the test methods have been established and shown to be able to produce repeatable, consistent results, there is further work that could be done. This further work would extend knowledge of how friction management products behave and improve impact of this work. Figure 148 shows how the outcomes/future work fits together and Table 15 summarises the key benefits and details.

1. Presence of grease detection using longitudinal vibration in the rail. Current work has focussed on one low traffic curve. To capture more data a field trial using a metro line would be beneficial. This would enable lots of repeats (all with similar trains) to be captured quickly. Additionally, data can be captured further from the lubrication site to assess carry-down of the grease from the lubrication site. This would benefit track operators/infrastructure managers as they will be able to assess how well the flange lubrication equipment is working.

2. Friction Modifier (FM) detection. As the longitudinal vibration in the rail has been shown to be affected by grease and contamination of the railhead, it can be assumed that FM's will also affect the vibration. Once the FM has dried (occurs very soon after wheel passes over the applicator), there is little transfer of product from wheel to rail. Therefore, conventional friction measurement devices (e.g. hand-push tribometer) cannot detect the presence of FM. A field trail measuring the longitudinal vibration at different distances down a track from an application site for the same train wold enable the carry-down performance to be assessed. As with item 1, this would benefit track

operators/infrastructure managers as they will be able to assess how well the application equipment is working and how far the benefits of the FM are seen.

3. Can longitudinal vibration in the rail be linked to track damage? Whilst carrying out the field trial at QRTC (see section 7.3.4) it was noticed that a defect in the track caused a large spike in the recorded vibration. A field trail that measures the vibration at a site known to have damage on it could be carried out to assess the sensitivity of the measurement equipment to track damage. This would lead into item 4.

4. Condition monitoring via longitudinal vibration. Field trails described in Chapter 7 showed how the longitudinal vibration in the rail is linked to products applied to the rail, vehicle speed, vehicle traction/braking and contamination of the rail. An accelerometer attached to the rail, linked to an Arduino and connected via mobile data could be used to create monitoring devices. These would be placed at strategic points (could be known problem areas) to record data continuously and alert the relevant people if vibration reaches a predetermined level. This would require an understanding of the 'normal' levels of vibration for that particular section of track to determine an appropriate alert level. For example, a device could be placed at a spot where leaf contamination is known to cause problems. The device measures the vibration, and if vibration is below the predetermined level, nothing happens other than data logging via upload to a server. When leaf contamination increases to cause wheel sliding and hence increasing the vibration above the predetermined level an email is sent to the relevant people. The data can then be analysed to see if it is a one off (potentially caused by wheel flat or oil contamination of that train) or if remedial measures are required. This benefits the railways by only applying remedial measures where required and reducing maintenance costs. This would also lead to an understanding of what vibrations are unacceptable (i.e. cause too much damage to track/train operation) and what the cause of the damage is.

5. Design of new application and friction management products. The test methods developed in this work can be used by equipment and product manufacturers to assess how new designs compare to old ones. This has the benefit that only the designs/formulations shown to be an improvement on existing ones are taken forward to costly field trials. This allows greater scope for innovation as more ideas can be tried out using simpler, cheaper test rigs in the laboratory.

6. Quality assurance. The laboratory tests developed (particularly the tackiness test due to its simplicity and speed) can be used at the end of a production line to show that the products meet agreed requirements.

7. Standards. The laboratory tests developed can be used in new/updated standards so that the railway industry is supplied with products/equipment that are designed and optimised for their intended use. Further laboratory and field validation would be required to determine the standard requirements. For example, in the SWR pick-up tests, how much grease is the minimum pick-up and where on the wheel should it be.

8. Modelling. Currently there are very few models that can incorporate third-body materials and products. The majority of models use one friction coefficient and are for dry wheel-rail contact. As more sophisticated models are developed, inputs are required to the models as well as validation of them. For example, an input could be the tackiness

of the grease from the tackiness test. The model would then calculate how much grease is picked-up and how far the carry-down distance is (taking into account all the other variables such as wheel-rail displacements, track geometry etc.). Based on this information, the model would update the friction coefficient for the gauge face, increasing the coefficient as distance from applicator increases. This benefits the railways as having models that accurately portray conditions in the field speeds up the rate of research and innovation that can be carried out.

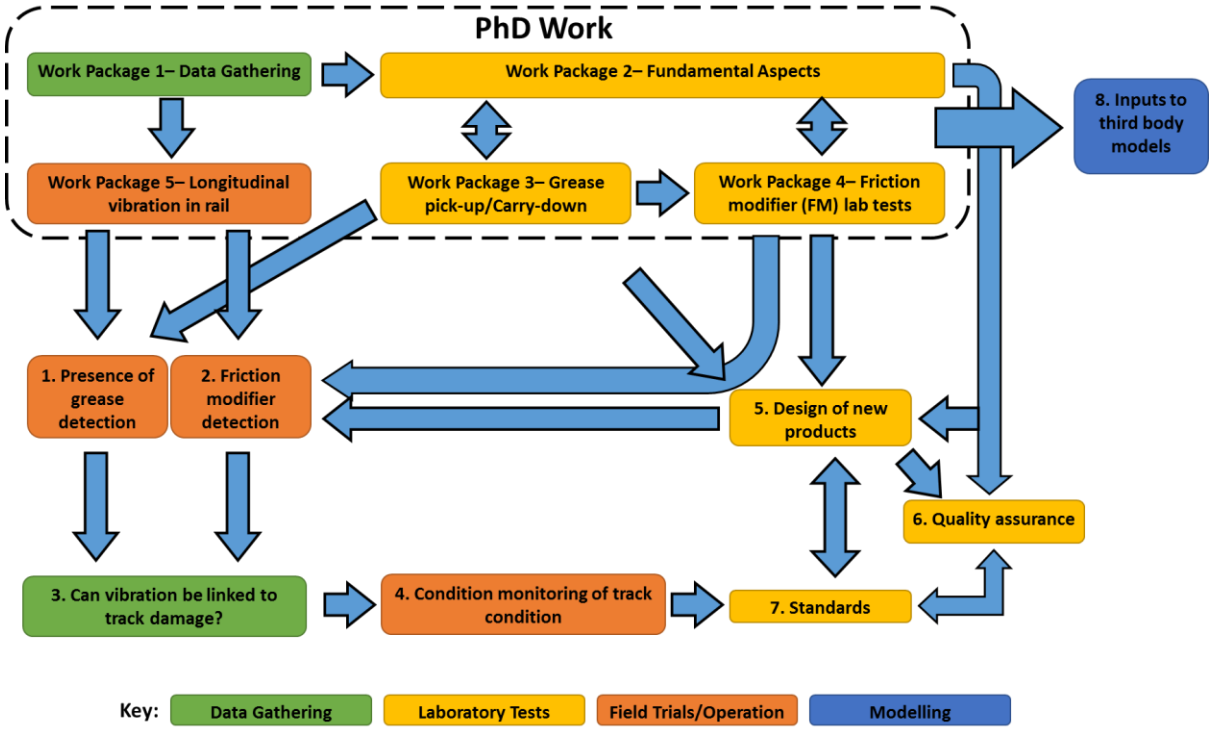

Figure 148- Flowchart of future directions of work

Work Item	Who Benefits	Details
1. Presence of grease detection	Track operators, infrastructure managers	Verify lubrication equipment is working effectively using longitudinal vibration devices. Detect carry-down distances of grease
2. FM detection	Track owners, track users, product manufactures	Detect how far FM is carried-down track using longitudinal vibration devices
3. Vibration and track damage	Track owners/ maintenance operators	Detect issues and severity earlier by increase in longitudinal vibration
4. Condition monitoring of track condition	Track owners and track users	Detect issues and severity earlier, use preventative maintenance where required. Uses mobile data enabled longitudinal vibration measurement devices
5. Design of new products/applicators	Equipment manufacturers	Test new product designs quickly and easily
6. Quality assurance	Friction management producers	Test products at end of production to ensure client requirements/standards met
7. Standards	Track owners, operators	Set minimum requirements new products/equipment has to meet
8. Inputs to third-body modelling	The railway industry	Results from tests used to validate and be inputs into models of wheel-rail interface

Table 15- Summary of future directions of work

10 Conclusions

The literature review detailed in chapter 2 identified that whilst there was plenty of research regarding friction management product performance, there was little research that considers the practical application of products to the railway. Additionally, the research that did look at product application (product pick-up/carry-down etc.), was mainly based on field research, which is costly in terms of time and money. This was due to the lack of laboratory test methods available that had been validated against field operation.

Figure 37 shows an ideal test procedure and so chapter 4 focussed on measuring parameters in the field that could be mimicked in the laboratory tests. This included measuring the size of grease bulbs on a GDU in the laboratory and field, and comparing them. It was found that the field bulbs had more variability due to different trains/wheel profiles passing over them, but the laboratory bulb represented field bulbs well. The pumpability and grease bulbs were also measured at different temperatures. This showed that temperature did change the size of the grease bulb but the variation was relatively small. Gauge face/wheel flange gaps were measured and video recorded as a train passed over a GDU. This showed the importance of the ability of the grease to form strings and how the gaps can be very small. This chapter is important as it enabled the laboratory tests to be designed to be as representative as possible.

Following on from the data-gathering phase, a number of new test methods were developed in the laboratory using small-scale and full-scale test rigs. Chapter 5 describes the development of a tackiness test. As this was a new method, a number of parameters had to be initially determined. The decision to focus on tackiness as a key property was chosen due to the video footage seen in Chapter 4. The test can differentiate between different formulations of the same grease, as well as modifying the method slightly to be able to suit a different application if required. The ability of the method to suit different applications is important as product manufacturers generally make products for a variety of uses and industries. The applicability of this method to other applications means that the product manufacturers can have one test rig to help them design new formulations or as part of a quality assurance procedure rather than have many bespoke rigs for each individual application.

Chapter 6 validates the use of a Scaled-Wheel Rig (SWR) in previous pick-up work by repeating the tests using a Full-Scale Test Facility. The work concluded that whilst there was differences the ranking of the different applicator bars and the trends seen were the same. However, how these results relate to field operation is an area where further work is requied. This chapter also developed a new test that measured grease carry-down using the SWR. This work concluded that where the grease is picked-up on the wheel is just as important as how much grease is picked-up by the wheel. This is because the results showed that if an applicator bar deposited grease too close to the flange tip, the grease did not enter the contact zone and was wasted. This emphasises that when designing laboratory tests, the whole system must be considered to ensure the laboratory test is representative of field results and to avoid recording misleading data.

Chapter 7 outlines two field trails measuring the longitudinal vibration in the rail as a train passes over measurement equipment. At the Severn Valley Railway (SVR), different locations around a curve after a lubricator site were measured. It was concluded that the longitudinal vibration decreased and frequency shifted slightly when there was more grease present on the gauge face. The frequency range of interest was 700-1200 Hz for the primary peak. Results also showed that the speed of the train affected the amplitude of the vibration (not the

frequency) and vibration in the rail was independent of the train travel direction. The second field trial took place at Quinton Rail Technology Centre (QRTC) and focussed on leaf contamination and the effect it has on braking. During braking, vibration increased due to more slip occurring in the wheel-rail interface. It concluded that severe leaf contamination leads to greater wheel slides during braking and more vibration. A shorter patch of leaf contamination gave repeatable low adhesion conditions. Comparisons between the two methods are difficult due to the different procedures and aims. However, it was shown that leaf contamination affects the vibration across the frequency range, whereas grease has the most impact in the 700-1200 Hz region. Additionally, the test method was sensitive enough that it was able to differentiate between train passes on a wet track (caused by dew) that was drying with each pass of the train.

Chapter 8 describes how the test methods developed in Chapters 5-6 were applied to Friction Modifier's (FM's) with little modification to the methods. It concluded that the tackiness test was able to differentiate between different FM's and that the tackiest FM gave the best pick-up in the SWR and FSTF tests. The SWR tests concluded that pick-up was independent of lateral displacement of the wheel and that different applicator bar positions gave different levels of pick-up. The FSTF tests concluded that slip and increasing lateral displacement of the wheel (reducing distance between wheel flange and gauge face), increased pick-up very slightly. It also concluded that increasing the load reduced pick-up due to more FM being squeezed out of contact for higher loads. As the tackiness, SWR, and FSTF tests gave the same ranking of FM's based on amount of pick-up, the final conclusion of this chapter was that the quick, small-scale tackiness test can be used to predict the outcome of the more realistic larger scale tests. Additionally, the fact that the SWR has no load, speed or slip control is not important due to the same ranking of FM's as the FSTF being given, despite the absolute values being different.

This work has led to the development of new test methods that can be used by product manufacturers to design and optimise new formulations of products or new equipment designs. This is because the new products/designs can be tested in the laboratory and compared to existing ones quickly and easily with only the successful, optimised final solutions being taken forward to costly, labour intensive field trails. This benefits the railway industry as it will lead to better performing friction management products. Additionally, standards can be created that incorporate these test methods to ensure that manufacturers produce products that meet a required standard. Furthermore, manufacturers can use these laboratory tests during quality assurance processes to prove that their products are of the required quality and meet the standard. This work has also linked different test scales together by repeating similar tests on different scales test rig and comparing results. This has the benefit that research on small-scale test rigs is more trusted as the methods have been validated using representative full-scale test rigs. Longitudinal vibration in the rail has been measured and been shown as an indicator of grease presence and of contamination by leaves on the rail. This can be used to validate further recommendations of the laboratory tests with respect to grease applicator bar set-up and different greases by measuring the carry-down of the grease. It is also hypothesised to be able to detect the presence of FM's. This is due to the sensitivity of the measurement equipment seen when measuring the vibration due to leaf contamination or dew on the rail. An extension of this work would be us the vibration measurement as a condition monitoring device for track damage or leaf contamination. This would enable preventative measures to be employed where and when necessary and monitoring of known problem sites to take place in real time. The grease and friction modifier tests can be used as inputs or to validate third-body models. This means that the models are more relatable to field conditions, as they will take into account more variables that are present in the real world. This leads to more accurate models that can be used by the railway industry to improve knowledge of the wheel-rail interface.

References

[1] R. Lewis, R. S. Dwyer-Joyce, S. R. Lewis, C. Hardwick, and E. A. Gallardo-Hernandez, "Tribology of the Wheel-Rail Contact: The Effect of Third Body Materials," *Int. J. Railw. Technol.*, vol. 1, no. 1, pp. 167–194, 2012.

[2] H. Tournay, "Guidelines to Best Practices for Heavy Haul Railway Operations," *International Heavy Haul Association*. pp. 2–45, 2001.

[3] H. R. Hertz, "Über die Beruhrüng fester elastischer Körper (on the contact of elastic solids)," *J. fur die reine und Angew. Math.*, vol. 92, pp. 156–171, 1882.

[4] K. L. Johnson, "Normal Contact of Elastic Solids: Hertz Theory," in *Contact mechanics*, Cambridge Press, 1985, pp. 84–106.

[5] R. Lewis and U. Olofsson, "Basic Tribology of the wheel-rail contact," in *Wheel–Rail Interface Handbook*, Woodhead Publishing Limited, 2009, pp. 34–57.

[6] A. Meierhofer, C. Hardwick, R. Lewis, K. Six, and P. Dietmaier, "Third body layer-experimental results and a model describing its influence on the traction coefficient," *Wear*, vol. 314, pp. 148–154, 2013.

[7] T. Telliskiv and U. Olofsson, "Contact mechanics analysis of measured wheel'rail profiles using the finite element method," *Proc. Inst. Mech. Eng. Part F-Journal Rail Rapid Transit*, vol. 215, no. 2, pp. 65–72, 2011.

[8] M. B. Marshall, R. Lewis, R. S. Dwyer-Joyce, U. Olofsson, and S. Björklund, "Experimental Characterization of Wheel-Rail Contact Patch Evolution," *J. Tribol.*, vol. 128, no. 3, p. 493, Jul. 2006.

[9] A. Rovira, A. Roda, M. B. Marshall, H. Brunskill, and R. Lewis, "Experimental and numerical modelling of wheel–rail contact and wear," *Wear*, vol. 271, no. 5–6, pp. 911–924, Jun. 2011.

[10] R. Stribeck, "Die wesentlichen Eigenschaften der Gleit und Rollenlager," *Zeitschrift Vereines deutche Ingenieure*, vol. 46, p. 86, 1902.

[11] R. Stock, L. Stanlake, C. Hardwick, D. Eadie, and R. Lewis, "Material concepts for top of rail friction management – classification, characterisation and application," *Wear*, vol. 366–367, Elsevier, pp. 225–232, Nov-2016.

[12] Y. Zhu, "Adhesion in the Wheel-Rail Contact under Contaminated Conditions," PhD Thesis, Royal Insitute of Technology, Stockholm, 2011.

[13] G. Vasic, F. Franklin, A. Kapoor, and V. Lucanin, "Laboratory simulation of low-adhesion leaf film on rail steel," *Int. J. Surf. Sci. Eng.*, vol. 2, no. 1/2, pp. 84–97, 2008.

[14] E. A. Gallardo-Hernandez and R. Lewis, “Twin disc assessment of wheel/rail adhesion,” *Wear*, vol. 265, no. 9–10, pp. 1309–1316, 2008.

[15] P. Swanson and R. Klann, “Abrasive wear studies using the wet sand and dry sand rubber wheel tests,” *Wear Mater.*, 1981.

[16] P. J. Bolton and P. Clayton, “Rolling—sliding wear damage in rail and tyre steels,” *Wear*, vol. 93, no. 2, pp. 145–165, 1984.

[17] R. Lewis and R. S. Dwyer-Joyce, “Wear mechanisms and transitions in railway wheel steels,” vol. 218, no. August, pp. 467–478, 2004.

[18] P. J. Blau, “How common is the steady-state? The implications of wear transitions for materials selection and design,” *Wear*, vol. 332–333, pp. 1–9, 2014.

[19] J. F. Archard, “Contact and rubbing of flat surfaces,” *J. Appl. Phys.*, vol. 24, no. 8, pp. 981–988, 1953.

[20] F. Braghin, R. Lewis, R. S. Dwyer-Joyce, and S. Bruni, “A mathematical model to predict railway wheel profile evolution due to wear,” *Wear*, vol. 261, no. 11–12, pp. 1253–1264, 2006.

[21] C. Hardwick, R. Lewis, and D. T. Eadie, “Wheel and rail wear-Understanding the effects of water and grease,” *Wear*, vol. 314, no. 1–2, pp. 198–204, Jun-2014.

[22] A. Rovira, A. Roda, R. Lewis, and M. B. Marshall, “Application of Fastsim with variable coefficient of friction using twin disc experimental measurements,” *Wear*, vol. 274–275, pp. 109–126, Jan. 2012.

[23] R. Lewis and U. Olofsson, “Mapping rail wear regimes and transitions,” *Wear*, vol. 257, no. 7–8, pp. 721–729, 2004.

[24] D. I. Fletcher, F. J. Franklin, and A. Kapoor, “Rail surface fatigue and wear,” in *Wheel-rail interface handbook*, 2009, pp. 280–310.

[25] A. Kapoor and J. A. Williams, “Shakedown limits in rolling-sliding point contacts on an anisotropic halfspace,” *Wear*, vol. 191, no. 1–2, pp. 256–260, 1996.

[26] S. L. Grassie, “Rail Corrugation,” in *Wheel–Rail Interface Handbook*, Woodhead Publishing Limited, 2009, pp. 349–376.

[27] S. L. Grassie and J. Kalousek, “Rail corrugation: characteristics, causes and treatments,” in *Proceedings of the Institution of Mechanical Engineers, Part F: Journal of Rail and Rapid Transit January*, 1993.

[28] L. Buckley-Johnstone, R. Lewis, D. Fletcher, K. Six, G. Trummer, and A. Meierhofer, “T1077: Modelling & quantifying the influence of water on wheel/rail adhesion levels,” London, UK, 2015.

[29] O. Polach, “Creep forces in simulations of traction vehicles running on adhesion limit,” *Wear*, vol. 258, no. 7–8, pp. 992–1000, 2005.

[30] J. Kalker, “A fast algorithm for the simplified theory of rolling contact,” *Veh. Syst. Dyn.*, no. 11, pp. 1–13, 1982.

[31] J. Giménez, A. Alonso, E. Gómez, and J. G. Gimé Nez, “Introduction of a friction coefficient dependent on the slip in the FastSim algorithm,” *Veh. Syst. Dyn.*, vol. 43, no. 4, pp. 233–244, 2005.

[32] M. Spiryagin, O. Polach, and C. Cole, “Creep force modelling for rail traction vehicles based on the Fastsim algorithm,” *Veh. Syst. Dyn.*, vol. 51, no. 11, pp. 1765–1783, Nov. 2013.

[33] E. A. H. Vollebregt, “Numerical modeling of measured railway creep versus creep-force curves with CONTACT,” *Wear*, vol. 314, no. 1–2, pp. 87–95, 2013.

[34] K. Six, A. Meierhofer, G. Müller, and P. Dietmaier, “Physical processes in wheel–rail contact and its implications on vehicle–track interaction,” *Veh. Syst. Dyn.*, vol. 53, no. 5, pp. 635–650, 2014.

[35] A. Meierhofer, “A new Wheel-Rail Creep Force Model based on Elasto-Plastic Third Body Layers,” PhD Theses- Graz University of Technology, 2015.

[36] C. Tomberger, P. Dietmaier, W. Sextro, and K. Six, “Friction in wheel-rail contact: A model comprising interfacial fluids, surface roughness and temperature,” *Wear*, vol. 271, no. 1–2, pp. 2–12, 2011.

[37] M. D. Evans, R. Lewis, C. Hardwick, A. Meierhofer, and K. Six, “High Pressure Torsion testing of the Wheel/Rail Interface,” in *Proceedings of 10th international conference on contact mechanics and Wear of Rail/Wheel Systems*, 2015.

[38] R. I. Popovici, “Friction in wheel - rail contacts,” PhD Thesis, University of Twente, 2010.

[39] R. Fries, C. Urban, N. Wilson, and M. Witte, “Modelling of Friction Modifier and Lubricant Characteristics for Rail Vehicle Simulations,” in *Proceedings of the 22nd International Association of Vehicle System Dynamics Symposium*, 2011, pp. 1–7.

[40] H. Harrison, T. McCanney, and J. Cotter, “Recent developments in coefficient of friction measurements at the rail/wheel interface,” *Wear*, vol. 253, no. 1–2, pp. 114–123, 2002.

[41] B. Allotta, E. Meli, A. Ridolfi, and A. Rindi, “Development of an innovative wheel-rail contact model for the analysis of degraded adhesion in railway systems,” *Tribol. Int.*, vol. 69, pp. 128–140, 2014.

[42] R. Lewis and J. Masing, “Static wheel/rail contact isolation due to track contamination,” *Proc. Inst. Mech. Eng. Part F J. Rail Rapid Transit*, vol. 220, no. 1, pp. 43–53, 2006.

[43] T. Johnson, “Understanding Aerodynamic Influences of Vehicle Design on Wheel/Rail Leaf Contamination,” 2006.

[44] P. M. Cann, “The ‘leaves on the line’ problem - A study of leaf residue film formation and lubricity under laboratory test conditions,” *Tribol. Lett.*, vol. 24, no. 2, pp. 151–158, 2006.

[45] Y. Zhu, U. Olofsson, and R. Nilsson, “A field test study of leaf contamination on railhead surfaces,” *Proc. Inst. Mech. Eng. Part F J. Rail Rapid Transit*, vol. 228, no. 1, pp. 71–84, 2014.

[46] O. Arias-Cuevas, Z. Li, and R. Lewis, “Laboratory investigation of some sanding parameters to improve the adhesion in leaf-contaminated wheel–rail contacts,” *F J. Rail*, vol. 224, pp. 139–157, 2010.

[47] S. R. Lewis and R. S. Dwyer-Joyce, “Effect of Contaminants on Wear, Fatigue and Traction,” in *Wheel-rail interface handbook*, Woodhead Publishing Limited, 2009, pp. 437–455.

[48] C. Hardwick, R. Lewis, and U. Olofsson, “Low adhesion due to oxide formation in the presence of NaCl,” in *Proceedings of 9th international conference on contact mechanics and wear of rail/wheel system*, pp. 27–30.

[49] B. T. White, J. Fisk, M. D. Evans, A. D. Arnall, T. Armitage, D. I. Fletcher, and R. Lewis, “A Study into the Effect of the Presence of Moisture at the Wheel / Rail Interface during Dew and Damp Conditions,” *Proc. 10th Int. Conf. contact Mech. Wear Rail/Wheel Syst.*, 2015.

[50] S. R. Lewis, R. Lewis, P. Richards, and L. E. Buckley-Johnstone, “Investigation of the isolation and frictional properties of hydrophobic products on the rail head, when used to combat low adhesion,” *Wear*, vol. 314, no. 1–2, pp. 213–219, 2014.

[51] S. Descartes, C. Desrayaud, E. Niccolini, and Y. Berthier, “Presence and role of the third body in a wheel-rail contact,” *Wear*, vol. 258, no. 7–8, pp. 1081–1090, 2005.

[52] T. M. Beagley, I. J. McEwen, and C. Pritchard, “Wheel/rail adhesion—Boundary lubrication by oily fluids,” *Wear*, vol. 31, no. 1, pp. 77–88, 1975.

[53] V. Reddy, G. Chattopadhyay, D. Hargreaves, and P. O. Larsson-Kråik, “Development of Wear-Fatigue-Lubrication Interaction Model for Cost Effective Rail Maintenance Decisions,” in *Proceedings of the First World Congress on Engineering Asset Management (WCEAM) 2006*, 2008, pp. 368–378.

[54] R. Stock, L. Stanlake, C. Hardwick, D. Eadie, and R. Lewis, “Material concepts for top of rail friction management – classification , characterization and application .,” in *Proceedings of 10th international conference on contact mechanics and Wear of Rail/Wheel Systems*, 2015.

[55] R. Lewis, E. A. Gallardo-Hernandez, T. Hilton, and T. Armitage, “Effect of oil and water mixtures on adhesion in the wheel/rail contact,” *Proc. Inst. Mech. Eng. Part F J. Rail Rapid Transit*, vol. 223, no. 3, pp. 275–283, 2009.

[56] O. Arias-Cuevas, Z. Li, R. Lewis, and E. A. Gallardo-Hernández, “Rolling-sliding laboratory tests of friction modifiers in dry and wet wheel-rail contacts,” *Wear*, vol. 268, pp. 543–551, 2010.

[57] Z. Li, O. Arias-Cuevas, R. Lewis, and E. A. Gallardo-Hernández, “Rolling–Sliding Laboratory Tests of Friction Modifiers in Leaf Contaminated Wheel–Rail Contacts,” *Tribol. Lett.*, vol. 33, pp. 97–109, 2008.

[58] O. Arias-Cuevas, Z. Li, and R. Lewis, “Investigating the lubricity and electrical insulation caused by sanding in dry wheel-rail contacts,” *Tribol. Lett.*, vol. 37, pp. 623–635, 2010.

[59] O. Arias-Cuevas, Z. Li, and R. Lewis, “A laboratory investigation on the influence of the particle size and slip during sanding on the adhesion and wear in the wheel-rail contact,” *Wear*, vol. 271, no. 1–2, pp. 14–24, 2011.

[60] R. Lewis and R. S. Dwyer-Joyce, “Wear at the wheel/rail interface when sanding is used to increase adhesion,” *Proc. Inst. Mech. Eng. Part F-Journal Rail Rapid Transit*, vol. 220, pp. 29–41, 2006.

[61] S. Kumar, P. K. Krishnamoorthy, and D. L. Prasanna Rao, “Wheel-Rail Wear and Adhesion With and Without Sand for a North American Locomotive,” *J. Eng. Ind.*, vol. 108, no. 2, pp. 141–147, May 1986.

[62] W. J. Wang, P. Shen, J. H. Song, J. Guo, Q. Y. Liu, and X. S. Jin, “Experimental study on adhesion behavior of wheel/rail under dry and water conditions,” *Wear*, vol. 271, no. 9–10, pp. 2699–2705, 2011.

[63] M. Omasta, M. Machatka, D. Smejkal, M. Hartl, and I. Křupka, “Influence of sanding parameters on adhesion recovery in contaminated wheel–rail contact,” *Wear*, vol. 322–323, pp. 218–225, Jan. 2015.

[64] S. R. Lewis, R. Lewis, J. Cotter, X. Lu, and D. T. Eadie, “A New Method for the Assessment of Traction Enhancers and the Generation of Organic Layers in a Twin-Disc Machine,” in *Proceedings of 10th international conference on contact mechanics and Wear of Rail/Wheel Systems*, 2015.

[65] W. J. Wang, T. F. Liu, H. Y. Wang, Q. Y. Liu, M. H. Zhu, and X. S. Jin, “Influence of friction modifiers on improving adhesion and surface damage of wheel/rail under low adhesion conditions,” *Tribol. Int.*, vol. 75, pp. 16–23, 2014.

[66] A. Matsumoto, Y. Sato, H. Ono, Y. Wang, M. Yamamoto, M. Tanimoto, and Y. Oka, “Creep force characteristics between rail and wheel on scaled model,” *Wear*, vol. 253, no. 1–2, pp. 199–203, Jul-2002.

[67] Y. Suda, T. Iwasa, H. Komine, M. Tomeoka, H. Nakazawa, K. Matsumoto, T. Nakai, M. Tanimoto, and Y. Kishimoto, “Development of onboard friction control,” *Wear*, vol. 258, no. 7–8, pp. 1109–1114, 2005.

[68] P. Temple, M. Harmon, R. Lewis, M. Burstow, B. Temple, and D. Jones, “Optimisation of grease application to railway tracks,” *Proc. Inst. Mech. Eng. Part F J. Rail Rapid Transit*, vol. 232, no. 5, pp. 1514–1527, 2018.

[69] M. C. Burstow and B. Temple, “Wheel/rail interaction for lubrication,” in *Presented at the Annual V/T SIC Seminar, RSSB, London*, 2015.

[70] J. Lundberg, M. Rantatalo, C. Wanhainen, and J. Casselgren, “Measurements of friction coefficients between rails lubricated with a friction modifier and the wheels of an IORE locomotive during real working conditions,” *Wear*, vol. 324–325, no. 1, pp. 109–117, Feb-2015.

[71] D. T. Eadie, D. Elvidge, K. Oldknow, R. Stock, P. Pointner, J. Kalousek, and P. Klauser, “The effects of top of rail friction modifier on wear and rolling contact fatigue: Full-scale rail-wheel test rig evaluation, analysis and modelling,” *Wear*, vol. 265, no. 9–10, pp. 1222–1230, Oct-2008.

[72] K. Matsumoto, Y. Suda, T. Fujii, H. Komine, M. Tomeoka, Y. Satoh, T. Nakai, M. Tanimoto, and Y. Kishimoto, “The optimum design of an onboard friction control system between wheel and rail in a railway system for improved curving negotiation,” *Veh. Syst. Dyn.*, vol. 44, no. sup1, pp. 531–540, 2006.

[73] K. Chiddick, B. Kerchof, and K. Conn, “Considerations in choosing a top-of-rail (TOR) material,” in *AREMA Annual Conference and Exposition*, 2014, pp. 1–21.

[74] D. T. Eadie, K. Oldknow, L. Maglalang, T. W. Makowsky, R. Reiff, P. Sroba, and W. Powell, “Implementation of wayside top of rail friction control on north american heavy haul railways,” in *7th World Congress on Railway Research*, 2006.

[75] M. G. Uddin, G. Chattopadhyay, and M. Rasul, “Development of effective performance measures for wayside rail curve lubrication in heavy haul lines,” *Proc. Inst. Mech. Eng. Part F J. Rail Rapid Transit*, vol. 228, no. 5, pp. 481–495, 2014.

[76] H. Chen, S. Fukagai, Y. Sone, T. Ban, and A. Namura, “Assessment of lubricant applied to wheel / rail interface in curves,” *Wear*, vol. 314, no. 1–2, pp. 228–235, 2014.

[77] S. Abbasi, U. Olofsson, Y. Zhu, and U. Sellgren, “Pin-on-disc study of the effects of railway friction modifiers on airborne wear particles from wheel–rail contacts,” *Tribol. Int.*, vol. 60, pp. 136–139, Apr. 2013.

[78] S. Achanta, M. Jungk, and D. Drees, “Characterisation of cohesion, adhesion, and tackiness of lubricating greases using approach–retraction experiments,” *Tribol. Int.*, vol. 44, no. 10, pp. 1127–1133, 2011.

[79] L. R. Rudnick, “Tackifiers and Antimisting Additives,” in *Lubricant Additives: Chemistry and Applications*, 2nd Editio., CRC Press, 2009, pp. 357–377.

[80] O. Steinhof and A. Kull, “Extensional flow properties of lubricating grease and the effect of tackiness additives,” in *Annual European Rheology Conference*, 2014.

[81] H. Strasburger, “Tacky Adhesion,” *J. Colloid Sci.*, vol. 13, pp. 218–231, 1958.

[82] BSI, “EN 15427- Railway applications — Wheel / rail friction management — Flange lubrication.” 2010.

[83] BSI, “EN 16028 Railway applications — Wheel / rail friction management — Lubricants for trainborne and trackside applications.” 2012.

[84] “NR/L3/TRK/3530/A01- Curve Lubricants.” Network Rail, 2012.

[85] D. T. Eadie, K. Oldknow, M. Santoro, G. Kwan, M. Yu, and X. Lu, “Wayside gauge face lubrication: How much do we really understand?,” *Proc. Inst. Mech. Eng. Part F J. Rail Rapid Transit*, vol. 227, no. 3, pp. 245–253, 2012.

[86] X. Lu, T. W. Makowsky, D. T. Eadie, K. Oldknow, J. Xue, J. Jia, G. Li, X. Meng, Y. Xu, and Y. Zhou, “Friction management on a Chinese heavy haul coal line,” *Proc. Inst. Mech. Eng. Part F J. Rail Rapid Transit*, vol. 226, no. 6, pp. 630–640, 2012.

[87] D. Elvidge, R. Stock, C. Hardwick, K. Oldknow, L. B. Foster, and R. Technologies, “The Effect of Freight Train Mounted TOR-FM on Wheel Life and Defects,” in *Proceedings of the Third International Conference on Railway Technology: Research, Development and Maintenance*, pp. 8–12.

[88] S. R. Lewis, R. Lewis, G. Evans, and L. E. Buckley-Johnstone, “Assessment of railway curve lubricant performance using a twin-disc tester,” *Wear*, vol. 314, no. 1–2, pp. 205–212, Jun-2014.

[89] R. Stock, D. T. Eadie, D. Elvidge, and K. Oldknow, “Influencing rolling contact fatigue through top of rail friction modifier application - A full scale wheel-rail test rig study,” *Wear*, vol. 271, no. 1–2, Elsevier B.V., pp. 134–142, May-2011.

[90] R. Stock, D. Eadie, and K. Oldknow, “Rail grade selection and friction management: a combined approach for optimising rail-wheel contact,” *Ironmak. Steelmak.*, vol. 40, no. 2, pp. 108–114, 2013.

[91] X. Lu, J. Cotter, and D. T. Eadie, “Laboratory study of the tribological properties of friction modifier thin films for friction control at the wheel/rail interface,” *Wear*, vol. 259, no. 7–12, pp. 1262–1269, Jul-2005.

[92] S. R. Lewis, R. Lewis, U. Olofsson, D. T. Eadie, J. Cotter, and X. Lu, “Effect of humidity, temperature and railhead contamination on the performance of friction modifiers: Pin-on-disk study,” *Proc. Inst. Mech. Eng. Part F J. Rail Rapid Transit*, vol. 227, no. 2, pp. 115–127, Jul. 2012.

[93] D. T. Eadie and M. Santoro, “Top-of-rail friction control for curve noise mitigation and corrugation rate reduction,” *J. Sound Vib.*, vol. 293, pp. 747–757, 2006.

[94] D. T. Eadie, M. Santoro, and J. Kalousek, “Railway noise and the effect of top of rail liquid friction modifiers: Changes in sound and vibration spectral distributions in curves,” *Wear*, vol. 258, no. 7–8, pp. 1148–1155, Mar-2005.

[95] S. L. Grassie, “Rail corrugation: Advances in measurement, understanding and treatment,” *Wear*, vol. 258, no. 7–8, pp. 1224–1234, Mar. 2005.

[96] M. Tomeoka, N. Kabe, M. Tanimoto, E. Miyauchi, and M. Nakata, “Friction control between wheel and rail by means of on-board lubrication,” *Wear*, vol. 253, no. 1–2, pp. 124–129, Jul-2002.

[97] D. T. Eadie, J. Kalousek, and K. C. Chiddick, “The role of high positive friction (HPF) modifier in the control of short pitch corrugations and related phenomena,” *Wear*, vol. 253, no. 1–2, pp. 185–192, Jul-2002.

[98] S. Aldajah, O. O. Aljayi, G. R. Fenske, and S. Kumar, “Investigation of Top of Rail Lubrication and Laser Glazing for Improved Railroad Energy Efficiency,” *J. Tribol.*, vol. 125, no. 3, p. 643, Jul. 2003.

[99] D. T. Eadie, M. Santoro, K. Oldknow, and Y. Oka, “Field studies of the effect of friction modifiers on short pitch corrugation generation in curves,” *Wear*, vol. 265, no. 9–10, pp. 1212–1221, Oct-2008.

[100] M. Chestney, N. Dadkah, and D. T. Eadie, “The effect of top of rail friction control on a european passenger system: the Heathrow express experience,” in *Proceedings of 8th International Contact mechanics and wear of rail/wheel systems conference*, 2009, pp. 591–598.

[101] C. Hardwick, S. Lewis, and R. Lewis, “The Effect of Friction Modifiers on Wheel/Rail Isolation at Low Axle Load,” *Wear*, vol. 271, no. 1–2, pp. 71–77, 2013.

[102] L. Buckley-Johnstone, M. Harmon, R. Lewis, C. Hardwick, and R. Stock, “Assessment of Friction modifiers performance using Two Different Laboratory Test-Rigs,” in *The Third International Conference on Railway Technology: Research, Development and Maintenance*, 2016, pp. 1–16.

[103] L. Zhou and R. Lewis, “Wheel-Rail Endpost Contact Characterisation using Ultrasound Reflectometry,” pp. 1–8, 2016.

[104] D. Jones, “Investigating Grease Pick-up and Carry Down using Laboratory and Field Measurements,” MEng Thesis, University of Sheffield, 2014.

[105] J. Kay and S. Chambers, “Preventing Flange Wear.”

[106] H. M. Tournay, “A future challenge to wheel/rail interaction analysis and design: Predicting worn shapes and resulting damage modes,” *Wear*, vol. 265, no. 9–10, pp. 1259–1265, 2008.

[107] Y. A. Areiza, S. I. Garcés, J. F. Santa, G. Vargas, and A. Toro, “Field measurement of coefficient of friction in rails using a hand-pushed tribometer,” *Tribol. Int.*, vol. 82, no. PB, pp. 274–279, Feb. 2015.

[108] M. Burstow, “Vehicle/Track System Interface Committee research areas: adhesion/ lubrication,” 2013.

[109] F. C. Robles Hernández, N. G. Demas, K. Gonzales, and A. a. Polycarpou, “Correlation between laboratory ball-on-disk and full-scale rail performance tests,” *Wear*, vol. 270, no. 7–8, pp. 479–491, 2011.

[110] W. Zhang, J. Chen, X. Wu, and X. Jin, “Wheel/rail adhesion and analysis by using full scale roller rig,” *Wear*, vol. 253, no. 1–2, pp. 82–88, 2002.

[111] X. S. Jin, W. H. Zhang, J. Zeng, Z. R. Zhou, Q. Y. Liu, and Z. F. Wen, “Adhesion experiment on a wheel/rail system and its numerical analysis.”

[112] K. Nagase, “A study of adhesion between the rails and running wheels on main lines: results of investigations by slipping adhesion test bogie.”

[113] J. D. Clarke, K. Hallas, R. Lewis, S. Thorpe, G. Hunwin, and M. J. Carré, “Understanding the friction measured by standardised test methodologies used to assess shoe-surface slip risk,” *J. Test. Eval.*, vol. 43, no. 4, pp. 723–734, 2015.

[114] D. I. Fletcher and J. H. Beynon, “Development of a machine for closely controlled rolling contact fatigue and wear testing,” *J. Test. Eval.*, vol. 28, no. 4, p. 267, 2000.

[115] D. I. Fletcher and S. R. Lewis, “Creep curve measurement to support wear and adhesion modelling, using a continuously variable creep twin disc machine,” *Wear*, vol. 298–299, pp. 57–65, Feb. 2013.

[116] RSSB, “Railway Wheelsets, Railway Group Standard GM/RT2466,” no. 3. 2010.

[117] P. Temple, M. Harmon, R. Lewis, M. Burstow, and B. Temple, “Optimisation of Grease Application to Railway Track,” in *The Third International Conference on Railway Technology: Research, Development and Maintenance*, 2016, pp. 1–16.

[118] P. Temple, “Optimisation of Grease Application to Railway Track,” MEng Thesis, University of Sheffield, 2015.

[119] D. Thompson, “2 Introduction to Rolling Noise,” in *Railway Noise and Vibration*, Elsevier, 2009, pp. 11–28.

[120] D. Thompson, “5 Wheel/Rail Interaction and Excitation by Roughness,” in *Railway Noise and Vibration*, Elsevier, 2009, pp. 127–174.

[121] C. F. Beards, “3.3 Modal analysis techniques,” in *Structural Vibration : Analysis and Damping*, London: Hodder Headline Group, 1996, pp. 125–128.

[122] L. B. Foster, “Trackside friction management ‘track parts’- Installation, operation and maintenance.” LB Foster, pp. 1–25, 2016.

Appendix A- Grading of Research Summary Table

Ref. Number	Number	Primary Category	Secondary Category	Criteria							Total Score
				1	2	3	4	5	6	7	
3	1	Wheel-Rail Contact	Modelling	Yes	Yes	Yes	Yes	Yes	No	No	5
6	2	Contaminants	Tribological Effect	Yes	Yes	No	Yes	Yes	No	No	4
7	3	Wheel-Rail Contact	Modelling	Yes	Yes	Yes	No	Yes	No	No	4
8	4	Wheel-Rail Contact	Tribological Effect	Yes	Yes	Yes	Yes	Yes	No	No	5
9	5	Wheel-Rail Contact	Modelling	Yes	Yes	Yes	Yes	No	No	No	4
12	6	Contaminants	Tribological Effect	No	Yes	Yes	Yes	Yes	No	Yes	5
13	7	Contaminants	Tribological Effect	Yes	Yes	Yes	No	Yes	No	No	4
14	8	Contaminants	Tribological Effect	Yes	Yes	Yes	No	Yes	No	No	4
15	9	Contaminants	Tribological Effect	Yes	Yes	Yes	No	Yes	No	No	4
16	10	Contaminants	Tribological Effect	Yes	Yes	Yes	No	Yes	No	Yes	5
17	11	Wheel-Rail Contact	Tribological Effect	Yes	Yes	Yes	No	Yes	No	No	4
19	12	Wheel-Rail Contact	Modelling	Yes	Yes	Yes	Yes	Yes	No	No	5
20	13	Wheel-Rail Contact	Modelling	Yes	Yes	Yes	Yes	Yes	No	No	5
21	14	Grease/Lubricant	Product Performance	Yes	Yes	Yes	No	Yes	No	No	4
22	15	Wheel-Rail Contact	Modelling	Yes	Yes	Yes	Yes	No	No	No	4
23	16	Wheel-Rail Contact	Modelling	Yes	Yes	Yes	No	Yes	No	Yes	5
25	17	Wheel-Rail Contact	Modelling	Yes	Yes	Yes	Yes	No	No	No	4
28	18	Contaminants	Tribological Effect	No	Yes	Yes	Yes	Yes	No	No	4
29	19	Wheel-Rail Contact	Modelling	Yes	Yes	Yes	Yes	No	No	Yes	5
30	20	Wheel-Rail Contact	Modelling	Yes	Yes	Yes	Yes	No	No	No	4
31	21	Wheel-Rail Contact	Modelling	Yes	Yes	Yes	Yes	No	No	No	4
32	22	Wheel-Rail Contact	Modelling	Yes	Yes	Yes	No	No	No	Yes	4
33	23	Wheel-Rail Contact	Modelling	Yes	Yes	Yes	Yes	No	No	No	4
34	24	Wheel-Rail Contact	Modelling	Yes	Yes	Yes	Yes	No	No	No	4
35	25	Wheel-Rail Contact	Modelling	No	Yes	Yes	Yes	Yes	No	Yes	5
36	26	Contaminants	Modelling	Yes	No	Yes	No	No	No	No	2
37	27	Wheel-Rail Contact	Tribological Effect	Yes	Yes	Yes	Yes	Yes	No	No	5
38	28	Contaminants	Modelling	No	Yes	Yes	Yes	Yes	Yes	Yes	6
39	29	Friction Modifiers	Modelling	Yes	Yes	Yes	No	No	No	Yes	4
40	30	Wheel-Rail Contact	Tribological Effect	Yes	Yes	No	No	Yes	No	Yes	4
41	31	Contaminants	Modelling	Yes	Yes	Yes	Yes	No	No	Yes	5
42	32	Contaminants	Tribological Effect	Yes	Yes	Yes	No	Yes	No	No	4
43	33	Contaminants	Modelling	Yes	Yes	Yes	Yes	No	No	No	4
44	34	Contaminants	Tribological Effect	Yes	Yes	Yes	No	Yes	No	No	4
45	35	Contaminants	Tribological Effect	Yes	Yes	Yes	No	No	No	Yes	4
46	36	Traction Enahncers	Product Performance	Yes	Yes	Yes	No	Yes	No	No	4
48	37	Contaminants	Tribological Effect	Yes	Yes	Yes	No	Yes	No	No	4
49	38	Contaminants	Tribological Effect	Yes	Yes	Yes	No	No	No	Yes	4
50	39	Traction Enahncers	Product Performance	Yes	Yes	Yes	No	Yes	No	No	4
51	40	Contaminants	Tribological Effect	Yes	Yes	Yes	No	No	No	Yes	4
52	41	Contaminants	Tribological Effect	Yes	Yes	Yes	No	Yes	No	No	4

53	42	Grease/Lubricant	Modelling	Yes	Yes	Yes	Yes	No	No	No	4
55	43	Contaminants	Tribological Effect	Yes	Yes	Yes	No	Yes	No	No	4
56	44	Friction Modifiers	Product Performance	Yes	Yes	Yes	No	Yes	No	No	4
57	45	Friction Modifiers	Product Performance	Yes	Yes	Yes	No	Yes	No	No	4
58	46	Contaminants	Tribological Effect	Yes	Yes	Yes	No	Yes	No	No	4
59	47	Contaminants	Tribological Effect	Yes	Yes	Yes	No	Yes	No	No	4
60	48	Traction Enahncers	Product Performance	Yes	Yes	Yes	Yes	Yes	No	No	5
61	49	Traction Enahncers	Product Performance	Yes	Yes	Yes	No	No	No	Yes	4
62	50	Contaminants	Tribological Effect	Yes	Yes	Yes	No	Yes	No	No	4
63	51	Traction Enahncers	Product Performance	Yes	Yes	Yes	No	Yes	No	No	4
64	52	Traction Enahncers	Product Performance	Yes	Yes	Yes	No	Yes	No	No	4
65	53	Friction Modifiers	Product Performance	Yes	Yes	Yes	No	Yes	No	No	4
66	54	Friction Modifiers	Product Performance	Yes	Yes	Yes	No	Yes	No	No	4
67	55	Friction Modifiers	Product Performance	Yes	Yes	Yes	No	No	No	Yes	4
68	56	Grease/Lubricant	Practical Considerations	Yes	Yes	Yes	Yes	Yes	No	No	5
70	57	Friction Modifiers	Product Performance	Yes	Yes	Yes	No	No	Yes	Yes	5
71	58	Friction Modifiers	Product Performance	Yes	Yes	Yes	Yes	No	Yes	No	5
72	59	Friction Modifiers	Practical Considerations	Yes	Yes	Yes	Yes	Yes	No	Yes	6
73	60	Friction Modifiers	Product Performance	No	Yes	Yes	No	No	No	Yes	3
74	61	Friction Modifiers	Product Performance	Yes	Yes	Yes	Yes	No	Yes	No	5
75	62	Grease/Lubricant	Practical Considerations	Yes	Yes	Yes	No	No	No	Yes	4
76	63	Grease/Lubricant	Product Performance	Yes	Yes	Yes	No	Yes	No	No	4
77	64	Friction Modifiers	Product Performance	Yes	Yes	Yes	No	Yes	No	No	4
78	65	Grease/Lubricant	Product Performance	Yes	Yes	Yes	No	Yes	No	No	4
80	66	Grease/Lubricant	Product Performance	No	Yes	Yes	No	Yes	No	No	3
81	67	Grease/Lubricant	Product Performance	Yes	Yes	Yes	No	Yes	No	No	4
86	68	Friction Modifiers	Product Performance	Yes	Yes	Yes	No	No	No	Yes	4
87	69	Friction Modifiers	Product Performance	Yes	Yes	Yes	No	No	No	Yes	4
88	70	Grease/Lubricant	Product Performance	Yes	Yes	Yes	No	Yes	No	No	4
89	71	Friction Modifiers	Product Performance	Yes	Yes	Yes	No	No	Yes	No	4
90	72	Friction Modifiers	Product Performance	Yes	Yes	Yes	No	No	Yes	No	4
91	73	Friction Modifiers	Product Performance	Yes	Yes	Yes	No	Yes	No	No	4
92	74	Friction Modifiers	Practical Considerations	Yes	Yes	Yes	No	Yes	No	No	4
93	75	Friction Modifiers	Product Performance	Yes	Yes	Yes	No	No	No	Yes	4
94	76	Friction Modifiers	Product Performance	Yes	Yes	Yes	No	No	No	Yes	4
96	77	Friction Modifiers	Product Performance	Yes	Yes	Yes	No	Yes	No	Yes	5
97	78	Friction Modifiers	Product Performance	Yes	Yes	Yes	No	No	No	Yes	4
98	79	Grease/Lubricant	Product Performance	Yes	Yes	Yes	No	Yes	No	No	4
99	80	Friction Modifiers	Product Performance	Yes	Yes	Yes	No	No	No	Yes	4
100	81	Friction Modifiers	Product Performance	Yes	Yes	Yes	No	No	No	Yes	4
101	82	Friction Modifiers	Practical Considerations	Yes	Yes	Yes	No	Yes	No	No	4
102	83	Friction Modifiers	Product Performance	Yes	Yes	Yes	No	Yes	Yes	No	5
103	84	Wheel-Rail Contact	Tribological Effect	No	Yes	Yes	Yes	No	Yes	No	4
104	85	Grease/Lubricant	Practical Considerations	No	Yes	Yes	Yes	Yes	No	Yes	5

105	86	Wheel-Rail Contact	Tribological Effect	No	Yes	Yes	No	No	No	Yes	3
106	87	Wheel-Rail Contact	Tribological Effect	Yes	Yes	Yes	No	No	No	Yes	4
107	88	Wheel-Rail Contact	Tribological Effect	Yes	Yes	Yes	No	No	No	Yes	4
109	89	Wheel-Rail Contact	Tribological Effect	Yes	Yes	Yes	No	Yes	Yes	No	5
110	90	Wheel-Rail Contact	Tribological Effect	Yes	Yes	Yes	Yes	Yes	No	No	5
111	91	Wheel-Rail Contact	Tribological Effect	Yes	Yes	Yes	Yes	Yes	No	No	5
112	92	Wheel-Rail Contact	Tribological Effect	Yes	Yes	Yes	No	No	Yes	No	4
114	93	Wheel-Rail Contact	Tribological Effect	Yes	Yes	Yes	No	Yes	No	No	4
115	94	Wheel-Rail Contact	Tribological Effect	Yes	Yes	Yes	No	Yes	No	No	4
117	95	Grease/Lubricant	Practical Considerations	Yes	Yes	Yes	Yes	Yes	Yes	No	6
118	96	Grease/Lubricant	Practical Considerations	Yes	Yes	Yes	Yes	No	No	No	4

Table 16- Summary table for grading of research